DETERMINING THE WATER USE, WATER AND NUTRITIONAL WATER PRODUCTIVITY OF MORINGA UNDER VARYING CROP MANAGEMENT PRACTICES

Report to the
Water Research Commission

Edited by

NA ARAYA

In collaboration with

S GOKOOL, SO AMOO, NA SITHOLE, N MULOVHEDZI, A NDAYAKUNZE, M MUTEMA, A CLULOW, M MENGISTU, H ARAYA & CP DU PLOOY

Agricultural Research Council – Vegetable, Industrial and Medicinal Plants
Roodeplaat, Pretoria

WRC Report No. 3171/1/24
ISBN 978-0-6392-0661-5

September 2024

Obtainable from
Water Research Commission
Bloukrans Building, Lynnwood Bridge Office Park
4 Daventry Street
Lynnwood Manor
PRETORIA

hendrickm@wrc.org.za or download from www.wrc.org.za

This is the final report of WRC project no. C2020/2021-00484.

EXECUTIVE SUMMARY

Moringa has multipurpose benefits to food, nutrition, human health and water security. Given its vast importance and environmental stress tolerance, the tree is often cultivated to produce nutritious leaves, pods and flowers. The tree productivity is dependent on crop management factors and environmental conditions, of which planting density, harvesting method, quantity and frequency of fertilization, water supply regimes, and climate types are amongst the major influencing factors. Thus, it is crucial to determine Moringa water use or evapotranspiration (ET) under different crop management practices and assess the consequent implications on water and nutritional water productivity of the crop. Very little is known, both locally and internationally, regarding optimum cultivation practices of Moringa for increased water and nutritional water productivity. Past research has focused primarily on the bio-active compound constituents and value-addition related to agro-processing for product development. To narrow the gaps in research, the Agricultural Research Council (ARC) in partnership with the Water Research Commission (WRC) implemented a project (Project C2020/2021-00484), from April 2021 to March 2024, aiming to determine the water use, water and nutritional water productivity of Moringa as influenced by different crop management practices. In order to meet the project aim, the following objectives were formulated: (1) to determine Moringa ET using the eddy covariance and remote sensing technologies; (2) to quantify Moringa ET under varying water supply regimes, and soil water conservation practices; (3) to determine the water and nutritional water productivity of Moringa under varying water supply regimes and soil water conservation practices, and (4) to predict ET and leaf yield of Moringa under varying soil water regimes and climatic conditions across South Africa using a soil water balance model.

In-situ measurements of crop evapotranspiration were conducted using an open-path eddy covariance system, on a 13-year-old Moringa stand established on a commercial farm located in the semi-arid area of Tooseng, Capricorn district municipality of the Limpopo Province, South Africa (24° 26' 59'' S, 29° 32' 58'' E, 822 m above sea level (masl)). These measurements were used to validate the METRIC EEFLUX (Mapping Evapotranspiration at High Resolution with Internal Calibration using the Earth Engine Flux) platform and an improved remote sensing modelling approach that combines fractional reference evapotranspiration with in-situ meteorological data to estimate daily Moringa crop evapotranspiration. This study also determined transpiration and transpiration coefficients of 9-year-old Moringa trees using sap flow measurements obtained with an improved stem heat balance approach in the semi-arid area of Roodeplaat, Pretoria. The data was used to parameterize and validate a canopy conductance physiological model to predict daily transpiration of Moringa. Additional crop evapotranspiration estimates of Moringa were conducted using a soil water balance approach, with the aid of automated capacitative soil water content sensors, irrigation controllers and rain gauges. These measurements were conducted under different crop management practices, including harvesting methods and frequencies, as well as soil water supply regimes (full irrigation – 20% management allowable depletion level (MADL) of plant available, moderate irrigation – 40% MADL and low irrigation – 60% MADL). The performance of crop models and research treatments tested in this study was evaluated using several statistical parameters, including coefficient of determination (R^2), mean absolute percent deviation (MAPD), root mean square error (RMSE), and Willmott index of agreement (d).

Daily Moringa ET obtained with the eddy covariance technique varied from 2.45 mm day^{-1} on a cloudy day to 4.28 mm day^{-1} on a hot sunny day. Daily crop coefficients (K_c) remained steadily constant throughout the experimental period, suggesting the presence of a drought adaptation mechanism in Moringa trees. Hourly and daily transpiration (T) measurements broadly showed a positive correlation between the measured sap flow and the involved microclimatic and morpho-physiological parameters. The average daily canopy conductance

ranged between 142 and 176 mmol m^{-2} s^{-1}, whereas the measured sap flow varied from 1.809-6.378 L/tree/day, which is equivalent to 1.06-3.75 mm/day. Additional crop evapotranspiration measurements conducted on 2-, 4- and 10-year-old Moringa trees using the soil water balance method in a semi-arid area of Roodeplaat, Pretoria, also revealed relatively low tree water consumption (1.3 to 12.0 L/tree/day^{-1}). This suggests that, in regions receiving sufficient rainfall, *Moringa oleifera* can be cultivated under rain-fed; however, implementation of climate-smart production systems, such as the in-situ rainwater harvesting, can bring added benefits to the Moringa tree. *Moringa oleifera* leaf production was significantly higher under moderate to low irrigation levels throughout the entire growing season. In terms of nutritional content, there was a significant interaction between growing period and water supply regimes on β-carotene (68.69 mg/100 g) and Fe (64.53 mg/100 g) with the highest value obtained under medium and high irrigation condition, respectively, while Na content did not vary significantly among different growing periods and water supply regimes tested. Vitamin C, total phenols, total flavonoids, Ca, Cu, K, Mg, Mn and Zn were largely influenced by the growing period. Vitamin C, total flavonoids and K content were significantly higher during the autumn growing period, Mg content was significantly higher during the autumn to winter growing period, while total phenols was significantly higher during the summer growing period. Water productivity was highly influenced by growing period and water supply regimes interaction mainly when the crop was still young, and also by these factors individually when the crop was well established. Moringa water productivity highest performance was obtained under low and medium irrigation treatment, with only rainfed treatments showed a good performance during the autumn and autumn-winter growing periods, with the lowest under high irrigation treatment during experimental period. It was also observed that Moringa water productivity was also influenced by weather variables as it increased and decreased with air temperatures and rainfall intensity during growing periods. Beta-carotene, Na, vitamin C and Zinc water productivity were significantly influenced by the interaction between water supply regime and growing period. Nutritional water productivity was significantly higher during the summer growing period, particularly for β-carotene (802.1 mg m^{-3}) and Na (445.0 mg m^{-3}) under the medium water supply regime, Zn (41.62 mg m^{-3}) under the low water regime. The autumn growing period was particularly beneficial for vitamin C accumulation (7554 mg m^{-3}) under the low water supply regime. These results indicated that nutritional content and nutritional water productivity were largely influenced by growing periods and the interaction between water supply regimes and growing period, while water productivity was influenced by both these factors and their interaction. Good predictions of daily Moringa ET (MAPE = 8%; RMSE = 0.28 mm/d and R^2 = 0.98) were obtained using fractional reference ET obtained using satellite imagery acquired by Landsat 7, 8 and 9 combined with alfalfa reference ET determined from in-situ measurements of meteorological variables. The overall performance of the AquaCrop model showed a good match between measured and simulated data for predictions of canopy cover (d = 0.98; RMSE = 5.4% and r = 0.98), fresh and dry seasonal yield (MAPD = 21.5-24.1%), soil water content and daily crop evapotranspiration. This suggests that the AquaCrop model (version 7.1) can be used to simulate Moringa responses to varying water supply regimes. A set of crop and soil parameters were developed to simulate Moringa productivity using the AquaCrop model. These parameters can be confidently applied to the AquaCrop model for simulation of Moringa productivity across a range of soil water supply regimes.

The information generated by implementing this project can be transferred to policy decision-makers, irrigation officers and consults, as well as farmers through technology transfer dissemination outputs, such as policy briefs, farmers' days, popular articles, scientific presentations and publications. This project conducted several informal farmers' days training events, conducted six oral presentations at national and international scientific conferences, produced four peer-reviewed scientific publications and four popular articles. The following new knowledge contributions were made to the scientific space through the above-mentioned technology transfer outputs: (1) accurate Moringa crop water use (crop ET and T) under various crop management practices; (2) nutritional content, water and nutritional water productivity under varying crop management practices; (3) first-time modelling of Moringa water use using a physiological model for prediction of T, soil water balance model for prediction of ET, remote sensing modelling approach for prediction of ET and simple, empirical regression models using canopy cover and stem area in-situ data; (4) a deeper understanding of the regulation of Moringa T; (5) field-based development of crop and transpiration coefficients, and (6) an assessment of the accuracy of eddy covariance for field-based Moringa ET measurements under limited fetch conditions. Adoption of the generated knowledge and tools will contribute to improved productivity of Moringa (both yield and nutritional content) using limited water resources, which will ultimately enhance food, nutrition and water security.

The aim and objectives of the project have been met. However, further research is warranted concerning measurements of Moringa crop ET and T in relation to associated environmental drivers across different climates, seasons and crop species, to improve the understanding of Moringa crop water use and enable parameterization/validation of crop models in an arid climatic condition. *Moringa peregrina* and *Moringa stenopetala* are the second and third most cultivated genotypes, following *Moringa oleifera*, due to their comparative great economic importance and increased nutritional properties. Other areas recommended for future research include water purification using Moringa seed, rainwater harvesting and conservation technologies combined with varying crop management practices, intercropping of Moringa with high-value crops such as vegetables and herbs, establishment of Moringa gardens at schools, households and communities, while exploring its potential for improving diets, water and soil conservation and quantify Moringa water footprints at field scale.

Apart from meeting the formulated research objectives, this project capacitated four students, one agricultural practitioner and nine farmers from the MOR-NUTRI Farm located in Tooseng, Limpopo province. Two of the capacitated students were registered for a PhD degree at the universities of KwaZulu-Natal and Pretoria, one registered for an MSc degree and another one registered for an Advanced Diploma at Tshwane University of Technology.

ACKNOWLEDGEMENTS

The following institutions and persons are acknowledged for their meaningful contribution to the successful completion and submission of this project final report:

Funding
Water Research Commission

Project implementation and management
Agricultural Research Council

Reference Group Members

Dr Luxon Nhamo	-	Water Research Commission (Project Manager)
Prof Sylvester Mpandeli	-	Water Research Commission
Dr Samkelisiwe Hlophe-Ginindza	-	Water Research Commission
Prof John Annandale	-	University of Pretoria
Prof Colin Everson	-	University of KwaZulu-Natal and University of Pretoria
Dr Brigid Letty	-	Institute of Natural Resources (non-profit company)
Dr Sebinasi Dzikiti	-	Stellenbosch University

Research Team Members

Dr Nadia Araya	-	Agricultural Research Council (Project Leader)
Dr Christian Philippus du Plooy	-	Agricultural Research Council
Mr Mduduzi Sithole	-	Agricultural Research Council
Dr Shaeden Gokool	-	University of KwaZulu-Natal
Dr Alistair Clulow	-	University of KwaZulu-Natal
Prof. Stephen Amoo	-	Agricultural Research Council
Dr Hintsa Araya	-	Agricultural Research Council
Dr Michael Mengistu	-	South African Weather Service
Prof Michael Savage	-	University of KwaZulu-Natal
Dr Macdex Mutema	-	Agricultural Research Council

Students

Mr Ntsieni Mulovhedzi (PhD student)	-	University of KwaZulu-Natal
Mr Ambroise Ndayakunze (PhD student)	-	University of Pretoria
Mr Floyd Nwamba (MSc student)	-	Tshwane University of Technology
Mr Graig Sithole (Intern)	-	Tshwane University of Technology
Ms Tintswalo Mathonsi (Agricultural Practitioner)	-	Tshwane University of Technology

Farmer

Mr Mathabatha Thushego	-	MOR-NUTRI Moringa Farm

Report structuring

Ms Johleen Malaka	-	Agricultural Research Council

CONTENTS

LIST OF TABLES

LIST OF FIGURES

LIST OF ABBREVIATIONS, ACRONYMS AND SYMBOLS

AATSR	Advanced Along-Track Scanning Radiometer
ARC-VIMP	Agricultural Research Council – Vegetable, Industrial and Medicinal Plants
EEF	Earth Engine Flux
ESI	Ecosystem Stress Index
ET_o	Reference evapotranspiration
ET	Crop evapotranspiration
E_s	Soil evaporation
GEE	Google Earth Engine
K_c	Crop coefficient
$K_{c\ mid}$	Crop coefficient during the mid-season under partial ground cover
$K_{c\ full}$	Crop coefficient during the mid-season under full ground cover
K_{cb}	Basal crop coefficient
K_e	Soil evaporation coefficient
K_t	Transpiration crop coefficient
LAI	Leaf area index
LE	Latent heat flux
MODIS	Moderate Resolution Imaging Spectroradiometer
NWP	Nutritional Water Productivity
RS	Remote Sensing
r_s^c	Bulk stomatal resistances of the canopy
r_a^c	Boundary layer resistance
r_a^s	Aerodynamic resistance from soil to canopy
r_a^a	Aerodynamic resistance from canopy to reference height
r_s^s	Soil surface resistance
R_n	Net radiation
R^2	Coefficient of determination
SABALI	Surface Energy Balance Algorithm for Land-Improved
SEBAL	Surface Energy Balance Algorithm for Land
SEBI	Surface Energy Balance Index
SEBS	Surface Energy Balance System
TSEB	Two Surface Energy Balance
UAV	Unmanned Aerial Vehicles
UKZN	University of KwaZulu-Natal
WRC	Water Research Commission
WUE	Water use efficiency

LIST OF UNITS

cm	Centimetre
g	Gram
kg	Kilogram
L	Litre
m	Metre
m/s	Metre per second
$MJ/m^2/s$	Megajoules per square metre per second
ml	Millilitre
mm	Millimetre
W/m^2	Watts per square metre

CHAPTER 1

INTRODUCTION AND BACKGROUND

Nadia Araya

Agricultural Research Council – Vegetable, Industrial and Medicinal Plants, Private bag X293, Pretoria, 0001, South Africa
Agricultural Research Council – Natural Resources and Engineering, Private bag X79, Pretoria, 0001, South Africa

Moringa is a multipurpose tree known for its beneficial role in food and nutrition security. In addition, the tree is used for medicinal and nutraceutical purposes to strengthen human health, due to its high antioxidant content, amongst others, which are effective against prostrate and skin cancers, tumors, aging and other diseases (Khazim Al-Asmari et al., 2015). The seeds of Moringa can be used for human consumption and as seed cake for livestock feed and soil fertility amelioration. The high oil content in the seeds demonstrates its potential for industrial uses as well (Ayerza, 2012), in the manufacturing of lubricants for machinery, biodiesel, perfumes and hairdressing products. The oil also has great potential market value, which can contribute to income generation for farmers. In addition, Moringa tree leaves are a good source of protein, with high potential to address nutritional deficiencies in ruminants, particularly in the dry season when natural pastures are low in protein and energy.

Given the vast importance of Moringa, the tree is often cultivated for the production of leaves, pods or both, and in some cases for fodder production. Crop management differs depending on the purpose of its cultivation. Production of leaves for human food consumption is normally done at higher planting densities or narrower plant spacing (0.75-1.0 m intra row x 1.0-2.0 m inter row) when compared to pod production (2.0-2.5 m x 2.5-5.0 m), being dependent on several factors including soils and climatic conditions (Radovich et al., 2009, Attia et al., 2014). Much higher planting densities, at considerably narrower plant spacing, are used for fodder production (0.15-0.2 m intra row x 0.2-0.5 m inter row) (Mabapa et al., 2017). Pruning is also an important factor influencing Moringa production, as it promotes branching, increased yields, and easy harvesting. Cutting back branches and tipping young Moringa trees, grown for leaf production, induce lateral branching to produce a multi-branched shrub, while old trees that are unproductive or too high for easy harvesting, can be cut back once per year (Crosby and Craker, 2007). There is insufficient information available regarding appropriate frequency and intensity of pruning of Moringa trees grown for leaf production. Moringa tree pod production also benefits from pruning. As reported by du Toit et al. (2020), light pruning (3 m from the ground) results in the highest quantity of buds and flowers. In South Africa, household gardeners and smallholder farmers commonly cultivate Moringa for leaf production, at their backyards and small areas of less than 1.0 ha (Mabapa et al., 2017). The main purpose of their production is to process the leaves into powder to be sold in local markets for income generation. Commercial farmers are mainly interested in pod production for biodiesel, as well as supply to cosmetic and food industries for glycerin production (due to its rich glyceride content) amongst other products (Susilorini et al., 2017). For this purpose, Moringa is cultivated in large areas up to 3000 or more hectares of land, through organized cooperatives, which are formed by small groups of local community members (Joubert, 2010). Therefore, large-scale production benefits not only commercial farmers, but also local communities in terms of income generation for sustainable livelihoods and human wellbeing.

Despite the complex management of the Moringa tree crop, there are knowledge gaps regarding optimum cultivation practices for increased yield and quality of the harvested fresh leaf produce (Leone et al., 2015; du Toit et al., 2020). In addition, there is a paucity of information on the potential of Moringa tree crop to protect agricultural soils against erosion, a major concern in the smallholder farming sector where agriculture is largely rain-fed based. Most of the research conducted to date has largely focused on assessing chemical, medicinal and nutritional properties of the plant. The Agricultural Research Council – Vegetable, Industrial and Medicinal Plants (ARC-VIMP) has made significant contributions to knowledge generation on Moringa (Ndhlala et al., 2014; Ntila et al., 2018; Mapfumo et al., 2019; Muhammad et al., 2019; Singh et al., 2019; Tshabalala et al., 2019a, b). ARC-VIMP's pioneering research on Moringa began more than 10 years ago, focusing largely on analytical studies of the bio-active compounds and value-adding research related to agro-processing for product development.

In April 2021, ARC-VIMP received funding approval from the Water Research Commission (WRC) to manage and implement a 3-year research project focusing on quantification of Moringa water use under varying crop management practices (Project No C2020/2021-00484). Two experimental sites were established at ARC-VIMP Roodeplaat research station semi-arid area, to investigate Moringa tree crop water use and related influencing factors. Research findings were presented during the 2nd International Symposium on Moringa, in November 2019 (Araya et al., 2019; Mokgehle et al., 2019; Ntsieni et al., 2019). Greater water use efficiency and nutritional water productivity was obtained from deficit irrigation at 60% depletion from maximum plant available water, indicating potential for irrigation water savings (500 000 L ha^{-1} can be saved over one growing season), which can be used for expansion of cultivated area to 2-3 times more, under limited availability of water resources. The current WRC funded Moringa Water Use project has also investigated crop water use under dryland conditions. In addition, since crop water use is highly variable across different soil water regimes and climatic conditions, crop simulation models were used to extrapolate site-specific experimental results to conditions where measurements have not been conducted. This can contribute to identification of suitable sites for production and more effective irrigation scheduling, which will result in irrigation water savings for improved water use efficiency. Such research outputs can contribute to a more effective implementation of the National Water Resources Management Strategy, which advocates a 50% growth in irrigated agriculture by 2030, as this can be more easily achieved through water savings and increased water use efficiency in crop production, due to limited water allocations made to the agricultural sector (Bonthuys, 2018). The research conducted under this project (C2020/2021-00484) provides first-time insight on Moringa tree water consumption determined using eddy covariance and sap flow technologies, which are reliable and accurate methods of measuring crop water use. In addition, the report provides recommendations on best crop management practices of Moringa under irrigated and dryland production for improved water use efficiency and nutritional water productivity of the crop.

The project aimed at determining the water use, water and nutritional water productivity of Moringa under varying crop management practices. The following objectives were formulated in order to meet the project aim:

- To determine Moringa ET using the eddy covariance and remote sensing technologies;
- To quantify Moringa ET under varying water supply regimes, and soil water conservation practices;
- To determine the water and nutritional water productivity of Moringa under varying water supply regimes and soil water conservation practices and
- To predict ET and leaf yield of Moringa under varying soil water regimes and climatic conditions across South Africa using a soil water balance model.

REFERENCES

Araya, N.A., Mulovhedzi, N., Araya, H.T., Amoo, S.O., du Plooy, C.P., Laurie, S., Mofokeng, M.M., 2019. Seed germination, seedling growth and physiology of *Moringa oleifera* under varying air temperature regimes: effect of growing medium and seed treatment. II International Symposium on Moringa, 10-13 November 2019, Pretoria, South Africa.

Attia, M.F., Shahin, M.F.M., Merwad, M.A., El-Hady, E.S., Haggag, L.F., 2014. Effect of Mineral, Organic and Bio-Fertilization on Productivity of Moringa plant under Saline Conditions in North Sinai. Middle East j. appl. sci., 4(4): 825-832.

Bonthuys, J., 2018. In-depth study sheds light on irrigated farming areas, water use. Irrigation Water Use. The Water Wheel July/August 2018.

Joubert, R., 2010. Moringa: A tree for all seasons. Farmer's Weekly.

Leone, A., Spada, A., Battezzati, A., Schiraldi, A., Aristil, J., Bertoli, S., 2015. Cultivation, genetic, ethnopharmacology, phytochemistry and pharmacology of *Moringa oleifera* leaves: an overview. Int. J. Mol. Sci., 16, 12791-12835.

Mabapa, M.P., Ayisi, K.K., Mariga, I.K., Mohlabi, R.C., Chuene, R.S., 2017. Production and Utilization of Moringa by Farmers in Limpopo Province, South Africa. Int. J. Mol. Sci., 12: 160-171.

Mabapa, M.P., Ayisi, K.K., Mariga, I.K., 2017. Effect of planting density and harvest interval on the leaf yield and quality of Moringa (*Moringa oleifera*) under diverse agroecological conditions of Northern South Africa. Int. J. Agron., 2017: 1-9.

Mapfumo, M., Lembede, B.W., Ndhala, A.R., Chivande, E., 2019. Effect of crude Moringa oleifera Lam. seed extract on the blood markers of metabolic syndrome in high-fructose diet-fed growing Sprague-Dawley rats. JCIM, 17(1).

Mokgehle, S.N., Mulovhedzi, N.E., Araya H.T., du Plooy, C.P., Amoo, S.O., Seepe, H.A., Laurie, S.M., Araya N.A., 2019. Phytochemical and nutritional composition of Moringa oleifera in response to varying water supply regimes. II International Symposium on Moringa, 10-13 November 2019, Pretoria, South Africa.

Mosase, E., Ahiablame, L., 2018. Rainfall and Temperature in the Limpopo River Basin, Southern Africa: Means, Variations, and Trends from 1979 to 2013. Water 2018, 10, 364.

Muhammad, N., Ibrahim, K.G., Ndhlala, A.R., Erlwanger, K., 2019. *Moringa oleifera* Lam. prevents the development of high fructose diet-induced fatty liver. S AFR J BOT, 129: 32-39.

Mulovhedzi, N., Savage, M.J., Araya, H.T., Amoo, S.O., du Plooy, C.P., Laurie, S., Araya, N.A., 2019. Water use efficiency of Moringa oleifera under different water supply regimes. II International Symposium on Moringa, 10-13 November 2019, Pretoria, South Africa.

Ndhlala, A.R., Mulaudzi, R., Ncube, B., Abdelgadir, H.A., du Plooy, C., Staden, J. van, 2014. Antioxidant, antimicrobial and phytochemical variations in thirteen *Moringa oleifera* Lam. Cultivars. Mol., DOI: 10.3390/molecules190710480(3).

Ntila, S. Ndhalala, A.R., Kolanisi, u., Abdelgadir, H., Siwela, M., 2018. Acceptability of a moringa-added complementary soft porridge to caregivers in Hammanskraal, Gauteng province and Lebowakgomo, Limpopo province, South Africa. South Afr J Clin Nutr, 1(1):1-7.

Radovich, T., 2009. Farm and Forestry Production and Marketing Profile for Moringa (Moringa oleifera). In: Elevitch, C.R. (ed.). Specialty Crops for Pacific Island Agroforestry. Permanent Agriculture Resources (PAR), Holualoa, Hawaii.

SAWS, 2018. Annual Climate Summary for South Africa. South African Weather Service. Public Document, WCS-CLS-CI-ACS-2018.

Singh, A.K., Rana, H.K., Tshabalala, T., Kumar, R., Gupta, A., Ndhala, A.R., Pandey, A.K.2019. Phytochemical, nutraceutical and pharmacological attributes of a functional crop Moringa oleifera Lam: An overview. S AFR J BOT, 129: 209-220.

Tshabalala, T., Ncube, B., Madala, N.E., Nyakudya, T.T., Moyo, H.P., Sibanda, M., Ndhlala, A.R., 2019. Scribbling the Cat: A Case of the “Miracle” Plant, *Moringa oleifera*. Plants, 8, 510.

Tshabala, T., Ndhalala, A.R., Abdelgadir, H.A., Staden, J. van, 2019. Potential substitution of the root with the leaf in the use of Moringa oleifera for antimicrobial, antidiabetic and antioxidant properties. S AFR J BOT, 129: 106-112.

CHAPTER 2

LITERATURE REVIEW

Nadia Araya[1,2], Ambroise Ndayakunze[1], Mduduzi Sithole[1], Sihle Floyd Nwamba[1] and Ntsieni Mulovhedzi[3]

[1]*Agricultural Research Council – Vegetable, Industrial and Medicinal Plants, Private bag X293, Pretoria, 0001, South Africa*

[2]*Agricultural Research Council – Natural Resources and Engineering, Private bag X79, Pretoria, 0001, South Africa*

[3]*School of Agricultural Sciences, University of Mpumalanga, Private bag X11283, Mbombela, 1200, South Africa*

2.1 METHODS USED FOR LITERATURE SEARCH

An integrated, qualitative, and systematic approach was used in this study to search, select and manage the available knowledge relating to Moringa water use and crop water use related drivers. This was integrated with the authors' expertise in this field to thoroughly discuss the most relevant topics in order to identify the current gaps in knowledge and to provide appropriate recommendations for future research to address these gaps. The literature search included online sources, peer-reviewed papers published in scientific journals, books and other publications such as popular articles. Published literature from universities, national research institutions, in the form of student theses and dissertations, conference proceedings, working papers, and project reports were also considered. A detailed literature search was conducted using various search engines such as Google, universities and the Agricultural Research Council's online databases.

2.2 PRODUCTION OF MORINGA

2.2.1 World production

Moringa oleifera Lam., commonly referred to as either horseradish tree due to the taste of its roots, or Drumstick tree given the shape of its pods, is indigenous to South Asia, particularly from India in Bengal (Paliwal et al., 2011; Sharma et al., 2011). The genus *Moringa* comprises of 13 species distributed around Africa, Madagascar, western Asia and the Indian subcontinent (Iqbal et al., 2006). These species are generally categorized into three sections: (1) Donaldsonia or the 'bottle tree' group, mostly from southern Africa and Madagascar, with swollen trunks and radially symmetrical flowers; (2) DysMoringa from north-eastern Africa, with thick and fleshy tuberous roots, and (3) Moringa to which *Moringa oleifera* belongs, from the Indian subcontinent and the Arabian Peninsula, with tough roots and bilaterally symmetrical flowers (Mahklouf, 2020). Table 2.1 presents all 13 species of the genus Moringa, including their native countries/regions. *Moringa oleifera* and *Moringa peregrina* Forssk. are the most cultivated species around the world due to their great economic importance and increased nutritional properties (Hassanein and Abdulah Al-Soqeer, 2018).

Table 2.1: Species of genus Moringa and their native countries/regions (Olson, 2002).

Species	Native countries/regions
Moringa arborea Verdc.	Kenya
Moringa rivae Chiov.	Kenya and Ethiopia
Moringa stenopetala (Baker f.) Cufod.	Kenya and Ethiopia
Moringa borziana Mattei	Kenya and Somalia
Moringa longituba Engl.	Kenya and Somalia
Moringa pygmaea Verdc.	Somalia
Moringa ruspoliana Engl.	Kenya, Ethiopia and Somalia
Moringa ovalifolia Dinter and A. Berger	Namibia and Angola
Moringa drouhardii Jum.	Madagascar
Moringa hildebrandtii Engl.	Madagascar
Moringa peregrina (Forssk.) Fiori	Arabia, Red sea and Dead sea
Moringa concanensis Nimmo	Sub-Himalayan tracts of India subcontinent
Moringa oleifera Lam.	Sub-Himalayan tracts of India subcontinent

Moringa has been widely naturalized in other tropical regions of the world (Figure 2.1). These regions include large parts of southern and eastern Asia, sub-Saharan Africa, north and South America, and Pacific islands (Gandji et al., 2018).

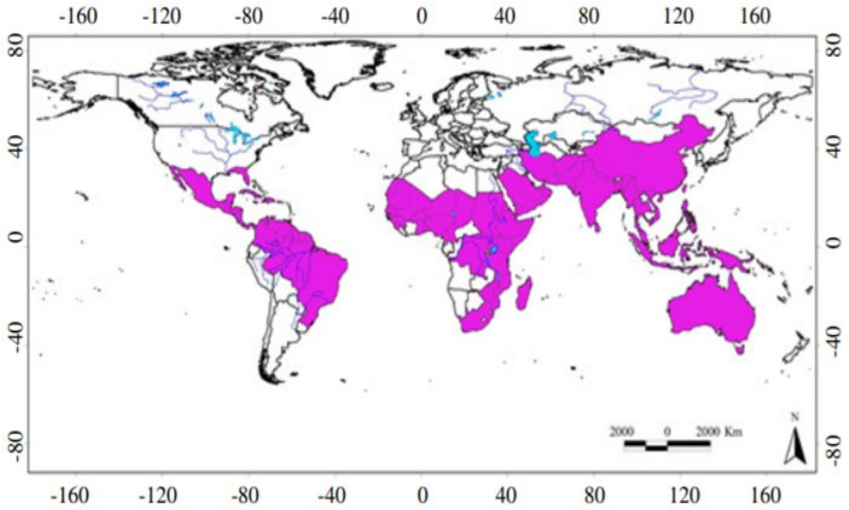

Figure 2.1: Countries where Moringa has been recorded as either native or naturalised (Adapted from Navie and Csurhes, 2010).

2.2.2 South African production

Moringa is majorly grown in six of the nine South African Provinces: Limpopo, Gauteng, Mpumalanga, KwaZulu-Natal, Free State and North West. Among these Provinces, it is mainly grown in the Limpopo Province by farmers and household gardeners, particularly in Capricorn, Mopani, Sekhukhune, Vhembe and Waterberg Districts (Mashamaite et al., 2021). In these areas, Moringa is primarily produced as a nutritional source, an income source and for health purposes. A socio-economic situational analysis conducted in the Limpopo Province (Vhembe district) concluded that, on average, a household produced a total of 53 kg of Moringa fresh leaves per year, and that production was highly variable across locations, depending on cultivation methods, genetic differences and climatic conditions (Maxwell, 2019). Another situational analysis conducted in the Limpopo Province revealed that farmers produce in relatively small areas, ranging from 0.25-1.0 ha (Bopape-Mabapa, 2019). In the Limpopo

Province, Moringa is commonly cultivated on medium textured soils, including loam sandy, sand loamy, clay loam and sandy clay loam, with a clay content varying from 16 to 56% (Bopape-Mabapa, 2019). The same study showed that tree age was quite variable, from as young as 1.0 to as old as 10-year old trees, indicating that farmers continue to plant and expand Moringa plantations, and that the establishment of Moringa trees in South Africa is relatively new (approximately 10 years ago). Figures 2.2 and 2.3 illustrate average annual temperature, soil type and total annual rainfall where Moringa is grown in Limpopo Province (Bopape-Mabapa, 2019).

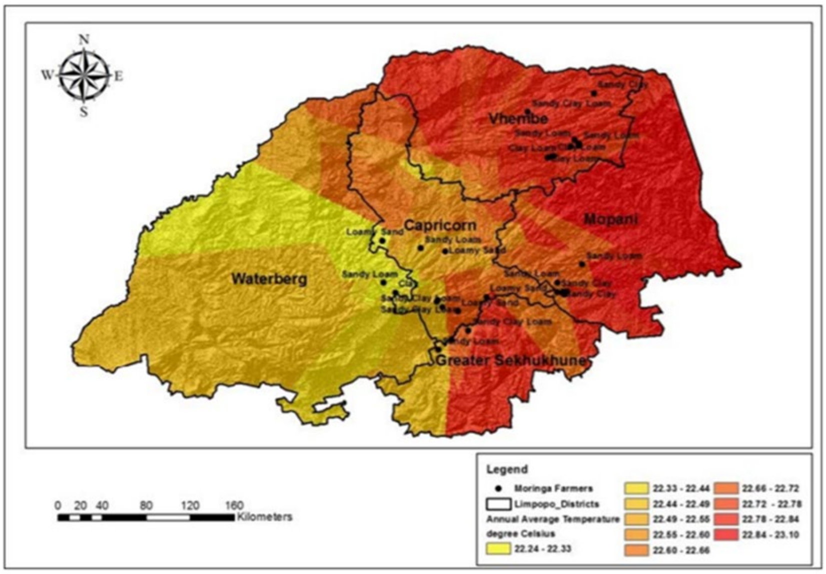

Figure 2.2: Average annual temperature and soil textural classes from various locations where Moringa is growing in Limpopo Province (Bopape-Mabapa, 2019).

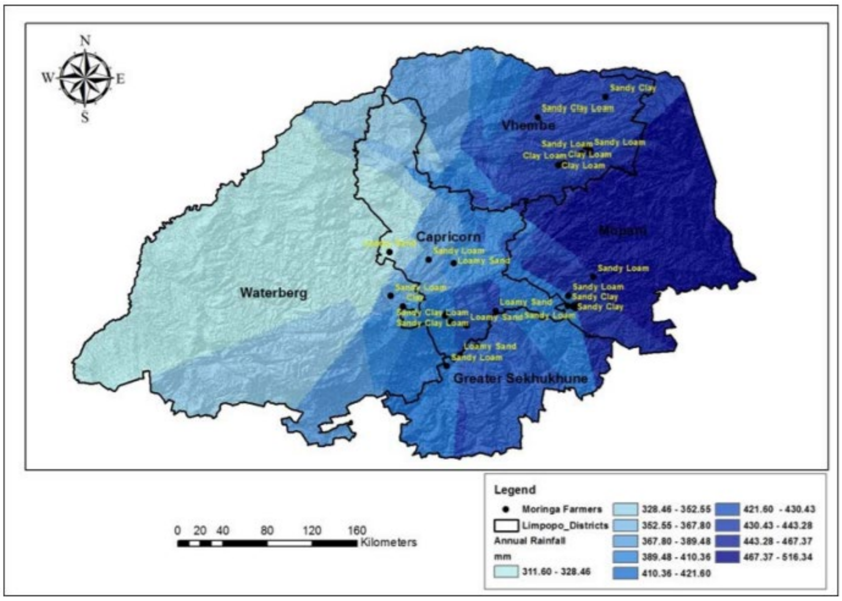

Figure 2.3: Total annual rainfall and soil textural classes from various locations where Moringa is growing in Limpopo Province (Bopape-Mabapa, 2019).

2.3 MORINGA TREE CHARACTERISTICS AND ASSOCIATED WATER RELATIONS

2.3.1 Morphology

The variation in morphological traits of Moringa has been investigated worldwide (Table 2.2), which was attributed to differences in ecological conditions where the species is grown, and crop management practices employed (Gandji et al., 2018). Some of the crop management practices identified as having an influence on morphological characteristics of Moringa include time of leaf harvesting, harvesting frequency, planting density, tree spacing and type of production system (Agoyi et al., 2015).

Table 2.2: Some morphological traits recorded for diverse populations of Moringa oleifera and physical properties of pods and seeds.

Morphological trait	Ferrao and Ferrao (1970)	Popoola et al. (2014)	Ganesan et al. (2014)	Agoyi et al. (2015)
Tree height range (m)	-	-	2.40-5.56	0.04-0.07
Trunk girth range (m)	-	-	0.54-2.19	0.05-0.10
Tree spacing (m)	-	-	1.5 x 5.0	0.2 x 0.3
Production system	-	-	Monoculture	Agro-Forest
Average pod length (cm)		38	57	31
Average pod diameter/width (cm)	-	2.19	8.52	1.89
Average fresh pod weight (g)			110	72.87
Average dry pod weight (g)	7.60	7.95	7.25	-
Average number of seeds/pod	12	12	20	-
Average number of locules/pod		12.9	-	-
Average seed weight (g)	0.299	0.302	-	-
Average weight of kernels/seed	0.212	0.225	-	-
Percentage weight of kernel in relation to entire seed	72.5	74.5	-	-
Percentage weight of hull in relation to entire seed	27.5	25.5	-	-

There are also clear morphological differences across different species of Moringa. For example, Figure 2.4 shows variability in tree and leaf morphology between the two most cultivated species of Moringa (*M. oleifera* and *M. peregrina*). Generally, *M. oleifera* genotypes have higher plant height, stem diameter and tree spread compared to *M. peregrina* genotypes (Hassanein and Abdulah Al-Soqeer, 2018). Another distinct morphological characteristic between the two species lies relates to their leaves, which are generally larger with a tripinnate subdivision pattern in *M. oleifera* as opposed to bipinnate and smaller leaves in *M. peregrina* (Hassanein and Abdulah Al-Soqeer, 2018).

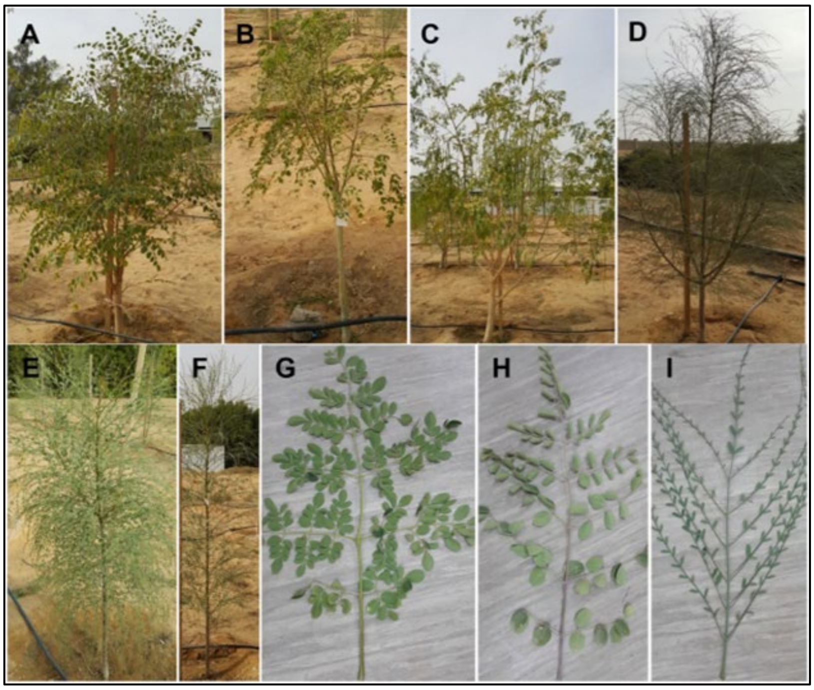

Figure 2.4: Variability in tree and leaf morphology between *M. oleifera* (A, B, C, G, H) and *M. peregrina* genotypes (D, E, F, I) (Hassanein and Abdulah Al-Soqeer, 2018).

Variations in agro-ecological conditions also seem to have an impact on the morphological growth of the tree. For example, Moringa trees grown in warm areas of Limpopo tend to lose their leaves much later in the season, with substantially reduced leaf senescence (Figure 2.5a). Trees grown in Gauteng Province very often lose their leaves completely during the cold, winter period of the year, and a complete die-back of the tree stem occurs (Figure 2.5b). This results in different regrowth patterns of stems and branches later in the season (persistence of one V-shaped main stem in warmer areas compared to the development of multiple stems from the ground-level tuber in colder areas, as shown in Figure 2.5). However, not much is known regarding the extent to which variations in ecological conditions and farmers' management practices influence morphological traits of the plant parts of *M. oleifera*, and this may have an impact on Moringa crop water use variations.

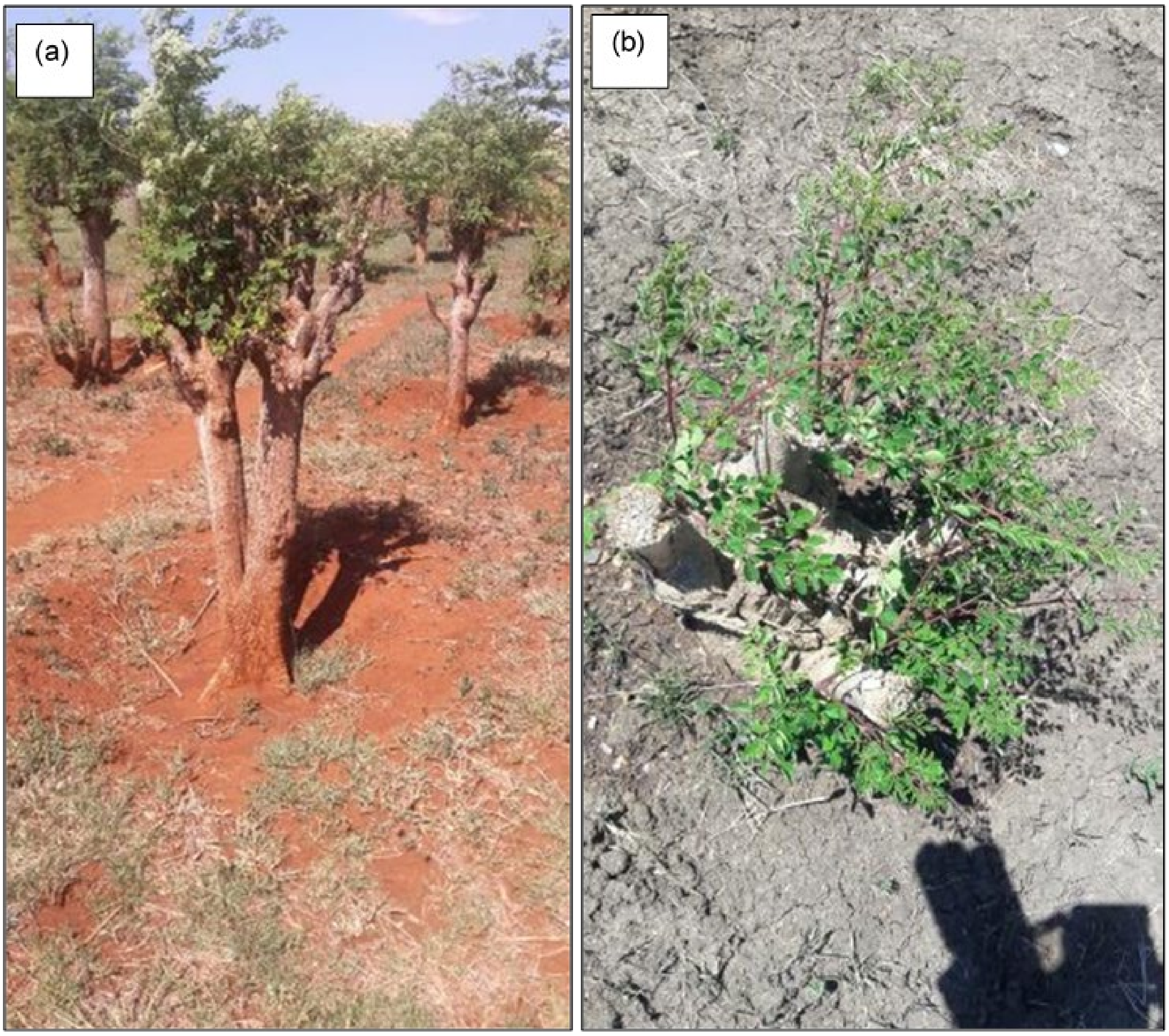

Figure 2.5: Variations in stem growth morphological characteristics in *Moringa oleifera* grown in warmer areas of Limpopo (a) and colder areas of Gauteng (b). The picture was taken at farmers' sites during the spring period, when the trees had just broken their dormancy after the winter period (Photos taken by Dr Nadia Araya on 20 October 2021).

Moringa oleifera trees develop a different rooting habit under different propagation methods. Seedlings develop swollen, tuberous, white taproots with a characteristic pungent odour, and very sparse lateral roots. Trees grown from seeds develop a deep, stout taproot with a wide-spreading system of thick, tuberous lateral roots. Taproots are unlikely to develop on trees propagated from cuttings (Parrotta, 2005).

2.3.2 Anatomy

The anatomical structure of various organs of *Moringa oleifera* has been investigated by Vyas (2019). Table 2.3 summarizes the anatomical characters that are present in various organs of *Moringa oleifera* and their significance.

Table 2.3: Moringa oleifera tree organs' anatomical characters and their significance for environmental stress regulation (Vyas, 2019).

Moringa oleifera tree organs' anatomical characters and their significance		
Stem	Root	Leaf
Character: young stem has 16-18 collateral vascular bundles in a ring. Pith is large and parenchymatous. Pericycle is composed of alternate groups of fibers and parenchyma cells Significance: presence of Parenchyma cells are responsible for metabolic functions, such as photosynthesis, and they help repair and heal wounds Character: old stem has a complete circular band of fibers. Cambium produces small amount of secondary phloem and large amount of secondary xylem (sapwood) Significance: the sapwood serves in water conduction	Character: young root has tetrarch xylem, while old root has a vascular cambium with 6-8 layers that produce many roundish vessel elements embedded in large number of xylem parenchyma cells Starch grains and tannin are observed in xylem parenchyma Significance: this explains the drought tolerance of old root compared to young ones. Starch grains and tannin stimulate high photosynthetic rates	Character: epidermal cells of adaxial surface are larger than cells of abaxial epidermis Significance: this is a mechanism of environmental stress regulation Character: palisade cells are elongated, present in a single row and have dense tanniferous content Character: leaf is hypostomatic with anomocytic Significance: stomata found only on the underside of the leaf, preventing excessive water losses during stress periods Character: fontiguous stomata at right angle to each other are also observed Significance: formation of contiguous stomata occurs when two adjacent meristemoids or meristemoids adjacent to mature stomata enlarge, divide equally into two guard cells and the guard cells joining each other

2.3.3 Physiology

The physiological characters of *Moringa oleifera* were investigated in Indonesia under different growing climatic regions (Wasonowati et al., 2019). Table 2.4 compares leaf stomata density and width, chlorophyll, quercetin and proline content in *Moringa oleifera* leaves grown in Pamekasan (with daily mean temperatures varying between 26.0 and 28.0°C, monthly total precipitation between 11 and 260 mm and a total annual precipitation of 1573 mm) and Sumenep Regencies of the East Java Province, Indonesia (with daily mean temperatures varying between 24.3 and 26.0°C, monthly total precipitation between 11 and 331 mm and a total annual precipitation of 1888 mm). *Moringa oleifera* developed higher physiological responses under cooler and wetter conditions in Sumenep compared to Pamekasan. The ability of *Moringa oleifera* to adapt to environmental stress conditions was evident through increased proline content in leaves. A study conducted on bhendi (*Abelmoschus esculentus* (L.) Moench.) plants showed that the amount of proline accumulated under stressed conditions supplied energy for plant growth and survival and thereby helped the plant to tolerate stress (Sankar et al., 2007). Another evidence of increased adaptation of the Moringa tree to variations in ambient air temperatures was revealed by a study conducted at Hatfield, Pretoria, where Moringa was grown in three temperature-controlled greenhouses (10/20°C, 15/25°C and 20/30°C) (Muhl et al., 2011). Leaves from the 10/20°C greenhouse had an average thickness of 0.239 mm, compared to 0.136 mm at 20/30°C. This is a 43.1% increase in leaf thickness, as a result of a mere 10°C decrease in temperature. Leaves were thicker mostly due to a broader spongy mesophyll layer. Despite larger stomata observed at the 20/30°C greenhouse, the lower stomatal index resulted in a significant 18.9% reduction in leaf conductance compared to the 10/20°C greenhouse. Although higher temperatures generally favoured Moringa tree growth, plants acclimatized to lower temperatures through physiological adaptations (Muhl et al., 2011).

Table 2.4: Leaf physiological traits of Moringa in two different climatic regions of Indonesia (Wasonowati et al., 2019).

Climatic region	Description	Density of stomata (mm^{-2})	The width of opening stomata (μm)	Total Chlorophyll ($mg\ g^{-1}$)	Proline (μmol proline, g^{-1})	Quercetin ($mg\ L^{-1}$)
Pamekasan	Daily mean temperatures varying between 26.0 and 28.0°C, monthly total precipitation between 11 and 260 mm and a total annual precipitation of 1573 mm	247.81 5.72	±2.81 ± 0.15	2.33±0.18	10.07±0,73	15.28±2.95
Sumenep	Daily mean temperatures varying between 24.3 and 26.0°C, monthly total precipitation between 11 and 331 mm and a total annual precipitation of 1888 mm	288.01 14.72	±2.84 ± 0.08	5.32±1.08	5.80±2.06	23.02±8.16

2.4 SUITABLE AGRONOMIC PRACTICES FOR MORINGA CULTIVATION

2.4.1 Climate

Moringa oleifera is widely dispersed globally (Palada, 2021) and can tolerate less fertile soils and harsh environmental conditions such as sweltering heat, recurrent droughts and light frosts (James and Zikankuba, 2017). Moringa is mainly grown in the tropical or subtropical semi-arid areas. The warm and humid semi-arid tropics were specifically noted as the optimal conditions for Moringa growth, which is very resilient to drought and thrives under annual rainfall of 250-3000 mm at altitudes lower than 600 m (Masih et al., 2019), although its development has also been reported at an altitude of up to 1200 m in the tropics or even 2000 m in some parts of the tropical zones (Price, 1985; Amaglo, 2006). The crop prefers direct sunlight and an optimum temperature range of 25-35°C while the cut-off upper and lower temperatures are 48°C (in the shade) (Palada et al., 2019) and -1 to 3°C (Godino et al., 2013), respectively. It must be noted that a study by Muhl et al. (2011) disclosed that relatively higher temperatures favoured the growth and development of the Moringa tree.

Jahn (1988) referred to *Moringa oleifera* as a fast growing, small-medium sized shrub with 5-12 m height, native to sub-Himalayan areas (Northern India), nowadays distributed in diverse ecosystems over Southeast Asia, Africa and South America. The growing habit of the Moringa tree is influenced by climates and can be either deciduous or evergreen to reflect the sub-tropics and the tropics, respectively. The Moringa tree grows naturally or is domesticated in plains, including in live hedges and household backyards, or evolves in the vicinity of the sandy bed rivers and streams under the tropical growing conditions (Olson, 2019). In addition, the nutritional value offered by the leaves of the Moringa tree was found to vary depending on the ecological factors which characterize different sites (Asante et al., 2014). Kumar et al. (2019) revealed that Moringa develops vigorously with an annual rainfall of 250-3000 mm and the soil with a pH in the range of the neutral point.

In the study on the tolerance of *Moringa oleifera* to freeze events, Motis and D'Aiuto (2012) reported that close to 50% survival can be expected with 6-month-old, mulched Moringa trees where brief spells of freezing temperatures occur. It was recommended that to ensure survival through freezing events, Moringa trees should be established early in the growing season to stimulate the woody tissue, while the tree base should be mulched.

2.4.2 Soil

Moringa possesses a long tuberous taproot, which enables it to adapt to different soil types, including those impoverished soils with limited or no fertilization (Mridha, 2015). Moringa trees thrive in well-drained sandy loam soils to offset their susceptibility to waterlogging, yet, they are able to grow in clayey soils (Price, 1985). *Moringa oleifera* can tolerate both acidic and basic soil types, with pH levels varying from 5.0 to 9.0 (Palada and Chang, 2003). Moringa can also tolerate salinity (up to 3 dS/m during germination and 8 dS/m once well established) (Nouman et al., 2014). Moringa growth is even not compromised by unfavourable poor marginal conditions of desert soils (Singh et al., 2012). However, Moringa trees provided with organic or inorganic fertilizers preserve adequate productivity. Likewise, Moringa can achieve its leaf and pod yield potential of acceptable quality if offered optimum agronomic and horticultural practices such as mulching and fertilization (Morton, 1991; Dania et al., 2014). In addition, lessened Moringa growth was reported to have resulted from the inadequacy or absence of fertilizers (Mahn et al., 2005). Nevertheless, the reports from the Madisha-Ditoro and Moletlane villages (Limpopo Province, South Africa, Mashela, 2017) revealed that the aboveground biomass of the Moringa seedlings grown on clay and sandy soils was practically the same and greater than that of calcareous and loam soils. With regard to the underground biomass, the clayey soils gave higher values than the sandy soils, while the biomass of the alkaline calcareous soil was the lowest. The results of leaf nutritional composition revealed no significant differences between the soil textural classes. Moreover, there was no significant correlation between soil and leaf nutritional compositions. The study concluded that Moringa can be produced in many locations and diverse soils of the Limpopo Province without negatively affecting leaf nutritional composition (Mabapa, 2019).

2.4.3 Pruning frequency and cut-back depth

Moringa as a multipurpose tree can be grown for diversified products such as biomass, seed, and oil. One approach for increased production is to focus on the purpose of producing the tree. Therefore, there is a need to have background information on the production of Moringa for a specific purpose under particular environmental conditions. Moringa yield production can be affected by various factors such as environment and climate (Ayerza, 2012).

The Moringa shrub grows fast and can provide substantial development and yield in just three months, even though the height of a fully grown tree fluctuates from 5-10 m (Liu et al., 2018). It must be noted that in terms of pod yields, flowering and pod setting are continuous in wet tropical areas (full-year rainfall), whereas dry tropical areas produce two pod harvests annually. Outside the tropics, for example in the Iberian Peninsula, only one summery pod harvest takes place (MO, 2016), although 3 to 5 cuttings for leaf yield can be carried out per season.

There have been numerous investigations on pruning intensities and frequencies with different outcomes (Mabapa et al., 2017; Truong et al., 2017; Abdullahi et al., 2021; Santos at al. (2021). It is known that pruning is crucial to Moringa production through the promotion of branching and increased reachable yields. In terms of pod production, Moringa trees can be pruned 3-5 months after transplanting by cutting back the uppermost 10 cm of the growing shoots. With regard to leaf production, the manipulation of the canopy depends on the age of Moringa trees.

Cutting back branches by 30 cm when it reaches 60 cm and tipping young Moringa trees, grown for leaf production, induce lateral branching to produce a multi-branched shrub, while old trees that are unproductive or too high for easy harvesting, can be cut back to 0.5-1 m above the ground level once per year (Mabapa et al., 2017).

2.4.4 Irrigation

The Moringa tree, particularly when propagated from seed, has a long taproot, which makes it more drought tolerant (Dalal et al., 2020; Dos Santos et al., 2017). It exhibits a certain degree of xerophytic behaviour (El-Boraie et al., 2020) making it able to survive in harsh climatic conditions, including barren soils (El-Sayed and Mahmoud, 2018). It can also adapt to conditions in most climatic zones of the world (El-Boraie et al., 2021; Fuglie and Sreeja, 2014). This offers potential for its cultivation under both irrigated and rainfed conditions.

Water is critical to crop growth and development particularly in the tropics due to increased atmospheric evaporative demand. Water requirements for Moringa depends on stage of growth and prevailing weather conditions. The crop is yet to be fully exploited on a commercial level in South Africa; hence, not much research work is known about its water requirements/consumption and the suitable irrigation practices. Most of the research conducted to date has been on tree morphology, chemistry, growing conditions, production, processing and utilisation (Mashamaite et al., 2021). Knowledge on crop water requirements and irrigation application frequency is crucial for managing the available water effectively.

Being drought tolerant, the tree crop does not require much watering for survival; however, adequate water amount is certainly important for optimal productivity. Moringa is raised from seeds, seedlings or cuttings. Seeds are used to raise the annual Moringa types, which require less frequent irrigation compared to the perennial types raised from cuttings. The annual Moringa types have highly succulent and fast spreading roots while the perennial types have hardy roots. The latter can be irrigated at 7 to 10-day intervals, while the former can be irrigated at 10-15 day intervals, depending on the soil t. However, there is need for more frequent watering in the early stages of Moringa growth, especially the first two months of establishment (Fuglie and Sreeja, 2014). Moringa trees will flower and produce pods whenever sufficient water is available (Fuglie and Sreeja, 2014).

Although Moringa exhibit xerophytic traits that make it drought tolerant, prolonged drought-stress reduces the plant water content with subsequent diminishing of leaf water potential and turgor loss, closure of stomata and inhibited photosynthesis. All these lead to dehydration, impaired metabolism processes, decreased and inhibited cell expansion, enlargement, growth and development of the plants, especially during the early stages of growth (Galgaye et al., 2020). The minimum annual rainfall requirement for Moringa was estimated at 250 mm with maximum at over 3 000 mm, but its roots are not tolerant to waterlogged soils because they have a tendency to rot (Fuglie and Sreeja, 2014). Mashamaite et al. (2021) also reported on the minimum annual rainfall requirement of 250 mm, but was conservative on the maximum annual rainfall requirement put at 1500 mm. Other annual precipitation requirements were estimated at 760-2500 mm (Leone et al., 2015). Dos Santos et al. (2017) estimated water requirements and crop coefficients for Moringa in different phenological stages over three months, and reported a cumulative evapotranspiration rate of 139.8 mm.

Despite a considerable number of irrigation driven studies done on Moringa, there are no studies aiming at assessing the optimal irrigation water requirement of this crop. El-Sayed and Mahmoud (2018) examined the effect of irrigation methods at different soil moisture depletion levels with various fertilizer sources on Moringa water consumptive use, water use efficiency, growth traits, yield and yield quality. Water consumption averaged 4259 m^3/ha, but the study does not report on the period of observation (El-Sayed and Mahmoud, 2018). In a different study of a similar nature, Muhl et al. (2013) reported that fruit setting was best in Moringa plants cultivated with 900 mm per year irrigation water. However, flower bud initiation was higher at lower watering regimes. Mashamaite et al. (2021) reported similar results for a trial performed in Gauteng Province, South Africa. In their study, Leone et al. (2015) reported a Moringa irrigation water requirement of less than 800 mm per year.

Similar to irrigation water requirement, not much is documented about the best irrigation water management practices to achieve optimal Moringa production. Irrigation water management is a tool or approach that ensures timely application of water for improved water use efficiencies and high yields. Daba and Tadese (2018) estimated the optimum water application frequency of Moringa seedlings and reported a general decrease of growth performance with decreasing frequency of water application and higher water application rates. Their study indicated the best growth performance with highest water application frequency of twice daily at the lowest water application rate of 1.5 litres per plot. In a different study, Dalal et al. (2020) compared the impact of different watering regimes on growth parameters that included plant height and days to first flowering. The study showed that treatments receiving 100% irrigation of the irrigation water requirement had the highest plant height. However, the number of days to first flush of flowers decreased with increasing moisture stress (Dalal et al., 2020). The results of a study by El-Boraie et al. (2021) agreed with observations made by Dalal et al. (2020). The positive influence of water restriction treatments decreased in the order of 100 > 80 > 60% of irrigation water requirement. However, the differences between 100 and 80% of water requirement application were not significant, which culminated into a recommendation to approve application of 80% of the required irrigation water in order save about 20% (El-Boraie et al., 2021). The results of a study by Abaker (2010) concurred with the above. The number of leaves and length of roots decreased with increasing irrigation interval reaching the lowest number in the seedlings irrigated every 8 days (Abaker, 2010). Nevertheless, Sale et al. (2015) reported that watering regimes had significant influence on stem diameter only. Overall, frequent application of low application rates appears to result in more favourable growth performance. However, frequent irrigation requires very careful planning and management to ensure that operations have sufficient water to maintain adequate supplies for plant production.

A suitable irrigation method needs to apply water to crops at a rate that satisfies demand. Both water quantity and quality are extremely important for successful crop production. In the case of Moringa, methods for irrigating this tree crop need to ensure that both the leaves and trunk are not kept wet for prolonged periods of time, which makes flooding and drip systems the most popular irrigation methods for the tree crop (Dalal et al., 2020; El-Boraie et al., 2020; 2021; El-Sayed and Mahmoud, 2018). However, some studies, e.g. El-Boraie et al. (2020), have used mini-sprinklers to irrigate Moringa under experimental conditions. If flood irrigation system in basins, beds, border or furrows is used, care need to be taken to avoid direct water contact with the trunk surface or base by creating earth mounts of radius 0.30-0.45 m around each tree. If drip irrigation is used, then the laterals and emitters are placed 0.30-0.45 m away from the main trunk or base of the tree. Direct water contact weakens the base of the tree against winds. Prolonged wet conditions on leaves promote incidences of diseases. Experimental results have shown the most positive influence was obtained from buried drip irrigation system (El-Boraie et al., 2021). In general, drip irrigation system demonstrated the capacity to improve crop productivity, reduce energy costs, improve irrigation efficiency and reduce water loss by deep percolation (El-Sayed and Mahmoud, 2018). These are the desired characteristics of an irrigation system because irrigation generally consume large volumes of water. Many countries across the world, particularly in the arid and semi-arid climatic zones, are grappling with water scarcity at a time when demand and competition for water is also stiffening.

2.4.5 Spacing and planting density

Moringa can be planted through direct seeding, cuttings or transplanting of seedlings. Cuttings can also either be planted directly or introduced in sacks in the nursery. The length of the mature cuttings should be 0.45-0.5 m and the breadth (width) 10 cm. For the purpose of intensive production, the planting spacing of the Moringa tree should be 3 x 3 m (between rows x within row) (Palada et al., 2019). It is also recommended to follow an east-west direction when planting the Moringa trees for adequate sunlight and airflow. In mixed cropping systems, Moringa is grown as an intercrop with high nutritional value crops such as vegetables and herbs (Palada et al., 2019). For the instance of alley-cropping, the between-row distance should be extended to 10 m. The planting spacing and density usually vary depending on the purpose of the living trees: food, fodder, live fence, live pole, etc. The areas unoccupied by the trees should constantly be weeded regardless of the spacing.

In general, as a function of different factors such as soils and climatic conditions, higher planting densities or narrower plant spacing (0.75-1.0 m (within-row) x 1.0-2.0 m (between-row)) are adopted to increase leaf production, whilst the opposite option is favourable for pod production (Radovich et al., 2009, Attia et al., 2014). For fodder production, extremely higher planting densities, with excessively smaller plant spacing, are used (0.15-0.2 m within-row x 0.2-0.5 m between-row) (Mabapa et al., 2017).

High density planting of Moringa for leaf biomass production has been studied by Foidl (2019). There are also other studies indicating that leaf biomass production can be maximized in limited area by increasing plant density (Patricio and Palada, 2017; Palada, 2017). A study conducted at Central Philippine University indicated that the highest fresh biomass of 30 t ha^{-1} was obtained from plant density of 40,000 plants ha^{-1} harvested at 8-week intervals. The lowest fresh leaf biomass was obtained at 10,000 plants ha^{-1}. Data on fresh leaf biomass from plants harvested at 4- and 6-week intervals at high density (40,000 plants ha^{-1}) suggest that these treatments are optimum when there is a monthly demand for fresh raw materials for leaf processing into Moringa by-products (Patricio and Palada, 2017). Amaglo et al. (2007) studied the effect of plant spacing and harvest frequency on Moringa fodder production and found that a wide spacing (5 × 15 cm) produced more leaf yield per plant than medium (5 × 10 cm) and close (5 × 5 cm) spacing. However, the total leaf yield per ha was higher in the closest spacing compared with medium and wide spacing (Patricio et al., 2017).

2.5 FIELD MANAGEMENT PRACTICES TO IMPROVE WATER USE EFFICIENCY AND NUTRITIONAL WATER PRODUCTIVITY

2.5.1 Deficit irrigation

Deficit irrigation (DI) strategy can be defined as irrigating with limited water to obtain maximum water use efficiency (WUE), nutritional water productivity (NWP) and acceptable yields instead of obtaining maximum yields (Tian et al., 2017). Therefore, this strategy is based on preventing excessive water stress in crop growing stages where the crop is highly sensitive to drought, thus, effectively monitoring the plant water status along the crop growing cycle becomes crucial (Poblet-Echeverria et al., 2014; Fernandez, 2014) (Figure 2.6).

Figure 2.6: Capacitative 10-Hs soil water sensors connected to an EM-50 datalogger to automatically monitor Moringa soil water content under different deficit irrigation regimes (Photo taken by Mr Ntsieni Mulovhedzi).

The strategy of deficit irrigation is regarded as a highly effective method for improving NWP and WUE (Garcia-Tajero et al., 2017; El-Sayed and Mahmoud, 2018), through subjecting plants to drought by decreasing the volume of water used or by decreasing the number of irrigations either throughout a specific growth stage or during the whole season (Fereres and Sariono, 2007; AbdEl-mageed et al., 2017). Again, it has been reported that a properly chosen DI strategy saves water and improves WUE without highly affecting yield (Geerts and Raes, 2009; Fernandez et al., 2013; Gomez-del-Champo, 2013; Ballester et al., 2014; Padilla-Diaz et al., 2016), and it normally has a positive impact on crop quality which in turn improves NWP (Fereres and Sariano, 2007; Geerts and Raes, 2009; Ruiz-sanchez et al., 2010; Mulovhedzi, 2017). Moreover, it is believed to increase the net income of farmers (Stroosnijder et al., 1987) because of the reduced cost of water and increased irrigation efficiency (Zigada-Lizarazu and Berliner, 2010). Therefore, in order to alleviate food insecurity, malnutrition, and to conserve scarce water resources in South Africa, there is a need to precisely quantify the effect of DI on nutritional content, NWP and WUE of Moringa tree crop, as this crop is gaining popularity amongst processing industries, and it is envisaged that the area under Moringa production will increase in the near future.

2.5.2 Rainwater harvesting and conservation

Small-scale farming communities in sub-Saharan Africa have fallen prey to the effects of global climate change and endure food insecurity, poverty and desolation. Rainwater harvesting (RWH) has the potential to alleviate the adverse impacts of climate change among smallholder farmers by capturing the additional water to support rainfed agriculture. In addition, RWH systems have been characterized as beneficial tools to mitigate the rampant severe water shortage of dryland crop production, especially during the critical crop growing stages (Oweis and Hachum, 2006). However, to render RWH systems more efficient and attractive to users, appropriate design and implementation are highly recommended. Only practically useful RWH systems can inspire reliability, technical and economic feasibility and water saving efficiency (Odhiambo et al., 2021). According to Hatibu and Mahoo (1999), RWH systems for rainfed agriculture can be classified into three main groups, based on the distance between the catchment (runoff) area and the cropped (runoff collection) area: In-situ RWH, internal (micro-catchment, MC) RWH and external (macro-catchment) RWH. RWH techniques have widely been used to resolve water scarcity for diverse aspects of ecosystems, including crop irrigation requirements, and to meet the water resource needs of a growing world population. However, there is a need to pursue a holistic assessment of the costs, benefits and impacts of alternative crop types and irrigation practices (Ghimire and Johnston, 2019).

South Africa is mostly characterized by dryland crop production predominated by small-holding farming and perennial water stress (Nhlabatsi, 2010). This is due to the fact that the country features among those with limited water resources and receives 500 mm (60 percent of the world average) average annual rainfall (DWA, 1994). Therefore, to ensure sustainable water supply in marginal areas and upgrade the productivity of small-scale rainfed agriculture, South Africa has to resort to innovative water sources such as the in-field RWH technique (Worku, 2006). Through this technique, the use of rainwater is streamlined by lessening the unproductive water losses (soil evaporation and runoff from the soil surface) while the rainwater productivity becomes optimal by increasing the productive water loss (crop transpiration) (Nhlabatsi, 2010). Likewise, new tillage technologies were also proposed to revolutionize crop production in the marginal rainfall areas of Zimbabwe through the conservation of fragile soils and the prolongation of the retained available water to crops (Wang et al., 2005; Rockstrom et al., 2009; Masaka et al., 2021). Furthermore, Mak-Mensah et al. (2021) found that rainwater use efficiency was upgraded by the implementation of tied-ridge-furrow RWH coupled with biochar for soil amendment and an enhanced agricultural productivity.

Amongst other platforms to combat the noxious effects of climate change and variability is to make use of tree crop species known to be more stress-tolerant than conventional seasonal crops, and can even stand hostile growing conditions. In addition, although the usually cultivated species can provide the required energy, they cannot satisfy the needs for dietary nutrients (Wang et al., 2011). Therefore, it is vital to diversify and prioritize the production of less investigated, locally adapted plant species that are utilized in rural communities for consumption either fresh or processed (Foyer et al., 2016; Mashamaite, 2021). Moringa is one species that could be considered under variable climatic conditions for positive outcomes through climate change adaptation and mitigation as well as life sustenance against food insecurity threats. Moringa production in South Africa is exclusively for leaf processing and consumption (Mabapa, 2019). Associating Moringa production with RWH and conservation can support sustainable food and nutrition availability while protecting the soil fertility and the environment at large. As a nutrient-dense crop, Moringa is usually cultivated in dryland farming, including in South Africa. Its manifold benefits can be enhanced if the production conditions are improved: water conservation and supply, soil conservation and amendment, etc. Moringa farmers around Limpopo and Gauteng Provinces have been implementing practices of RWH, particularly the in-situ technique (Figure 2.7a) or simply soil water conservation through the use of mulching (Figure 2.7b).

Figure 2.7: Commercial Moringa oleifera plantations established at farmers' sites: (a) in the Limpopo Province using in-situ rainwater harvesting on 11-year-old trees and (b) in the Gauteng Province using mulching as a soil water conservation technique on 8-year-old trees (Photos taken by Mr Ntsieni Mulovhedzi and Dr Nadia Araya).

2.6 CROP WATER USE MEASUREMENT METHODS

Due to increased competition for limited water resources in South Africa, there is a need for continuous improvement on crop water use measurements and modelling of crop water use to improve irrigation practices in the agricultural sector. This is crucial especially in countries like South Africa, where the arid and semi-arid climatic conditions, with erratic rainfall dominate the country. This is aggravated by the effect of climate change, which may lead to exacerbated water shortages in the near future.

Therefore, without doubt, agricultural practices consume large volumes of water. Thus, efforts with respect to rational and efficient use of this natural scarce resource have been made through robust technologies that allow accurate measurements of crop evapotranspiration (ET), which contributes to a good estimate of crop water requirements and adequate irrigation management (Lacerda and Turco, 2015). As Pocas et al. (2020) stated, efficient irrigation management depends on the availability of accurate information about crop water requirements. There are a number of approaches available for field quantification of ET, each with a different principle of operation, advantages and disadvantages, including differences of acquisition cost, expertise to interpret the raw data and degree of complexity (Jarmain et al., 2009; Allen et al., 2011; Euser et al., 2013). Consequently, numerous researchers have reported several approaches for quantifying ET in both field and orchards, where ET data can be quantified from crop and soil information as well as from meteorological, for instance, surface renewal, chambers, sap flow, lysimeters, Bowen ratio, soil water balance, residual energy balance and eddy covariance system (Doorenbos and Pruitt, 1977; Jensen et al., 1990; Dugas et al., 1991; Malek and Bingham, 1993; Allen et al., 1998; Rana and Katerji, 2000; Wilson et al., 2001; Burt et al., 2005; Jarmain et al., 2009; Mengistu and Savage, 2010; Teixeira and Bastiaanssen, 2011; Mauder et al., 2013 Kool et al., 2014; dos Santos et al., 2017; Anapalli et al., 2020). Thus, in order to use the available water resources efficiently, it is compulsory to carry out measurements of evapotranspiration for different crops. This must be done at a high temporal and spatial resolution, while accounting for variability in weather conditions, physiological and morphological characteristics of the crop and soil types (Santos et al., 2020). The available crop water use measurement methods can be grouped into hydrological, meteorological and plant physiological approaches as detailed in the next section (Dugas and Bland, 1989; Baldocchi et al., 2003; Savage et al., 2004; Payero and Imark, 2008; Unlu et al., 2010; Alfieri et al., 2012; Kool et al., 2014).

2.6.1 Hydrological approaches

2.6.1.1 Lysimeters

Lysimeters are considered the most dependable and precise tool for determining plant water use, developing crop coefficient functions for specific crops and they frequently serve as validation for other approaches, as they have been used for decades by numerous researchers (Howell et al., 1991; Fisher, 2012; Kool et al., 2014). Moreover, lysimetry is a direct approach of measuring ET (Alfieri et al., 2012; Fisher, 2012), which is generally appreciated for its simplicity (Lascano et al., 1987). Furthermore, Drexler et al. (2004) stated that the lysimetry method might be the only approach available that allows for the direct measurement of the total water loss from a vegetated surface. In this approach, the ET of the crop is generally quantified by recording the mass loss difference using a weighing scale, which can subsequently be converted to crop water per unit of time in L day^{-1} or the depth of water used over a defined area (Beeson et al., 2017). Lysimeters of many different designs, shapes, sizes and measurement system have been built over the years, such as the one shown in Figure 2.8.

Figure 2.8: Lysimeter measuring evapotranspiration for a young peach tree (Photo taken from Zambrano-Vaca C).

Therefore, early weighing lysimeters often contain mechanical mechanisms and electrical circuitry to obtain relatively high-resolution measurements and required regular maintenance (fisher, 2012). While micro-lysimeters normally consist of a small cylinder, typically 0.1-0.3 m in diameter and depth, which is pushed into the soil surface to retrieve and undisturbed soil sample. The micro-lysimeter is then carefully excavated, sealed at the bottom and weighed, it is then placed back in the soil, sometimes inside a collar, level with the soil surface. Then, after a period micro-lysimeter is reweighed, the change in mass being directly proportional to evaporation from the soil (Alfieri et al., 2012). Numerous researchers have used this approach to estimate ET and soil evaporation (E), in order to develop crop coefficients (Kc) for various crops, such as turfgrass (Devitt et al., 1992), strawberry (Clark et al., 1996), broccoli and lettuce (Bryla et al., 2010), watermelon (Shukla et al., 2012). However, this approach has high operational costs and is labour intensive (fisher, 2012), time consuming (Trambonze et al., 1998), unable to provide accurate measurements during irrigation or rainfall (Thompson et al., 1997; Flumignan et al., 2011) and limited representation of field condition due to small sampling area (Daamen et al., 1993; Alfieri et al., 2012). Although with all these limitations, various researchers have successfully used this approach for measuring E from the soil surface of irrigated crops (Plauborg, 1995; Ibraimo, 2018; dos Santos et al., 2017).

2.6.1.2 Soil water balance

The soil water balance (SWB) approach determines the ET component as the residual of the budget of a defined system of interest (Annandale et al., 1999; 2007; Kool et al., 2014). Therefore, the water balance for an area under study, relates water inputs (supply), outputs and changes in soil water storage (Perry, 1996) (Figure 2.9).

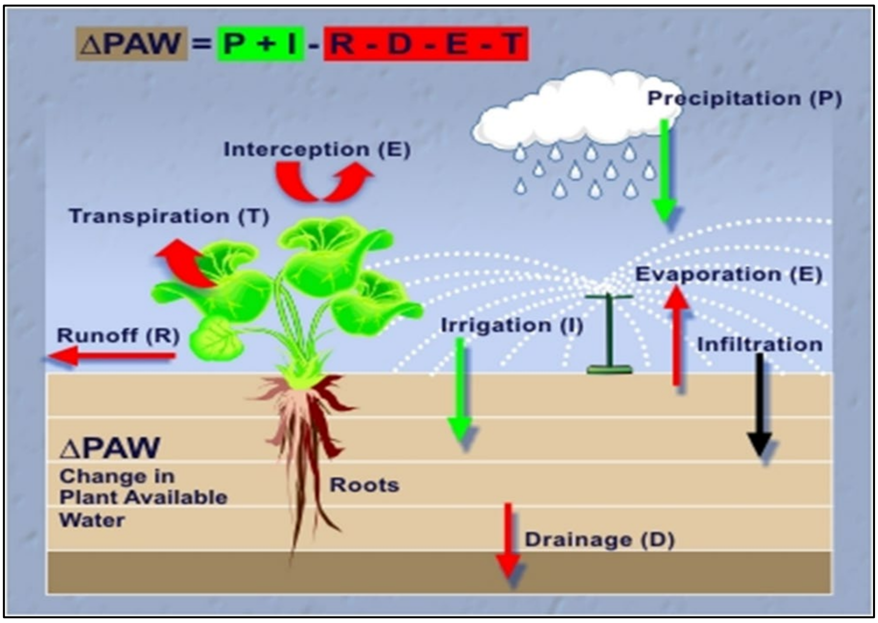

Figure 2.9: Schematic diagram of soil water balance components (Gassman et al., 2010).

Moreover, components included in the budget equation depend on the size and time scale of the system of interest (Kool et al., 2014). Since ET is a component of the SWB, it can be calculated from the water balance of an appropriate control volume of soil indirectly (Ranna and Katerji, 2000; Event et al., 2012), using the following equation:

$$ET = P+I+U-R-D-\Delta S \quad (2.1)$$

where ET is evapotranspiration (mm), P is precipitation (mm), I is irrigation (mm), U is upward capillary rises into the root zone (mm), R is runoff (mm), D is deep percolation beyond the root zone (mm) and ∆S is change in root zone soil water storage (mm).

Changes in plant storage, lateral flow and capillary rise are routinely neglected. The water balance is only practical as an approach to estimate water use when evapotranspiration is relatively large, otherwise small errors in measurements of other components can results in large errors in estimated ET (Hillel et al., 1998). Recently numerous researchers successfully use the SWB equation to estimate ET of different crops, including alfalfa (Kuslu et al., 2010), sweet potato (Masango, 2014; Mulovhedzi, 2017), and wheat (Imukova et al., 2016).

2.6.2 Micrometeorological approaches

2.6.2.1 Eddy covariance

A good knowledge of turbulent fluxes of sensible heat (H) and latent heat (λE) is of crucial importance for crop water management purposes, particularly in arid and semi-arid areas which are characterized by hot air Tz and scanty rainfall. Therefore, as reported by numerous authors, for quantification of ET exchanges from cropping systems, the eddy covariance (EC) approach is the most accurate, advanced, robust, non-invasive, direct and sound micro meteorological theory-based measurement method (Baldocchi and Mayers, 1991; Wofsy et al., 1993; Wilson et al., 2001; Parent and Anctil, 2012; Shurpali et al., 2013; Tallec et al., 2013; Anapalli et al., 2018). Furthermore, the EC approach is an independent system for quantification of turbulent fluxes H and λE (Brotzge and Crawford, 2003) (Figure 2.10).

Figure 2.10: Eddy covariance system measuring sweet potato evapotranspiration at the Agricultural Research Council – Vegetable, Industrial and Medicinal Plants research station (Photo taken by Mr Ntsieni Mulovhedzi).

The EC method provides a direct measure of the vertical turbulent flux of a scalar entity of interest F_S across the mean horizontal stream lines (Swinbank, 1951) providing fast response sensors (≈10 Hz) for the wind vector and scalar entity of interest are available (Meyers and

Baldocchi, 2005). For a sufficiently long averaging period over horizontally homogeneous surface, the flux is expressed as:

$$F_s = \rho_a \overline{w's'} \tag{2.2}$$

where ρ_a is the density of air, w is the vertical wind speed and s is the concentration of the scalar of interest. The primes in Equation (x) indicate fluctuation from a temporal average (i.e. $w' = w - \overline{w}$; $s' = s - \overline{s}$) and the over bar represents a time average. The vertical wind component is responsible for the flux across a plane above a horizontal surface. Based on Equation (3), the sensible heat flux H can be expressed as:

$$H = \rho_a c_p \overline{w'T_s{}'} \tag{2.3}$$

where c_p is the specific heat capacity of air, w' denotes the fluctuation from the mean of the vertical wind speed, and T_s' is the fluctuation of air temperature from the mean. The averaging period of the instantaneous fluctuations, of w ' and s ' should be long enough (30 to 60 minutes) to capture all of the eddy motions that contribute to the flux (Meyers and Baldocchi, 2005).

The EC technique, when properly applied, can be used routinely for direct measurements of surface layer fluxes of momentum, heat, water vapour, and carbon dioxide between a surface and turbulent atmosphere (Savage et al., 1997; Massman, 2000; Massman and Lee, 2002; Finnigan et al., 2003). Like other micrometeorological methods, an adequate fetch is required for the EC method; a fetch to height ratio greater than 100 is usually considered adequate (Wieringa, 1993).

The EC measurements of w' should ideally be at a height that allows small-sized eddies between the anemometer transducer to be sensed (Savage et al., 1995). If the sensor height is too close to the canopy small-sized eddies may not be sensed, resulting in a possible underestimation of the flux. Savage et al. (1995) suggested that measurements, under unstable conditions above short turf grass surface, at a height of 1 m above the plant canopy should be sufficient without need of corrections for spectral attenuation of the eddy structures from spatial averaging.

The EC method requires sensitive, expensive instruments to measure high frequency wind velocities and scalar quantities. Besides, eddy covariance data need rigorous quality control and filtering, such as anemometer tilt correction (coordinate rotation, planar fit), spike detection, and trend removal (Meyers and Baldocchi, 2005). Sensors must measure vertical wind speed, sonic temperature and atmospheric humidity with sufficient frequency response to record the most rapid fluctuations important to the diffusion process (Drexler et al., 2004).

Crop water use using the EC method can be expressed as the total evaporation (soil evaporation + transpiration + interception) in mm or m^3 for the growing period (Mengistu et al., 2016). The EC technique estimates total evaporation (crop water use) directly using vertical fluxes of wind speed and water vapour (Equation x) and/or indirectly as the residual of the shortened energy balance equation using the sensible heat flux, H (Equation y). Neglecting advection and the stored canopy heat, the shortened energy balance equation is used to estimate the latent energy flux λE (W m^{-2}), which is the energy equivalent of total evaporation as:

$$\lambda E = Rn - G - H \quad (2.4)$$

where: Rn is the net irradiance (W m^{-2}), G the soil heat flux (W m^{-2}), and H the sensible heat flux (W m^{-2}).

Over the last years, the EC approach has become a standard tool to study the exchange of energy, carbon dioxide (CO_2) and water vapour (H_2O) between the earth's surface and atmosphere by interpreting covariance measurements of vertical wind velocity (w) (Verman et al., 1990; Lenschow, 1995; Massmam, 2000; Baldocchi et al., 2003). Moreover, Drexler et al. (2004) in their review mentioned that there are very few evapotranspiration quantification approaches that work well for an hourly time-step, and in some cases, they do not even work well for a daily time-step. However, with exception of the EC approach from which direct measurements of the vertical turbulent flux are obtained, depending on a theoretical framework and unquestionable assumptions (Swinebank, 1951; Savage et al., 2004; Meyers and Baldocchi, 2005; Jarmain et al., 2009; Savage et al., 2010).

Theoretically, this approach is based on the observation that fluxes of λE and H in the atmosphere, which are driven by the covariance between vertical wind speed and the wind vector or turbulence (Garratt, 1992). In other words, this means that the transport of scalar between the atmosphere and canopies is mostly governed by air turbulence. Arya (2001) reported that in turbulent flow, wind velocity components and a scalar quantity transported by this wind vary irregularly in space and time. Therefore, these scalars closely follow the turbulent motion if they are sufficiently small (Swinbank, 1951). This approach directly measures fluxes of H and λE using high frequency measurements of CO_2 and H_2O concentration, scalar properties such as air temperature (Tz), and w, over the scales of hundreds to thousands of metres of distance (Drexler et al., 2004).

In the EC approach, the net ecosystem exchange of H_2O and CO_2 is quantified by tracking and measuring the turbulent transport of eddies carrying CO_2 and H_2O in the plant canopy boundary layer of the atmosphere (Anapalli et al., 2020). Moreover, Van kesteren et al. (2013) and Hipps et al. (1998) reported that the EC approach drives turbulent fluxes using high frequency point sampling measurements. With three-dimensional wind speed (u, v, w) as well as the air Tz which is normally measured by a sonic anemometer, and H_2O and CO_2 concentration commonly with open-path gas analyzer (Schotanus et al., 1983; Baldocchi and Mayers, 1991; Jarmain et al., 2009; Van kesteren et al., 2013).

According to Odhiambo and Savage (2009), when using this approach there are no assumptions made about the land surface properties, such as aerodynamic roughness, zero plane displacement or measurement height and no corrections for atmospheric stability are required. In addition, the EC system is simple to carry around and can be set up in various landscapes with relative ease and is less labour intensive compared to other approaches such as the soil water balance and lysimetry (Evett et al., 2012). The EC approach involves measurements that are usually at a frequency of 10-20 Hz of two atmospheric variables, w and water pressure from which λE is computed directly following many corrections (Brutsaert, 1982; Drexler et al., 2004; Jarmain et al., 2009; Savage et al., 2010).

Thus, for accurate EC measurements, there is a need to have enough fetch, which can simply be defined as the distance across a uniformly rough surface or as the relative influence of upwind surface source to H and λE, measured at a height above the uniformly rough canopy surface from the location of instrumentation until where there is a discontinuous change in surface roughness (Savage et al., 1997; Savage, 2010). The fetch to height ratio of 100:1 is generally considered enough; however, a greater fetch is advantageous (Wieringa, 1993; Kaimal and Finnigan, 1994; Jarmain et al., 2009).

Just like any other approach, the main disadvantage of EC system is that is stringent and requires many post processing corrections, favourable wind directions, carefully sensors positioning and alignment (Drexler et al., 2004; Mengistu and Savage, 2010). Furthermore, Baldocchi and Mayers (1991) and Foken (2006) reported that this approach needs a homogeneous surface without disturbance between the surface and the instrument height. Furthermore, the EC approach is costly and requires high maintenance, the closure is forced, and the eddy diffusivities of heat and moisture must be assumed equal (Brotzge and Crawford, 2003). In addition, Li et al. (2008) reported that under conditions of scanty mechanical and thermal turbulence the EC approach tends to underrate fluxes. Consequently, the energy balance deficit is on average found to be between 20 and 25% (Wilson et al., 2001; Hendricks Franssen et al., 2010; Gebler et al., 2015), which means that the λE flux of actual ET estimated from EC measurements shows potentially a strong underestimation, thus, failing to close the surface energy balance. This is usually the main disadvantage of the EC approach (Aubinet et al., 2000; Wilson et al., 2002; Texeira and Bastiaanssen, 2009; Leuning et al., 2012; Gebler et al., 2015).

Without doubt, H and λE are vital components of the shorten energy balance equation (Savage et al., 2010), therefore, EC approach in combination with radiation and soil heat flux measurements, it provides precise data to better understand the processes regulating ecosystem-atmosphere exchange, the surface energy balance measurements also helps to check the reliability of this approach (Wofsy et al., 1993; Schmid, 1994; Aubinet et al., 2000; Baldocchi et al., 2001; law et al., 2002; Baldocchi, 2003; Barr et al., 2006; Baldocchi, 2008; Lu et al., 2018).

Thus far, studies conducted in different areas have found an average EC energy balance closure ranging between 0.75 and 0.87 (Wilson et al., 2002; Li et al., 2005). Even though with all above mentioned disadvantages, the EC approach has proven to be the most accurate and numerous studies have been successfully conducted in South Africa and around the world to estimate seasonal water use of both orchards and field crops, for instance sparse irrigated olive tree (Ezzahar et al., 2007), mixed grass land communities (Savage et al., 2010), sugar cane (Pakoktom et al., 2013), pecan tree (Ibraimo, 2018), cotton (Anapalli et al., 2020) and sweet potato (Mulovhedzi et al., 2020).

Therefore, quantifying ET of Moringa using EC system will contribute important knowledge on the exact amount of water that this crop requires in a growing season, in order to satisfy the atmospheric evaporative demand of a given location and provide data that can be used to extrapolate ET measurements to other climatic conditions, thereby improving yield and use of water in a sustainable manner.

In the EC approach, it is crucial to verify the energy balance closure. According to numerous researchers, energy balance closure is the ratio of the sum of turbulent fluxes to available heating (Gu et al., 1999; Wilson et al., 2002). During the last four decades it has become clear that the energy balance at the earth surface could not be closed with experimental data (Foken and Oncley, 1995). The sum of Rn and the G was found in most areas to be larger than the sum of turbulent fluxes of H and λE (Anderson et al., 1984; Verma et al., 1986; Mahrt, 1998; Foken, 2008). According to various studies, most field measurements have failed to show closure of the surface energy balance (MacNail and Shuttleworth, 1975; Dugas et al., 1991; Fritschen et al., 1992; Stannard et al., 1994; Lloyd et al., 1997; Twine et al., 2000). Furthermore, direct estimates of H, λE fluxes, available energy Rn, G and storage almost always indicate an incomplete energy balance closure (Aubinet et al., 2000; Oncley et al., 2002; Wilson et al., 2002; Culf et al., 2004).

Within the micrometeorological community, the evaluation of the surface energy balance closure is a standard way for assessing data quality (Aubinet et al., 2000; Wilson e al., 2002; Brotzge and Crawford, 2002; Liu et al., 2006). Past studies have shown that the energy imbalance typically ranges from about 5-30% and its source is dependent on various errors that might occur (any noise in the entire measurement system will act to degrade the correlations and reduce the flux). Moreover, numerous researchers have hypothesized several explanation of this system imbalance which includes; consumption of net radiation by photosynthesis, different footprints for energy and flux, error in available energy measurements, lack of steady state condition, improper choice of averaging period, high frequency corrections not perfect, no perfect choice for coordinate rotation, measurements error, neglected energy sinks, loss of low or high frequency contribution to the turbulence fluxes, neglected transport processes of the surface layer fluxes (such as horizontal and vertical advection) and its subsequent dissipation away from the EC tower due to processes not measured by EC (Black et al., 1996; Mahrt, 1998; Aubinet et al., 2000; Twine et al., 2000; Massman and Lee, 2002; Oncley et al., 2002; Turnipseed et al., 2002; Wilson et al., 2002; Hipps et al., 2006; Oucley et al., 2007; Kidson et al., 2010; Consoli, 2013). Nonetheless, the energy balance closure problem can be corrected by using procedures such as Bowen ratio (BR), where authors argued that closure should be forced by increasing H and λE by keeping the measured BR, for example turbulent flux is assumed constant (Kidston et al., 2010; Gebler et al., 2015). Therefore, the effect of forcing closure is examined by adding to the water vapour and CO_2 fluxes according to the ratio of H as described in Twine et al. (2000), in order to match the available energy. To verify precision of turbulent flux measurements with the EC system, one simple measure is to check for conservation of energy, so that the sum of turbulence fluxes of H and λE must balance the available energy Rn and G (Hipps et al., 2006). This check provides estimates of reliability of fluxes, as well as the presence of bias.

2.6.2.2 Remote Sensing

The adoption of remote sensing as a micrometeorological tool for improving agriculture has been widely accepted across the globe by scientists in the research community, because it has the ability to capture spatial explicit information of a heterogeneous environment (an area varying in climate, soil properties, topography and elevation), in a way that saves time and resources, unlike the in-situ based system which requires calibration and cannot be automated to function for a long period without observation (Andreu et al., 2019). The process of measuring biophysical factors using in-situ based methods such as eddy covariance has been studied over a long period of time. There is a lot of confidence in the accuracy of its output, and it has been proven that the system is ideally suited for homogenous environments. In spatial variable areas, there would be a need to have more flux towers situated in different parts of the area to accurately detect the observed parameters. This would make the process more costly (Mhawej et al., 2020).

The types of remote sensing systems used to acquire crop water use data are normally dependent on the objectives which serve the knowledge required by the researchers and farmers. These objectives include the need to understand factors which affect crops (such as yield, the need for irrigation, areas affected by diseases, fertilizer which might be required and how the crop grows during its different stages by observing factors such as rainfall, evapotranspiration, soil moisture content, etc.) (Figure 2.11). The impacts of climate change have become more evident over the years, which are reflected through an increase in variability of rainfall patterns, higher temperatures and water shortages. These are amongst the major reasons why decision-makers require more information on how to become efficient in human interaction with water and related drivers (Dehkordi et al., 2020).

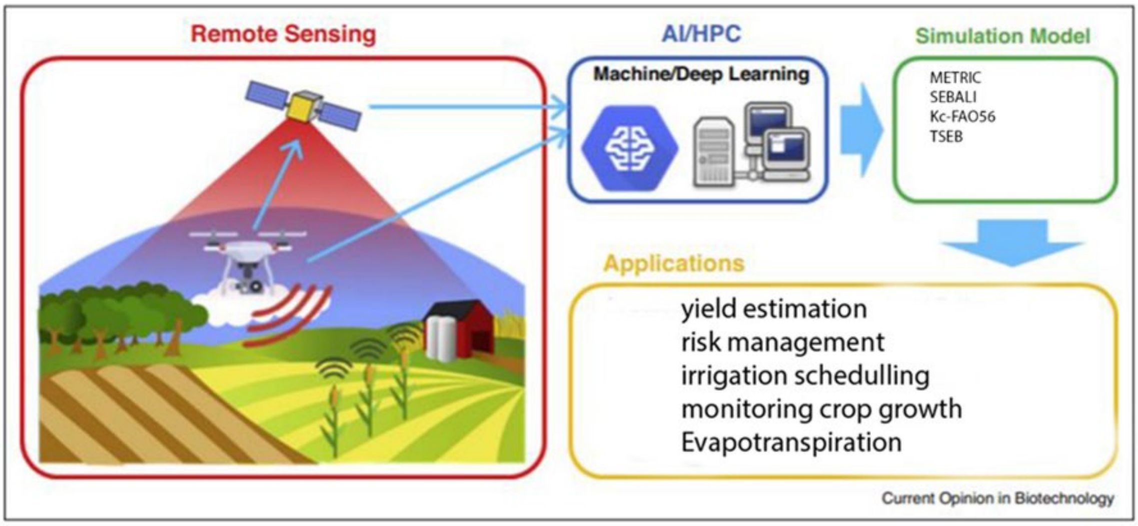

Figure 2.11: The remote sensing application process (Jung et al., 2021).

Andreu et al. (2019) conducted a study focused on assessing the validity of Remote Sensing as a monitoring tool for water use and water stress in two sites located within the African savanna ecosystem. The savanna ecosystem is characterized grasslands, with scattered trees and shrubs with limited water supply, frequent droughts, and sensitive to change from climate and land-use practices. This study was encouraged by the need to improve measurement methods for better planning and decision-making by the water resources management. The aim behind this project was to develop a reliable monitoring tool to detect water use and water stress of the ecosystem, by quantifying the crop evapotranspiration (ET_c) from the remotely sensed data. As shown in Figure 2.12, the sites were in Skukuza and Malopane. They both had flux towers installed to validate the results produced by the models using the remotely sensed data during the summer and winter months.

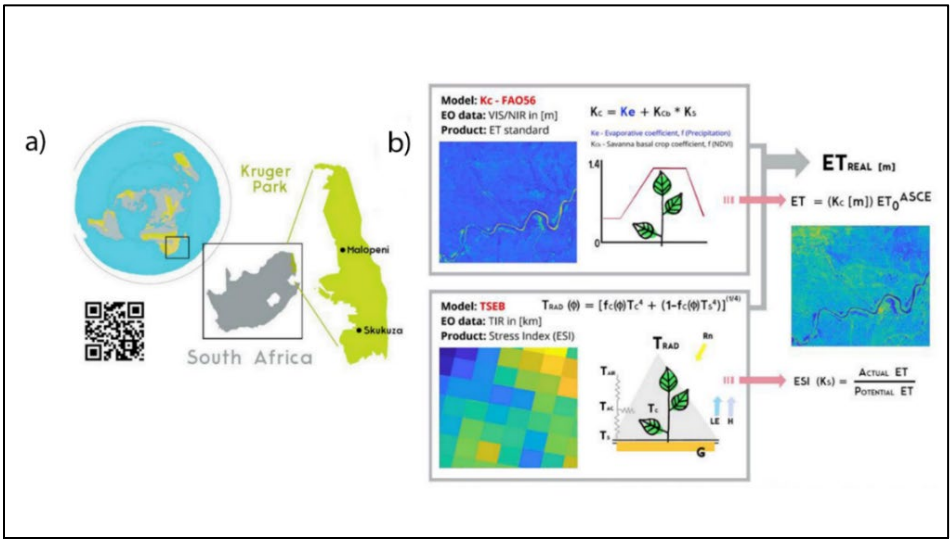

Figure 2.12: Location of sites used to assess the validity of remote sensing as a monitoring tool for water use and water stress within the African savanna ecosystem (a) and an illustration of how the Kc-FAO56 and the Two Based Energy Balance (TSEB) models process remotely sensed data through integration to derive a high resolution estimated Evapotranspiration of the ecosystem (b) (Andreu et al., 2019).

The K_c-FAO56 model used a SPOT 4 and 5 satellite imagery for ET output data (the NDVI data was obtained from a Multispectral sensor, which has a 10 m resolution). The Two Surface Energy Balance (TSEB) model acquired data from the Advanced Along-Track Scanning Radiometer (AATSR) which has a 1 km resolution using Land surface temperature as input data and Ecosystem Stress Index (ESI) as output data that had to be downscaled to a finer resolution (Table 5). Literature has shown that there is a strong correlation between estimated ET and biomass of a crop (Mhawej et al., 2020; Koech and Langlat, 2018). According to the results, incorporating the Ecosystem Stress index in the estimation of ET_c was significant in increasing accuracy in comparison to the measured data which is shown the Table 2.5 below. It is recommended that in-situ measurements be available when dealing with Remote Sensing data due to its high dependence on assumptions which can make it difficult to detect cause of error.

Table 2.5: Evapotranspiration results obtained in Skukuza by the Kc-FAO56 alone and Kc-FA056 plus ESI versus the in-situ flux tower measurements from 2010 to 2012 (Andreu et al. (2019).

Month	Year	ET measured In-situ (mm day^{-1})	ET estimated using Kc-FAO56 + ESI (mm day^{-1})	ET estimated using Kc-FAO56 (mm day^{-1})
April	2010	3.6	2.6	4.3
May	2010	1.7	1.1	3.72
September	2010	0.5	0	0
October	2010	0.3	0	0
December	2010	4	3.1	5.02
May	2011	2.2	1.5	6.48
August	2011	0.6	0.1	0
May	2012	1.1	0.5	0.22
RMSD against the measured data			0.6	1.3

Jin et al. (2021) conducted a study using drone imagery to assess the impact of applying biochar on water use efficiency and growth monitoring of rice. This experiment was facilitated in an area of 160 m^2 experiencing severe drought (long-term mean annual precipitation was 1547 mm) at the Enrique Jimenez Nunez station in Costa Rica. The drone used in this investigation was a DJI M600 Pro Hexacopter with the ability to capture hyperspectral and thermal imagery with a mass of 6 kg, 30 minutes flying time at 30 m above field of view. The evapotranspiration (ET) data collected by the drone was validated by an in-situ micro meteorological station in the area. The ET values from Remote Sensing and in-situ measurements had a high correlation. This is supported by the evidence which indicates that biochar application increases soil water availability, results in less nutrient loss and reduces the probability of plant water stress (Dehkordi et al., 2020). Various methods have been used in South Africa to estimate crop ET, study energy and soil water balance components as well as groundwater recharge (Table 2.6).

Table 2.6: Methods that have been used to obtain evapotranspiration data using Remote Sensing in South Africa (Gibson et al., 2013).

Type	Study Focus	Parameters	Temporal Scale	Spatial scale/ Scale	Reference
Review	Methodology	ET, energy balance	Instantaneous, day, week, month	Field/10 m	Allam et al. (2021)
Operational	Agricultural water use efficiency	ET, energy balance	weekly, for a period of 12 months	Field/Farm 30 m	Singels et al. (2014)
Historic	Catchment water Use	ET, rain, runoff, groundwater recharge	Day, month, year for 1 year	Catchment/1 km	Gibson et al. (2009)
Operational	Catchment scale planning and water allocation	ET, rain, rain-ET	weekly, for a period of 12 months	Field/ Catchment	WE Consult (2011)

The freely available sensors responsible for data acquisition are MODIS, Landsat and Sentinel. MODIS satellite has a 1 km resolution and a daily time stamp. This sensor is good for obtaining temporal information for a larger area. However, its low resolution makes It difficult to rely on the sensor's output when dealing with local-scale results. Landsat-8 has a 30 m resolution and a revisit time of 16 days. The satellite produces high-resolution images which is advantageous for consistent long-term observations for local-scale area. The Sentinel-2 satellite can capture a spatial heterogeneous land cover to extent of being able to distinguish the different types of vegetation in that area and the state of the plants due to its high resolution of 10 m and a revisit time of 5 days. The limitations with the use of this satellite include the need for cloud cover absence and inadequate representation of thermal infrared observations. The identification of an appropriate satellite to gather data from is dependent on the site specifications (Table 6) (Gibson et al., 2013; Andreu et al., 2019).

When it comes to data processing of estimated evapotranspiration there are four different methods that have been adopted over the years which include deterministic, empirical, vegetation index and the commonly used parameterization of the energy balance. Models are not sensor dependent. For a long time, the most used Energy Balance models were the Surface Energy Balance Index (SEBI), Surface Energy Balance System (SEBS), and the Surface Energy Balance Algorithm for Land (SEBAL). The advantages of these models were: they are freely available, easily accessible, and there are very few assumptions required. The main limitation was their high requirement for input data. This limitation has been bridged with the development of the Surface Energy Balance Algorithm for Land-Improved (SEBALI) in 2020, which requires less inputs and calibrated in a way that is able to estimate the right values for Hot/Cold pixels in agricultural areas. However, the model has been commercialized therefore it is not easily accessible to everyone, just like the Mapping Evapotranspiration using Internalized Calibration (METRIC) model (Allam, 2021).

Technological advancements in Remote Sensing have resulted in the development of products such as MOD16, METRIC Earth Engine Flux (EEF), and SEBALI Google Earth Engine (GEE). The function of a product is to provide processed information using Cloud Computing. The process of Cloud Computing refers to the migration from traditional Remote Sensing methods to the use of online engines as the hosts responsible for managing and processing remotely sensed data (Google Earth is an example of an engine). This new way of processing data is advantageous when it comes to analyzing spatially variable, long-term High-resolution imagery, in a way that is less time-consuming. The challenges which come with these systems include the lack of control over site-specific characteristics; because of that the product may or may not produce an ideal replication of the site specifications. The SEBALIGEE product is slightly different from other products, since the code can be edited which makes crop water use estimates more site-specific (Allam et al., 2019; Mhawej et al., 2020)).

The adoption of Remote Sensing offers the following potential opportunities and challenges for crop water use measurements:

Opportunities

1. The application of Remote Sensing has the potential to improve relationships between crop water use, and potential yield forecasting. This process has not been widely accepted due to the issues associated with lack of easy access to high spatial and temporal resolution imagery. The satellites commonly used in recent agricultural research projects related to water use at a local scale (farm-scale) include Landsat 8 and Sentinel 2. The other challenge associated with the reliance of capturing data using satellites is the disturbance from cloud coverage which results in loss of information more common during the rainy season (Mhawej et al., 2020);
2. A new form of remote sensing with a lot of potential for crop parameter estimates is the adoption of Unmanned Aerial Vehicles (UAV). However, the cost remains a limiting factor (currently the ARC spends approximately R50 000 per flight, Personal Communication data). The multispectral and thermal imagery produced by drones is convenient because of reduced cloud cover problems. The user can readily acquire plant canopy temperature to determine the crop water use. This relationship has been well received in the agriculture and remote sensing literature. The multispectral imagery can be used to obtain water use in pasture, cereal crops, fruit trees and grapevines (Koech and Langlat, 2018).
3. The technological advancement in drone capabilities is more likely going to make UAVs more affordable for farmers if the right models are developed which could reduce the number of flights required. This would solve the cost limiting factor affecting researchers. The near future is going to have more drone features that enable efficient communication with irrigation systems (Gupta et al., 2019).

Challenges

1. There is no accessible Remote Sensing information addressing *Moringa oleifera* crop water use. The limited Remote Sensing research that has been done on the crop and is accessible to the public domain include biomass yield quantification (Tshabalala et al., 2021) and spatial distribution of Moringa cultivation across suitable agro-ecological regions (Tshabalala et al., 2020), while Remote Sensing studies conducted to determine the water use of other crops grown under similar conditions (Andreu et al., 2019) show that it is possible to obtain valuable information on water use of *Moringa oleifera* which would add to the body of knowledge that is currently available.
2. The process of Remotely Sensed data using cloud computing is still new, which creates room for more development on the system in the future. The accuracy of information produced through products has not been tested in all environments. Even though the method has proved to work in large-scale areas, there is still a need to validate it at a local scale. Further developments on Remote Sensing technology will allow future reduction of costs associated with the acquisition of its information. These costs include equipment required for processing, experience needed by the person who will use the information and the time spent to learn and understand the process.

3. Improvements on Moringa crop water use estimates using an in-situ process will address key gaps in Moringa water use knowledge, due to the method's Cloud Computing increased accuracy relative to traditional Remote Sensing methods.

2.6.3 Plant physiology approaches

2.6.3.1 Chamber

For years, chambers have been used to quantify fluxes of H_2O and CO_2 between the land surface and the atmosphere (Lundegardh, 1927, 1928; Wohlfahrt et al., 2005; Aubinet et al., 2012; Acosta et al., 2013). This method is based on measurements of changes in gas concentration in a closed volume, from which gas exchange between the soil surface and the atmosphere is estimated (Musgrave and Moss, 1961). Moreover, chambers can be static or dynamic using an absorption agent to integrate flux over a period of time for former, and for latter by measuring the differences in concentration between inflow and outflow of air (Iritz et al., 1997). Furthermore, Kool et al. (2014) stated that chamber is generally comprised of a closed, often hemispherical, volume placed either directly on the soil surface or on a pre-installed collar, with a pump inside that circulates gas to an external IRGA (Infrared gas analyser) (Kool et al.,2014). Thus, according to Leuning and Foster (1990) this approach is exceptional in providing T data that can be used for comparative purpose amongst different irrigation treatments. Therefore, various researchers have used chambers of different sizes to directly measure the exchange of H_2O and CO_2 between the atmosphere, plant organs, soil (Monteith, 1990; Leuning and Foster, 1990; Denmead et al., 1993, Wohlfahrt et al., 2005; Acosta et al., 2013) and whole tree for instance Eucalyptus saligna (Barton et al., 2010), Spruce tree (Medhurst et al., 2006) (Figure 2.13).

Figure 2.13: A whole-tree chamber quantifying fluxes of CO_2 and H_2O (Photo taken from https://www.researchgate.net/publication/259153552 on 12/12/2021).

Chambers are portable and can be placed on the plant for the measurement; they are then removed before the plant can respond physiologically to the changing environment. Chamber measurements are relatively simple to operate and adaptable to a wide variety of studies, they can be used for the gap-filling of the EC data. Moreover, they are useful to partition the net fluxes of CO_2 into their components (gross primary production and respiration) (Reicosky and Peter, 1977, Pavelka et al., 2018). However, the disadvantage of this approach is that in most cases errors can occur when measurements are done on trees growing in open fields because the presence of the chamber changes leaf energy balance Also, measurements with this approach are usually for short period of time and affect the environmental conditions where measurements are done for instance they alter the temperature, radiation, and wind conditions and vapour pressure deficit inside the chamber comparing to that outside (Denmead, 1984; Wong and Dunin, 1987; Legg, 1988 Monteith, 1990; Leuning and Foster, 1990; Denmead et al., 1993; Pérez-Priego et al., 2010). However, even though with this limitation, chambers are generally considered accurate, and therefore a good method to measure transpiration (Kool et al., 2014), again, they can be useful for making replicated measurements in small plots (Dugas et al., 1997) and is the most used flux measurement approach (Denmead, 2008).

2.6.3.2 Sap flow

Thermometric methods of sap flow measurements were invented in 1930, and over the years many developments and new derivations have continued to appear in order to improve the performance of sap flow sensors (Marshall, 1958; Granier, 1985; Baker and van Bavel, 1987; Cermák et al., 2004; Vandegehuchte and Steppe, 2013). This method is a thermal-based technique to quantify water flow through the stem following varying methodologies, and can mainly be classified into heat balance, heat pulse and constant heater methods (Baker and Van Bavel, 1987; Steinberg et al.,1989; Kool et al., 2014). Sap flow technique allows the transpiration from whole-tree to be continuously measured directly with adequate accuracy (Dugas, 1990; Schulze et al., 1985; Dugas, 1990; Bethenod et al., 2000) (Figure 2.14).

Figure 2.14: Thermocouples and a heat temperature probe installed on the trunk of a seven-year-old macadamia tree to measure sap flow movement through the xylem (Photo taken by Dr Nadia Araya).

In addition to the advantages mentioned above, the sap flow method measures total sap flow through the whole plant and sap flux density (Vandegehuchte and Steppe, 2013). They use pulsed or continuous heating and track temperature changes caused by convective heat transport by moving sap in different plant organs along the transpiration pathway (Goldstein et al., 1998; Burgess et al., 2000). Over the years various researchers have used this approach on woody stems, vegetables, and grasses to quantify transpiration, for instance Banana trees (Lu et al., 2002), sugarcane (Chabot et al., 2005), sweet cherry trees (Juhasz et al., 2013), macadamia trees (Taylor et al., 2013), tomato (Hanpin et al., 2017), Apple trees (Mobe et al., 2020). From all these studies, sap flow yielded acceptable temporal patterns of plant T and these results have often compared well with independent measurements (McCulloh et al., 2007) and with ET at larger scales (Wilson et al., 2001). Sap flow systems are easy to replicate and the probes are automatic (Granier et al., 1996), these systems are inexpensive, easy to use and readily interfaced with data loggers for remote operation, so continuous records of plant water use with high time resolution can be obtained, and they can be used anywhere with very little disturbance to the site (Smith and Allen, 1996; Wullschleger et al., 1998; Poyatos et al., 2016). However, like any methodology, sap flow also has its own limitations. These include incomplete contact of the probe with the sapwood, natural temperature gradients, the need for species-specific calibrations and parameters, uncertainty in baseline flow estimates, wounding effects and sensor drift, the magnitude of the time lag between sap flow and transpiration, changes in spatial patterns of T (Cermak and Kucera, 1981; Schulze et al., 1985; Granier et al., 1996; Burgess et al., 2001; Traver et al., 2010;

Vandegehuchte and Steppe, 2013; Poyatos et al., 2016). However, even though with all this limitation this approach has highly contributed to addressing important concept of the mechanisms of stem water storage dynamics (Goldstein et al., 1998). Therefore, according to Smith and Allen (1996), the use of sap flow approach is becoming increasingly popular, thus, they are likely to play an important role in future efforts to come up with solutions on how to improve the use of scarce natural water resources in sustainable manner.

2.7 CROP WATER USE MODELLING APPROACHES

Various modelling approaches are used to predict crop water use, starting from simple, empirical approaches to the more complex, mechanistic approaches (Rana and Katerji, 2000; Egea et al., 2011; Dong et al., 2014; Kool et al., 2014; Verhoef and Egea, 2014; Subedi and Chávez, 2015). Simple, empirical approaches are more easily parameterized, but they are often site-specific, whilst mechanistic approaches can be more widely transferred, provided that the required, often difficult to determine, input parameters are accurately obtained (Leenhardt et al., 1995). Depending on the central principle for estimating crop water use, these modelling approaches can be categorized into three main groups: (1) soil water balance approaches, which predict crop water use as the residual difference between soil water inputs (rainfall and irrigation) and outputs (runoff, drainage and changes in soil water storage within the root zone) (Leenhardt et al., 1995); (2) crop coefficient approaches, which make use of a crop coefficient that integrates the effect of characteristics distinguishing a typical crop from the grass reference (Allen et al., 1998); and (3) stomatal conductance approaches, which model the response of stomata to changes in the local environmental conditions of the crop (Damour et al., 2010). A description of each category of modelling approaches is presented below.

2.7.1 Soil water balance approach

Soil water balance models for the estimation of crop water use can be grouped in two main categories: (1) simple models (which use the cascading or tipping bucket principle to estimate root water uptake) and (2) complex models (which model root water uptake using soil water infiltration and redistribution functions) (Rana and Katerji, 2000; Dong et al., 2014). In simple models, the soil is treated as a collection of water reservoirs, filled by rainfall and/or irrigation and emptied by crop ET and drainage (Leenhardt et al., 1995; Rana and Katerji, 2000). Examples of such models include those where the soil profile is treated as a bucket into which water flows until it is full, or more advanced ones where the soil profile is divided into different layers, with water cascading from upper to lower layers when the upper layers reach field capacity (de Jong and Bootsma, 1996). An example of such models include the one-dimensional Soil Water Balance (SWB) model (Annandale et al., 1999). In complex models, the water flow in the soil is described by mathematical functions of soil water movement, such as the two-dimensional Richard's equation. The HYDRUS-2D and SWB-2D soil water balance models are clear examples of models within this category (Skaggs et al., 2004; Annandale et al., 2004).

The simple and complex approaches of soil water balance modelling both present advantages and disadvantages. The applicability of complex models is constrained by the accuracy of pseudo-transfer functions used for the estimation of water transfer and by the procedures used for estimating the boundary conditions of the soil-plant-atmosphere system. However, in simple models, although they are simpler, there are difficulties in determining the soil water storage as a function of the soil and root depth (Rana and Katerji, 2000). The availability of data often determines which modelling approach can be used. More advanced soil water balance modelling approaches generally require daily or hourly observations of rainfall and estimated potential ET. Simpler models require less soil input parameters (field capacity and permanent wilting point values, either single values applicable to the entire soil profile, or a set of values of each layer) than more complex models (which require water retention characteristics and hydraulic conductivity functions for each soil layer). Simple modelling approaches often give accurate estimates of water use for annual crops (de Jong and Bootsma, 1996; Dong et al., 2014). Complex models, on the other hand, may be more suitable for estimating crop water use of perennial tree crops, as these often simulate multiple-dimensional water movement in the soil, which better accounts for root water uptake for T and variability of E_s due to non-uniform wetted areas (Annandale et al., 2004). In these models, crop ET is computed using a mechanistic supply or demand-limited approach (Skaggs et al., 2004; Annandale et al., 2004).

Even though complex models may be difficult to operate, the estimated ET may be more accurate, provided that the required hydraulic parameters (such as soil water content at saturation, residual soil water content and saturated hydraulic conductivity) are well determined (Leenhardt et al., 1995; Skaggs et al., 2004). Failing to meet the input parameter requirements, the soil water balance approach may not be accurate enough to estimate crop ET. This is particularly true for tree species where complex soil-plant-atmosphere continuum interactions occur, which are often aggravated by the fact that such plant species exhibit high levels of stomatal control that can override the effect of root water uptake, in which the functional principle of soil water balance models is based (Dong et al., 2014). This may help explain why the applicability of soil water balance models is very limited for tree species.

2.7.2 Crop coefficient approach

The simplest and most widely used form of the crop coefficient approach consists of estimating crop ET by multiplying the reference crop ET (ET_o), by a single crop coefficient (K_c). Estimates of crop ET using this approach represent ET rates under well-watered, optimal management conditions (Allen et al., 1998):

$$\mathrm{ET} = \mathrm{K_c}\ \mathrm{ET_o} \tag{2.5}$$

Reference crop evapotranspiration was initially conceptualized as the evapotranspiration rate from a hypothetical short grass reference surface, growing under optimum management conditions (Allen et al., 1998). Later on, Pereira et al. (1999) suggested that, for more accurate predictions of crop ET, ET_o should be distinctly defined for three groups of crop categories based primarily on crop height, namely 0.12 m (short grass), 0.5 to 0.7 m (alfalfa) and 2.0 to 3.0 m (tall maize). This was suggested considering the fact that the aerodynamic resistance parameter initially included in the ET_o equation developed by Allen et al. (1998) is highly variable depending on crop height and density (Pereira et al., 1999). As a result, a more standardized form of the Penman-Monteith equation was developed, which applies for both, short and tall vegetation (Allen ,,,,,,,,,,2006; Pereira et al., 2015):

$$\mathrm{ET_o} = \frac{0.408\Delta(\mathrm{R_n}-\mathrm{G})+\gamma\left(\frac{\mathrm{C_n}}{\mathrm{T_a}}+273\right)\mathrm{u_2}(\mathrm{e_s}-\mathrm{e_a})}{\Delta+\gamma(1+\mathrm{C_d}\mathrm{u_2})} \tag{2.6}$$

where ET_o is the standardized reference ET, in mm d^{-1} for daily time steps, or mm h^{-1} for hourly or shorter time steps; Rn is the calculated net radiation at the crop surface, MJ m^{-2} d^{-1} for daily time steps, or MJ m^{-2} h^{-1} for hourly or shorter time steps; G is the soil heat flux density at the soil surface, MJ m^{-2} d^{-1} for daily time steps, or MJ m^{-2} h^{-1} for hourly or shorter time steps; T_a is the mean daily or hourly air temperature at 1.5 to 2.5 m height, °C; u_2 is the mean daily or hourly wind speed at 2 m height, m s^{-1}; e_s is the saturation vapour pressure at 1.5 to 2.5 m height, kPa, calculated for daily time steps as the average of saturation vapour pressure at maximum and minimum air temperature and for hourly time steps using hourly average air temperature; e_a is the mean actual vapour pressure at 1.5 to 2.5 m height, kPa; Δ is the slope of the saturation vapour pressure-temperature curve, kPa $^{\circ}C^{-1}$; ϒ is the psychometric constant, kPa $^{\circ}C^{-1}$; Cn is the numerator constant that changes with reference type and calculation time step, K mm s3 Mg^{-1} d^{-1} or K mm s3 Mg^{-1} h^{-1}; C_d is the denominator constant that changes with reference type and calculation time step, s m^{-1}. Values for parameters Cn and Cd are given in Table 2.7 (Pereira et al., 2015).

Table 2.7: Values for Cn and Cd coefficients for calculation of reference ET (Pereira et al., 2015).

Calculation time step	Short reference, ET_o (Clipped grass)		Tall reference, ETr (Alfalfa)		Units for ET_o, ET_r	Units for Rn, G
	Cn	Cd	Cn	Cd		
Daily	900	0.34	1600	0.38	mm day^{-1}	MJ m^{-2} day^{-1}
Hourly daytime	37	0.24	66	0.25	mm hr^{-1}	MJ m^{-2} hr^{-1}
Hourly night-time	37	0.96	66	1.7	mm hr^{-1}	MJ m^{-2} hr^{-1}

The effects of crop characteristics on the estimation of ET, using Equation 5, are accounted for by including a single K_c, which takes into consideration the effects of crop type, variety and development stage, as well as, differences in resistance to T, crop height, crop roughness, reflection, ground cover and crop rooting characteristics (Allen et al., 1998). Values of K_c will also fluctuate as affected by climatic conditions and crop management practices (Wang et al., 2007).

As values of K_c fluctuate throughout the growing season, as influenced by changes in climate, tree size and canopy development, various models have been developed to adjust K_c according to these changes, in order to obtain more accurate predictions of crop ET (Allen et al., 1998; Johnson et al., 2000; Sammis et al., 2004; Wang et al., 2007; Allen and Pereira, 2009; Samani et al., 2011). Changes in climate may result in variations in the length of the different growth stages, thus affecting the shape of the Kc curve (Sammis et al., 2004) or in the magnitude of K_c values, as a result of variations in wind speed (u2) and minimum daily relative humidity (RH_{min}) from one climatic region to another (Allen and Pereira, 2009). Increased u_2 and decreased RH_{min} cause the ratio of ET over grass ET_o to increase due primarily to differences in roughness between taller agricultural crops and the clipped grass reference (Allen and Pereira, 2009). This is the reason why Allen et al. (1998) suggested that K_c values published in FAO-56, which were developed under sub-humid climatic conditions at $u_2 = 2$ m s^{-1} and $RH_{min} = 45\%$, should be adjusted to specific conditions of u_2 and RH_{min} for more accurate estimates of crop ET using grass ET_o. The procedure developed by Allen et al. (1998) for the adjustment of Kc due to differences in roughness is, however, limited to use with K_c values published in FAO-56 only. While changes in K_c due to intra and inter seasonal climatic variations are well accounted for using ET_o when estimating crop ET with the FAO-56 model, the procedure does not consider the influence of climate on the rate of canopy development, which is quite significant for some deciduous fruit tree species like pecans for example (Miyamoto, 1983; Sammis et al., 2004; Wang et al., 2007; Samani et al., 2011). In an attempt to overcome this limitation, researchers have developed simple models using thermal time to adjust the shape of the K_c curve in order to account for changes in the rate of canopy development (Sammis et al., 2004; Marsal et al., 2014). Simple thermal time or growing degree day (GDD) equations accumulate thermal time linearly with increasing temperature above a constant crop-specific base temperature, which makes them easily applicable to conditions where they were developed (Samani et al., 2011), but perhaps less applicable outside the area of calibration.

2.7.3 Stomatal conductance approach

Stomatal conductance is most often described using mathematical expressions, which represent physical and physiological characteristics of the biological process being studied (Damour et al., 2010). The most common models fall within two main categories, namely: (1) models applied at the leaf level, which include multiplicative models of environmental influences and models of stomatal behaviour; (2) models applied at the canopy level, which include those that are based on the Penman-Monteith resistance model (Leuning, 1990; Leuning, 1995; Rana and Katerji, 2000; Pereira et al., 2006; Damour et al., 2010). In both categories of models, stomatal conductance is estimated taking into account both canopy properties and meteorological conditions. Models applied at the leaf level may not be able to provide accurate estimations of T for an entire canopy due to the fact that changes in stomatal conductance are highly variable: (1) at the leaf level, due to changes in stomatal characteristics (stomatal density and pore length), different exposure of leaves to solar radiation due to shading by other leaves in a canopy and orientation of parts of an irregularly shaped leaf with respect to the solar beam, variations in water potential gradients as a result of internal resistances to water movement through the leaf, and fluctuations in the solute potentials of guard cells; and (2) at the canopy level, due to all the reasons described earlier, and as a result of the configuration of leaves within a plant canopy, where leaves may touch one another, and as a result, their individual boundary layers may overlap (Jarvis and McNaughton, 1986). The Jarvis-Stewart model is a clear example of stomatal conductance models applied at the leaf level, in which the g_s response is integrated to quantum flux density (QFD, μE m^{-2} s^{-1}), leaf temperature (Tl, ºC), leaf-to-air vapour pressure deficit calculated at leaf temperature (VPDl, kPa), ambient CO_2 concentration (Ca, ppm) and leaf water potential (ψ, MPa), according to the following equation (Jarvis, 1976):

$$g_s = f(Q_{FD})(T_l)(VPD_l)(C_a)(\psi) \qquad (2.7)$$

Noting all the limitations with the use of stomatal conductance models applied at the leaf level, it is very important to consider modelling stomatal conductance at the canopy level, i.e. canopy conductance (gc), in order to obtain more accurate estimates of whole-plant T. In this case, the effects of changes in the fluxes of heat and water vapour from all the individual leaves are likely to accumulate and lead to substantial changes in the saturation VPD around the leaves within the canopy (Jarvis and McNaughton, 1986). In order to predict these effects on T, the resultant changes in saturation VPD that will occur at the canopy level, as a result of the changes in stomatal conductance should be estimated. With such consideration models of gc were developed, which estimate an unweighted total of stomatal conductances of all the leaves within a canopy (Leuning et al., 1995; Whitehead, 1997; Wang and Leuning, 1998; Granier et al., 2000; Leuning et al., 2008; Whitley et al., 2009; Egea et al., 2011; Villalobos et al., 2013; Ding et al., 2014). The Penman-Monteith resistance model based on the “big-leaf” approach is a clear example of a model in which g_c is obtained by scaling-up measurements of gs, conducted on individual leaves using a portable gas exchange device, to the canopy level using average leaf area index (LAI) measurements for the entire canopy (Whitehead, 1997).

In an attempt to provide direct estimates of crop ET, the Shuttleworth-Wallace model was developed, in which the crop ET is estimated using two distinct Penman-Monteith resistance equations, i.e. one for the crop (for estimation of transpiration – T) and the other for the soil surface (for estimation of soil evaporation – E_s) expressed as follows (Zhao et al., 2015):

$$E_s = \left[1 + \frac{R_s R_a}{R_c(R_s+R_a)}\right]^{-1} \frac{\Delta A + \left(\frac{\rho_a c_p VPD - \Delta r_a^s (R_n - G)}{r_a^a + r_a^s}\right)}{\Delta + \gamma\left(\frac{1+r_s^s}{r_a^a + r_a^s}\right)} \quad (2.8)$$

$$T = \left[1 + \frac{R_c R_a}{R_s(R_c+R_a)}\right]^{-1} \frac{\Delta A + \left(\frac{\rho_a c_p VPD - \Delta r_a^c A_s}{r_a^a + r_a^c}\right)}{\Delta + \gamma\left(\frac{1+r_s^c}{r_a^a + r_a^c}\right)} \quad (2.9)$$

where Δ is the slope of saturation vapour pressure curve (kPa K^{-1}); γ is psychrometric constant (kPa K^{-1}); r_s^c and r_a^c are bulk stomatal resistances of the canopy (estimated by inverting values of gc modelled using the "big-leaf" approach) and boundary layer resistance (s m^{-1}), respectively; r_a^s and r_a^a are aerodynamic resistances from soil to canopy and from To reference height (s m−1), respectively; r_s^s is soil surface resistance (s m^{-1}).

Penman-Monteith resistance models include climatic (Rn and VPD) and parametric variables (r_a^a and r_s^c) (Zhao et al., 2015) which strongly influence modelling results. Vapour pressure deficit in particular must be measured very accurately and r_s^c must be precisely modelled for appropriate estimates of crop water use (Rana and Katerji, 1998). This has made the initial version of the Shuttleworth-Wallace model hard to parameterize, and as a result, a simplified format of its representation was developed to estimate E_s using the Priestley-Taylor formula (Li et al., 2010):

$$E_s = \alpha_E \tau \frac{\Delta}{\lambda(\Delta+\gamma)}(R_n - G) \quad (2.10)$$

$$\begin{cases} \tau \le \tau_c, \alpha_E = 1 \\ \tau > \tau_c, \alpha_E = \alpha - (\alpha - 1)(1-\tau)/(1-\tau_c) \end{cases} \quad (2.11)$$

where αE is the coefficient of the Priestley-Taylor formula with relevance to light interception, Tc and α is 0.55 and 1.3, respectively. The use of Priestley-Taylor formula has made the estimation of the Es component relatively easier and more applicable using the Shuttleworth-Wallace model, because it requires more easily obtainable parameters and is valid for humid and sub-humid regions (Kool et al., 2014). However, the procedure does not account for variability of E_s due to changes in the wetted surface area and wetting frequency as affected by irrigation and rainfall events, which is crucial for accurate E_s predictions. While researchers have tried to simplify the formulation of E_s component of the Shuttleworth-Wallace model, nothing has been done to address the challenges of modelling the T component. The most critical point of the Penman-Monteith model for tall orchard crops is the estimation of r_s^c which is determined by inverting values of gc modelled using the "big-leaf" approach. Thus, g_c should be modelled mechanistically. The problem is that g_c is estimated as a function of g_s measured on single leaves and average LAI measurements for the entire canopy, using the "big-leaf" approach, by scaling-up stomatal conductance from a leaf to canopy level, which is not trivial and an adequate solution has yet to be found, particularly for semi-arid environments. An improved method of estimating g_s was proposed to minimise this problem, in which the canopy is divided into various layers and g_s is estimated for each layer and weighted with the LAI for each layer using a multi-layer approach (Leuning et al., 1995), or in which the canopy is divided into two distinct layers of sunlight and shaded leaves using a "two-leaf" approach (Wang and Leuning, 1998; Ding et al., 2014). Either of the described methods may result in erroneous estimates of g_c due to the use of averaged g_s and LAI for each sub-layer to estimate g_c for the entire canopy.

In order to overcome such limitations, Villalobos et al. (2013) proposed a different approach, in which gc is modelled directly using measurements of T. The approach used to predict gc with the model of Villalobos et al. (2013) is based on the concept that canopy assimilation is proportional to radiation interception. This approach was found acceptable for well-coupled crops where the ratio of aerodynamic conductance (g_a) to g_c is generally sufficient high (Villalobos et al., 2000; Orgaz et al., 2007). Estimates of g_c are subsequently used to derive crop parameters (a and b), through a linear regression of (fIPAR*Rs)/g_c against VPD, which are subsequently used for direct estimates of daily T (mm day^{-1}) using the following equation:

$$\mathrm{T} = 37.08 \times 10^{-3} \frac{\mathrm{f_{IPAR} R_S}}{\mathrm{a+b\,VPD}} \frac{\mathrm{VPD}}{P_a} \tag{2.12}$$

where fIPAR is the fraction of photosynthetically active radiation intercepted by the canopy (dimensionless), Rs is the total daily solar radiation (J m^{-2} d^{-1}), Pa is the atmospheric pressure (kPa), VPD is vapour pressure deficit (kPa), the coefficient 37.08 × 10^{-3} incorporates the conversion of units for Joules of solar radiation to mol quanta and from mol to kg of H_2O, and a and b are the intercept and slope of the linear function relating (fIPAR*R_s)/g_c to VPD.

2.8 CASE STUDIES ON MORINGA

2.8.1 Crop yield

Globally Moringa is mainly produced in India with about 1.1 to 1.3 million tons of tender fruits produced every year from 380 km^{-2}, for human consumption and medicinal purpose (Talreja, 2010). In Africa, the crop is mainly produced in Ghana, Senegal and Malawi for the same purposes mentioned above (Booth and Wickens, 1988). However, in South Africa the Moringa industry is increasing steadily, with most being grown on small-scale farms and is normally consumed as a nutritional supplement in several rural communities (Muhl et al., 2011; Pakade e al., 2013). Thus far, Moringa is currently gaining popularity amongst processing industries, therefore, some commercial farmers have also shown an interest in Moringa cultivation due to its multipurpose values, and they have started growing it (Pakade et al., 2013). The tree can grow in versatile conditions including dry tropical, subtropical and humidity regions, different soil types, with exception of waterlogged condition (Ramachandran et al., 1980; Morton, 1991; Palada and Chang, 2003; Makinde, 2013). Even under tough climatic conditions, Moringa still produces acceptable yield, which is evidenced by numerous researchers who reported different values of Moringa biomass and dry matter yield grown under different field management practices and agro-climatic conditions (Table 2.8).

Table 2.8: Biomass, leaf and dry matter yield of the Moringa tree crop cultivated under different growing conditions.

Source	Yield (kg ha^{-1})	Plant density (Trees ha^{-1})	Climate
Mabapa et al. (2020) (South Africa)	160.06-447.9 (dry matter)	1 250-5 000	Tropical
El-Sayed et al. (2018) (Egypt)	3 114-4 894 (fresh leaf)	66 666	Sub-tropical
Isah et al. (2014) (Niger)	3 100-10 400 (dry matter)		Sahel climatic zone
González-González and Crespo-López (2016) (Cuba)	4 820-11 340 (dry matter)	20 000	Tropical Savanna
Amaglo et al. (2006) (Ghana)	2 500-30 000 (fresh leaf)	1 332 000-4 000 000	Tropical

2.8.2 Nutritional content

All parts of Moringa are edible, however, researchers have reported that the leaves are the most nutritious part of Moringa and have been used to combat malnutrition particularly amongst infant and nursing mothers as well as most people in rural areas (Makinde, 2013; Adamu et al., 2017). Moringa leaves are rich in carotene, vitamins A, B, C and E, essential amino acids, and minerals elements, constitute a rich and scarce combination of bioactive secondary metabolism such as flavonoids, glucosinolates and phenolic acids, which have the potential to curb and treat different diseases and can improve food and nutritional security in Southern Africa (Fuglie, 2001; Bosch et al., 2004; Fahey, 2005; Anwar et al., 2007; Pandey et al., 2011; Nouman et al., 2014). Moreover, nutritionist in developing countries have gathered information and evidence that in most people who stays in rural areas there is a deficiency of essential micronutrients such as Fe, Zn and vitamins such as A in the food that they eat every day (United Nations, 1997). Therefore, without doubt, the shortage of enough Vitamin A, Fe and Zn is a common problem, mainly in Southern Africa. Thus, the lack of vitamin and micronutrients especially in most children has placed Moringa in a recognizable state as it is the source of the essential micronutrients (Table 2.9). Therefore, without doubt this tree crop has the potential to curb hidden hunger that is affecting most of Southern Africa communities, most importantly this crop can also help in improving livelihoods for poor in rural areas.

Table 2.9: Nutritional content (beta-carotene, iron and zinc) of fresh Moringa leaves.

Source	Beta-carotene (mg/100 g)	Iron (mg/kg)	Zinc (mg/kg)
Price (2000)	16.3	282	-
Mapaba (2019)	-	138-364	10.70-28.70
Luhlaza-ISS (2019)	-	50.89-283.02	22.00-51.64
Fuglie (2001)	16.3	282	-
Saint Sauveur and Broin (2010)	4.0-8.0	180-280	15.00-30.00
Leone et al. (2015)	17.62-66.00	-	-
Moyo et al. (2011)	-	490	31.03

The variation in nutritional content of Moringa is attributed to several factors such as differences of field management practices, harvesting periods, environmental factors and maturity of leaves (Sant Sauveure and Broin, 2010). Therefore, it is important to investigate how different irrigation levels and other agronomic factors affects the nutritional content of this crop, which in turn will help to improve the nutritional water productivity (NWP) and water use efficiency (WUE) of this crop.

2.8.3 Crop water use

Knowledge of Moringa crop water use/evapotranspiration (ET) grown under standard conditions (nutrients and water non-limited). Therefore, without a doubt this knowledge is crucial in scheduling irrigation, optimizing crop production and modelling ET of this crop, which is envisaged that areas under its production in South Africa will increase in near future. Thus, the ability to quantify, predict ET or water requirement of Moringa can result in better satisfying the crop water needs, thereby improving crop productivity, WUE and use of this scarce resource in a sustainable manner.

Numerous authors have reported that Moringa tree has been found growing in areas receiving mean annual rainfall of between 200-1500 mm (Morton, 1991; Odee, 1998; Reyes-Sanchez, 2006; Pandey et al., 2011; Adebayo et al., 2017; Mabapa, 2019). These values of Moringa water requirements were based on mean annual rainfall received under various areas. Moreover, Luhlaza-ISS (2019) reported that Moringa was normally irrigated two to five litres of water per tree once or twice per week by different small-scale farmers in South Africa. Nonetheless, Sant Sauveur and Broin (2010) reported that it is crucial to irrigate the Moringa tree two to three times per week during the first three months after planting. The study conducted by dos Santos et al. (2017) was the only one which reported Moringa water use of 139.8 mm, measured over a three-month growth season, using a lysimeter in Brazil.

Therefore, globally there is limited information regarding water use or water requirement of this tree crop. This simply means that this crop has been studied very little, especially regarding water use under different climatic conditions. Thus, in this regard there is a huge need to quantify the water requirements of this crop. As this information is extremely important in terms of crop water management, including use in crop models to extrapolate measured results to other areas, in order to improve Moringa productivity and WUE.

2.8.4 Water use efficiency and nutritional water productivity of Moringa crop tree

About 85% of the available water under arid and semi-arid areas is used for irrigation purposes, however, inappropriate irrigation practices exacerbate the impact of water scarcity worldwide (Ezzahar et al., 2007). Since Moringa is highly adaptable to arid and semi-arid climate conditions, it is predicted that the area under its production will considerably increase in South Africa. Thus, knowledge of WUE (a concept introduced decades ago that connect water use and yield) and NWP (a new concept that connects water use, yield and nutritional content of crops) (Briggs and Shants, 1913; Ranault and Wallender, 2000; Nyathi et al., 2016), are extremely important as they can help in designing irrigation systems and irrigation regimes that are suitable for Moringa production (Garcia-Tejero et al., 2013). Moreover, this information is appropriate since there are very few detailed studies on WUE of this crop under different irrigation treatments (Mabapa et al., 2018; El-sayed et al., 2018; Hassan et al., 2019) (Table 2.10). There are no detailed studies reported in literature with regard to NWP of Moringa, which clearly demonstrates the huge gap in knowledge concerning this field.

Table 2.10: Moringa tree crop water use efficiency under different irrigation treatments.

Source	Irrigation method	Treatment (%)	Fresh yield (kg ha^{-1})	Water use (m^3 ha^{-1})	WUE (kg m^{-3})
Mapaba et al. (2018)	-	Rainfed	-	-	0.12-0.34
		50% SMD	1963-2268	4232-4365	0.46-0.52
		75% SMD	2225-2274	-	0.52-0.54
El-Sayed et al. (2018)	Flood				
		50% SMD	2117-2383	-	0.49-0.56
		75% SMD	2464-2430	-	0.58-0.58
El-Sayed et al. (2018)	Drip				
		100% SMD	-	-	0.65-0.71
		50% SMD	-	-	0.45-0.66
Hasan et al. (2019)	Drip	20% SMD	-	-	0.32-0.53

The values of WUE reported by Mabapa et al. (2018) and Hasan et al. (2019) were determined using portable photosynthesis system which quantify gaseous exchange on plant leaf, with the highest WUE obtained under 100% FC for the latter. However, the study conducted by EL-Sayed et al. (2018) was the only one where WUE was determined as yield/seasonal water consumptive (kg m^{-3}), with the highest WUE obtained under 75% soil moisture depletion treatment. This simply shows that this crop tree has the ability to produce acceptable yield even under scarce water condition. However, without doubt there is limited information on WUE and NWP of Moringa crop tree, thus there is a need to quantify ET with ET quantification approaches such as EC system, SWB or micro lysimeter in order to detail the effects of different irrigation levels on water use efficiency of this crop, which in turn will improve crop water management under arid and semi-arid conditions.

2.9 CONCLUSIONS AND RECOMMENDATIONS

Moringa is native to the African and Asian continents, but its cultivation has rapidly expanded to various regions around the world, including America, Australia and Europe. There are 13 species of the genus Moringa, but only two are the most cultivated species around the world (*Moringa oleifera* and *Moringa peregrina*) due to their great economic importance and high nutritional properties. In South Africa, Moringa is primarily produced in the Limpopo Province by smallholder and emerging commercial farmers as well as household gardeners, particularly in Capricorn, Mopani, Sekhukhune, Vhembe and Waterberg Districts, where the climatic conditions are relatively warm. There is a need to investigate the potential for Moringa cultivation in other provinces, which may be relatively cold, but through appropriate crop management, the crop can attain comparable productivity to that obtained in warmer regions.

The morphological characteristics of Moringa (tree height, trunk girth diameter), seed/pod and leaf yields are highly variable depending on crop management factors (time of leaf harvesting, harvesting frequency, planting density, tree spacing, and type of production system), genetics (cultivar) and environmental conditions (soil type and climate). Moringa crop productivity is also likely to be influenced by variations in crop physiological and anatomical characteristics. Very few studies have investigated the influence of crop management practices and changes in environmental conditions on crop productivity, water use efficiency and nutritional water productivity. The available literature suggests that Moringa grows well in tropical and sub-tropical semi-arid climates, with warm and humid environmental conditions and a range of rainfall amounts (200-3000 mm) and soil types. This indicates that Moringa is quite tolerant to both drought and waterlogging conditions. However, very few studies have looked at Moringa crop responses to varying water supply regimes and soil types, which could lead to an underestimation of the crop potential yields, especially in areas where the crop has not been studied. The limited research that is available on Moringa has mostly been generated from the Limpopo Province. Hence, there is a need to conduct further research in other Provinces with potential for cultivation of Moringa such as the Gauteng Province.

There is little to non-existent scientific information on Moringa crop responses in relation to water supply under dryland and irrigated conditions. Hence, there is a need to conduct research to optimize Moringa crop productivity, by testing a range of climate-smart production practices, including rainwater harvesting and conservation and deficit irrigation strategies. Such factors must be optimized in combination with the identification of best crop management practices (planting densities, pruning/cut-back methods and fertilization) in order to achieve greater crop productivity in terms of water use efficiency and nutritional water productivity. Based on only one study that was conducted, Moringa uses 423 to 436 mm of water annually. The water use efficiency of the crop varies from 0.12 to 0.53 kg m^{-3}, being highly influenced by water supply regimes, while the crop nutritional water productivity has not been reported. Therefore, there is a need to investigate Moringa crop responses to a range of crop management practices and environmental conditions in order to identify efficient crop water use practices for increased water use efficiency and nutritional water productivity. Several approaches are available to quantify crop water use, each with advantages and disadvantages. Approaches offering reliable data collection, such as the eddy covariance technique and crop-specific adjusted remote sensing approaches, should be prioritized at a large-scale of measurements. Whereas on a short-scale of field measurements, where heterogeneous crop growth patterns are expected, in-situ measurement methods such as sap flow and soil water balance should be considered for Moringa crop water use quantification.

ACKNOWLEDGEMENTS

This literature review document was financially supported by the Water Research Commission of South Africa (WRC Project No. C2020/2021-00484). All post-graduate students involved in the project as well as ARC-VIMP staff are thanked for their contributions to this document.

REFERENCES

Abdelaty, H.S., Hosny, A.M., Abdelhamid, A.N., Abdalla, A.M., 2022. Effect of irrigation water quantity and salinity level on growth and internal chemical contents of Moringa plants. Egypt. J. Chem., 65(12), 79-85.

Araya, A., Habtu, S., Hadgu, K.M., Kebede, A., Dejene, T., 2010. Test of AquaCrop model in simulating biomass and yield of water deficient and irrigated barley (*Hordeum vulgare*). Agric. Water Manag., 97, 1838-1846.

Bello, Z.A., Walker, S., 2016. Calibration and validation of AquaCrop for pearl millet (*Pennisetum glaucum*). Agric. Crop Pasture Sci, A-M, http://dx.doi.org/10.1071/CP15226

Bello, Z.A., Walker, S., 2017. Evaluating AquaCrop model for simulating production of amaranthus (*Amaranthus cruentus*) a leafy vegetable, under irrigation and rainfed conditions. Agric. For. Meteorol., 247, 300-310.

Daba, M., 2016. Miracle tree: a review on multi-purposes of *Moringa oleifera* and its implication for climate change mitigation. J. Earth Sci. Clim. Change, 7(8), 1-5.

Devkota, S., Bhusal, K.K., 2020. *Moringa oleifera*: A miracle multipurpose tree for agroforestry and climate change mitigation from the Himalayas – A review. Cogent food agric., 6(1), 1-8.

El-Boraie, F.M., El Shafay, R.M.M., Elhagarey, M.E., 2021. Morphological and chemical characterizes responses of *Moringa oleifera* yield to localized irrigation systems, water restriction and fertilizers. Int. j. adv. Res, 9(2), 509-523.

Er-Raki, S., Bouras, E., Rodriguez, J.C., Watts, C.J., Lizarraga-Celaya, C., Chehbouni, A., 2021. Parameterization of the AquaCrop model for simulating table grapes growth and water productivity in an arid region of Mexico. Agric. Water Manag., 245, 1-10.

Ezzine, H., Metougui, M.L., Boukcim, H., Abbas, Y., 2023. Physiological responses of three field-grown species (*Ceratonia siliqua, Eucalyptus camaldulensis*, and *Moringa oleifera*) to water deficits in a Mediterranean semi-arid climate. Sci. Rep., 13, 1-10.

FAO, 2023. Chapter 2. Users guide. AquaCrop Version 7.1. Reference manual. Food and Agriculture Organization (FAO) of the United Nations, 1-370.

Feng, D., Li, G., Wang, D., Wulazibieke, M., Cai, M., Kang, J., Yuan, Z., Xu, H., 2022. Evaluation of AquaCrop model performance under mulched drip irrigation for maize in Northeast China. Agric. Water Manag., 261, 1-10.

Gopalakrishnan, L., Doriya, K., Kumar, D.S., 2016. *Moringa oleifera*: A review on nutritive importance and its medicinal application. Food Sci. Hum. Wellness, 5, 49-56.

Grosshagauer, S., Pirkwieser, P., Kraemer, K., Somoza, V., 2021. The future of Moringa foods: a food chemistry perspective. FRONT NUTR, 8, 1-9.

Ibraimo, N.A., Taylor, N.J., Steyn, J.M., Gush, M.B., Annandale, J.G., 2016. Estimating water use of mature pecan orchards: A six stage crop growth curve approach. Agric. Water Manag., 177, 359-368.

Jadon, A., Patil, A., Jadon, S., 2022. A comprehensive survey of regression based loss

functions for time series forecasting. arXiv:2211.02989v1 [cs.LG], 1-13.

Jalil, A., Akhtar, F., Awan, U.K., 2020. Evaluation of the AquaCrop model for winter wheat under different irrigation optimization strategies at the downstream Kabul River Basin of Afghanistan. Agric. Water Manag., 240, 1-8.

Jo, W.J., Shin, J.H., 2021. Development of a transpiration model for precise tomato (*Solanum lycopersicum* L.) irrigation control under various environmental conditions in greenhouse. Plant Physiol. Biochem., 162, 388-394.

Kisekka, I., De Jonge, K.C., Ma, L., Paz, J., Douglas-Mankin, K., 2017. Crop modeling applications in agricultural water management. Transactions of the ASABE, 60(6), 1959-1964.

Li, L., Chen, S., Yang, C., Meng, F., Sigrimis, N., 2020. Prediction of plant transpiration from environmental parameters and relative leaf area index using the random forest regression algorithm. J. Clean. Prod., 261, 1-13.

Martínez-Romero, A., L'opez-Urrea, R., Montoya, F., Pardo, J.J., Domínguez, A., 2021. Optimization of irrigation scheduling for barley crop, combining AquaCrop and MOPECO models to simulate various water-deficit regimes. Agric. Water Manag., 258, 1-16.

Mokgehle, S., Araya N., Mofokeng, M., Makgato, M., Amoo, S., Maboka, K., du Plooy and Araya, H., 2022. Regrowth response and nutritional composition of *Moringa oleifera* to cutting back in three agro-ecological zones in South Africa. Horticulturae, 8(963), 1-11.

Mulovhedzi, N.E., Araya, N.A., Mengistu, M.G., Fessehazion, M.K., du Plooy, C.P., Araya H.T., van der Laan, M., 2020. Estimating evapotranspiration and determining crop coefficients of irrigated sweet potato (*Ipomoea batatas*) grown in a semi-arid climate. Agric. Water Manag., 233, 1-9.

Muhl, Q.E., Toit, E.S., Robbertse, P.J., 2011. *Moringa oleifera* (Horseradish tree) leaf adaptation to temperature regimes. Int J Agric Biol ., 13, 1021-1024.

Muhl, Q.E., du Toit, E.S., Steyn, J.M., Apostolides, Z., 2013. Bud development, flowering and fruit set of *Moringa oleifera* Lam. (Horseradish Tree) as affected by various irrigation levels. JARTS, 114(2), 79-87.

Nash, J. E., Sutcliffe, J. V., 1970. River flow forecasting through conceptual models part I — A discussion of principles. J. Hydrol. 10, 282-290.

Nyathi, M.K., van Halsema, G.E., Annandale, J.G., Struik, P.C., 2018. Calibration and validation of the AquaCrop model for repeatedly harvested leafy vegetables grown under different irrigation regimes. Agric. Water Manag., 208, 107-119.

Nyathi, M.K., Mabhaudhi, T., Van Halsema, G.E., Annandale, J.G., Struik, P.C., 2019. Benchmarking nutritional water productivity of twenty vegetables – A review. Agric. Water Manag., 221, 248-259.

Nunes, H.G.G.C., Farias, V.D.S., Sousa, D.P., Costa, D.L.P., Pinto, J.V.N., Moura, V.B., Teixeira, E.O., Lima, M.J.A., Ortega-Farias, S., Souza, P.J.O.P., 2021. Parameterization of the AquaCrop model for cowpea and assessing the impact of sowing dates normally used on yield. Agric. Water Manag., 252, 1-14.

Poppe, M., 2016. Simulating the water footprint of woodies in Aquacrop and Apex. Master Thesis, University of Twente, Water Engineering and Management, 1-102.

Raes, D., Steduto, P., Hsiao, T.C., Fereres, E., 2023. AquaCrop Version 7.1. Chapter 3 Calculation procedures. Reference manual. Food and Agriculture Organization (FAO) of the United Nations, 1-163.

Steduto, P., Raes, D., Hsiao, T.C., Fereres, E., Heng, L., Izzi, G., Hoogeveen, J., 2008. AquaCrop: a new model for crop prediction under water deficit conditions.

Shyamli, P.S., Pradhan, S., Panda, M., Parida, A., 2021. De novo whole-genome assembly of *Moringa oleifera* helps identify genes regulating drought stress tolerance. Front. Plant Sci., 12, 1-14.

Steduto, P., Raes, D., Hsiao, T.C., Fereres, E., Heng, L., Izzi, G., Hoogeveen, J., 2014. AquaCrop: a new model for crop prediction under water deficit conditions. Options Méditerranéennes, Series A (80), 285-292.

Singh, J., Knapp, H.V., Arnold, J.G., Demissie, M.. 2005. Hydrologic modeling of the Iroquois River watershed using HSPF and SWAT. J. American Water Resources Assoc. 41(2): 361-375.

Swanson, D.A., 2015. On the relationship among values of the same summary measure of error when it is used across multiple characteristics at the same point in time: An examination of MALPE and MAPE. Review of Economics & Finance. ID: 1923-7529-2015-03-01-14, 1-14.

Wang, H., Cheng, M., Liao, Z., Guo, J., Zhang, F., Fan, J., Feng, H., Yang, Q., Wu, L., Wang, X., 2023. Performance evaluation of AquaCrop and DSSAT-SUBSTOR-Potato models in simulating potato growth, yield and water productivity under various drip fertigation regimes. Water Manag., 276, 1-20.

Wellens, J., Raes, D., Fereres, E., Diels, J., Coppye, C., Adiele, J.G., Ezui, K.S.G., Becerra, L., Selvaraj, M.G., Dercon, G., Heng, L.K., 2022. Calibration and validation of the FAO AquaCrop water productivity model for cassava (*Manihot esculenta* Crantz). Agric. Water Manag., 263, 1-10.

Willmott, C.J., Matsuura, K., 2005. Advantages of the mean absolute error (MAE) over the root mean square error (RMSE) in assessing average model performance. Clim. Res. 30, 79-82.

Zhang, C., Xie, Z., Wang, Q., Tang, M., Feng, S., Cai, H., 2022. AquaCrop modeling to explore optimal irrigation of winter wheat for improving grain yield and water productivity. Agric. Water Manag., 263, 1-10.

Zeleke, K.T., Wade, L.J., 2012. Evapotranspiration estimation using soil water balance, weather and crop data. Evapotranspiration – Remote Sensing and Modeling, pg 41-58.

CHAPTER 3

DAILY DETERMINATION OF MORINGA EVAPOTRANSPIRATION AND CROP COEFFICIENTS USING THE EDDY COVARIANCE TECHNIQUE

Nadia Araya[1,2], Mduduzi Sithole[1], Ntsieni Mulovhedzi[1,4,5], Macdex Mutema[2], Alistair Clulow[3,4], Michael Savage[4] and Ian du Plooy[1]

[1]Agricultural Research Council – Vegetable, Industrial and Medicinal Plants, Private bag X293, Pretoria, 0001, South Africa
[2]Agricultural Research Council – Natural Resources and Engineering, Private bag X79, Pretoria, 0001, South Africa
[3]Centre for Water Resources Research, School of Agricultural, Earth and Environmental Sciences, University of KwaZulu-Natal, Pietermaritzburg, South Africa.
[4]Discipline of Agrometeorology, School of Agricultural, Earth and Environmental Sciences, University of KwaZulu-Natal, Pietermaritzburg 3209, South Africa
[5]School of Agricultural Sciences, University of Mpumalanga, Private bag X11283, Mbombela, 1200, South Africa

3.1 INTRODUCTION

Moringa (*Moringa oleifera* Lam.) is considered a drought-tolerant crop, capable of surviving dry seasons and prolonged dry spells. This is mainly due to its long tuberous taproot that grows very deep into the soil to absorb water and minerals from the sub-soils (Mashamait et al., 2021). A study conducted on deficit irrigation in a semi-arid climatic region, revealed the best performance of Moringa under reduced water supply (low irrigation of 300 mm/annum resulted in high bud initiation, although fruit set was delayed compared to 600 and 900 mm/annum, Mashamait et al., 2021). Similarly, greater water use efficiency was observed for Moringa grown for leaf production when irrigation was maintained at 60% depletion from maximum plant available water (Mulovhedzi et al., 2019). These studies have shown that it is necessary to limit water supply to enhance re-branching and flower initiation prior to floral initiation, but this should be followed by sufficient irrigation to ensure pollination, fruit set, and high pod yield (Mashamait et al., 2021). Therefore, there is a need to accurately quantify Moringa water use throughout the entire growing period, especially for pod production. This would enable an assessment of the variability of crop water needs as influenced by differences in growth stages and weather conditions.

Several methods have been used to measure crop water use, which vary in their degree of accuracy, complexity and affordability. According to Rana and Katerji (2000) and Allen et al. (2011a), these methods can be grouped into different categories based on their specific approaches to determine crop water use. These include hydrological approaches (lysimetry and soil water balance), micrometeorological approaches (energy balance: Bowen ratio, eddy covariance, surface renewal and scintillometry methods), remote sensing (remote sensing energy balance and satellite-based crop ET using vegetation index methods from satellite images or aerial photography) and plant physiology approaches (sap flow/sap flux density methods and chamber systems). Most of these methods, such as the energy balance and micrometeorological methods, are demanding in terms of the accuracy of measurements and operation skills, require expensive equipment and very often difficult to deploy them in remote areas or to use them to create large networks to monitor spatio-temporal changes. Despite these limitations, it is still very important to conduct crop water use measurements in order to characterize water use in tree crops and identify the most relevant driving factors. This will enable analysis of irrigation efficiencies and scheduling, in addition to parameterization and validation of crop models for the estimation of crop water use. The eddy covariance method is amongst the most popular technologies for determining field-scale crop ET.

The eddy covariance method obtains turbulent ET flux data by calculating the covariance of fluctuations in the vertical wind velocity and in the physical quantity to be measured (Foken et al., 2012). The covariance of vertical wind speed and vapour density over a 30 min or an hourly time-scale gives a direct estimate of latent heat flux (LE), which is equivalent to actual crop ET (Rana and Katerji, 2000). Instantaneous values of wind speed can be measured using a sonic anemometer, while vapour density can be obtained using a fast response hygrometer or an infrared gas analyser. Both measurements are performed at a typical frequency of 5-20 Hz (Rana and Katerji, 2000). The use of a fast response hygrometer to measure vapor density can be expensive and can create high-frequency fallout caused by the physical separation of the hygrometer from the sonic anemometer. As a result, LE is normally computed as a residual of the energy balance to avoid this problem, thus making accurate measurements of net radiation and soil heat flux (G), as well as air temperature and wind speed which are used to compute sensible heat (H), extremely important in order to minimize the closure error (Allen et al., 2011a). Alternatively, LE can be obtained through direct measurements using an infrared gas analyser (IRGA), which in some designs is incorporated into the 3D sonic anemometer. In both methods to obtain LE, the lack of closure in the energy balance obtained using the eddy covariance technique is still a common problem (Allen et al., 2011a). As a rule, estimates of the scalar turbulent fluxes of H and LE are generally underestimated and the available energy (Rn + G) is usually overestimated (Wilson et al., 2002; Foken, 2008). The lack of closure of the energy balance has implications for how energy flux measurements should be interpreted and how these estimates should be compared with model simulations (Foken, 2008).

The energy balance closure is typically poor during nocturnal periods due to weak turbulent mixing, and better during daytime periods (afternoons better than mornings), possibly suggesting the underestimation of storage terms, which are usually larger in the mornings (Wilson et al., 2002). Several other possible causes of lack of closure in the energy balance have been suggested, such as horizontal advection, energy used by photosynthesis, change in storage of heat in the developing boundary layer below the instrumentation (causing flux divergence), frequency response of the sensor, separation and misalignment of sensors, error or bias in Rn or G measurement and insufficient fetch (the upwind distance from the tower with uniform features required to ensure that the measurement is representative of the underlying surface, usually set at a minimum of 1:100 m as a rule of Thumb or 100 m of upwind distance of vegetation for every metre above the ground up to the uppermost temperature and/or humidity sensor (Mahrt, 1998; Twine et al., 2000; Stewart and Howell, 2003; Allen et al., 2011a; Foken, 2008).

In general, the discrepancy in energy balance closure is a bias that varies from 0 to 30% (Twine et al., 2000). Wilson et al. (2002) found an average lack of closure of 20%, which prevailed in all the different vegetation types monitored and under climatic conditions ranging from Mediterranean to temperate and arctic; while Wang et al. (2020) determined a closure error of 22% over wheat and maize fields cultivated on a rotational basis in North China Plain. Contrarily, ET measurements conducted in South Africa over a sweet potato field revealed much higher closure error (around 47%), which was attributed to several factors including malfunctions of sensors during rainfall conditions (Mulovhedzi et al., 2020). The magnitude of this discrepancy in the energy balance closure can be assessed using various methods reported in the literature (Twine et al., 2000; Wilson et al., 2002; Harper, 2014). One of the most common methods to assess the energy balance closure error is through the calculation of the energy balance ratio (EBR), which is the ratio between cumulative sums of LE + H and Rn – G, with EBR = 1 representing full closure (Twine et al., 2000). The energy balance closure error is often resolved assuming that the Bowen ratio (β) is measured accurately by the eddy covariance system and adjusting both LE and H to preserve β and conserve energy (Twine et al., 2000; Consoli and Papa, 2013).

The eddy covariance system has similar advantages to the Bowen ratio energy balance method. Both methods can also be used indirectly to determine soil evaporation (E_s) from a cropped field, as the difference between measured crop ET and transpiration (T) measured with a sap flow method (Zeggaf et al., 2008; Holland et al., 2013). However, like most methods, it also has disadvantages which include a high number of corrections needed in order to obtain accurate estimates of crop ET, the energy balance closure error is often in the range of 10-30% and it requires substantial fetch (generally between 50-100 times the height of the instruments above the zero-plane displacement height) (Allen et al., 2011a). Accurate measurements of crop ET can, however, be done using the eddy covariance system, provided that the basic requirements are fulfilled, which include the following (Allen et al., 2011a; Allen et al., 2011b): establishment of an adequate fetch; sufficient elevation of the instrumentation above the canopy to reduce roughness sub-layer distortions and to increase eddy size to match the sensor path length; corrections of the eddy covariance flux measurements and use of qualified personnel, with knowledge of physics of turbulence.

The accuracy and representativeness of crop ET measurements conducted using the eddy covariance technique make it possible to determine a crop coefficient, which integrates the effects of characteristics that distinguish field crops from a well-managed, short grass surface. Such crop coefficients have tremendous potential in guiding irrigation scheduling and improving the efficiency of water resources utilization, particularly in water-scarce countries like South Africa.

3.1.1 Study aim

- The aim of this study is to determine Moringa evapotranspiration and crop coefficients on a daily basis using the eddy covariance technique, to validate satellite-based remote sensing ET estimates, with the ultimate goal of improving irrigation scheduling and water resources planning at the farm-scale across different climatic conditions in South Africa.

3.1.2 Study objectives

- To quantify evapotranspiration and water use efficiency of Moringa grown in different semi-arid regions;
- To estimate K_c values of Moringa under varying climatic conditions;
- To assess the usefulness of the FAO-56 single crop coefficient approach to estimate evapotranspiration and irrigation water requirement of Moringa.

3.2 RESEARCH METHODOLOGY

3.2.1 Description of the study site

In-situ evapotranspiration measurements are being conducted using the eddy covariance technique on a commercial Moringa farm located in the district of Capricorn, Tooseng, Limpopo Province (24° 26' 59'' S, 29° 32' 58'' E, 822 m above sea level (masl)). These in-situ measurements of crop ET will be used to parameterize and validate remote sensing cloud-based computing models of crop water use. The site has a 1.4-ha (120 x 120 m) Moringa farm, including an agro-processing facility owned by a sole emerging commercial farmer (Figure 3.1). The field is mostly composed of *Moringa oleifera* trees, which were planted in 2013 with a tree spacing of 2 x 2 m (Figure 3.2). The farm is equipped with a drip irrigation system (one dripper per tree delivering 1.6 L of water per hour). A monocropping production system is used, with organic fertilization and planting basins around each tree to optimize rainfall and irrigation water utilization. Weed control is usually done using a grass mower and brush cutters.

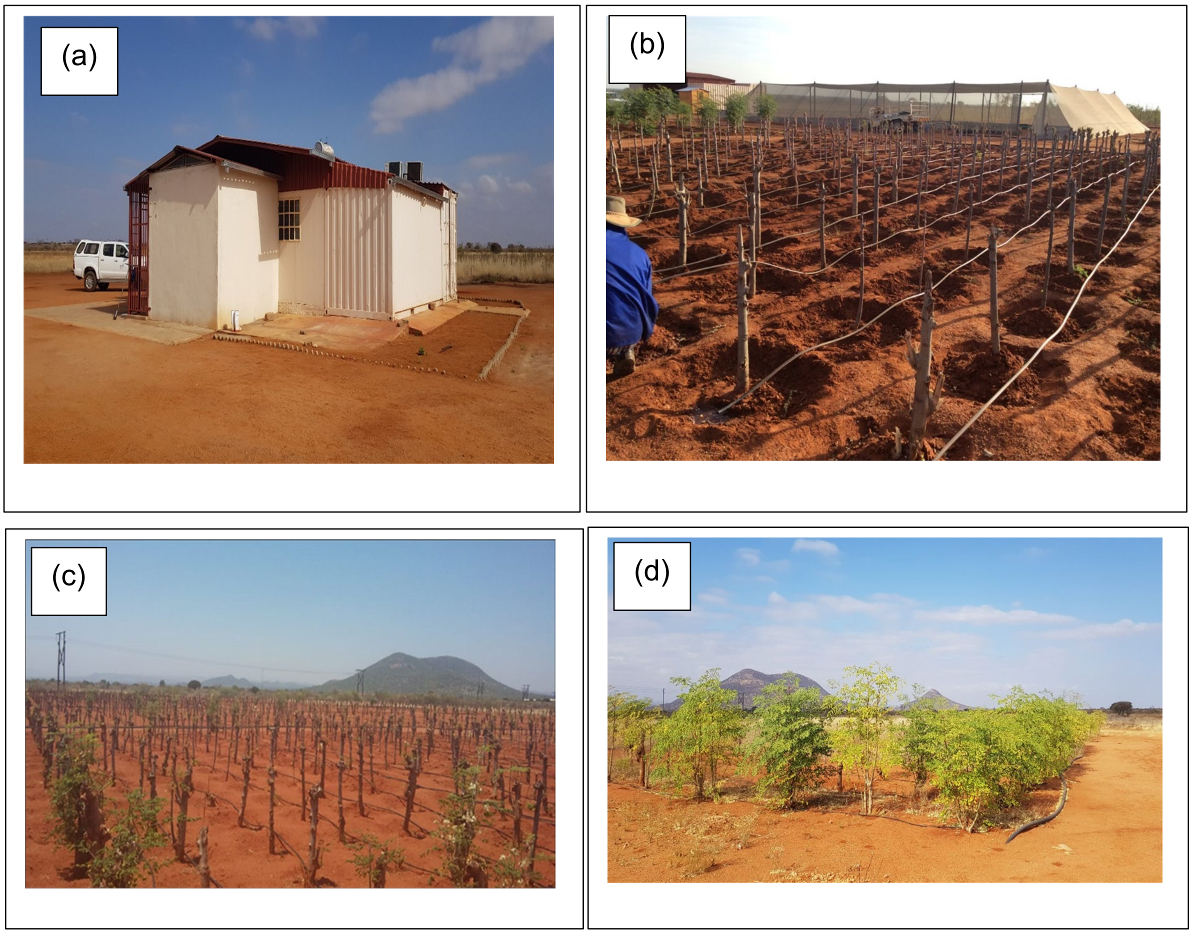

Figure 3.1: Agro-processing facility for drying, grinding and packaging fresh harvestable leaves and pods of Moringa for product development (a); In-situ rainwater harvesting with planting basins around trees (b); A pressure-compensated drip

Figure 3.2: An 8-year old Moringa stand established in 2013 at Tooseng research site, Limpopo province (Picture taken by Mr Ntsieni Mulovhedzi in December 2021).

Based on long-term climatic data for the site, monthly averages of minimum temperatures vary between 3.4°C in July and 20.5°C in January, while maximum temperatures vary 24.5°C in July and 33.0°C in February (Figure 3.3). The wettest month (with the highest rainfall) is January (74 mm), while the driest month (with the least rainfall) is July (0 mm). The site receives a total of 448 mm of rainfall and 1433 mm of reference evapotranspiration annually, resulting in a water deficit of 985 mm (69% shortage of water supply).

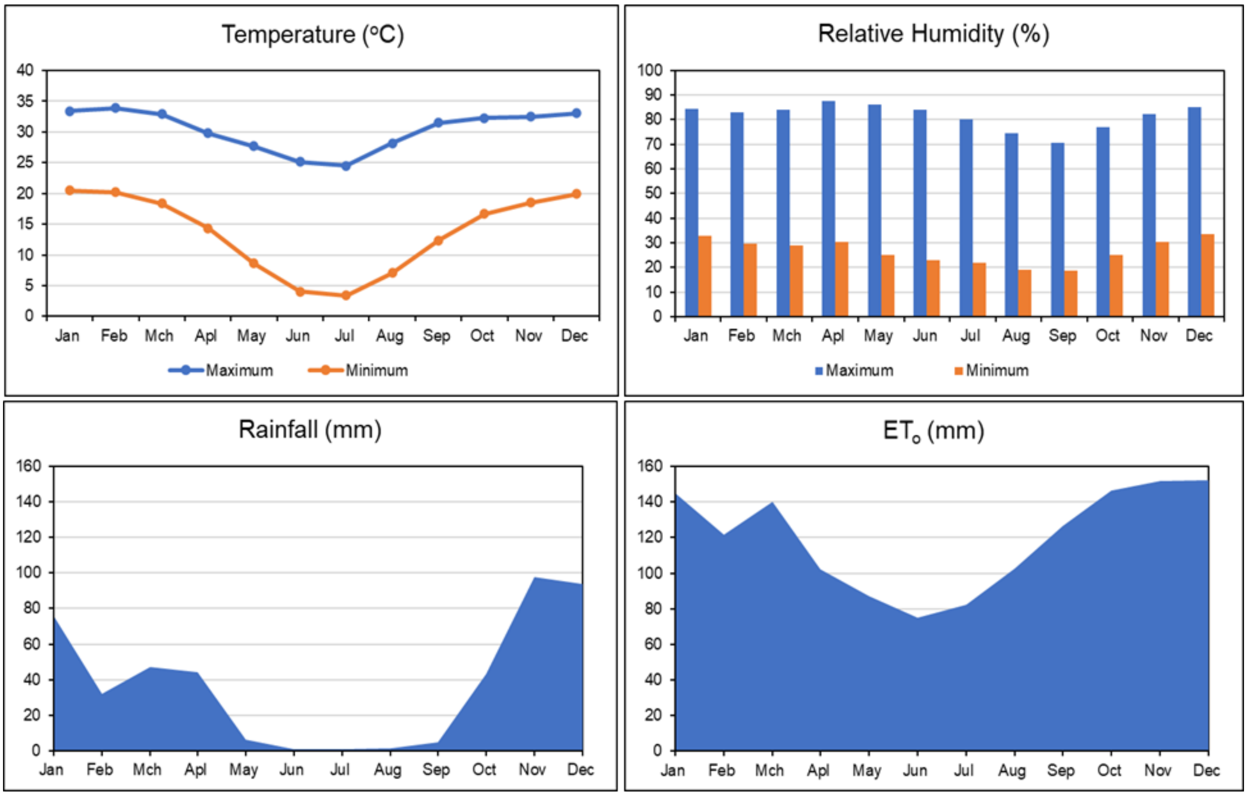

Figure 3.3: Long-term (15 years) monthly average data of temperature and humidity and totals of rainfall and reference evapotranspiration (ET_o) at Tooseng research site, South Africa (Data supplied by ARC, Institute for Soil, Climate and Water).

Prior to the commencement of the trial (December 2021), soil samples were collected for 0-30, 30-60 and 60-90 cm soil layers, and sent to the Institute for Soil, Climate and Water of the ARC for analysis of chemical and physical soil properties. Table 3.1 presents the obtained results. The soil at the study site has a loamy sand texture with 78-84% sand, 2-4% silt and 14-18% clay (Figure 3.4). The macro and micronutrient composition is relatively low, which warrants the need for supplemental fertilization. The Moringa industry is generally organic and, as a result, farmers are very sceptical to apply inorganic fertilizers. The research team will therefore recommend to the farmer an application of organic soil amendments such as Bone Meal or Bat Guano commercial fertilizer in order to improve the fertility of the soil. These fertilizers are rich in minerals, calcium, phosphorus, iron, magnesium and zinc.

Table 3.1: Soil chemical and physical properties for 0-30, 30-60 and 60-90 cm soil profile layers at Tooseng study site prior to the commencement of the trial during the 2021/22 growing season.

Chemical elements	**Units**	**0-30 cm soil layer**	**30-60 cm soil layer**	**60-90 cm soil layer**
Phosphorous (P)-Bray 1	mg kg^{-1}	0.79	0.58	0.26
Potassium (K)	mg kg^{-1}	124.00	109.00	96.30
Calcium (Ca)	mg kg^{-1}	549.00	425.00	519.00
Magnesium (Mg)	mg kg^{-1}	230.00	188.00	258.00
Sodium (Na)	mg kg^{-1}	21.40	14.50	16.00
Iron (Fe)	mg kg^{-1}	8.42	8.50	10.50
Zinc (Zn)	mg kg^{-1}	0.39	0.27	0.14
Manganese (Mn)	mg kg^{-1}	15.00	15.50	17.70
Copper (Cu)	mg kg^{-1}	1.72	1.57	1.88
Organic matter	%	1.42	1.38	1.64
pH (H_2O)	-	7.57	6.91	6.64
Physical properties				
Sand	%	84.00	84.00	78.00
Silt	%	2.00	2.00	4.00
Clay	%	14.00	14.00	18.00
Soil type	-	Loamy sand	Loamy sand	Loamy sand
Bulk density	Ton m^{-3}	1.37	1.47	1.37
Field capacity	m^3 m^{-3}	0.19	0.19	0.19
Permanent wilting point	m^3 m^{-3}	0.10	0.10	0.10

Figure 3.4: A 1.0 m soil profile being excavated to collect soil samples prior to the beginning of the trial at Tooseng, Limpopo province (Picture taken by Mr Ntsieni Mulovhedzi).

3.2.2 Installation of the eddy covariance system

A complete open-path eddy covariance system (EC 150, Campbell Scientific Inc., Logan, Utah, USA) was installed to quantify crop ET directly and indirectly. Three dimensional wind velocity and temperature fluctuations were measured using a CSAT3 sonic anemometer (Campbell Scientific Inc., Logan, Utah, USA). Water vapour concentration was measured using a fast-response EC 150 CO_2 / H_2O open-path gas analyser (Campbell Scientific. Inc., Logan, Utah, USA) as part of the EC system. The EC data was logged at 30 minute intervals, with subsequent storage in a CR5000 data logger (Campbell Scientific Inc., Logan, Utah USA). Additional sensors including an NR-Lite net radiometer (Kipp and Zonen, delft, The Netherlands), thermocouples, a time domain reflectometer (TDR) and soil heat flux plates were used for measuring the remaining components of the energy balance in order to complete the energy balance equation. In the beginning of the measurements (17 December 2021), all sensors were installed at a height of 2.0 m above the 1.5 m canopy height and thereafter, the placement of sensors was increased to 2.6 m (around mid-February) when the trees attained a height of 2.1 m. All sensors were placed on a 6 m tower which was situated around the middle of the plot, but closer to the one end where the prevailing wind dominates (facing North) in Tooseng, Limpopo province. This was done to obtain enough fetch for the EC measurements accounting for all desired wind directions and atmospheric stabilities in order to improve the energy balance closure. Thus, considering the standard rule of thumb for fetch requirement on eddy covariance systems (100:1), the Moringa stand had at least 50 m of a homogeneous and flat upwind surface towards the desired wind direction and atmospheric stability. Three soil heat flux plates (HFT-S, REBS, Seattle, WA) were installed at the depth of 0.08 m below the soil surface and thermocouple soil temperature averaging probes were installed at the depths of 0.02 and 0.06 m to measure the heat stored above soil heat flux plates. Volumetric soil water content for the top 0.06 m soil is being measured using two CS616 probes. The EC system estimates sensible heat fluxes (H) based on measurements of the turbulent boundary layer above the canopy (Rana and Katerji, 2000). The air flow is assumed to be made up of a large number of eddies, each having three-dimensional components (horizontal and vertical) (Nagler et al., 2005). The sensors installed on the tower measure water content of the air, vertical component of wind speed, and air temperature at 10 Hz. Direct ET measurements are done using a 3-D sonic anemometer and an open-path gas analyser, while the indirect measurements are achieved using the shortened energy balance equation. Figure 3.5 illustrates a complete EC system installed on an 8-year old Moringa stand at Tooseng research site, Limpopo province. The data is averaged every 30 min (Nagler et al., 2005).

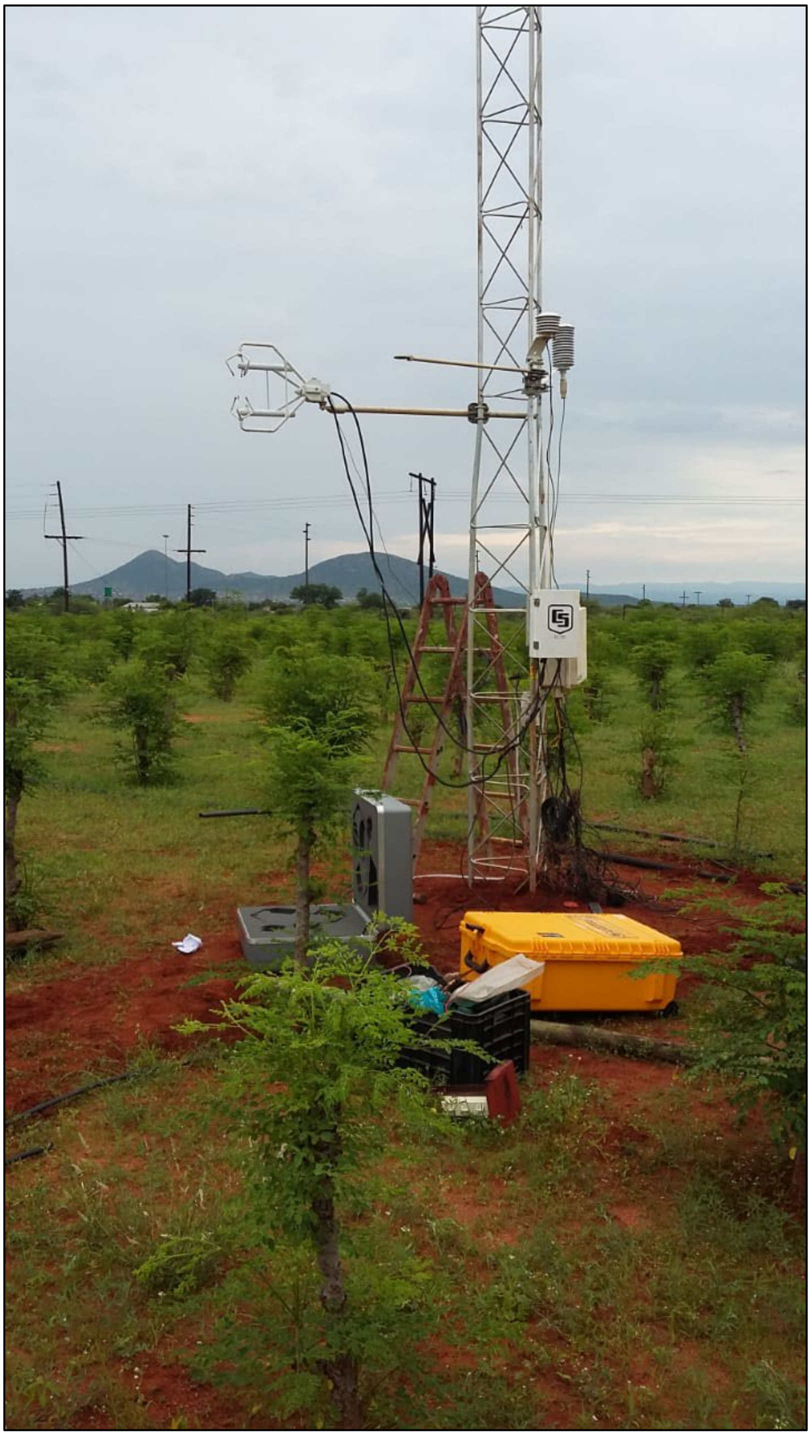

Figure 3.5: A complete eddy covariance system installed on an 8-year old Moringa stand to measure evapotranspiration at Tooseng research site, Limpopo province (Picture taken by Mr Ntsieni Mulovhedzi).

The EC flux measurements allow crop ET to be calculated directly, whereas additional instruments allow the surface energy balance to be calculated indirectly, as indicated in Equation 1 (Twine et al., 2000). These measurements will be conducted throughout the entire experimental period to check the validity of ET measurements in order to assess the energy balance closure using the Bowen ratio method, as described by Twine et al. (2000).

$$Rn - G = LE + H \tag{3.1}$$

where Rn is the net radiation measured above the canopy using a net radiometer, G is soil heat flux measured using soil heat flux plates, LE is latent energy flux (evaporation multiplied by the latent heat of vaporization) which was measured using an open path gas analyzer, H is sensible heat flux measured using a sonic temperature sensor.

Daily ET (mm day^{-1}) was calculated from LE measured using the EC system following the equation below:

$$ET\ (\text{mm day}^{-1}) = 86400 \times (LE/(\lambda \rho w) \tag{3.2}$$

where LE (W m^{-2}) is the 24-h sum of latent heat fluxes measured using the EC system, λ is the specific latent heat of vaporization of water per unit mass (2.454 MJ kg^{-1}), and ρw (kg m^{-3}) is the density of water. The factor 86400 allows conversion from seconds to days.

3.2.3 Assessment of energy balance closure error

Surface energy balance closure for the EC system measurements was determined for the period of experimental measurements (three window periods from the 17th of December 2021 to the 8th of March 2022) at the half-hourly time scale. Estimates of the turbulent fluxes (LE + H) from the EC system were subsequently compared to estimates of the available energy (R_n – G) using the energy balance method in order to determine the energy balance closure using the Bowen ratio method (Twine et al., 2000; Wilson et al., 2002; Nagler et al., 2005). This method assumes that R_n – G was correctly measured by the EC system, so that both values of H + LE could be increased according to the ratio of H and LE in order to balance Equation (1), as described by Blanken et al. (1997) and Twine et al. (2000). Where unacceptable energy balance closure error was found (above 30%), adjustments were considered by computing the difference between (LE + H) and (R_n – G) flux values measured at the same time and divide the product by two. Then the final value would be used to compensate values of LE + H (Blanken et al., 1997; Twine et al., 2000; Cleverly et al., 2002; Hipps et al., 2002; Scott et al., 2004; Nagler et al., 2005).

The surface energy balance closure was analysed by plotting the sum between H + LE (turbulent fluxes) against the R_n – G (available energy) using good quality data for seven days during the measurement period (18th to 25th December 2021). Stannard et al. (1994) stated that if all components of energy balance are measured with accuracy, independently, and sum to zero, it shows that the EC measurements are good, and the energy balance equation is satisfied. In such a case, the linear equation of H + LE against R_n – G should have a slope close to one and an intercept close to zero.

3.2.4 Eddy covariance system footprint analysis

Most footprint models are based on the Monin-Obukhov stability length (Monin and Obukhov, 1954), a height-independent stability parameter, defined as:

$$L = \frac{T}{kg} \cdot \frac{\rho_{air} c_p}{H} \cdot u_*^3 \tag{3.3}$$

where T is the air temperature (K), In this expression, since the sensible heat flux density H is positive under "normal unstable" daytime conditions, L > 0. Some of the literature defines sensible heat flux density H as positive for these conditions. The Monin-Obukhov stability length L contains all of the parameters associated with free and forced convection except height z. The ratio k (z-d)/L is therefore regarded as an absolute dimensionless measure of stability at height z. The Monin-Obukhov stability length L (m), also referred to as the Obukhov length, has the dimensions of length and is essentially independent of height.

The Hsieh et al. (2000) model is analytically based, combines the results from a Lagrangian stochastic model and uses dimensional analysis. Their model results were in good agreement with those calculated by detailed Eulerian and Lagrangian models. They used eddy covariance (EC) latent energy flux density measurements collected along a transect as confirmation of the model estimates.

For their work using potatoes, a relatively short crop, Hsieh et al. (2000) ignored d and z_0 relative to z_m. This may result in negligible error for measurement heights about 2 m or more. However, for taller vegetation, d and z_0 cannot be ignored.

Their model involved redefining a length scale, z_u (m), for which Savage et al. (2004) showed:

$$z_u = (z_m - d) \cdot \frac{z_m - d}{z_m - (z_o + d)} \cdot \left(\ln\frac{z_m - d}{z_o} - 1 + \frac{z_o}{z_m - d}\right) \tag{3.4}$$

Using the outputs from the Lagrangian model of Thomson (1987), for a range of stability conditions,

In the vertical direction, the atmospheric boundary layer consists of the surface layer with approximately constant turbulent fluxes and the outer layer above. The surface layer is approximately 10% of the atmospheric boundary layer in vertical extent. It is in this lower 10% that MOST is applied. In terms of stability, the atmospheric boundary layer can be classified as convective, unstable, neutral, stable-continuous and stable-sporadic (Deardorff, 1978):

+ convective: (z-d)/L>0.5 for which buoyancy dominates. The vertical profiles of the mean wind speed and air temperature are almost uniform. The term "mixed layer" is therefore used to describe this state;

+ unstable: 0.02 < (z-d)/L ≤ 0.05 for which there may be significant wind shear;

+ neutral: -0.02 < (z-d)/L ≤ 0.02;

+ stable-continuous: -0.2 ≤ (z-d)/L < -0.02 for which turbulence is mechanically driven;

+ stable-sporadic: (z-d)/L < -0.2 for which only a very shallow layer next to the soil surface is turbulent in character.

The relationships have been extended to allow for a zero-plane displacement height.

Hsieh et al. (2000) expressed x/L, the horizontal distance x to the MO length L, as a function of their similarity parameters D and P, the ratio of the length scale z_u to L using:

D = 0.28 and P = 0.59 for unstable conditions,

D = 0.97 and P = 1 for near neutral and neutral conditions, and D = 2.44 and P = 1.33 for stable conditions.

Hence, the 90% fetch to measurement height ratio x/z_m is given by:

$$x/z_m = \frac{9.491}{k^2\, z_m} \cdot D\, z_u^P\, |L|^{1-P} \tag{3.5}$$

Hsieh et al. (2000) used a restricted condition for near neutral conditions, viz., $|z_u/L| < 0.04$. Using an approach similar to Calder (1952) and Gash (1986), they also showed that the peak location of the footprint, x_{peak} (m), can be calculated using:

$$x_{peak} = \frac{D\, z_u^P\, |L|^{1-P}}{2\, k^2} \tag{3.6}$$

The Hsieh et al. (2000) model is analytically based, combines the results from a Lagrangian stochastic model and uses dimensional analysis. Their model results were in good agreement with those calculated by detailed Eulerian and Lagrangian models. They used EC latent energy flux density measurements collected along a transect as confirmation of the model estimates.

The 90% fetch to measurement height ratio is given by:

$$x/z_m = \frac{2 \times 9.491}{z_m} \cdot x_{peak} \tag{3.7}$$

3.2.5 Determination of crop coefficients

Daily K_c values were calculated following the single crop coefficient method, as the ratio of crop ET measured by the EC system to the reference evapotranspiration (ET_o), following the equation below:

$$\mathrm{K_c} = \frac{\mathrm{ET}}{\mathrm{ET_o}} \tag{3.8}$$

ET_o was calculated according to the FAO Penman-Monteith equation using daily weather data measured at the study site (Allen et al., 1998):

$$\mathrm{ET_o} = \frac{0.408\Delta(\mathrm{Rn}-\mathrm{G})+\gamma\frac{900}{\mathrm{T}+273}\mathrm{u_2}(\mathrm{e_{s-e_a}})}{\Delta+\gamma(1+0.34\mathrm{u_2})} \tag{3.9}$$

where γ is the psychrometric constant (kPa °C^{-1}), T is air temperature at 2 m height (°C), u_2 is wind speed at 2 m height in (m s^{-1}), e_s is saturation vapour pressure (kPa), e_a is actual vapour pressure (kPa) and Δ is the slope of the vapour pressure curve (kPa °C^{-1}).

In this report, daily K_c values were reported only for the period when the crop was growing without infestation of pests (17 December 2021 to 31 January 2022).

3.2.6 Weather variability monitoring

Daily weather variables (wind speed, solar radiation, temperature, relative humidity, rainfall and reference evapotranspiration) were measured by an automatic weather station installed in close proximity to the experimental site. Additional in-situ measurements of air temperature, relative humidity and dew point were conducted and recorded every 30 min using a data logger

(Decagon Devices). A pyranometer (Decagon Devices) was installed in the open-field to measure the incident solar radiation at 30 min intervals.

3.2.7 Monitoring of changes in soil water content

Automated 10-HS capacitive soil water sensors were installed in one soil profile at depths of 0.30, 0.60 and 0.90 m to monitor changes in soil water content and advise on irrigation scheduling (Figure 3.6). The sensors were connected to an EM50 data logger (Decagon Devices) to automatically log the data at every 30 min interval.

Figure 3.6: Capacitative 10HS sensors connected to an EM50 data logger to monitor changes in soil water content up to 90 cm below the soil surface at Tooseng research site, Limpopo province (Picture taken by Dr Nadia Araya).

3.2.8 Recording of growth and yield crop parameters

Tree growth (leaf area index, plant height, stem circumference and diameter, tree depth and width) and yield parameters (fresh and dry weight of leaves) are being recorded at every harvest. The materials used for these measurements included a tape measure, scale, vernier caliper and ceptometer. Leaf fresh yield was measured on-site right after the harvest to avoid mass losses. To date, two harvests have been conducted since the beginning of the experimental period, on 17 December 2021 and 01 February 2022. Leaf dry yield was obtained by oven-drying fresh samples at 45°C for three consecutive days.

3.3 RESULTS AND DISCUSSION

3.3.1 Weather variability during the experimental period

During the experimental period (17 December 2021 to 08 March 2022), daily maximum air temperatures varied between 23 and 40°C, while minimum temperatures varied between 14 and 22°C. During the 100 days of experimental measurements, the atmospheric conditions were mostly composed of clear sky days (with solar radiation varying between 20 and 30 MJ m^{-2} day^{-1}, except for three days that were overcast with solar radiation decreasing to up to 5 MJ m^{-2} day^{-1}. Rainfall was quite well distributed from the 17th of December to the 29th of January, with a total of 100 mm. After this period, there was a prolonged dry spell of about one month until the 29th of February. The region receives a moderate wind, fluctuating between 0.23 and 1.04 m s^{-1} (Figure 3.7).

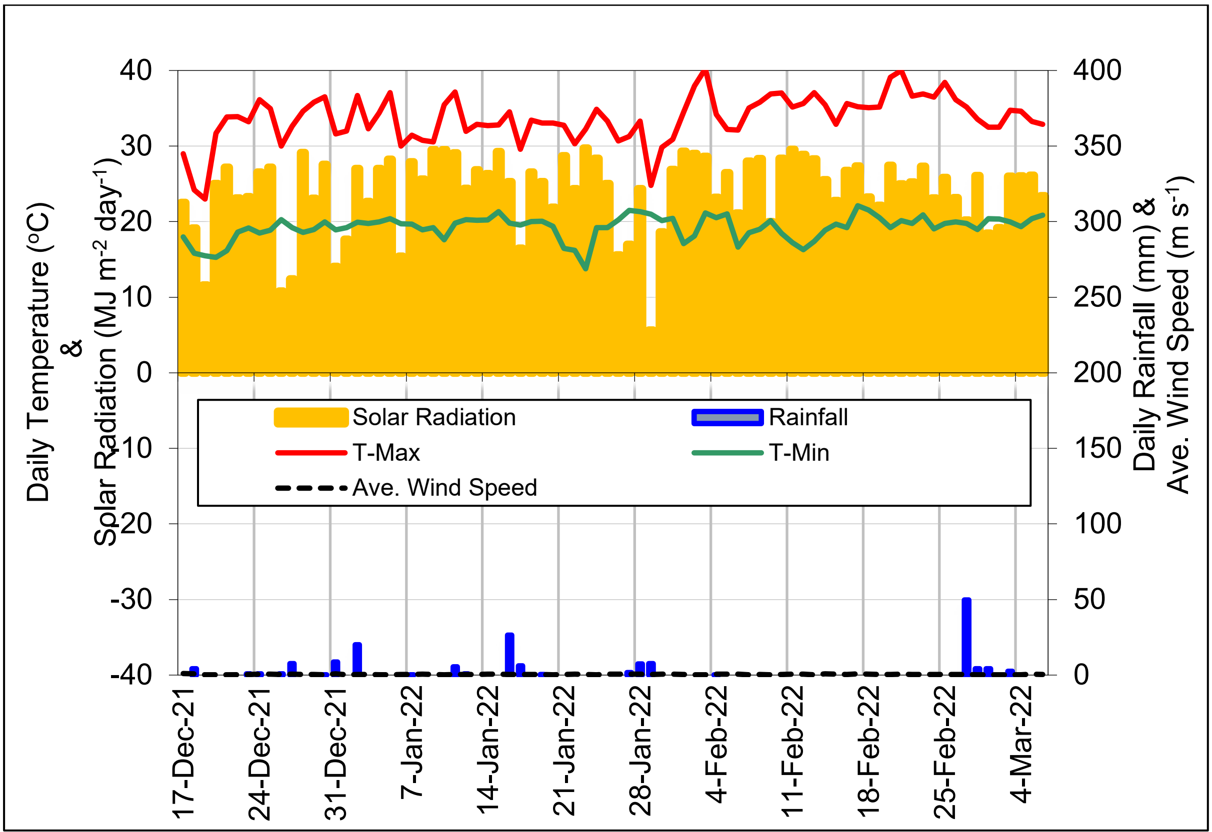

Figure 3.7: Weather variability during the experimental period (17 December 2021 to 08 March 2022) at Tooseng research site, Limpopo province.

Daily values of grass reference evapotranspiration (ET_o), which represent the condition of the atmospheric evaporative demand, were quite high almost during the entire experimental period, reaching a maximum of 6.3 mm day^{-1}, which was mainly explained by the occurrence of increased incident solar radiation during that day (the highest values observed during the experimental period). On cloudy and rainy days, ET_o decreased up to 1.26 mm day^{-1} (Figure 3.8).

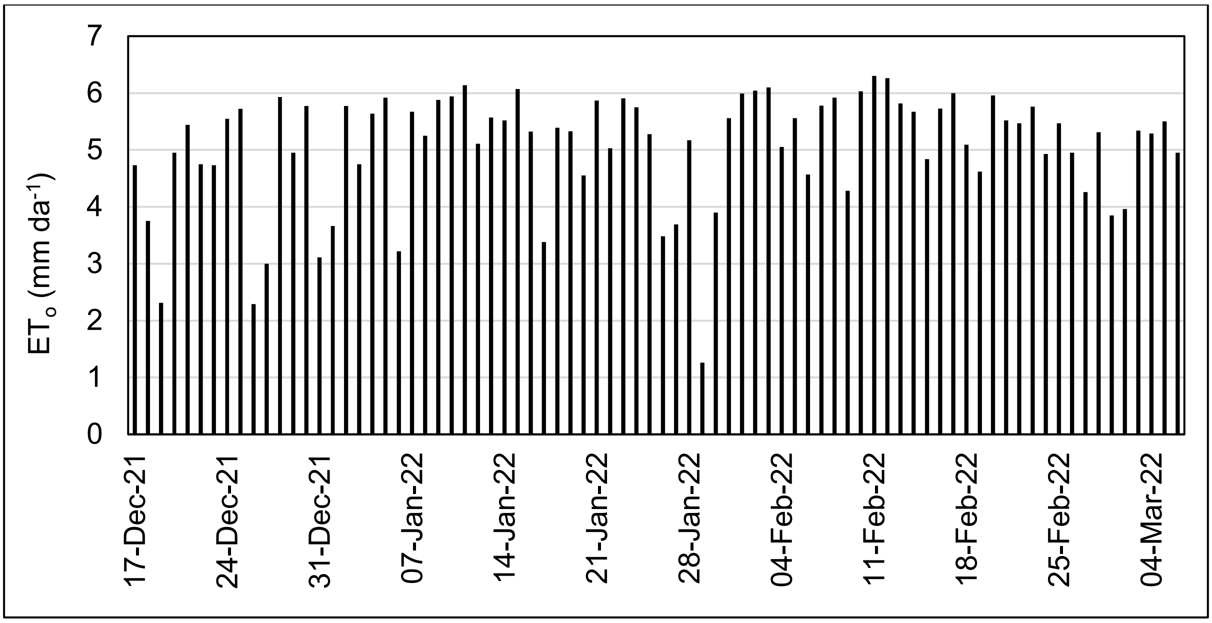

Figure 3.8: Reference evapotranspiration variability during the experimental period (17 December 2021 to 08 March 2022) at Tooseng research site, Limpopo province.

3.3.2 Water supply versus atmospheric demand during the experimental period

During the period when rainfall was reasonably well distributed (17 December to 29 January), there was typically no irrigation application. The total amount of irrigation (48 mm) was mostly applied during the dry period, from the 8th to the 23rd of February. Irrigation was applied through drip lines (one dripper per tree with a delivery rate of 1.6 litres per hour). Each irrigation event typically lasted for 6 h (Figure 3.9).

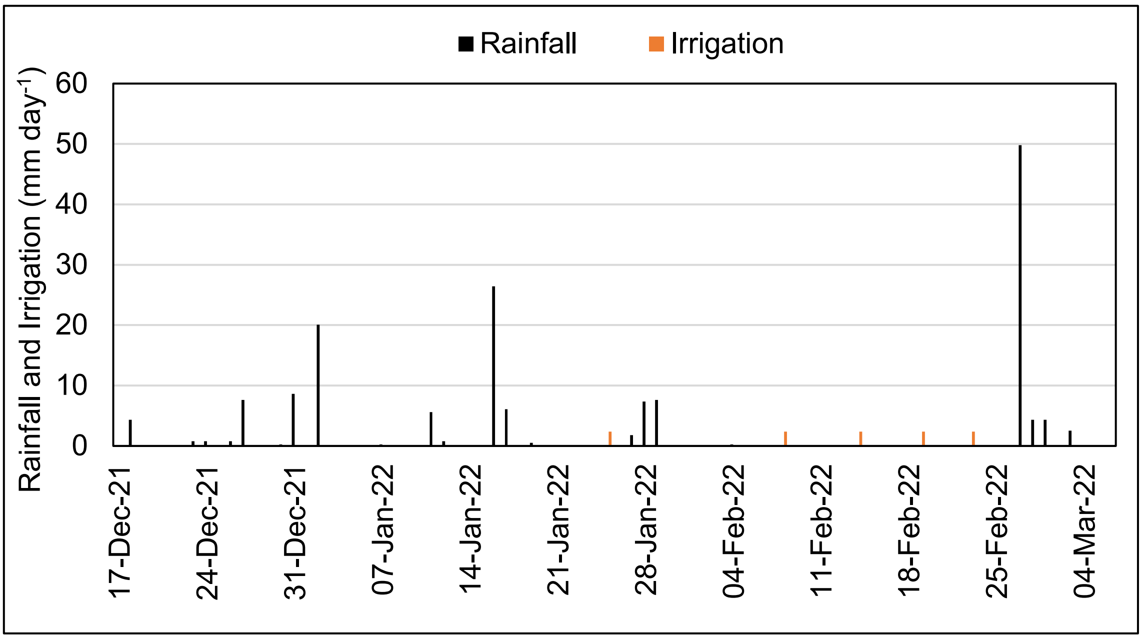

Figure 3.9: Daily rainfall and irrigation variability during the experimental period (17 December 2021 to 08 March 2022) at Tooseng research site, Limpopo province.

The total cumulative water supply (irrigation plus rainfall) was sufficient to meet the crop water demands (ET). However, it is important to note that the Moringa trees were well managed from the 17th of December until the end of January (period represented by a sharp increase of crop ET in Figure 3.10). After this period (from the beginning of February), there was an uncontrollable outbreak of bush crickets in the field, which devastated the Moringa plantation. The trees lost their leaves very rapidly, as crickets are active leaf feeders. This has impacted the Moringa water use research negatively. The amount of irrigation applied was only 20% of the total amount of water (rainfall plus irrigation) supplied to the Moringa stand.

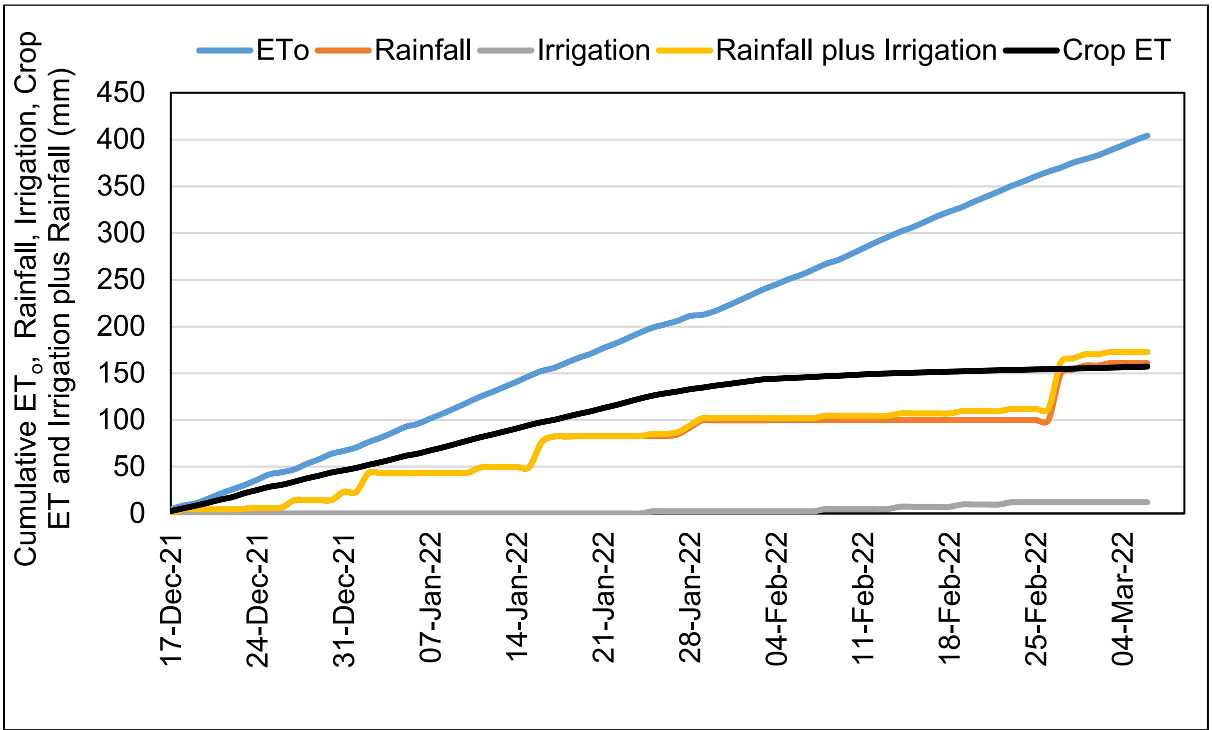

Figure 3.10: Cumulative reference evapotranspiration (ET_o), rainfall, irrigation, crop evapotranspiration (ET) and rainfall plus irrigation during the experimental period (17 December 2021 to 08 March 2022) at Tooseng research site, Limpopo province.

3.3.3 Changes in soil water content

The loamy sand soil at Tooseng study site has a relatively low water content at field capacity (0.19 m^3 m^{-3}). Although measurements of soil water content started later during the experimental period (24th February), it was possible to deduct that the 8-year old trees were not water stressed during this period. Volumetric soil water content for the top 10 to 60 cm (represented by the sensor installed at 45 cm) remained at 83 to 95% of field capacity (Figure 3.11b). However, the bottom layer (represented by the sensor installed at 75 cm), was under saturation for more than a week, which might have brought negative implications for root water and nutrient uptake due to reduced oxygenation. The data also suggests that, the loamy sand soil at Tooseng experimental site has a compacted layer below the 60 cm soil depth. Laboratory soil texture analysis results revealed lower sand and higher clay content at the bottom 60-90 cm soil layer. This soil condition might restrict root development and water uptake. The first 10 cm top layer on the other hand, dries out very fast, suggesting increased soil evaporation rates. Changes in soil water content following a reduction cycle show that soil evaporation varies from 1.1 to 1.6 mm per day. This corresponds to 26-38% of the daily ET, particularly after a rainfall or irrigation event.

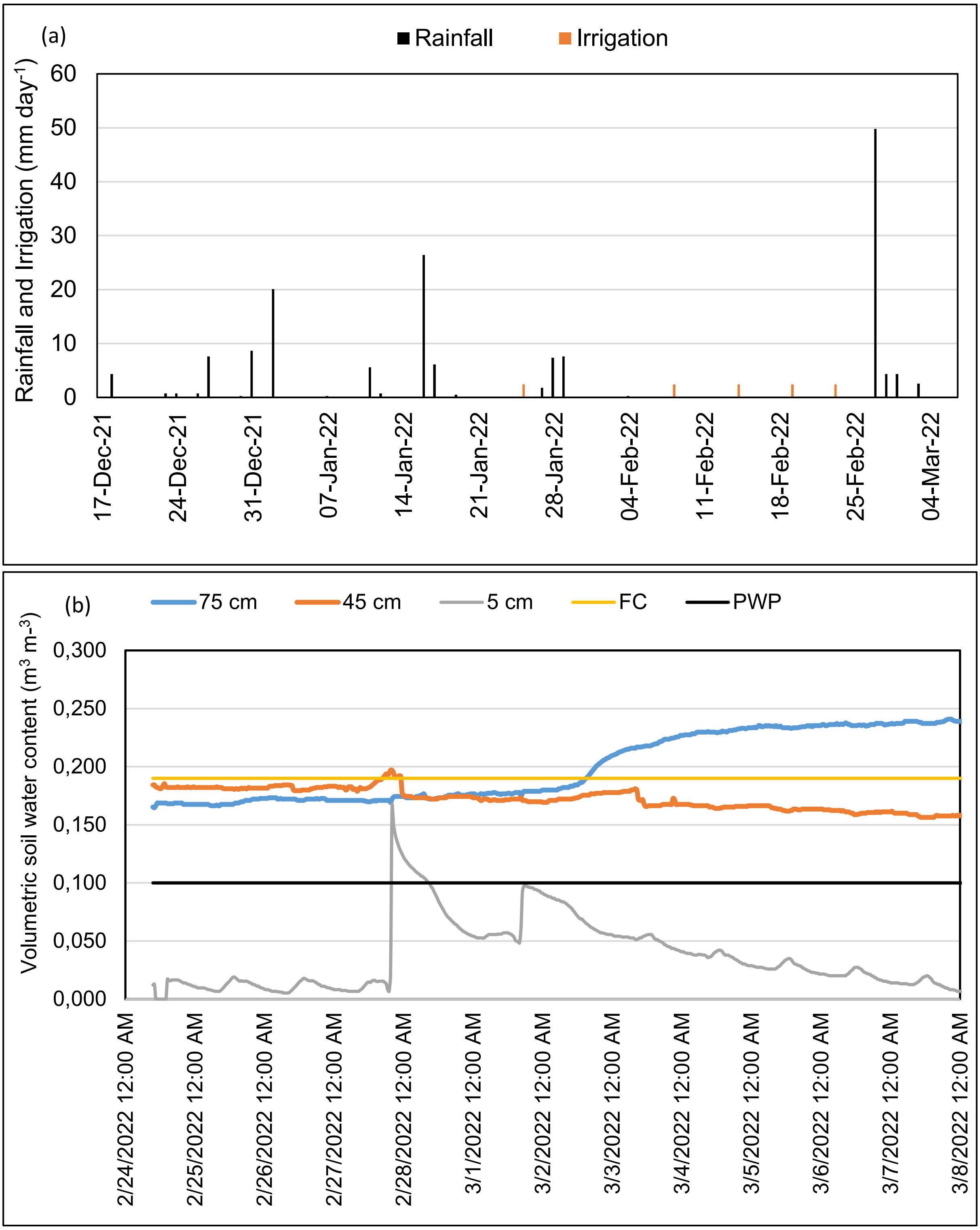

Figure 3.11: Changes in soil water content for the first 0-10, 10-60 and 60-90 cm soil layers (a), as influenced by rainfall and irrigation (b) during the experimental period (17 December 2021 to 08 March 2022) at Tooseng research site, Limpopo province. Volumetric water content at field capacity and permanent water content are also illustrated.

3.3.4 Surface energy balance closure for an 8-year-old Moringa stand in the Limpopo Province

Prior to data reporting on crop evapotranspiration, the surface energy balance closure was assessed to verify the accuracy of crop water use measurements using the eddy covariance technique (Figure 3.12). A perfect closure would result in the sum of the estimated latent energy (LE) and sensible heat flux (H) to be equivalent to the difference of net radiation (Rn) and soil heat flux (G). A perfect energy balance closure is impossible to obtain due to several factors, including possible occurrence of horizontal advection, energy used by photosynthesis, change in storage of heat in the developing boundary layer below the instrumentation (causing flux divergence), frequency response of the sensor, separation and misalignment of sensors, error or bias in Rn or G measurement and inadequate fetch that may occur in the field. Therefore, the data set obtained in this study was not an exception. There was a closure error of 19%, which is acceptable considering all the above-mentioned errors that may occur in the field and assumptions made in the eddy covariance data analysis and processing. The energy balance closure error obtained in this study is within the range of acceptable values published in the literature (up to 30%, Twine et al., 2000; Wilson et al., 2002; Wang et al., 2020). Therefore, no corrections were required in the collected dataset.

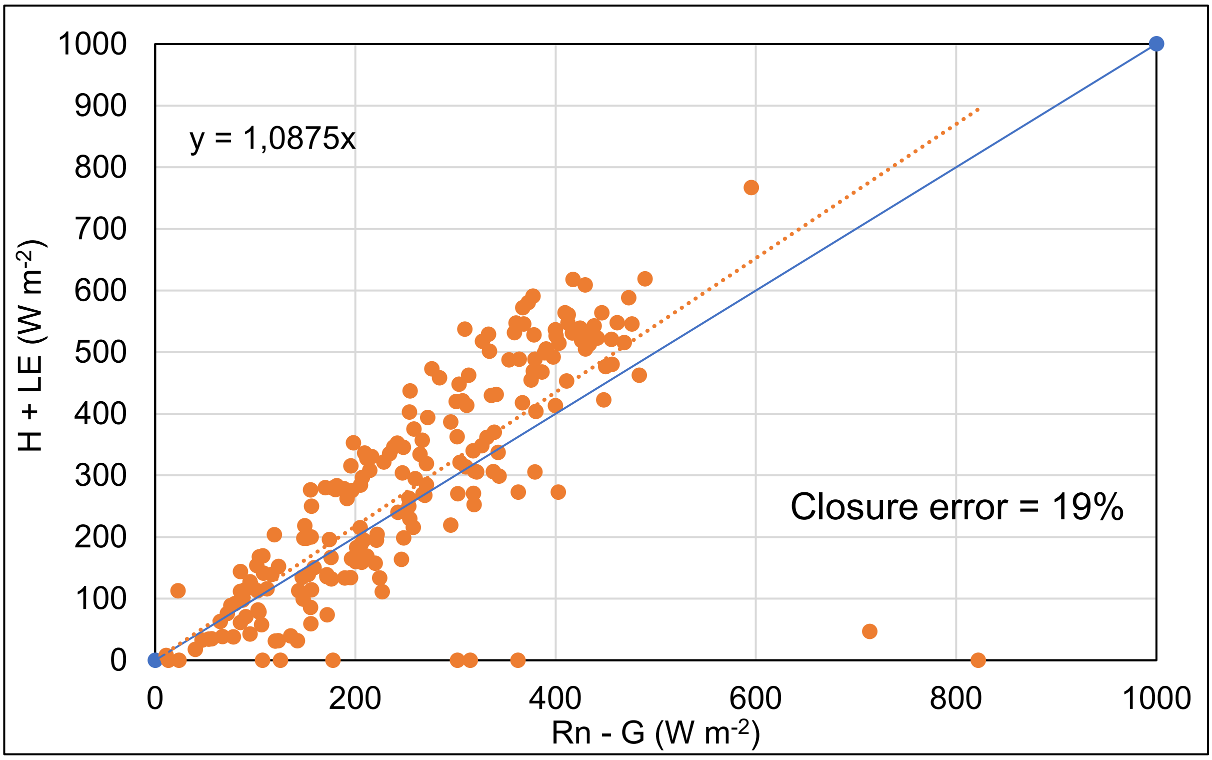

Figure 3.12: Scatterplots of (LE + H) against (Rn – G): uncorrected 30 min daytime data during the experimental period (17 December 2021 to 06 March 2022) at Tooseng research site, Limpopo province. The dashed line represents the linear regression line, the continuous line the 1:1 line, the regression equation and energy balance closure error are also given.

3.3.5 Eddy covariance flux footprint analysis over an 8-year old Moringa stand

A footprint analysis was undertaken to observe the relative contribution of upwind surface sources to the measured downwind sensible heat and latent energy fluxes, because measurements were made on a Moringa stand with limited fetch. The 90% fetch to measurement height ratio analysis over the entire flux measurement period (November 2022 to April 2023) indicates that more than 90% of the measured flux was coming from the upwind fetch distance of approximately 50 m, and very seldom turbulent fluxes went beyond 100 m when the prevailing wind speed reached peaks above 7 m/s (Figure 3.13). The peak location of the footprint, in other words, the distance from the anemometer in the direction from which the largest relative individual contribution to the flux originates (X_{peak}), was a maximum of 46 m during the experimental period. (Figure 3.14). This demonstrates that, the measured fluxes were within the fetch.

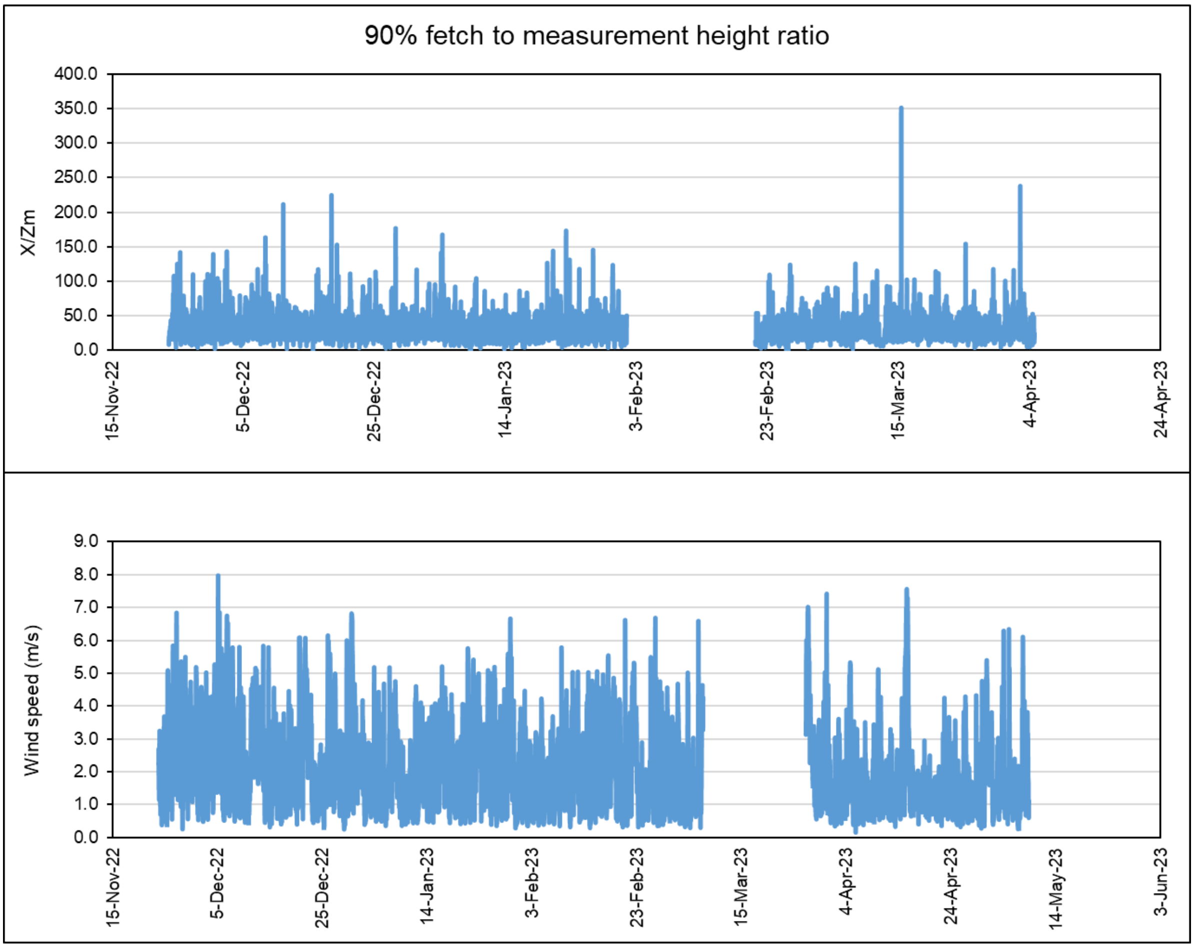

Figure 3.13: The 90% fetch to measurement height ratio analysis over the entire flux measurement period (November 2022 to April 2023) at the study site.

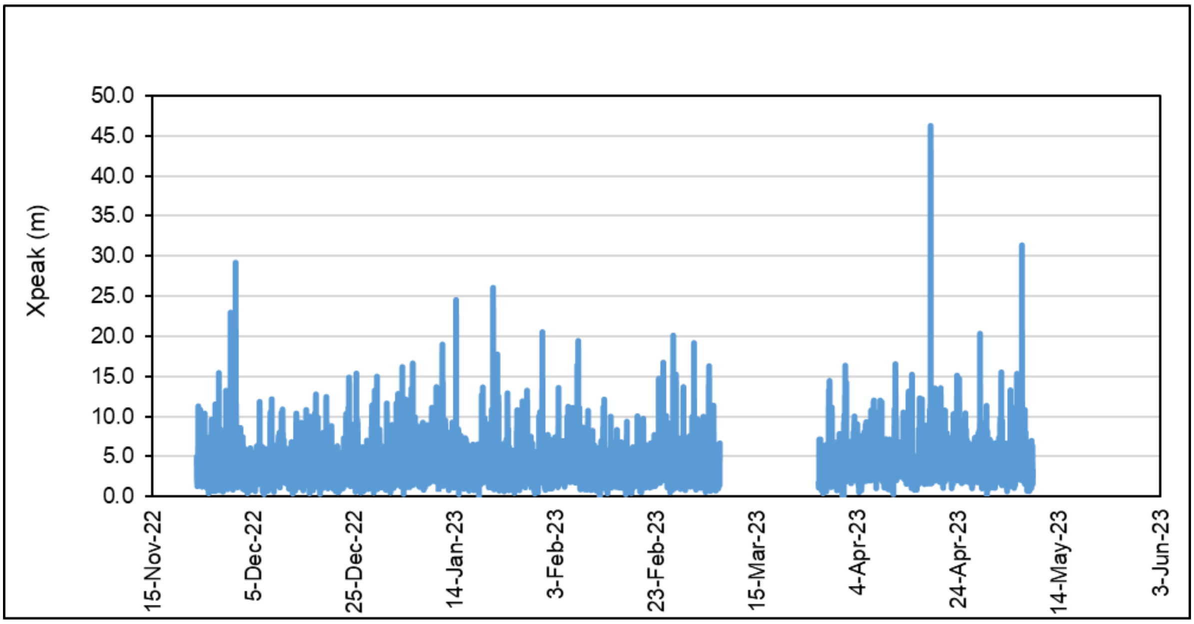

Figure 3.14: Footprint peak distance during the experimental period (November 2022 to April 2023) at the study site.

3.3.6 Daily variability of Moringa crop evapotranspiration as influenced by changes in atmospheric evaporative demand

In season 1, from the 17th of December to the 24th of January, there was an adequate crop management, whereas, from the 25th of January to the end of the measurement period the crop had been affected by the cricket outbreak, which destroyed the canopy of Moringa trees, leaving the stand almost leafless (Figure 3.15). During the period of good crop management, daily Moringa crop evapotranspiration varied between 2.1 mm on a cloudy day (with relatively low ET_o values) to a maximum of 4.3 on a less warm day (with ET_o below the maximum values) (Figures 3.15 and 3.16). This suggests that Moringa crop water use tends to be limited under conditions of increased atmospheric evaporative demand, which might be a physiological strategy of the crop to adapt and adjust to environmental stress.

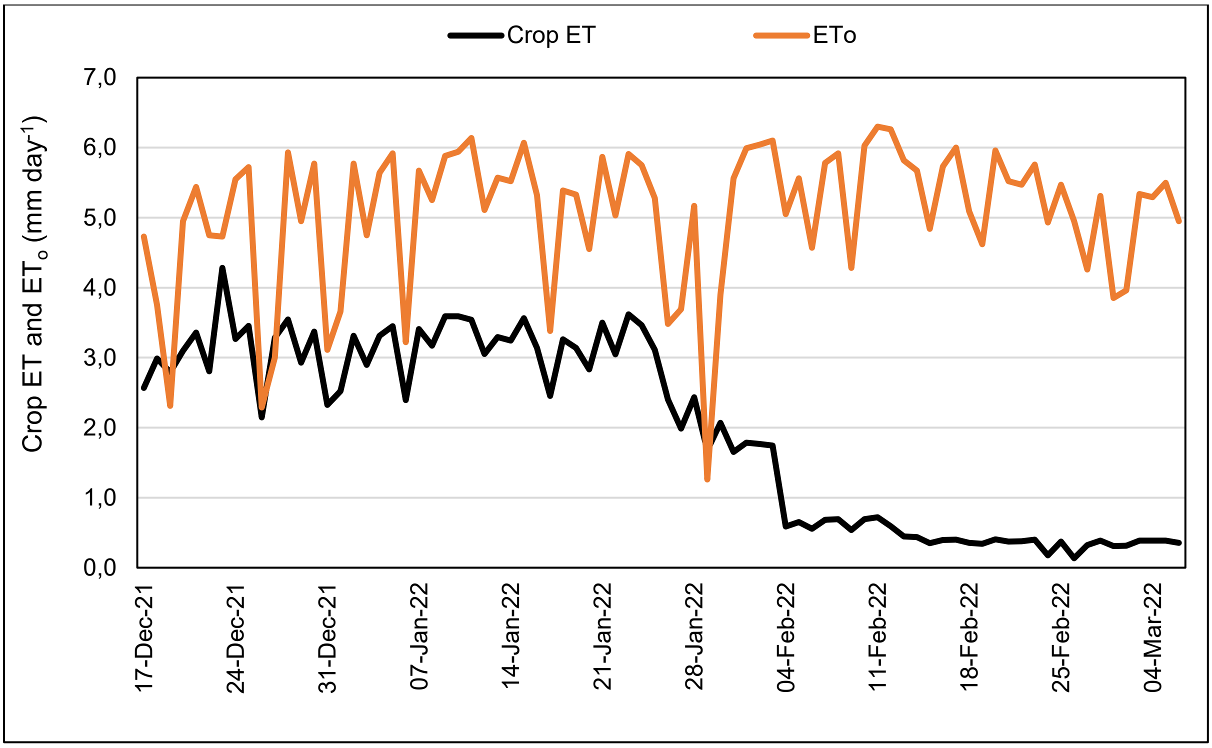

Figure 3.15: Daily crop evapotranspiration and reference evapotranspiration variability during the experimental period (17 December 2021 to 08 March 2022) at Tooseng research site, Limpopo province.

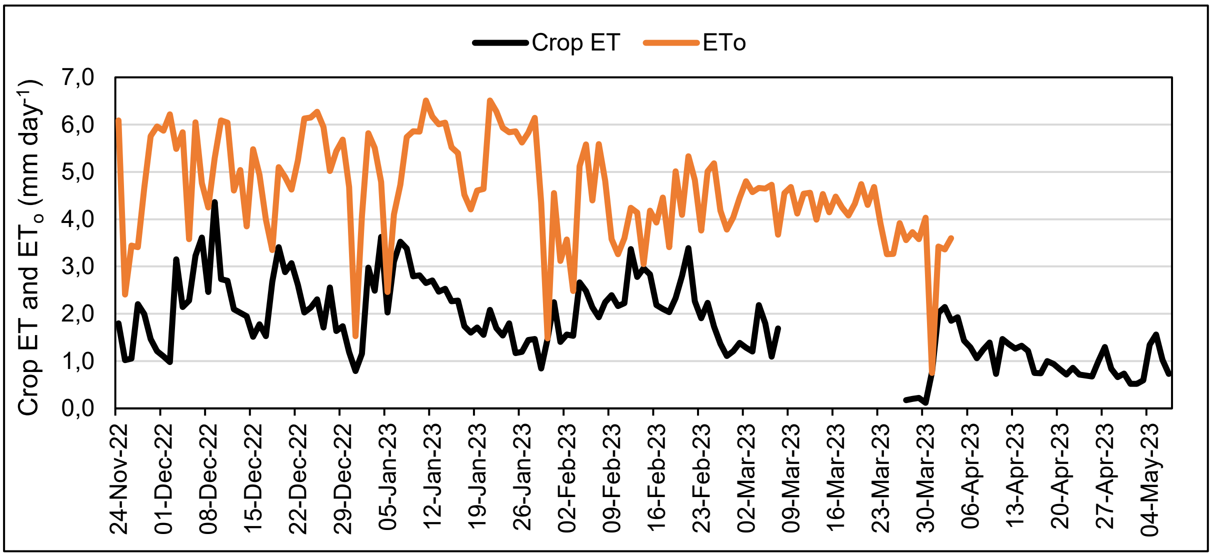

Figure 3.16: Daily crop evapotranspiration and reference evapotranspiration variability during the experimental period (24 November 2022 to 07 May 2023) at Tooseng research site, Limpopo province.

3.3.7 Crop coefficients

The drought adaptation of Moringa was also evident in the curve of crop coefficients (K_c). The K_c curve remained steadily constant with an increase in the atmospheric evaporative demand (Figure 3.17). Typical K_c values of Moringa were around 0.58 from the 17th of December to the 24th of January. This relatively low K_c value of Moringa indicates that the tree requires relatively low amounts of water irrespective of the increased atmospheric evaporative demand. Spikes in K_c values as a result of adverse environmental conditions (cloudy/rainy days) were removed from the data set, as shown in Figure 3.15.

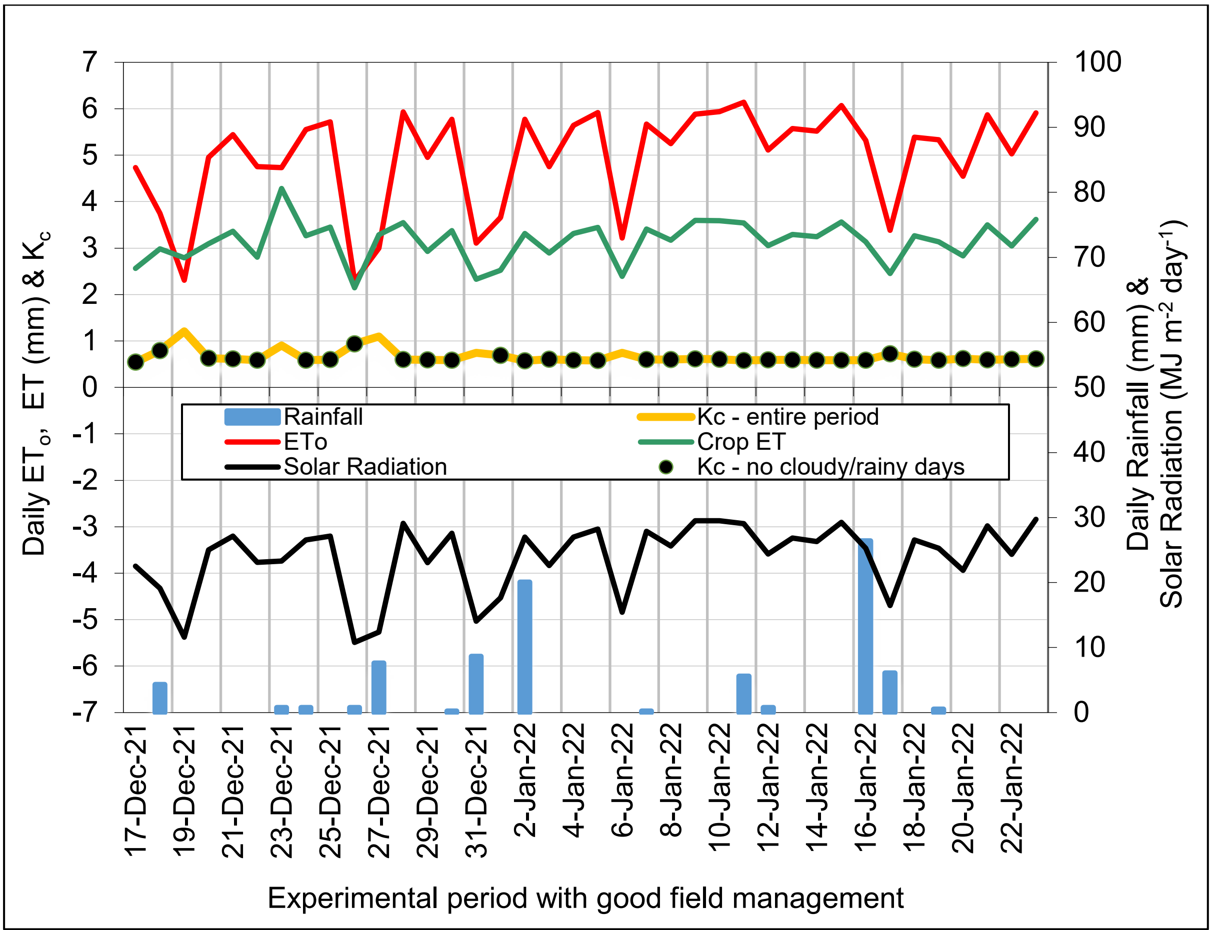

Figure 3.17: Variability of crop coefficients (K_c) during the experimental period when the Moringa stand was not affected by the cricket outbreak, excluding cloudy/rainy days (dotted line) and otherwise (solid line), for 8-year old Moringa trees in relation to reference evapotranspiration (ET_o). The occurring solar radiation and rainfall values are also shown for the experimental period with good crop management (17 December 2021 to 23 January 2022) at Tooseng experimental site, Limpopo province.

3.3.8 Growth parameters

At the beginning of the measurement period (17 December 2021), the 8-year old Moringa trees were 1.46 m tall, with a stem diameter of 9 cm and a canopy cover of 66% (Table 3.2). A few days after the start of the cricket outbreak, the trees lost leaves and, as a result, the canopy cover was much lower (49%), although the trees had grown taller with larger lateral branching

Table 3.2: Growth parameters (tree height, stem diameter, canopy width and depth, leaf area index and fractional interception of photosynthetic active radiation on an 8-year old Moringa stand at Tooseng research site, Limpopo province.

Harvest	Date	Height (m)	Stem diameter (m)	Canopy width (m)	Canopy depth (m)	LAI (cm^2/cm^2)	FI of PAR (%)
1	17/12/2021	1.46	0.09	0.78	0.79	2.8	66
2	01/02/2022	2.11	0.09	1.76	1.6	1.38	49

3.3.9 Leaf fresh and dry yield

The obtained fresh and dry yield of leaves was in agreement with the recorded growth parameters (Table 3.3). Leaf fresh and dry yield at the start of the measurement period were 600 and 143 kg/ha, but after the cricket outbreak, it reduced to 225 and 45 kg/ha, respectively. These yields are significantly lower than those reported in the literature for leaf production in South Africa using a similar planting density of 2500 plants per hectare (224-339 kg ha^{-1} leaf dry yield, Mabapa et al., 2020). The poor performance of the Moringa stand at Tooseng research site is mainly attributed to low soil fertility and soil structural problems at the bottom layers, which limit tree root expansion, leading to reduced water and nutrient uptake. The moisture percentage in Moringa leaves varied from 20 to 24%.

Table 3.3: Leaf fresh and dry mass as well as moisture content of 8-year-old Moringa trees at Tooseng research site, Limpopo province.

Harvest	Date	Leaf fresh mass (kg/tree)	Leaf dry mass (kg/tree)	Leaf fresh mass (kg/ha)	Leaf dry mass (kg/ha)	Leaf moisture content (%)
1	17/12/2021	0.24	0.057	600	143	24
2	01/02/2022	0.09	0.018	225	45	20

3.4 RESEARCH CHALLENGES

The challenges experienced during the experimental period include a sudden outbreak of Roesel bush crickets (*Metrioptera roeselii*) at the end of an intensive rainfall period (when 93 mm of rain fell within 30 days, which is about 60% of the total rainfall amount occurring during the experimental period). Bush crickets are a group of insects belonging to the order Orthoptera. They are plant-eating insects that grow to about 5 cm in size and have long protruding antennae and strong mandibles. According to the South African National Biodiversity Institute (SANBI), the species are native and widely distributed in Namibia, Botswana, Zimbabwe and South Africa (particularly found in Limpopo and Northern Cape provinces). Figure 3.15 shows a bush cricket climbing on one of the Moringa stems (circled in red) at Tooseng research site on 11 February 2022.

Figure 3.18: A Roesel bush cricket (*Metrioptera roeselii*) climbing onto a Moringa tree stem at Tooseng experimental site, Limpopo province (Picture taken by Dr Nadia Araya).

Bush crickets are frequently found in grassy and low vegetation places. This outbreak occurred in the beginning of February 2022, when the trees attained maximum foliage (above 86% of canopy cover) as a result of non-limiting soil water supply conditions. This period of maximum vegetation cover was likely to result in increased accumulation of protein particularly on the leaves, which offered a conducive environment for bush crickets to lay eggs and massively reproduce at a rapid rate. The cricket outbreak had a negative impact on crop water use measurements conducted with the eddy covariance technique, as most of the Moringa biomass was eaten. Due to this sudden loss in yield, it was not possible to determine water productivity of Moringa during the measurement period.

Another major challenge encountered by the research team was the fault that occurred in the smart battery charger that supplies electrical power continuously to the battery operating the eddy covariance system. To address the problem, two 100 Amp-hour deep cycle batteries were connected in parallel and frequent visits were conducted to the experimental site to change batteries and ensure continuous data collection and recording during this period. The research being conducted on the site also revealed depleted nutrients in the soil, which might have affected the productivity of Moringa. Therefore, it is recommended that an application of organic soil amendment materials such as kraal manure and compost be conducted to improve soil fertility and water holding capacity, which will ultimately result in improved crop productivity and income generation for the farmer.

3.5 CONCLUSIONS AND RECOMMENDATIONS

This study investigated the first application of an eddy covariance technique to determine Moringa crop water use in order to develop site-specific crop coefficients. Daily crop ET varied from 2.45 mm day^{-1} on a cloudy day to 4.28 mm day^{-1} on a hot sunny day. Daily crop coefficients (K_c) remained steadily constant throughout the experimental period at about 0.6, suggesting the presence of a drought adaptation mechanism in Moringa trees. The cumulative ET during the period when the crop was actively growing (17 December 2021 to 29 January 2022) was 136 mm, while the atmospheric evaporative demand (ET_o) was 216 mm, resulting in an average K_c value of 0.62. During this period, the crop canopy cover increased from 49 to 86%. Further studies should focus on collecting crop ET and ET_o data in different climates and seasons so as to improve the understanding of Moringa crop water use. In addition, the effective water use of Moringa (transpiration) should be quantified to assess the crop evapotranspiration partitioning and inform on water-efficient irrigation and soil water conservation strategies.

ACKNOWLEDGEMENTS

This work was financially supported by the Water Research Commission of South Africa (WRC Project No. C2020/2021-00484). Technical support, data collection and processing by postgraduate students (Mr Ntsieni Mulovhedzi and Mr Sihle N'Wamba) and ARC staff (Dr Nadia Araya, Mr Ernest Malatjie, Mr Takalani Tuwani, Mr Mfuzi Makwakwa and Dr Ian du Plooy) are highly appreciated. The research team also wishes to thank the following people: Mr Vivek Naiken, Prof. Alistair Clulow, Dr Shaeden Gokool (from the University of KwaZulu-Natal), Dr Michael Mengistu (from the South African Weather Service) and Mr Sibusiso Boyi (from Campbell Scientific Africa (Pty) Ltd.) for their valuable advice during the installation of the eddy covariance system. Ms Irene Nel (from ARC – Natural Resources and Engineering) is thanked for providing a complete set of weather data for the experimental site. Our gratitude is extended to Dr Salmina Mokgehle (former ARC employee) for assisting with the research site identification and selection. Last but not least, our deepest appreciation to Moringa farmers (Mr Tushego and Pa Madala) for being so cooperative and supportive of all the research activities on their farm.

REFERENCES

Allen RG, Pereira LS, Raes D, Smith M 1998. Crop evapotranspiration guideline for computing crop water requirements. FAO. Irrigation and Drained Paper 56. Rome. Italy, p 299.

Allen RG, Pereira LS, Howell TA and Jensen MA 2011a. Evapotranspiration information reporting: I. Factors governing measurement accuracy. Agric. Water Manag., 98: 899-920.

Allen RG, Pereira LS, Howell TA and Jensen MA 2011b. Evapotranspiration information reporting: II. Recommended documentation. Agric. Water Manag., 98: 921-929.

Blanken PD, Black TA, Yang PC, Den Hartog G, Neumann HH, Nesic Z, Novak MD, Staebler R, Lee X 1997. Energy balance and surface conductance of a boreal aspen forest: Partitioning over story and understory components. J. Geophys. Res., 102: 28915-28927.

Burba GG and Anderson DJ 2010. A brief practical guide to eddy covariance flux measurements principles and workflow examples for scientific and industrial applications. LI-COR Niosciences, Lincoln, USA.

Cleverly JR, Dahm CN, Thibault JR, Gilroy DJ, Coonrod JEA 2002. Seasonal estimates of actual evapotranspiration from Tamarix ramosissima stands using 3-dimensional eddy covariance. J. Arid Environ., 52: 181-197.

Consoli S and Papa R 2013. Corrected surface energy balance to measure and model the evapotranspiration of irrigated orange orchards in semi-arid Mediterranean conditions. Irrig. Sci, 31: 1159-1171.

Ding R, Kang S, Li F, Zhang Y, Tong L, Sun Q 2010. Evaluating eddy covariance method by large-scale weighing lysimeter in a maize field of northwest China. Agric. Water Manag., 98: 87-95.

Foken T 2008. The energy balance closure problem: an overview. Ecol. Appl., 18: 1351-1367.

Foken T, Aubinet M, Leuning R 2012.The eddy covariance method. In Aubinet, M., Vesala, T. and Papale, D. (eds). Eddy covariance. A practical guide to measurement and data analysis. Springer, New York.

Harper WV 2014. Reduced major axis regression: teaching alternatives to least squares. In Makar, K., de Sousa, B. and Gould, R. (eds.), Sustainability in statistics education. Proceedings of the Ninth International Conference on Teaching Statistics (ICOTS9, July 2014), Flagstaff, Arizona, USA.

Hipps LE, Ivans S, Johnson DA, Saliendra NZ 2002. Eddy covariance and Bowen ratio estimates of water vapor and CO_2 fluxes over crested wheatgrass. 25th Conference, Agric For Meteorol., 19-23.

Holland S, Heitman JL, Howard A, Sauer TJ, Giese W, Ben-gal A, Agam N, Kool D and Havlin J 2013. Micro-Bowen ratio system for measuring evapotranspiration in a vineyard interrow. Agric For Meteorol., 177: 93-100.

Mabapa MP, Ayisi KK and Mariga IK 2020. Biomass production and nutritional composition of Moringa oleifera under different planting spacings in a semi-arid condition of the northern South Africa. AJFAND, 20:15857-15875.

Mahrt L 1998. Flux sampling errors for aircraft and towers. JTECH, 15: 416 429.

Machakaire ATB, Steyn JM and Franke AC 2021. Assessing evapotranspiration and crop coefficients of potato in a semi-arid climate using Eddy Covariance techniques. Agric. Water Manag., 255: 1-11.

Mashamait CV, Pieterse PJ, Mothapo PN, Phir EE 2021. *Moringa oleifera* in South Africa: A review on its production, growing conditions and consumption as a food source. S. Afr. j. sci., 117: 1-7.

Mulovhedzi N, Savage MJ, Araya HT, Amoo SO, du Plooy CP, Laurie S and Araya NA, 2019. Water use efficiency of Moringa oleifera under different water supply regimes. II International Symposium on Moringa, 10-13 November 2019, Pretoria, South Africa.

Mulovhedzi NE, Araya NA, Mengistu MG, Fessehazion MK, du Plooy CP, Araya HT and van der Laan M 2020. Estimating evapotranspiration and determining crop coefficients of irrigated sweet potato (*Ipomoea batatas*) grown in a semi-arid climate. *Agric. Water Manag., 233: 1-9.*

Nagler PL, Scott RL, Westenburg C, Cleverly JR, Glenn EP, Huete AR 2005. Evapotranspiration on western US Rivers estimated using the enhanced vegetation index from MODIS and data from eddy covariance and Bowen ration flux towers. Remote Sens. Environ., 97: 337 351.

Pieterse PJ, Mothapo PN, Phiri EE 2021. Moringa oleifera in South Africa: A review on its production, growing conditions and consumption as a food source. S. Afr. j. sci., 117:1-7.

Rana G and Katerji N 2000. Measurement and estimation of actual evapotranspiration in the field under Mediterranean climate. Eur J Agron EUR J AGRON, 13: 125-153.

Scott CA, Bastiaanssen WGM, Ahmad MD 2003. Mapping root zone soil moisture using remotely sensed optical imagery. ASCE. J IRRIG DRAIN ENG, 129: 326-335.

Stannard DI, Blanford JH, Kustas WP, Nichols WD, Amer SA, Schmngge TJ, Wettz MA 1994. Interpretation of surface flux measurements in heterogeneous terrain during the monsoon experiment. Water Resour. Res., 83: 375 406.

Stewart BA and Howell TA 2003. Encyclopaedia of water science. Marcel Dekker Inc., New York, USA.

Twine TE, Kustas WP, Norman JM, Cook DR, Houser PR, Meyers TP, Prueger JH, Starks PJ and Wesely ML 2000. Correcting eddy covariance flux underestimates over a grassland. Agric For Meteorol., 103: 279-300.

Wang F, Ma D, Zhao W, Lu Y, Zhou D, Zhang J, Chen L and Huang P 2020. A validation of eddy covariance technique for measuring crop evapotranspiration on different time scales in the North China Plain. Can. J. Soil Sci., 101: http://dx.doi.org/10.1139/CJSS-2020-0050.

Wilson K, Goldstein A, Falge E, Aubinet M, Baldocchi D, Berbigier P, Bernhofer C, Ceulemans R, Dolman C, Field H, Grelle A, Ibrom A, Lawl BE, Kowalski A, Meyers T, Moncrieff J, Monson R, Oechel W, Tenhunen J, Valentini R and Verma S 2002. Energy balance closure at FLUXNET sites. Agric For Meteorol., 113: 223-243.

Zeggaf AT, Takeuchi S, Dehghanisanij H, Anyoji H and Yano T 2008. A Bowen ratio technique for partitioning energy fluxes between maize transpiration and soil surface evaporation. J. Agron., 100: 988 996.

CHAPTER 4

DAILY DETERMINATION OF MORINGA TRANSPIRATION USING THE SAP FLOW METHOD

Ambroise Ndayakunze[1,2], Martin Steyn[2], Ian du Plooy[1] and Nadia Araya[1,3]

[1]*Agricultural Research Council – Vegetable, Industrial and Medicinal Plants, Pretoria, South Africa*
[2]*University of Pretoria, Department of Plant and Soil Sciences, Pretoria, South Africa*
[3]*Agricultural Research Council – Natural Resources and Engineering, Pretoria, South Africa*

4.1 INTRODUCTION

The direct assessment of crop-specific water use (WU) can be implemented through a number of methods, including the heat balance-based sap flow (SF) (Li et al., 2022). The daily plant SF is affected by microclimatic factors such as solar radiation (SR), vapor pressure deficit (VPD), relative humidity (RH), air temperature (Ta), soil water content (SWC) (Guerrieri et al., 2019), and to a great extent, photosynthetically active radiation (PAR) (Zhang et al., 2015; Zhou et al., 2015). The recorded crop SF also depends on physiological factors such as canopy width and leaf area index (LAI) (Guerrieri et al., 2019).

Sap flow measurements from individual stems can be upscaled to the entire tree and stand (Duan et al., 2017). Earlier investigations on upscaling of transpiration (T) prioritized tall trees or vegetation types with a high canopy density, using independent variables such as woodland area (Hatton et al., 1995), canopy overlap (Xiong et al., 2008), sapwood area (Jaskierniak et al., 2015), and trunk diameter at breast height (Zhang et al., 2011). The validity of upscaling outcomes significantly depended on the scalar multipliers of the independent variables between the trees and the stand. However, for appropriate irrigation scheduling, there is a need to determine evapotranspiration (ET) precisely, which requires the input of local data that are not always available. Additionally, some techniques such as drainage lysimeters and eddy covariance equipment are not only highly inaccessible, but also their maintenance is controversial (Anapalli et al., 2018). In this regard, the state-of-the-art agricultural system models are cheap, viable, and widely accepted tools for developing location-specific crop ET data for irrigation scheduling and developing crop-ET response functions for more accurate determination of crop water needs.

Efficient water management can be improved through a determination of the effect of different factors on SF. Nonetheless, the nexus of SF and the controlling factors remains unintelligible, whereas no genuine model has yet been adopted for the prediction of SF change of several tree species including Picea crassifolia Kom (Li et al., 2022), Moringa (*Moringa oleifera* Lam.) (Mashamaite et al., 2021) and many more. Therefore, this study aimed at estimating T of Moringa by measuring the SF of intact main stems using an improved heat balance technique. The specific objectives of this study were to: (1) measure branch and stem SF of irrigated mature Moringa trees, (2) upscale the measured SF from stem-level to tree- and stand-level, (3) and identify the major morpho-eco-physiological parameters that affect daily SF.

4.2 MATERIALS AND METHODS

4.2.1 Description of the study site

The study was conducted on a 9-year-old, drip-irrigated Moringa stand (*Moringa oleifera* Lam., cultivar PKM1), during the autumn growing period of the 2021/22 season at the Roodeplaat Experimental Farm of the Agricultural Research Council – Vegetable, Industrial and Medicinal Plants (ARC-VIMP) (25°35'S, 28°21'E, 1164 m.a.s.l.). The study area lies within the semi-arid and sub-tropical regions, with an average annual rainfall of 650 mm predominantly derived from the summer season (mainly October-March). The range of the average daily air temperatures (Ta) fluctuates from 8-34°C (summer), and 4-23°C (winter), whereas January and July are the hottest and coldest months, respectively (Mokgehle *et al.,* 2022). The end of autumn is characterized by little or no rainfall while wintry frost is inexorable. In line with the United States Department of Agriculture (USDA) taxonomic system, the soil texture of the study site is classified as loamy, while the respective slope and soil depth are 0.5-1% and > 1.2 m.

4.2.2 Environmental and morpho-eco-physiological parameters

Key eco-physiological parameters were monitored on an hourly basis in order to complement the main SF study. These eco-physiological parameters included leaf stomatal conductance (gs) using a porometer, PAR and leaf area index (LAI) using a Decagon ceptometer, leaf chlorophyll content (SPAD) using a Minolta SPAD meter, and leaf chlorophyll fluorescence using a Handy PEA fluorometer. In addition, morphological parameters such as number of stems per tree, stem diameter (D) and leaf area (LA) were also recorded. Monitoring of hourly weather conditions such as Ta (minimum, average, maximum), as well as SR were conducted using a Tinytag TV-4500 datalogger smart sensor and a pyranometer, respectively. Values of wind speed (u) were obtained from the nearest automatic weather station. The reference evapotranspiration (ET_0) during the experimental period was computed using the Penman-Monteith equation (Allen *et al*., 1998). Daily measured SF (from 12 to 31 May 2022) was used to develop regression models linked to the various microclimatic and morpho-eco-physiological parameters.

4.2.3 Sap flow measurements

Sap flow (SF) sensors of varying sizes (10-25 cm diameter) were installed on main stems and branches to determine T of two representative trees (Tree 1 and Tree 2) selected based on a survey study conducted across the entire Moringa stand. Details of the theory and installation of the SF system can be found in Dynamax Inc. (2007). The stem heat balance approach (EXO-Skin sap flow sensors, Dynamax Inc.) was adopted for the current study, and the SF was recorded and logged every 15 min using a CR1000 data logger (Campbell Sci. Inc., Logan, UT, USA). The measured SF data were converted into hourly and daily timescales, whereas the recorded stem- and branch-level SF was upscaled to the whole stand level, using leaf area (LA) and stem area (SA). Daily tree and stand T were calculated as the accumulation of the hourly SF.

4.3 RESULTS AND DISCUSSION

4.3.1 Environmental and leaf stomatal conductance characteristics

The micro-climatic conditions (Table 4.1) influenced the changes in leaf stomatal conductance (g_s) characteristics (Figure 4.1). Although the weather conditions at the study site were mostly partly cloudy, interspersed with a few clear days, especially towards the end of the study period (Table 4.1), there were clear differences in g_s across the study period and experimental trees (Figure 1). In addition, Tree 2 was morphologically larger than Tree 1. Values of g_s were, on average, higher in Tree 2 (159.2 mmol m^{-2} s^{-1}) compared to Tree 1 (143.6 mmol m^{-2} s^{-1}). This is mainly attributed to the larger size of the former (four stems of D between 1.0 and 2.5 cm and canopy LA of 2.1 m^2) compared to the latter (two stems of D between 1.6 and 2.6 cm and canopy LA of 0.69 m^2). Values of g_s generally increased under high conditions of atmospheric evaporative demand (ETo between 3.9 and 4.2 mm/d), particularly at high values of daily SR (29.5-30.4 MJ/m^2/d), Tmax (23.4-24.0°C) and VPD (1.55-1.65 kPa).

Table 4.1: The microclimatic conditions during the sap flow study.

Dates (May 22)	Day of Year	Tmin[a] (°C)	Tmax[a] (°C)	Tave[a] (°C)	u[b] (m/s)	SR[c] (MJ/m^2/d)	VPD[d] (kPa)	ETo[e] (mm)
12	132	14.37	20.65	17.83	0.49	15.48	3.06	2.70
13	133	14.37	20.65	17.83	0.53	15.89	3.06	2.76
14	134	15.66	37.40	25.92	0.44	13.75	1.33	3.24
15	135	15.43	41.29	27.86	0.96	10.91	1.34	3.92
16	136	7.30	18.70	10.10	0.59	14.19	1.20	2.06
17	137	5.80	21.20	12.30	0.45	14.09	1.26	2.20
18	138	3.50	19.30	10.50	0.36	12.54	1.21	1.93
19	139	3.50	21.20	10.50	0.50	15.63	1.27	2.28
20	140	3.80	20.90	12.00	1.28	14.47	1.24	2.13
21	141	2.20	14.10	8.50	0.82	5.68	0.83	1.07
22	142	0.00	18.40	8.70	0.53	15.12	1.05	2.10
23	143	1.99	19.20	10.29	1.19	13.32	1.24	1.98
24	144	1.49	21.06	11.24	0.55	20.09	0.61	2.78
25	145	0.48	23.81	12.39	0.55	29.52	1.57	4.10
26	146	0.23	24.03	12.39	0.45	29.92	1.55	4.21
27	147	2.49	23.40	12.42	0.45	30.45	1.64	3.97
28	148	2.74	22.90	12.38	0.47	30.00	1.64	4.23
29	149	2.64	21.98	12.16	0.75	28.20	1.52	3.81
30	150	2.49	20.37	10.00	0.78	26.02	1.27	3.62
31	151	-3.27	18.71	8.60	1.40	26.07	1.01	3.26

[a]Tmax, Tmin and Tave: maximum, minimum and average temperatures, respectively; [b]u: wind speed; [c]SR: solar radiation; [d]VPD: vapour pressure deficit; and [e]ETo: reference evapotranspiration.

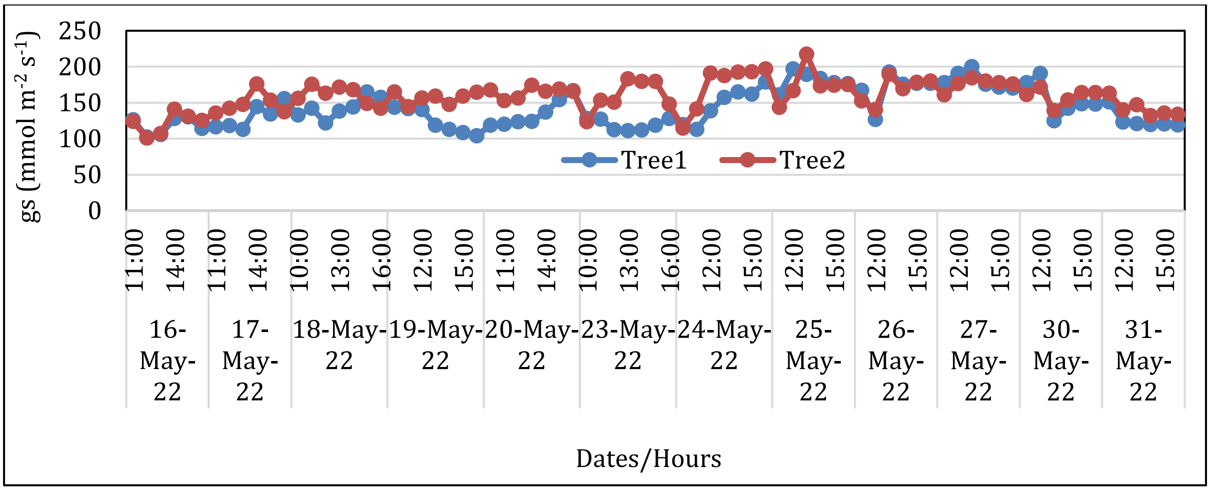

Figure 4.1: Variability of Moringa leaf stomatal conductance during the study period.

4.3.2 Sap flow characteristics

The hourly and daily sap flow results are given in Figure 4.2. The cyclic trend of hourly measurements indicates the peaks in the mornings and the troughs at night, with Tree 1 always registering lower daily SF and short peaks than Tree 2. In a study conducted by Fan et al. (2022) on golden pears, SF peaks also occurred in the mornings and not in the afternoons, although Uddin et al. (2014) opined that SF of Tulipwood trees raised continuously throughout the day and peaked in mid-afternoon, prior to declining in the late afternoon. The highest peak for Tree 2 (2.6 L/tree/hr) and Tree 1 (0.7 L/tree/hr) occurred on a relatively warm clear sky day (ETo = 4.2 mm/d and T = 4.2, and 2.0 mm/d, respectively). The variation in the magnitude of the peaks was mostly guided by the prevailing weather conditions, as also reported by Duan et al. (2017). The minimum observed daily SF were 0.09 and 1.13 mm/d for Tree 1 and Tree 2, respectively, which occurred under relatively low atmospheric evaporative demand conditions (2.7 mm/d). The present study also proved that the hourly and daily SF of the combined branches were on average approximately 25% lower than the sap flow of the respective main stems. This corroborates the findings obtained by Burgess et al. (2008) and Roddy et al. (2013). Roddy et al. (2013) also established the SF imbalance between branches and main stems and attributed the difference to various factors affecting the root-to-leaf continuum such as positional variability, capacitance (storage) and hydraulic resistance.

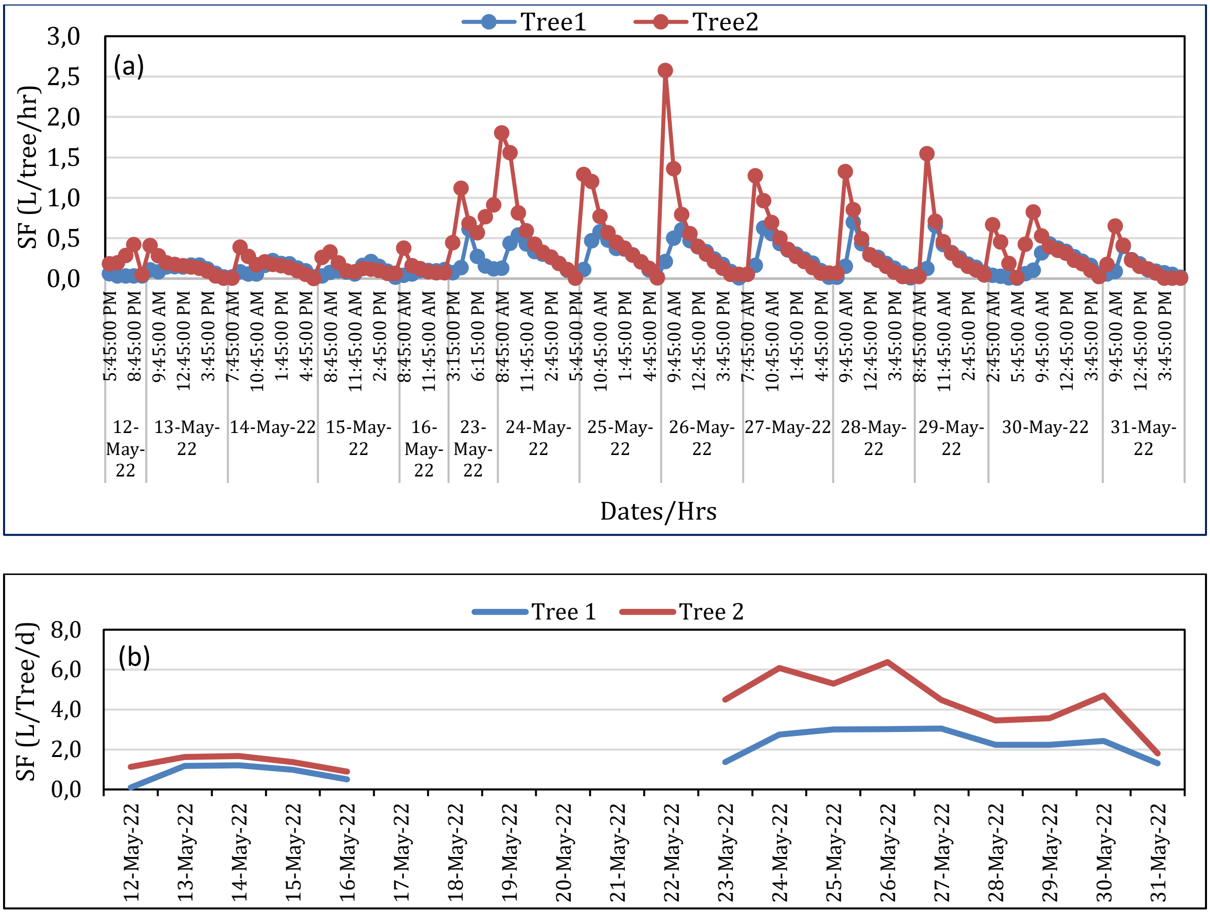

Figure 4.2: Hourly (a) and daily (b) Moringa sap flow (SF) during the study period.

4.3.3 Response of sap flow to microclimatic and morpho-eco-physiological conditions

The sap flow of Moringa trees was influenced by micro-climatic and morpho-eco-physiological conditions. As shown in Table 4.2, the hourly and daily records showed a strong positive correlation between the measured SF and related microclimatic and morpho-eco-physiological drivers (R^2 up to 0.877), except with Ta_{min} which resulted in very poor correlation (R^2 = 0.0267). The marked response of sap flow to ETo, Ta_{max} and VPD was reflected in R^2 of 0.83, 0.80 and 0.78, respectively. The literature indicated that SF is generally driven by climatic conditions, including air temperature and VPD (Zhao et al., 2016). Although SR and Ta_{ave} (with R^2 of 0.75 and 0.62, respectively) were not the leading drivers during the course of the current study, it is well-documented that a strong correlation links SF and these microclimatic factors (Guerrieri et al., 2019), and to a great extent, PAR (Zhang et al., 2015; Zhou et al., 2015). On the contrary, wind speed was inversely proportional to SF with an R^2 of 0.75. In general, SF rates mostly slow down as Ta and VPD lessen, and RH increases (Hentschel et al., 2016). This was confirmed in the current study, particularly for Ta_{max} and Ta_{ave}, as well as for other atmospheric variables such as SR, VPD and ETo. Additionally, SF was reported to preserve a strong dependence on the morpho-physiological conditions (Guerrieri et al., 2019; Fan et al., 2022). For instance, the response of SF to stomatal closure enables the assessment of water stress, water loss and T rate, particularly in woody plants (Noun et al., 2022). During the present study, LA, SA, g_s and chlorophyll fluorescence (maximum quantum efficiency of PSII = variable chlorophyll fluorescence/maximum chlorophyll fluorescence (Fv/Fm) were correlated with SF, with an R^2 of 0.73-0.88. In terms of morpho-physiological parameters, SF was primarily driven by SA, followed by g_s and Fv/Fm.

Table 4.2: Relationship between daily Moringa transpiration and microclimatic or morpho-physiological variables.

	Variables	Equations	R^2
Microclimatic	Maximum temperatures (°C)	y = 0.37x – 4.4412	0.796
	Minimum temperatures (°C)	y = 0.0696x – 3.5065	0.027
	Average temperatures (°C)	y = 0.468x – 1.7028	0.624
	Vapour pressure deficit (kPa)	y = 2.5605x + 0.1467	0.780
	Wind speed (m/s)	y = 1.8886x + 5.0656	0.748
	Solar radiation (MJ/m^2/day)	y = 1242x + 0.3713	0.749
	Reference evapotranspiration (mm)	y = 0.9908x + 0.0767	0.832
Morphological	Leaf area (m^2/m^2)	y = 9.3309ln(x) + 21.05	0.727
	Stem area (cm^2)	y = 3.8078ln(x) + 6.3585	0.877
Physiological	Stomatal conductance (mmol/m^2/s^1)	y = 0.0367x – 2.1618	0.851
	SPAD	y = 0.4088x – 13.835	0.712
	Fv[a]/Fm[b]	y = 207.7x – 150.31	0.822
	FI_{PAR}[c]	y = 19.534x – 12.005	0.728

[a]Fv: variable chlorophyll fluorescence; [b]Fm: maximum chlorophyll fluorescence; [c]FI_{PAR}: the fractional interception of the photosynthetically active radiation.

4.4 CONCLUSIONS AND RECOMMENDATIONS

In irrigated mature Moringa trees, the total branch SF diverged from the respective main stem SF by 25%. Moringa tree T was highly influenced by tree size (determined by the number of stems per tree and stem area, as well as by the changes in g_s). The major microclimatic influencing variables were ETo, followed by Ta_{max} and VPD. It is recommended that similar measurements be conducted in other species of the genus Moringa and across a range of climatic conditions, for better understanding of Moringa water use dynamics.

ACKNOWLEDGEMENTS

The authors would like to thank the Water Research Commission (Project No C2020/2021-00484) for funding this research, the Agricultural Research Council for project management and research implementation, as well as the University of Pretoria for student capacity building while implementing this research.

REFERENCES

Alam, M.S., Lamb, D.W., and Warwick, N.W.M. 2021. A canopy transpiration model based on scaling up stomatal conductance and radiation interception as affected by leaf area index. Water 13, 252. https://doi.org/10.3390/w13030252.

Allen, R.G., Pereira, L.S., Raes, D., and Smith, M. 1998. Crop evapotranspiration: Guidelines for computing crop water requirements. FAO Irrigation and Drainage Paper 56. FAO, Rome, Italy.

Anapalli, S.S., Green, R.G., Reddy, K.N. and Marek, G. 2018. Application of an energy balance method for estimating evapotranspiration in cropping systems. Agric. Water Manage. 204. doi: 10.1016/j.agwat.2018.04.005.

Burgess, S.S.O., and Dawson, T.E.D. 2008. Using branch and basal trunk sap flow measurements to estimate whole-plant water capacitance: a caution. Plant Soil 305, 5-13.

Duan, L.M., Lv, Y., Yan, X., Liu, T.X., and Wang, X.X. 2017. Upscaling stem to community-level transpiration for two sand-fixing plants: Salix gordejevii and Caragana microphylla. Water 9, 361. doi:10.3390/w9050361.

Fan, B., Liu, Z., Xiong, K., Li, Y., Li, K., and Yu, X. 2022. Influence of environmental factors on the sap flow activity of the golden pear in the growth period of Karst area in Southern China. Water 14, 1707. https://doi.org/10.3390/w14111707.

Guerrieri, R., Belmecheri, S., Ollinger, S.V., Asbjornsen, H., Jennings, K., Xiao, J., Stocker, B.D., Martin, M., Hollinger, D.Y., Bracho-Garrillo, R., et al., 2019. Disentangling the role of photosynthesis and stomatal conductance on rising forest water-use efficiency. Proc. Natl. Acad. Sci. 116, 16909-16914.

Hatton, T.J., and Wu, H.I, 1995. A scaling theory to extrapolate individual tree water use to stand water use. Hydrol. Process. 9, 527-540.

Hentschel, R., Hommel, R., Poschenrieder, W., Grote, R., Holst, J., Biernath, C., Gessler, A., and Priesack, E. 2016. Stomatal conductance and intrinsic water use efficiency in the drought year 2003: a case study of European beech. Trees 30, 153-174.

Ibraimo, N.A. 2018. Water use of deciduous and evergreen tree nut crops: a case study using pecans and macadamias. PhD Thesis. Department of Plant and Soil Sciences, University of Pretoria, South Africa.

Jaskierniak, D., Benyon, R., Kuczera, G., and Robinson, A. 2015. A new method for measuring stand sapwood area in forests. Ecohydrol. 8, 504-517.

Li, Y.H., Chen, Q., K.N., and Wang, Z.X. 2022. The accuracy improvement of sap flow prediction in Picea crassifolia Kom. based on the back-propagation neural network model. Hydrol. Processes. https://doi.org/10.1002/hyp.14490.

Mashamaite, C.V., Pieterse, P.J., Mothapo, P. N., and Phiri, E.E. 2021. Moringa oleifera in South Africa: a review on its production, growing conditions and consumption as a food source. S. Afr. J. Sci. 117(3/4), 1-7.

Mokgehle, S., Araya, N., Mofokeng, M., Makgato, M., Amoo, S., Maboka, K., du Plooy, C., and Araya, H., 2022. Regrowth response and nutritional composition of Moringa oleifera to cutting back in three agro-ecological zones in South Africa. Horticulturae 8, 963. https://doi.org/10.3390/horticulturae8100963.

Nash, J. E., and Sutcliffe, J. V. 1970. River flow forecasting through conceptual models part I: a discussion of principles. J. Hydrol. 10, 282-290.

Noun, G., Lo Cascio, M., Spano, D., Marras, S., and Sirca, C. 2022. Plant-based methodologies and approaches for estimating plant water status of Mediterranean tree species: a semi-systematic review. Agronomy 12, 2127. https://doi.org/10.3390/agronomy12092127.

Roddy, A.B., and Dawson, T.E. 2013. Novel patterns of hysteresis in the response of leaf level sap flow to vapour pressure deficit. Acta Horticulturae 991, 261-267.

Uddin, J., Smith, R., Hancock, N., and Foley, J. 2014. Evaluation of sap flow sensors to measure the transpiration rate of plants during canopy wetting and drying. J. Agric. St. doi:10.5296/jas.v2i2.6134.

Villalobos, F.J., Testi, L., Orgaz, F., García-Tejera, O., Lopez-Bernal, A., González-Dugo, M.V., Ballester-Lurbe, C., Castel, J.R., Alarcón-Cabañero, J.J., Nicolás-Nicolás, E., et al., 2013. Modelling canopy conductance and transpiration of fruit trees in Mediterranean areas: a simplified approach. Agric. Forest Meteorol. 171-172, 93-103.

Xiong, W., Wang, Y.H., Yu, P.T., Liu, H.L., Xu, L.H., Shi, Z.J., and Mo, F. 2008. Variation of sap flow among individual trees and scaling up for estimation of transpiration of Larix principis-rupprechtii stand. Sci. Silvae Sin. 44, 34-40.

Zhang, J.G., He, Q.Y., Shi, W.Y., Otsuki, K., Yamanaka, N., and Du, S. 2015. Radial variations in xylem sap flow and their effect on whole-tree water use estimates. Hydrol. Process. 29, 4993-5002.

Zhang, Y.T., Liang, F.C., Chang, S.L., Shi, Q.D., Li, X., and Lu, J.J. 2011. Scaling up for transpiration of Pinaceae schrenkiana stands based on 8 hm2 permanent plots in Tianshan Mountains. Acta Ecol. Sin. 31, 3330-3339.

Zhao, L.J., Wang, L.X., Cernusak, L.A., Liu, X.H., Xiao, H.L., Zhou, M.X., and Zhang, S.Q. 2016. Significant difference in hydrogen isotope composition between xylem and tissue water in Populus euphratica. Plant Cell Environ., 39, 1848-1857.

Zhou, H., Zhao, W., Zheng, X., and Li, S. 2015. Root distribution of Nitraria sibirica with seasonally varying water sources in a desert habitat. J. Plant Res. 128, 613-622.

CHAPTER 5

WATER USE OF MORINGA UNDER VARYING WATER SUPPLY REGIMES

Ntsieni Mulovhedzi[1,2,3], Michael Savage[2] and Nadia Araya[1,3]

[1]Agricultural Research Council –Vegetable, Industrial and Medicinal Plants, Private bag X293, Pretoria, 0001, South Africa
[2]University of KwaZulu-Natal, Private Bag X01, Pietermaritzburg, 3209, South Africa
[3]Agricultural Research Council – Natural Resources and Engineering, Private bag X79, Pretoria, 0001, South Africa
[4]School of Agricultural Sciences, University of Mpumalanga, Private bag X11283, Mbombela, 1200, South Africa

5.1 INTRODUCTION

Moringa (*Moringa oleifera*) is one of the most important and utilized trees worldwide (Paliwal et al., 2011; Sharma et al., 2011). It is mainly grown in tropical and subtropical climates and parts of the world where temperatures are relatively high (Gandji et al., 2018). Moringa is considered to be one of the most nutritious tree crops in the world and commonly grown for its edible leaves, which contain high levels of Vitamin A, B and C, calcium, potassium, iron and protein, which are required for healthy living (Pandey et al., 2011; Nouman et al., 2014). The tree has multi-purpose uses, including water purification, medicinal and industrial applications, thus offering a great potential to improve food and nutrition security in South Africa. Most importantly, Moringa seeds can be used as a source of biofuel which is derived from agricultural products and is a renewable source of energy that can be used in many applications such as fueling vehicles, generating electricity and heating homes (Ofor and Nwufo, 2011).

Moringa originates from Agra and Oudh, in the northwest region of India, South of the Himalaya Mountains (Jules and Paull, 2008). Commercial production of Moringa in South Africa is still developing, which makes it difficult to quantify the area under its production, but there are various farmers producing Moringa, especially among the smallholder farmers in rural areas, mainly as food supplements (Muhl et al., 2011). Moringa is planted mainly in the rainy season, and is considered a drought tolerant crop (Atabani et al., 2014), although several studies have reported on its growth under a range of rainfall conditions (200-1500 mm) (Morton, 1991; Reyes-Sanchez, 2006; Pandey et al., 2011; Mabapa, 2019). Actual crop water use studies on the crop are practically nonexistent; there is only one study conducted in a hot semi-arid area of Brazil that reported a cumulative Moringa water consumption of 139.8 mm over an experimental period of 150 days (dos Santos et al., 2017). The experimental trees were one-year-old, planted at 3 x 3 m spacing on a circular drainage lysimeter, and the total reference evapotranspiration during the experimental period was 130.97 mm. Based on this study, Moringa water consumption was above the atmospheric evaporative demand, which resulted in crop coefficients up to 1.73. From day 240 to day 290 after transplanting, daily reference evapotranspiration varied from 4.0 to 6.0 mm, while crop water use fluctuated from 2.0 to 10.0 mm per day. A technical report published by de Saint Sauveur and Broin (2010) supported the increased water demand in Moringa, indicating that the tree requires irrigation for optimum leaf production, especially if seasonal rainfall is lower than 800 mm. The increased water supply is particularly important during the crop' reproduction phase to ensure optimum pollination, fruit set and yield (Muhl et al., 2013). Reduced water supply or water stress conditions are particularly beneficial for Moringa in the beginning of the inflorescence period, as it promotes high bud initiation (Muhl et al., 2013). Changes in soil water content around the rhizosphere of a six-year-old Moringa tree are more evident in the upper soil layers (the first 40 cm from the soil surface), while soil water content from the deeper layers (below 40 cm) remains practically unchangeable (Muhl et al., 2013). This suggests that the effective root zone of a Moringa tree lies within the top 40 cm soil profile. Further studies are required to investigate Moringa tree responses to varying soil water supply regimes, and their influence on the tree leaf production, which is particularly important for Moringa agro-processing and product development.

5.1.1 Study aim

To improve irrigation scheduling of Moringa cultivated for leaf production, through appropriate quantification of the tree water requirements.

5.1.2 Study objectives

- To evaluate changes in soil water content around the rhizosphere of Moringa tree as affected by varying soil water supply regimes;
- To evaluate Moringa tree growth and physiological responses to varying soil water supply regimes;
- To quantify Moringa tree leaf yield under varying soil water supply regimes;
- To determine Moringa tree water consumption under varying soil water supply regimes.

5.2. METHODOLOGY

5.2.1 Description of the study site

The study was conducted on a one to two-year-old Moringa (*Moringa oleifera*) plantation (Figure 5.1) established from seedlings, located at the Roodeplaat Experimental Farm of the Agricultural Research Council – Vegetable, Industrial and Medicinal Plants (ARC-VIMP) (25°35'N, 28°21'E, 1164 metres above sea level (masl)) in Gauteng Province, South Africa, over two consecutive summer growing seasons (from January to June), in 2018/2019 and 2019/2020.

Figure 5.1: A two-year-old Moringa plantation used to investigate the influence of varying soil water supply regimes on tree productivity and water use at ARC-VIMP.

The region experiences summer rainfall, with an average of about 650 mm per annum (Jovanovic and Annandale, 1999). The study area has a semi-arid climate, with average daily air temperatures ranging from 8-34°C in summer and 4-23°C in winter (Beletse et al., 2013). Prior to commencement of the trial in August 2019, a 1.5 x 1.5 x 1.5 m soil trench was dug for soil texture, volumetric soil water content (θ) at field capacity (FC), and permanent wilting point (PWP) determination. Soil samples were retrieved from 0-35 cm, 35-70 cm and 70-100 cm depths for soil texture, FC and PWP determination using standard laboratory procedures involving a hydrometer and pressure plate apparatus at the Institute for Soil, Climate and Water of the ARC. The soil samples were collected using a manual soil auger. This was done to determine chemical and physical properties of the soil at the study site (Table 5.1). The soil at the study site is classified as a Hutton soil form (Soil Classification Working Group, 1991), with a sandy clay texture.

Table 5.1: Soil chemical and physical properties across a one-meter soil profile at the study site prior to commencement of the field trial in August 2018.

Mineral elements	**Units**	**Soil layer**		
		0-35 cm	**35-70 cm**	**70-100 cm**
Phosphorous (P)-Bray 1	mg kg^{-1}	54.55	12.47	2.79
Potassium (K)	mg kg^{-1}	196.00	129.00	103.00
Calcium (Ca)	mg kg^{-1}	733.00	838.00	787.00
Magnesium (Mg)	mg kg^{-1}	204.00	278.00	268.00
Manganese (Mn)	mg kg^{-1}	26.90	17.40	15.40
Sodium (Na)	mg kg^{-1}	11.50	21.50	22.20
Iron (Fe)	mg kg^{-1}	10.8	8.06	7.68
Zinc (Zn)	mg kg^{-1}	6.88	1.09	0.97
Copper (Cu)	mg kg^{-1}	4.03	2.70	2.02
Ammonium-nitrogen (NO_4-N)	mg kg^{-1}	8.11	8.03	7.47
Nitrogen (N)	%	0.06	0.06	0.05
Nitrate-nitrogen (NO_3-N)	mg kg^{-1}	1.73	1.46	1.21
pH (H_2O)	–	7.16	7.21	7.15
Physical elements				
Sand	%	36.7	30.1	26.6
Silt	%	13.4	13.7	14.1
Clay	%	49.9	56.2	59.3
Field capacity	m^3 m^{-3}	0.337	0.351	0.358
Permanent wilting point	m^3 m^{-3}	0.210	0.210	0.210
Bulk density	kg m^{-3}	1241	1196	1113
Exchangeable / extractable cations				
Sodium (Na)	cmol(+)/kg	0.025	0.048	0.089
Potassium (K)	cmol(+)/kg	0.465	0.332	0.248
Calcium (Ca)	cmol(+)/kg	0.998	1.367	1.292
Magnesium (Mg)	cmol(+)/kg	5.710	6.573	6.137
S-Value	cmol(+)/kg	7.197	8.321	7.767
CEC	cmol(+)/kg	5.445	10.019	8.589

5.2.2 Experimental design, research treatments and trial layout

A 25 x 15 m piece of land was divided into 12 experimental plots of 8 x 4 m. Each experimental plot was planted with nine trees, spaced at 2 x 1 m. Four experimental treatments (high, medium, low irrigation levels, as well as rainfed) were laid out in a randomized complete block design with three replications (Figure 5.2).

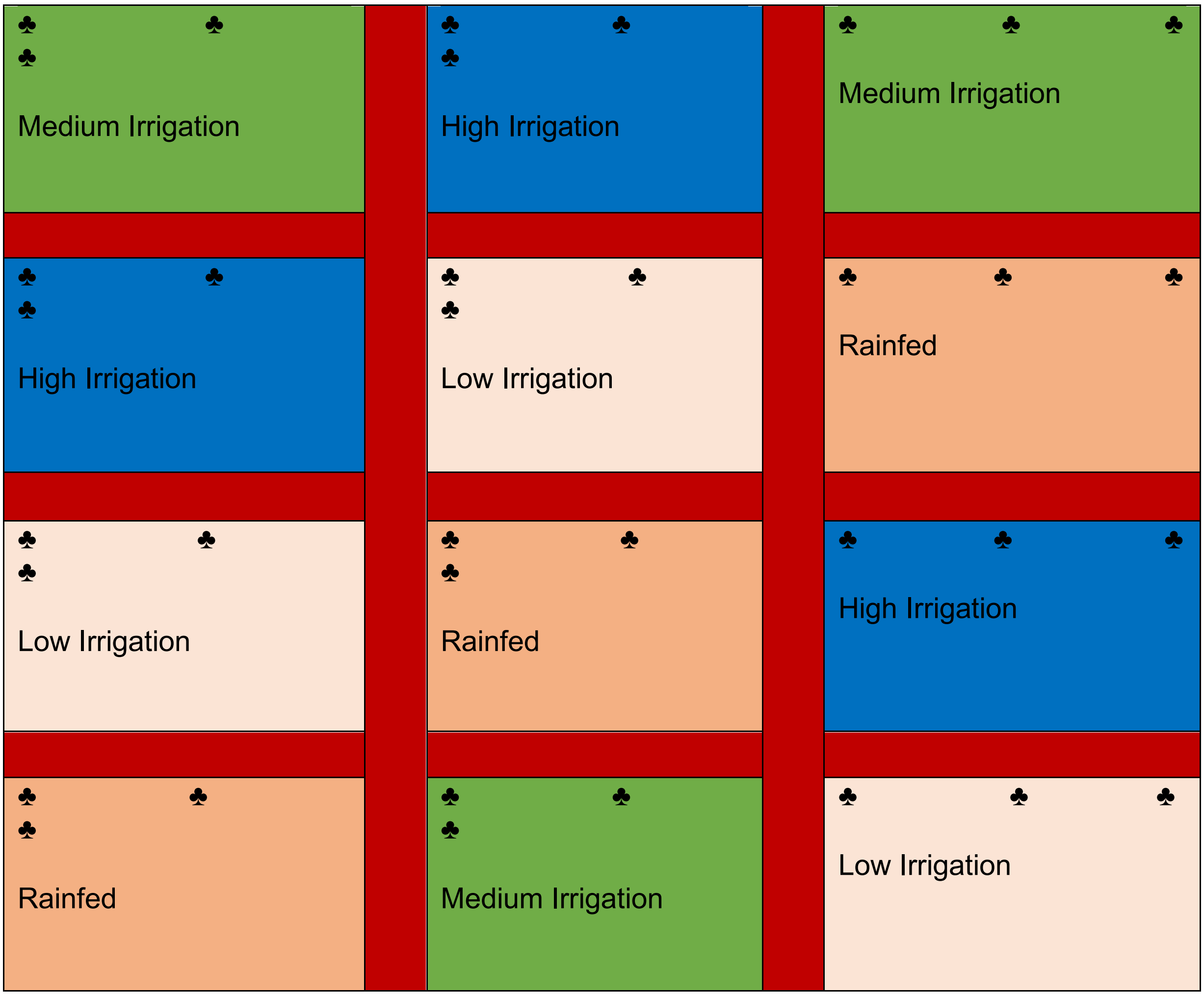

Figure 5.2: Field layout of the soil water supply regime Moringa trial at ARC-VIMP.

5.2.3 Irrigation scheduling and soil water content monitoring

The irrigation levels investigated during the trial period were defined as follows: (1) high irrigation, applied every day except on rainy days; (2) medium irrigation, applied once every three days and (3) low irrigation, applied once every week. The rainfed treatment depended solely on prevailing rainfall conditions. Irrigation was administered through drip lines (25 mm main lines and 15 mm lateral lines), one dripper per tree delivering 2.5 L/hr per tree. This resulted in a wetted diameter of 60 cm per dripper per tree. Changes in soil water content were monitored using 10HS capacitative soil water sensors (Campbell Scientific Inc., Logan, Utah, USA) connected to an EM50 datalogger (Campbell Scientific Inc., Logan, Utah, USA) to record the data automatically daily (Figure 5.3). Three soil water content sensors were installed per treatment to measure changes in soil water content from 0-35 cm, 35-70 cm and

70-100 cm. The cumulative irrigation amount per treatment was recorded using water meters installed on the main lines.

Figure 5.3: An EM50 datalogger connected to 10-HS capacitative soil water content sensors to record data automatically daily on a 2-year-old Moringa plantation at ARC-VIMP.

5.2.4 Weather data monitoring

Daily reference evapotranspiration (ET_o) for the measurement period was calculated using the FAO-56 Penman-Monteith equation (Allen et al., 1998) from weather data obtained from an automatic weather station (AWS). The AWS was located within 500 m of the Moringa plantation on an open stretch of mown, rain-fed grass and was 50 m north of natural vegetation, which consisted of sparse shrubs and grasslands. The weather parameters recorded were wind speed, solar radiation, temperature, relative humidity, and rainfall. Quality assessment and quality control of the data was performed according to the procedures described by Allen (2008). Quality of the data was found to be good, and no corrections were necessary.

5.2.5 Crop growth, physiology and yield monitoring

During both growing seasons, fractional interception of photosynthetically active radiation (FI_{PAR}) and leaf area index (LAI) were measured non-destructively using a Decagon Sunfleck ceptometer (Decagon, Pullman, Washington, USA) to monitor canopy development and the relationship between canopy development and crop water use. Maximum values were recorded at each harvest, during three consecutive harvests per growing season. This was done under clear sky days, between 12:00 and 14:00 pm.

Tree yield (fresh and dry mass) was measured at the end of each growing period, for three harvests per season using a portable field scale. The sample size consisted of two trees per treatment per replication. Trees were cutback to 80 cm from the ground surface, all the harvestable leaves were stripped off the branches and twigs for fresh yield determination. Immediately after taking the fresh weight of each sample, the fresh material was taken to an oven and dried at 70°C to a constant mass for dry yield determination. Leaf chlorophyll content and stomatal conductance were also taken once per growing period at each harvest using a SPAD and porometer, respectively.

5.2.6 Crop water use determination

Moringa tree water use was determined using the soil water balance method, taking into account the following principles: (1) rain or irrigation reaching a unit area of soil surface may infiltrate into the soil, or leave the area as surface runoff; (2) the infiltrated water may evaporate directly from the soil surface or be taken up by the tree for productivity via transpiration; (3) drain downward beyond the root zone as deep percolation, or (4) accumulate within the root zone (Zeleke and Wade, 2012). The soil water balance calculations were based on the conservation of mass principle, which states that change in soil water content (ΔS) of a crop root zone is equal to the difference between the amount of water added to the root zone, Q_i, and the amount of water withdrawn from it, Q_o (Hillel, 1998) in a given time interval expressed as in Equation 5.1.

$$\Delta S = Q_i - Q_o \tag{5.1}$$

Then, ΔS was used to determine crop evapotranspiration (ET), as follows:

$$ET = P + I + U - R - D - \Delta S \tag{5.2}$$

where ΔS = change in root zone soil water content storage, measured automatically on a daily basis, using 10HS capacitative soil water content sensors; P = Precipitation measured by an automatic weather station and manual rain gauges installed on-site; I = Irrigation monitored using water meters installed on the main lines of each treatment; U = upward capillary rise into the root zone, R = runoff and D = deep percolation beyond the root zone were estimated using AquaCrop modelling version 4 (Raes et al., 2012). Groundwater table was assumed to be present at a constant depth of 2 m below soil surface, while values of R were estimated using the Curve Number method embedded in the AquaCrop modelling procedure. Soil physical characteristics (particle size distribution, bulk density, FC, PWP and typical hydraulic conductivity values for a sandy clay soil) were used for model parameterization, while model testing was conducted with the aid of actual soil water content measurements at different depths of the soil profile.

5.2.7 Statistical analysis

Statistical analysis of variance (ANOVA) was performed on the observations of Moringa tree for the four soil water supply regimes investigated across different growth periods (John and

Quenouille, 1977) after testing the homogeneity of the experimental error variances using Bartlett's test (Bartlett, 1937). The residuals were examined for deviations from normality, and outliers causing skewness were removed. Fisher's least significant difference (LSD) was calculated at the 5% level to compare means for significant effects (Ott, 1998). Analysis was done using let Genstat for Windows 18th Edition (VSN International, 2015).

5.3. RESULTS AND DISCUSSION

5.3.1 Weather variability during the experimental period

During the experimental period (October 2018 to May 2020), maximum and minimum daily air temperatures fluctuated from 19.18-38.52°C and 2.48-20.64°C, respectively in 2018/19 and 16.58-38.31°C and 8.68-21.47°C, respectively in 2019/20. Daily solar radiation varied from 13.67-27.91 MJ m^{-2} s^{-1} in 2018/19, while in 2019/20 it fluctuated from 5.09-29.56 MJ m^{-2} s^{-1} (Figure 5.4). The 2019/20 season had noticeably higher and more erratic rainfall (a total of 981 mm, with December as the wettest month) compared to the 2018/19 season (501 mm occurring more evenly throughout the year).

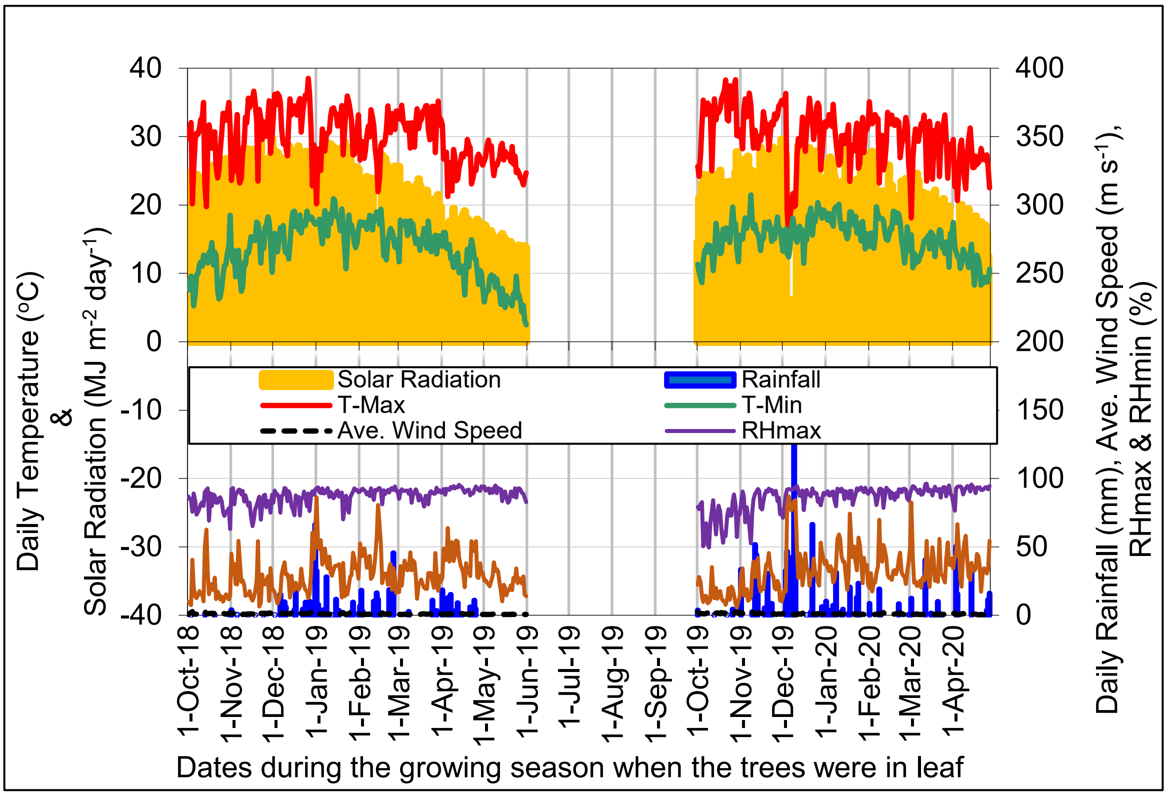

Figure 5.4: Daily weather variability (solar radiation, rainfall, maximum and minimum air temperature and relative humidity, as well as wind speed) during the experimental period at Roodeplaat Experimental Farm of ARC.

5.3.2 Changes in soil water content as influenced by rainfall, irrigation and reference evapotranspiration

The volumetric soil water content across different layers within a one-meter soil profile was quite different among the four soil water supply regimes investigated (Figure 5.5). The high irrigation treatment (water supplied every day for 20 min each time, except during rainy days) registered the highest volumetric soil water content (approximately 0.34 m^3/m^3 across the entire soil profile), which was very close to that at field capacity (0.348 m^3/m^3). Despite the high wetness, it was possible to note that the highest fluctuation in soil water content occurred with the first 35 cm soil layer, whereas the deeper soil layers remained practically unchangeable. A similar wetting pattern was observed with the medium/moderate irrigation treatment (application of irrigation every three days for 20 min at a time). The top 35 cm soil layer showed a maximum depletion of 10% from field capacity, while the deeper layers (35-100 cm) remained steadily wet at nearly field capacity. The depletion level in the lowest irrigation regime (water supply one a week for 20 min each time) reached a maximum of 25% from field capacity (the 2018/19 season showed a more pronounced depletion level compared to the 2019/20 season). Similarly, the rainfed water supply treatment revealed sharper decline in soil water content in the first experimental season compared to the second season. This is associated to variations in the occurrence of rainfall (a total of 501 mm in the first season compared to 900 mm in the second season, Figures 5.6 and 5.7). The data also showed severe decline in soil water content across the entire 1.0 m soil profile for the rainfed treatment, demonstrating that because of aggravated water stress, Moringa trees were able to access water from deeper layers as a strategy to maintain crop productivity. Similar changes in soil water content were reported by Muhl et al. (2013) for a 6-year-old Moringa plantation cultivated in a semi-arid area of Pretoria.

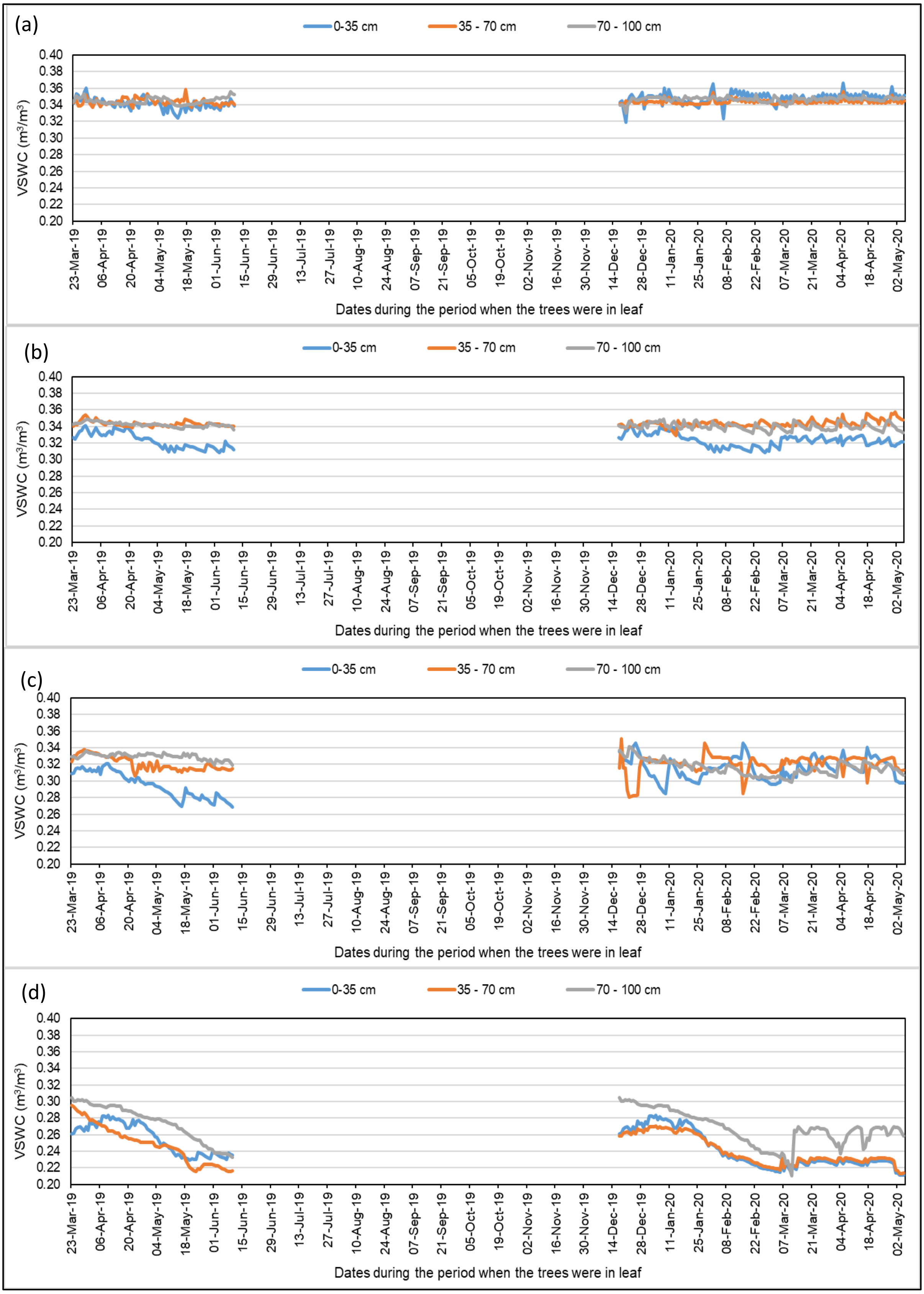

Figure 5.5: Changes in soil water content per soil layer on a 2-year-old Moringa plantation as affected by varying soil water supply regimes (high – a; medium – b; low – c and rainfed irrigation – d) at ARC-VIMP.

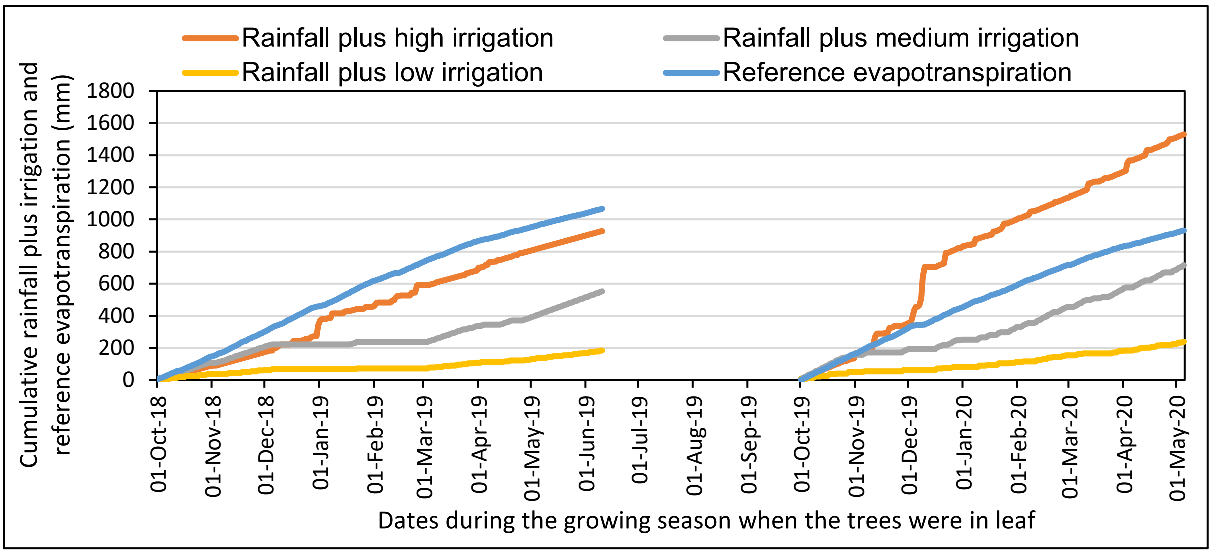

Figure 5.6: Seasonal cumulative rainfall plus irrigation and reference evapotranspiration under varying soil water supply regimes during the experimental period 2018/19-2019/20 at ARC-VIMP.

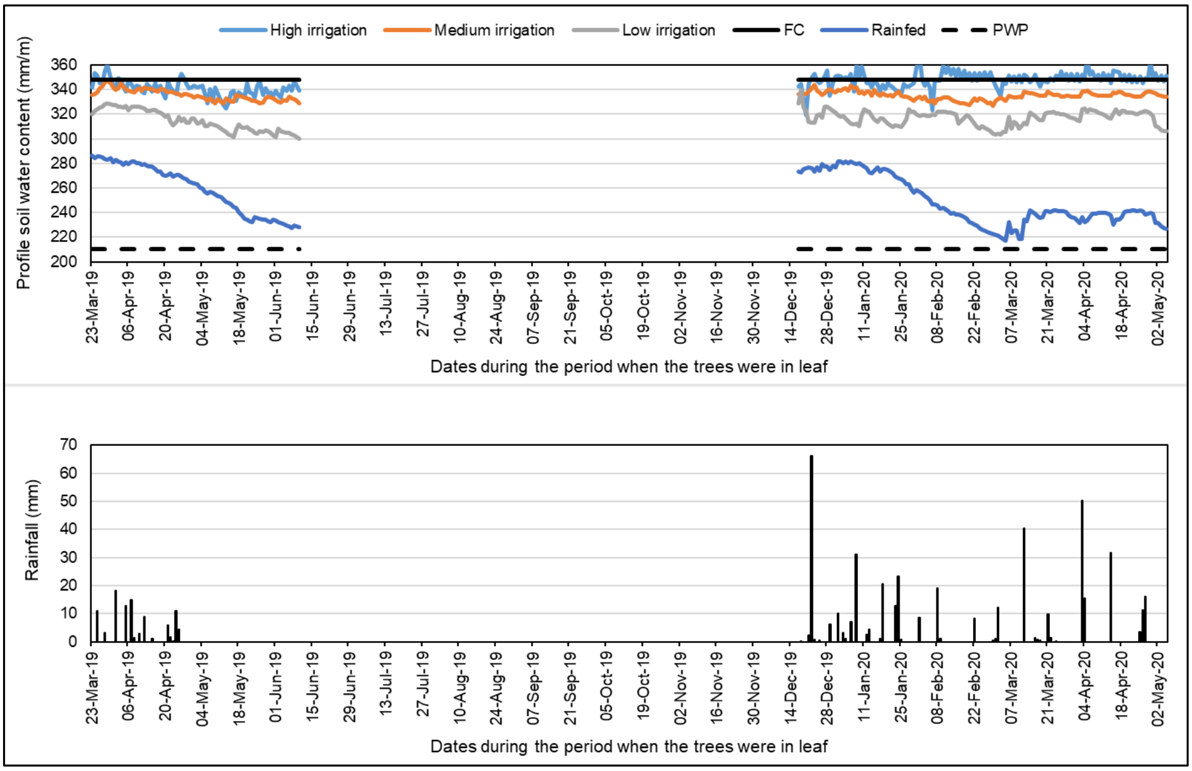

Figure 5.7: Average profile changes in soil water content as influenced by rainfall on a 2-year-old Moringa plantation under varying soil water supply regimes at ARC-VIMP.

5.3.3 Moringa tree growth and physiology in response to varying soil water supply regimes

An analysis of variance across the various soil water supply regimes investigated at different growth periods, revealed significant effects of these factors individually, while their overall interaction did not show any significant influence on the growth and physiology of the Moringa tree (Table 5.2). A similar crop response was observed across two consecutive seasons of experimental research. Soil water regime showed a more significant effect on the growth and physiological response on Moringa than the harvest/growth period. The highest order interaction or single factor was further analyzed using Fisher's least significant difference (LSD) calculated at the 5% level to compare means for significant effects (Tables 5.3-5.6). In general, the highest Moringa growth (in terms of LAI, PAR and tree height) was observed with the medium irrigation regime, while the rainfed treatment showed the poorest performance. The rainfed treatment showed exceptionally high leaf surface temperatures, because of severe water stress imposed on the crop. Leaf stomatal conductance of Moringa was only affected by variation in soil water supply regimes in the first season of measurements, which is probably because this season received much lower rainfall (a total of 500 mm) compared to the second season (which received a total of 900 mm) (Figure 5.8). Moringa did not reveal a clear response as influenced by the harvest/growth period, but in general, the second harvest period seemed to result in the highest significantly different growth and physiological response. Harvesting early or late in the season seemed to affect the productivity of the crop at a times.

Table 5.2: Analysis of variance for the effect of soil water supply regimes and harvest periods on growth and physiological parameters of Moringa trees cultivated at Roodeplaat.

		LAI ($m^2 m^{-2}$)		PAR (%)		Tree height (cm)		Leaf chlorophyll content (SPAD)		Leaf stomatal conductance (mmol $m^{-2} s^{-1}$)		Leaf temperature (°C)	
Source of variation	df	SS	MS	SS	MS	SS	MS	SS	MS	SS	MS	SS	MS
						2018 2019							
Soil water regime (SWR)	3	1.41889	0.47296***	889.75	296.58**	435.639	145.213**	406.347	135.449***	509412	169804***	8.4656	2.8219***
Harvest period (HP)	2	4.17722	2.08861***	1340.28	670.14**	5488.722	2744.361***	112.237	56.119***	93401	46701.ns	0.6289	0.3144 ns
SWR X HP	6	0.09611	0.01602ns	54.99	9.16ns	19.278	3.213ns	76.632	12.772*	141765	23627ns	1.8778	0.3130ns
Residual	16	0.20667	0.01292	232.72	112	15.7522	7.000	59.344	3.709	314880	19680	2.4333	0.1521
Total	35	6.07889		2653.24		6146.306		667.176		1212252		15.7522	
						2019-2020							
Soil water regime (SWR)	3	4.32333	4.32333***	1241.5	413.83**	2041.47	1398.5***	797.01	265.67***	90011	30004ns	3.6408	1.2136*
Harvest period (HP)	2	6.40722	3.20361***	112.46	56.23ns	102811.7	51405.9***	46.59	23.30ns	22182	11091.ns	0.42	0.21ns
SWR X HP	6	0.54833	0.54833ns	47.53	7.92ns	595.8	99.3ns	45.65	7.61ns	57826	9638.ns	3.3	0.5500ns
Residual	16	0.54833	0.05153	494.95	30.93	1877.1	117.3	166.91	10.43	231727	14483	3.4733	0.2171
Total	35	12.49222		2041.47		110740.3		1125.13		574704		13.4475	

Table 5.3: The effect of soil water supply regime and harvest period on leaf area index during two consecutive growing seasons.

Factor	LAI (m^2 m^{-2})			
	2018-2019			
Soil water regime	High Irrigation 1.578b	Medium Irrigation 1.833a	Low Irrigation 1.678b	Rainfed 1.289c
Harvest period	Harvest 1 1.250c	Harvest 2 2.058a	Harvest 3 1.475b	
	2019-2020			
Soil water regime	High Irrigation 2.556c	Medium Irrigation 3.111a	Low Irrigation 2.844b	Rainfed 2.178d
Harvest period	Harvest 1 3.192a	Harvest 2 2.158c	Harvest 3 2.667b	

Table 5.4: The effect of soil water supply regime and/or harvest period on photosynthetic active radiation during two consecutive growing seasons.

Factor	PAR (%)			
	2018-2019			
Soil water regime	High Irrigation 61.56b	Medium Irrigation 68.39 a	Low Irrigation 64.38ab	Rainfed 54.76c
Harvest period	Harvest 1 54.16c	Harvest 2 68.88a	Harvest 3 63.77b	
	2019-2020			
Soil water regime	High Irrigation 68.59c	Medium Irrigation 75.66a	Low Irrigation 72.82b	Rainfed 60.10 d

Table 5.5: The effect of soil water supply regime and harvest period on tree height during two consecutive growing seasons.

Factor	Tree height (cm)			
	2018-2019			
Soil water regime	High Irrigation 80.44b	Medium Irrigation 84.22a	Low Irrigation 80.44b	Rainfed 74.67c
Harvest period	Harvest 1 89.67a	Harvest 2 86.42b	Harvest 3 62.00c	
	2019-2020			
Soil water regime	High Irrigation 197.30b	Medium Irrigation 215.00a	Low Irrigation 205.00b	Rainfed 186.30c
Harvest period	Harvest 1 170.8b	Harvest 2 156.3c	Harvest 3 186.3a	

Table 5.6: The effect of soil water supply regime and/or harvest period on leaf chlorophyll content during two consecutive growing seasons.

Factor	Leaf chlorophyll content (SPAD)			
	2018-2019			
Soil water regime	High Irrigation	Medium Irrigation	Low Irrigation	Rainfed
	49.72c	56.48a	52.78b	47.54d
Harvest period	Harvest 1	Harvest 2	Harvest 3	
	51.47b	53.87a	49.55c	
	2019-2020			
Soil water regime	High Irrigation	Medium Irrigation	Low Irrigation	Rainfed
	51.65c	59.32a	55.27b	48.53d

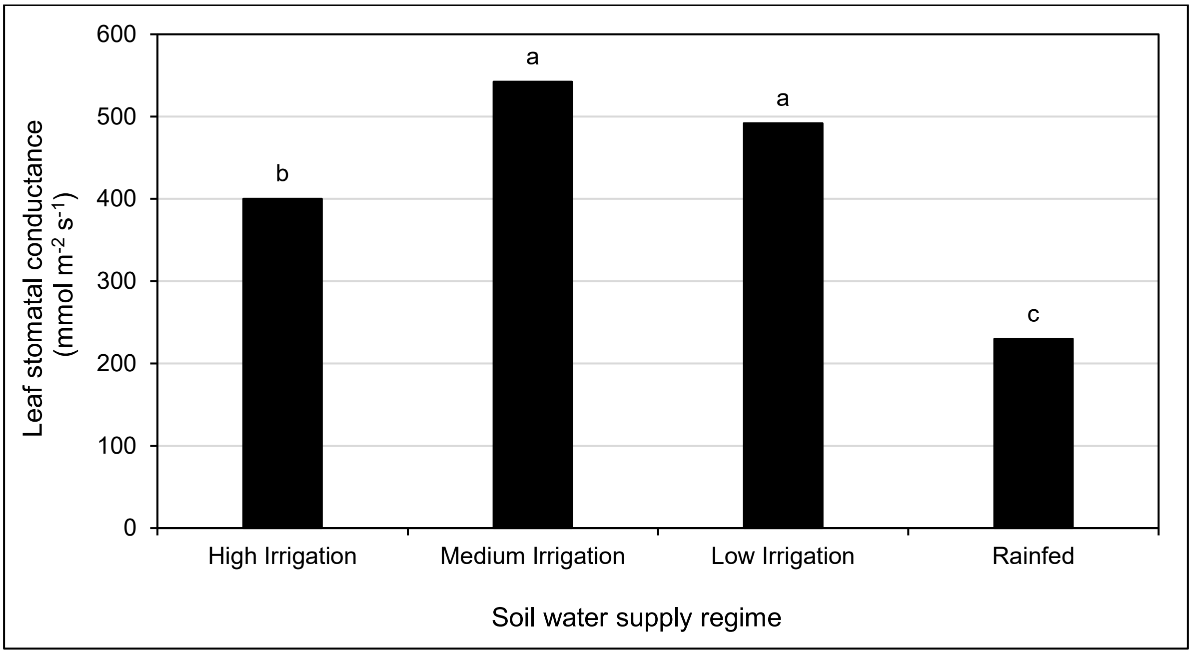

Figure 5.8: The effect of soil water supply regime on leaf stomatal conductance of Moringa during the 2018-2019 growing season.

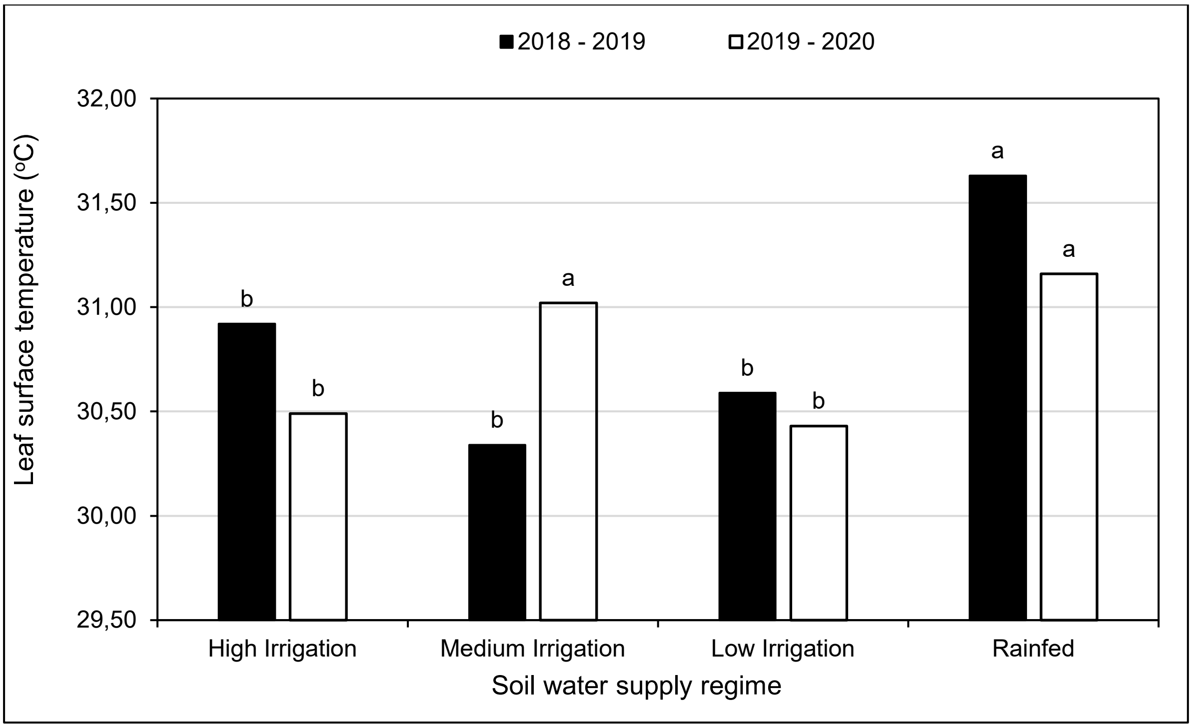

Figure 5.9: The effect of soil water supply regime on leaf surface of Moringa during two consecutive growing seasons.

5.3.4 Moringa tree yield in response to varying soil water supply regimes

Similarly to its growth and physiological response, Moringa yield was significantly higher under the medium irrigation regime, followed by the low irrigation regime, whilst the high irrigation and rainfed treatments showed the poorest crop yield (both fresh and dry leaf yield were the lowest under these treatments) (Tables 5.7-5.10). This shows that both extremes of soil water supply (too high or too low) are detrimental to Moringa crop productivity. The interaction between soil water supply regime and harvest period was significant only in the first season of growth, which is probably attributed by the fact that the tree was relatively young and more susceptible to the effect of water stress, particularly in the beginning or late in the season. This might also be related to the prevailing weather conditions and canopy during the growing season, as these periods coincide with relatively low canopy foliage and lower temperatures particularly in spring and autumn periods. Seasonal yield of Moringa (Table 5.10 and Figure 5.10), considerably increased from 2018-2019 (maximum of 1.0- and 0.2-ton ha^{-1} for fresh and dry yield, respectively) to 2019-2020 (maximum of 7.0- and 1.5-ton ha^{-1} for fresh and dry yield, respectively). This demonstrates the evident fast growth pattern in Moringa trees. Based on these results, it is possible to infer that the moisture content in Moringa leaves is approximately 80% of the total biomass weight.

Table 5.7: Analysis of variance for the effect of soil water supply regimes and harvest periods on yield parameters of Moringa trees cultivated at Roodeplaat.

Source of variation	df	Fresh leaf yield (ton ha^{-1}) SS	Fresh leaf yield (ton ha^{-1}) MS	Dry leaf yield (ton ha^{-1}) SS	Dry leaf yield (ton ha^{-1}) MS
			2018-2019		
Soil water regime (SWR)	3	0.0714219	0.0238073***	0.004475	0.00149167***
Harvest period (HP)	2	0.0963449	0.0481724***	0.00976872	0.00488436***
SWR X HP	6	0.0189898	0.00108417**	0.00108417	0.00018069*
Residual	16	0.0114587	0.01292	0.00075511	0.00004719
Total	35	0.2050259		0.01651322	
			2019-2020		
Soil water regime (SWR)	3	4.32333	1.5332**	0.206248	0.068749**
Harvest period (HP)	2	21.3202	10.6601***	1.039064	0.519532***
SWR X HP	6	0.8417	0.1403ns	0.044108	0.007351ns
Residual	16	2.2993	0.1437	0.128214	0.008013
Total	35	30.03		1.453809	

Table 5.8: The effect of soil water supply regime and harvest period on Moringa fresh leaf yield during two consecutive growing seasons.

Fresh leaf yield (ton ha^{-1})				
2018-2019				
	Soil water regime			
Harvest period	High Irrigation	Medium Irrigation	Low Irrigation	Rainfed
Harvest 1	0.2277ef	0.283cd	0.2513cd	0.1213f
Harvest 2	0.34ab	0.367a	0.3533a	0.327abc
Harvest 3	0.2427de	0.349ab	0.306bc	0.191g
2019-2020				
Soil water regime	High Irrigation	Medium Irrigation	Low Irrigation	Rainfed
Fresh leaf yield (ton ha^{-1})	1.9b	2.357a	2.053ab	1.371c
Harvest period	Harvest 1	Harvest 2	Harvest 3	
Fresh leaf yield (ton ha^{-1})	2.621a	0.849c	2.291b	

Table 5.9: The effect of soil water supply regime and harvest period on Moringa dry leaf yield during two consecutive growing seasons.

Dry leaf yield (ton ha^{-1})				
2018-2019				
	Soil water regime			
Harvest period	High Irrigation	Medium Irrigation	Low Irrigation	Rainfed
Harvest 1	0.04333 ef	0.06067d	0.05367de	0.1213f
Harvest 2	0.08700ab	0.09167a	0.08933ab	0.327abc
Harvest 3	0.05067de	0.08667ab	0.07400c	0.04500 g
2019-2020				
Soil water regime	High Irrigation	Medium Irrigation	Low Irrigation	Rainfed
Fresh leaf yield (ton ha^{-1})	0.3908b	0.4917a	0.4343ab	0.2849c
Harvest period	Harvest 1	Harvest 2	Harvest 3	
Fresh leaf yield (ton ha^{-1})	0.5828a	0.1738c	0.4448b	

Table 5.10: Analysis of variance for the effect of soil water supply regimes on seasonal yield parameters of Moringa trees cultivated at Roodeplaat.

Source of variation	df	Seasonal fresh leaf yield (ton ha^{-1}) SS	MS	Seasonal dry leaf yield (ton ha^{-1}) SS	MS
		2018-2019			
Soil water regime (SWR)	3	0.218225	0.072742***	0.0128917	0.0042972***
Residual	16	0.0118	0.01292	0.0007833	0.0001306
Total	35	0.001967		0.014025	
		2019-2020			
Soil water regime (SWR)	3	13.4892	4.4964**	0.58	0.193333***
Residual	16	1.5683	0.2614	0.055	0.009167
Total	35	16.3692		0.68	

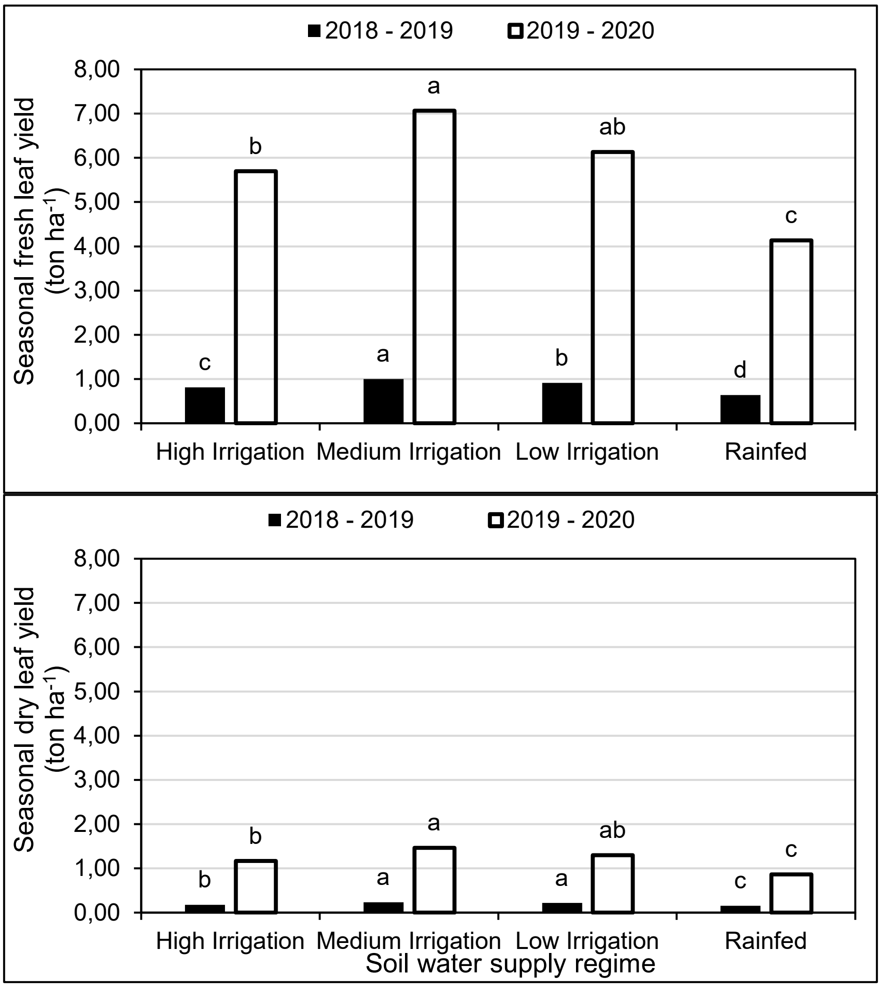

Figure 5.10: The effect of soil water supply regime on seasonal fresh (a) and dry (b) leaf yield of Moringa during two consecutive growing seasons.

5.3.5 Moringa crop water use under varying soil water supply regimes

The total cumulative water consumption of a Moringa tree per harvest/growth period summed 71.0 to 88.5 mm under the high irrigation regime, followed by 44.7 to 58.9 mm under the medium irrigation regime, 28.4 to 55.9 mm under the low irrigation regime, while the rainfed treatment showed the lowest tree water consumption of 34.2 to 52.3 mm. The tree water consumption remained practically unchangeable from season one to season two, although the tree growth and yield increased considerably from one season to another. This suggests that the Moringa tree does not use a lot of water; instead, it uses water very efficiency for maximum crop productivity. Tree water use was on average 0.6 to 1.8 mm day^{-1} during harvest 2 of 2018/19, 0.9 to 1.9 mm day^{-1} during harvest 3 of 2019/19, 1.2 to 1.7 mm day^{-1} during harvest 1 of 2019/20, 0.9 to 1.7 mm day^{-1} during harvest 2 of 2019/20 and 0.8 to 1.6 mm day^{-1} during harvest 3 of 2019/20 (Figure 5.11). The atmospheric evaporative demand, on the other hand, was much higher (averaging 2.5 to 4.4 mm day^{-1}). A study conducted by Azam at al. (2020) supports the present findings, as the growth performance of 5-year-old Moringa trees (shoot length, leaf score and number of branches) increased by maintaining the soil water content at 70% of field capacity as compared to 100% field capacity. Both studies contradict the findings reported by dos Santos et al. (2017) for 1-year-old Moringa trees grown in drainage lysimeters in a semi-arid area of Brazil, in which much higher daily tree water use was reported (between 2.0 and 10.0 mm day^{-1}). The huge discrepancy of Moringa crop water use findings between the two studies is likely attributed to differences in the methodology used to estimate crop water use, as well as cultivation environments (drainage lysimeter versus open-field). Further studies are encouraged using more robust crop water use methods, physiological (example of sap flow) and micrometeorological approaches (example of eddy covariance) for better inferences on Moringa crop water use.

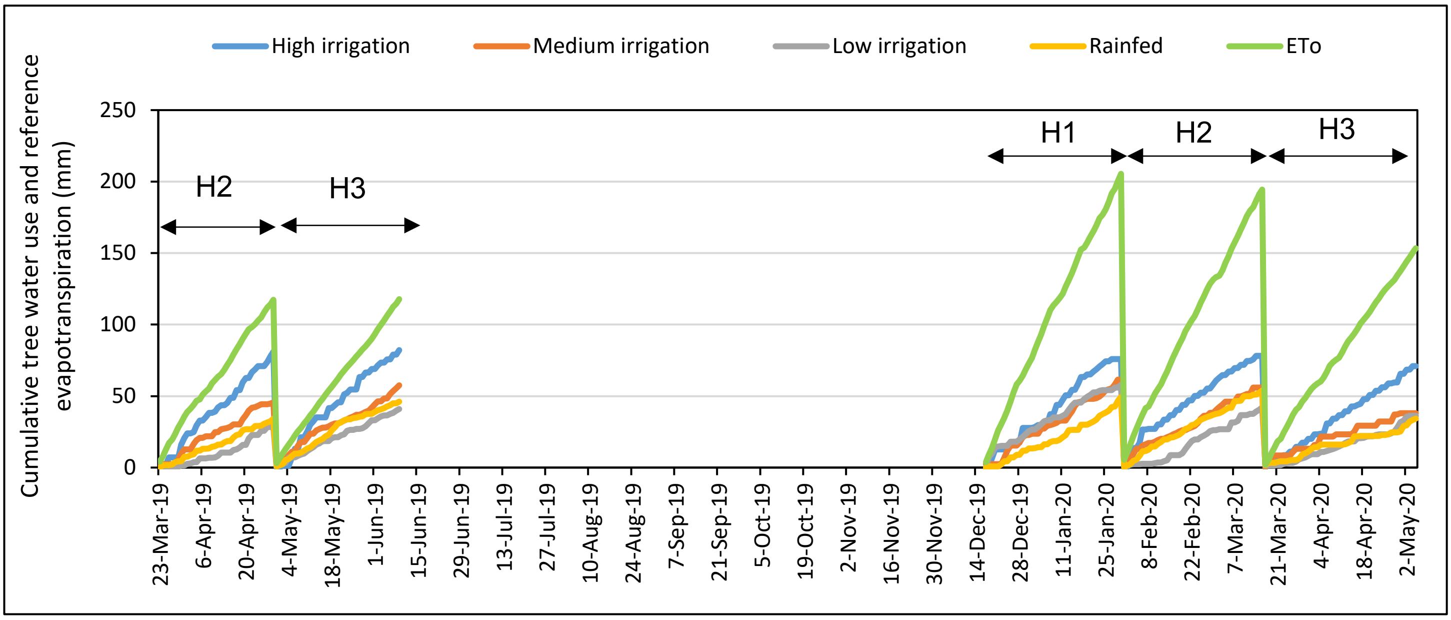

Figure 5.11: Moringa tree water use during different growth periods (H1, H2 and H3) and soil water supply regimes.

5.4 CONCLUSIONS AND RECOMMENDATIONS

The growth, physiology and yield of two-year-old *Moringa oleifera* trees was investigated in response to varying soil water supply regimes and harvest/growth periods. The productivity of Moringa trees (growth and yield parameters) increased considerably from one- to two-year-old trees. However, the crop water use remained practically unchangeable across the seasons. The total cumulative crop water use per growth period (about 45 days) varied from 28.4 mm under low irrigation to 88.4 mm under high irrigation, which results in a daily average water consumption of 0.63 to 1.9 mm day^{-1}. Moringa crop productivity was significantly higher under the moderate irrigation regime, followed the low irrigation regime imposed, while high irrigation and rainfed water supply regimes resulted in the poorest crop productivity. Based on these findings, Moringa young Moringa trees (1- to 2-year-old) should be irrigate one every three days for 3.0 to 4.5 mm of water at a time.

ACKNOWLEDGEMENTS

This work was financially supported by the Water Research Commission of South Africa (WRC Project No. C2020/2021-00484). Technical support, data collection and processing by postgraduate student Mr Ntsieni Mulovhedzi and ARC staff (Dr Nadia Araya, Mr Ernest Malatjie, Mr Takalani Tuwani, Mr Mfuzi Makwakwa and Dr Ian du Plooy) are highly appreciated. Ms Irene Nel (from ARC – Natural Resources and Engineering) is thanked for providing a complete set of weather data for the experimental site.

REFERENCES

Allen, R.G., 2008. Quality assessment of weather data and micrometeological flux – impacts on evapotranspiration calculation. J. Agric. Meteorol., 64, 191-204.

Allen, R.G., Pereira, L.S., Raes, D., Smith, M., 1998. Crop Evapotranspiration: Guidelines for Computing Crop Water Requirements, Irrigation and Drainage Paper 56. United Nations FAO, Rome http://www.fao.org/docrep/X0490E/ X0490E00.htm

Atabani, A.E., Mofijur, M., Masjuki, H.H., Badruddin, I.A., Kalam, M.A., Chong, W.T., 2014. Effect of Croton megalocarpus, Calophyllum inophyllum, Moringa oleifera, palm and coconut biodiesel diesel blending on their physico-chemical properties. Indian j. crop sci., 60 (0), 130-137.

Azam, S., Nouman, W., Ubaid-ur Rehman, U., Ahmed, Gull, T., Shaheen, M., 2020. Adaptability of Moringa oleifera Lam. under different water holding capacities. S AFR J BOT, 129; 299-303.

De Saint Sauveur, A., Broin, M., 2010. Growing and processing moringa leaves. Moringa Association of Ghana. Available at http//miracletree.org/moringadoc/ moringa book.

Dos Santos, C.S., Montenegro, A.A.A., Márcio, A.L., Dos Santos, M.A.L., Pedrosa, E.M.R,, 2017. Evapotranspiration and crop coefficients of Moringa oleifera under semi-arid conditions in Pernambuco. Rev. Bras. Eng. Agric. Ambient., 21: 840-845.

Gandji, K., Chadare, F.J., Idohou, R., Salako, V.K., Assogbadjo, A.E., Glèlè Kakaï, R.L., 2018. Status and utilisation of *Moringa oleifera* Lam.: a review. Afr. Crop Sci. J., 26 (1), 137-156.

Hillel, D., 1997. Small scale irrigation for arid zones: Principles and options, Development monograph No. 2 , FAO, Rome.

Jules J, Paull RE. 2008. The Encyclopedia of Fruit & Nuts. CABI. pp. 509-510.

Paliwal, R., Sharma, V., Pracheta, Sharma, S., Yadav, S., Sharma, S., 2011. Antinephrotoxic effect of administration of Moringa oleifera Lam in amelioration of DMBA-induced renal carcinogenesis in Swiss albino mice. Biol. Med. 3(2):27-35.

Pandey, A., Pradheep, K., Gupta, R., Nayar, E.R., Bhandari, D.C., 2011. 'Drumstick tree' (*Moringa oleifera* Lam.): a multipurpose potential species in India. Genet. Resour. Crop Evol., 58, 453-460.

Mabapa, M.P.B., 2019. Yield characteristics, carbon capture and chemical composition of Moringa oleifera under diverse planting population and agro-ecological conditions of the Limpopo Province. PhD thesis, University of Limpopo, Limpopo, South Africa.

Morton, J.F., 1991. The horseradish tree, Moringa pterygosperma (Moringaceae) – A boon to arid lands? Econ. Bot. 45, 318-333.

Muhl, Q.E., Du Toit, E.S., Robbertse, P.J., 2011. Moringa oleifera (horseradish tree) leaf adaptation to temperature regimes. Int J Agric Biol., 13: 1021-1024.

Muhl, Q.E., Du Toit, E.S., Steyn, J.M., Apostolides, Z., 2013. Bud development, flowering and fruit set of Moringa oleifera Lam. (Horseradish Tree) as affected by various irrigation levels. JARTS 114 (2), 79-87, ISSN 1612-9830.

Nouman, W., Siddiqui, M.T., Basra, S.M.A., Khan, R.A., Gull, T., Olson, M.E., Munir, H., 2014. Response of Moringa oleifera to saline conditions. Int J Agric Biol . 14, 757-762.

Ofor, M.O., Nwufo, M.I., 2011. The search for alternative energy sources: Jatropha and moringa seeds for biofuel production. JASR*.* 2011, *11*, 87-94.

Ott, R.L., 1998. An Introduction to Statistical methods and data analysis. Belmont, California: Duxbury Press: 807-837.

Reyes-Sánchez N 2006. Moringa oleifera and Cratylia argentea: Potential fodder species for ruminants in Nicaragua, Doctoral thesis No. 2001:1. (SLU Acta Universitatis Agriculture Science, Uppsala).

Raes, P., Steduto, T.C., Hsiao, E., Fereres, 2012. AquaCrop Calculation procedures. AquaCrop version 3, Chapter 3, 1-120.

Sharma, V., Paliwal, R., Sharma, P., Sharma, S. 2011. Phytochemical analysis and evaluation of antioxidant activities of hydroethanolic extract of *Moringa oleifera* Lam. Pods. J. Pharm. Res. 4: 554-557.

VSN International, 2015. Genstat for Windows 18th Edition. VSN International, Hemel Hempstead, UK. Web page: Genstat.co.uk.

Zeleke, K.T., Wade, L.J., 2012. Evapotranspiration estimation using soil water balance, weather and crop data. In book Evapotranspiration – Remote Sensing and Modeling, IntechOpen, Chapter 3, 41-58.

CHAPTER 6

WATER USE OF MORINGA UNDER VARYING TREE SPACING, RAINWATER HARVESTING AND CONSERVATION PRACTICES

Nadia Araya[1,3], Ambroise Ndayakunze[1,2], Sihle N'Wamba[1] and Hintsa Araya[1]
[1]*Agricultural Research Council – Vegetable, Industrial and Medicinal Plants, Pretoria, South Africa*
[2]*University of Pretoria, Department of Plant and Soil Sciences, Pretoria, South Africa*
[3]*Agricultural Research Council – Natural Resources and Engineering, Pretoria, South Africa*

6.1 INTRODUCTION

Moringa (*Moringa oleifera* Lam.) is a fast-growing and drought-tolerant tropical and subtropical tree species with multiple purposes. The tree can withstand unfavourable growing conditions and adapt to a wide range of environments (Mabapa et al., 2017; Aditama et al., 2021; Mokgehle et al., 2022). However, the species is confronted with the challenges of low commercial potential due to limited exploitation, and the scanty research thereof, largely with regard to the crop water use (WU) and morpho-ecophysiological characteristics (Vasconcelos et al., 2019). Moreover, there are knowledge gaps towards optimum cultivation practices for increased yield and quality of the harvested fresh leaf produce (Leone et al., 2015; du Toit et al., 2020). Further, nothing is known about the potential of the Moringa tree crop to protect agricultural soils against erosion, a major concern in the smallholder farming sector where agriculture is largely rain-fed.

Most of the literature on Moringa rather focused on assessing the chemical, medicinal and nutritional characteristics of the plant. Finally, the harvesting of Moringa leaves also deserves a renewed attention, as farmers mostly employ the cut-back method (which consists of cutting-back the tree branches and twigs by 30 cm when it reaches 60 cm high, followed by stripping off all productive leaves), for being relatively quick, thus reducing the harvesting time and labour costs (Mokgehle et al., 2022). However, Mabapa (2019) reported that stripping off productive leaves directly from the tree at the base of the petioles, without any removal of branches or twigs, can potentially enhance tree lateral branching, water use efficiency, regrowth, and leaf biomass production. The frequency at which Moringa farmers harvesting the trees for leaf agro-processing purposes has also not been investigated enough (Mabapa, 2019).

Moringa production in South Africa is essentially for agro-processing and a minority for consumption of leaves, which both are reported to make a positive contribution to poverty alleviation, food and nutrition security as well as job creation (Mabapa, 2019). In addition, although Moringa is underutilized, it remains one of the species that are beneficial options for climate change adaptation and mitigation under harsh climatic conditions (Mabapa, 2019). Thus, combining Moringa production with rainwater harvesting (RWH) and conservation can potentially support sustainable food and nutrition availability while protecting the soil fertility and the environment at large. This must specifically be prioritized in semi-arid and arid regions of the African continent, where crop and livestock productivity and farmer livelihoods are constraint by inadequate water availability and soil degradation. These regions have to adopt, maintain and enhance measures that conserve soil and water resources (SWC) (Bagula et al., 2022; Diop et al., 2022; Obala et al., 2022; Bufebo et al., 2023). Technologies of SWC include measures such as cultural (cover crops, conservation agriculture), vegetation (grass strips, agroforestry systems), structural (terraces, RWH structures) and land management practices (fertilisation, composting, manuring). In general, these different categories of SWC overlap or are involved in substantial synergies (Roose, E., 2015; Bufebo et al., 2023).

Therefore, the multiple benefits of Moringa can be consolidated if cultivation takes into account an integration of optimum management practices of tree spacing, population density as well as rainwater harvesting and conservation.

6.1.1 Study aim

To improve water management of Moringa cultivated for leaf production, through appropriate quantification of the tree water requirements under varying crop management practices.

6.1.2 Study objectives

- To evaluate changes in the tree rhizosphere soil water content, leaf yield and water use of Moringa trees grown under the in-situ rainwater harvesting and conservation production system, as affected by varying harvesting methods and frequencies;
- To evaluate changes in soil water content, leaf yield and water use of Moringa trees grown under varying tree spacing;

6.2 RESEARCH METHODOLOGY

6.2.1 Rain-fed and irrigation trials

6.2.1.1 Description of the study sites

A rain-fed trial was established on a four-year-old Moringa (*Moringa oleifera* Lam.) plantation (Figure 6.1), located at the Roodeplaat Experimental Farm of the Agricultural Research Council – Vegetable, Industrial and Medicinal Plants (ARC-VIMP) (25°35'N, 28°21'E, 1164 metres above sea level (masl)) in Gauteng Province, South Africa. The plantation was established from seedlings in the 2018-2019 growing season, on medium textured soils (Table 6.1). The research trial began in September 2021, and is expected to end in June 2023, after the completion of two experimental seasons.

Figure 6.1: A four-year-old Moringa plantation used to investigate the influence of different harvesting methods and frequencies of Moringa cultivated for leaf production under the in-situ rainwater harvesting and conservation system at ARC-VIMP.

The plantation shown in Figure 6.2 was 50 x 40 m in size, and comprised of 12 experimental plots of 160 m^2 each. The experimental trees were spaced at 2 x 1 m apart. The distance between blocks and experimental plots was 2 m. The in-situ rainwater harvesting and conservation system comprised of planting basins of 80 cm in diameter and 20 cm in depth, filled with local grass chips. Regular weeding was conducted manually. Talborne Organics (Vita Nitro-boost 8:1:1(10)), a scientific formulated complete organic fertilizer, was applied at a rate of 150 g/tree (60 kg/ha N) two weeks after every harvesting. Macro and micronutrient levels (Table 6.1) were generally higher on the second (30-60 cm), followed by the third (60-90 cm) soil layer compared to the top layer (0-30 cm). This suggests that there is a more active root nutrient uptake by Moringa trees from the upper soil layer 0-30 cm compared to deeper layers. The pre-trial major nutrient content of the soil was inadequate in terms of nitrogen levels throughout the entire profile (0.01-0.064%), whereas it was found sufficient for phosphorus (3.18-37.7 mg/kg) and potassium particularly from 30-90 cm soil profile (117-200 mg/kg) (Adebayo et al., 2017).

Table 6.1: Soil chemical and physical properties for 0-30, 30-60 and 60-90 cm profile layers at Roodeplaat study site prior to the commencement of the trial during the 2021/22 growing season.

Chemical elements	**Units**	**0-30 cm soil layer**	**30-60 cm soil layer**	**60-90 cm soil layer**
Total Nitrogen (N)	%	0.01	0.072	0.064
Phosphorous (P)-Bray 1	mg kg^{-1}	3.18	37.7	3.9
Potassium (K)	mg kg^{-1}	57.6	200	117
Calcium (Ca)	mg kg^{-1}	652.0	726	913
Magnesium (Mg)	mg kg^{-1}	270.0	252	332
Sodium (Na)	mg kg^{-1}	37.3	9.2	37
Iron (Fe)	mg kg^{-1}	6.48	14.1	61.9
Zinc (Zn)	mg kg^{-1}	0.212	10.9	2.57
Manganese (Mn)	mg kg^{-1}	18.10	93.2	171.0
Copper (Cu)	mg kg^{-1}	1.85	6.85	5.15
Organic matter	%	2.08	0.031	0.039
pH (H_2O)	-	7.60	6.60	6.86
Physical properties				
Sand	%	74.0	66.0	54.0
Silt	%	8.0	6.0	6.0
Clay	%	18.0	28.0	40.0
Soil type	-	Loamy sand	Sandy clay loam	Sandy clay
Bulk density	Ton m^{-3}	1.267	1.167	1.233
Field capacity (FC)	m^3 m^{-3}	0.19	0.30	0.40
Permanent wilting point (PWP)	m^3 m^{-3}	0.10	0.17	0.24

The irrigation trial began in January 2022 and is expected to end in March 2024. The trial is being implemented on the Roodeplaat Experimental Farm of the Agricultural Research Council – Vegetable, Industrial Medicinal Plants (ARC-VIMP). According to the USDA taxonomic system, the soil texture of the study site is classified as medium textured (Table 6.2). The status of the slope and the soil depth is 0.5-1% and > 1.2 m, respectively. The study crop is 10-year old Moringa (*Moringa oleifera Lam*., cultivar PKM1) (Figure 6.3). The Moringa crop plant was levelled (pruned) on 24 November 2022 to improve stand uniformity and better response of research treatments.

Figure 6.2: A 10-year-old Moringa plantation used to investigate the influence of various sustainable agricultural practices of Moringa cultivated for leaf production at ARC-VIMP.

Table 6.2: Soil chemical and physical properties for the top layer 0-30 cm on the 10-year-old Moringa plantation established at ARC-VIMP.

Chemical elements	**Units**	**0-30 cm**	**30-60 cm**	**60-90**
Total Nitrogen (N)	%	0.01	0.072	0.064
Phosphorous (P)-Bray 1	mg kg^{-1}	3.18	37.7	3.9
Potassium (K)	mg kg^{-1}	57.6	200	117
Calcium (Ca)	mg kg^{-1}	652.0	726	913
Magnesium (Mg)	mg kg^{-1}	270.0	252	332
Sodium (Na)	mg kg^{-1}	37.3	9.2	37
Iron (Fe)	mg kg^{-1}	6.48	14.1	61.9
Zinc (Zn)	mg kg^{-1}	0.212	10.9	2.57
Manganese (Mn)	mg kg^{-1}	18.10	93.2	171.0
Copper (Cu)	mg kg^{-1}	1.85	6.85	5.15
Organic matter	%	2.08	0.031	0.039
pH (H_2O)	-	7.60	6.60	6.86
Physical properties				
Sand	%	74.0	66.0	54.0
Silt	%	8.0	6.0	6.0
Clay	%	18.0	28.0	40.0
Soil type	-	Loamy sand	Sandy clay loam	Sandy clay
Bulk density	Ton m^{-3}	1.267	1.167	1.233
Field capacity	m^3 m^{-3}	0.19	0.30	0.40
Permanent wilting point	m^3 m^{-3}	0.10	0.17	0.24

6.2.1.2 Experimental factors, treatments, design and layout

The rain-fed trial was conducted as a randomized complete block design (RCBD), with four treatments and three replications. Treatments comprised of combinations of two factors, each involving two levels: harvesting method (cut-back “farmer’s practice” and stripping-off) and harvesting frequency (30 and 60 days). The trial layout is shown in Figure 6.4.

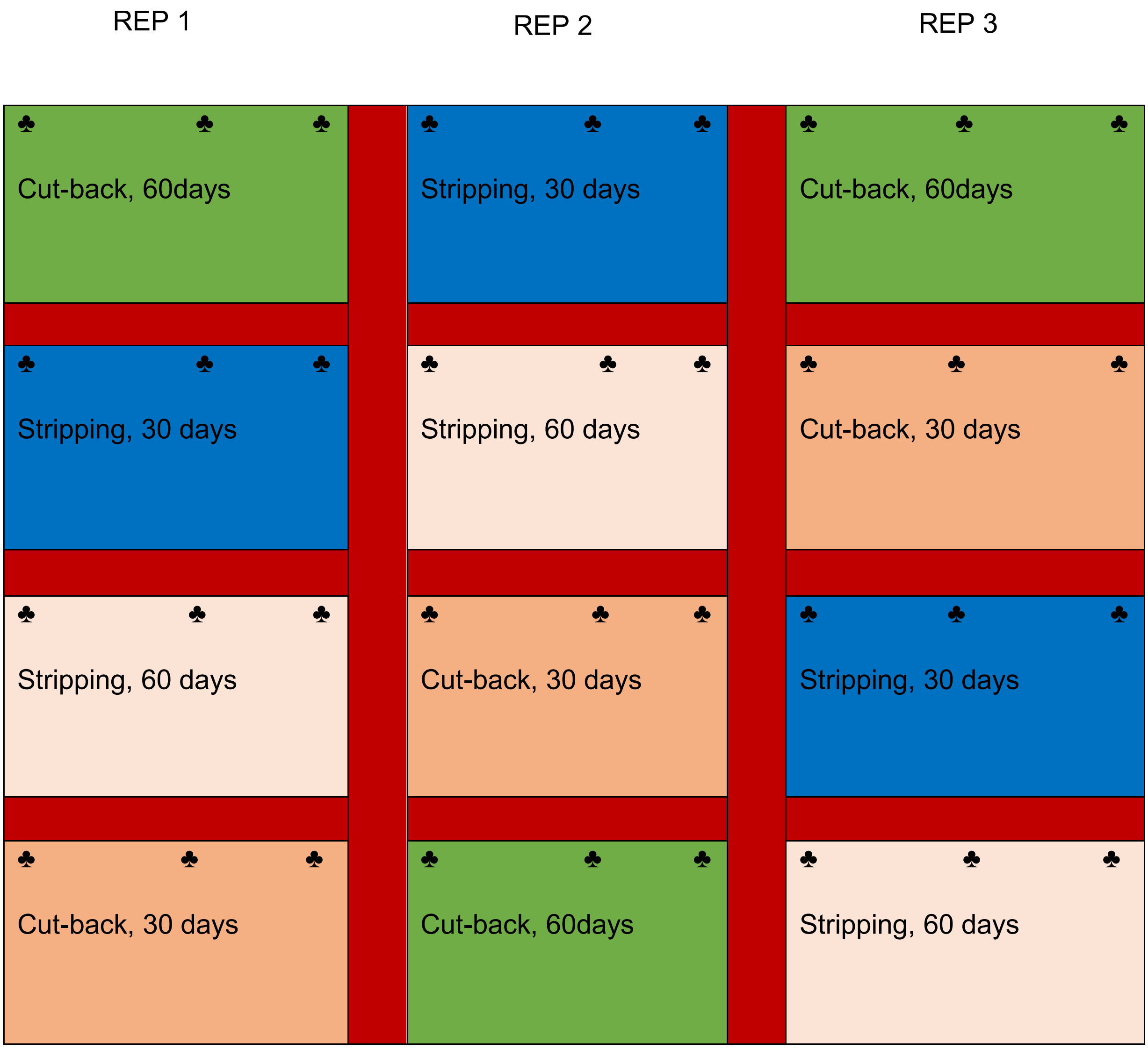

Figure 6.4: Field layout for the in-situ rainwater harvesting and conservation trial at ARC-VIMP.

The irrigation trial was laid out as a 3-factor split split-plot under a randomized complete block design (RCBD), with three replicates (Figure 6.5). The following factors were included:

(1) Tree spacing – main plot (S, 1.0 x 1.0 m and 1.0 x 1.5 m);
(2) Water regimes combined with soil conservation – subplot (R, conventional rain-fed, grass-mulched and well-watered, plastic-mulched and water-stress and grass-mulched and water-stress);

(3) Organic soil amendment – sub-subplot (F, kraal manure and compost).

In order to meet the objectives of this deliverable, this progress report will only present overall averages of tree performance for the two tree spacing levels investigated.

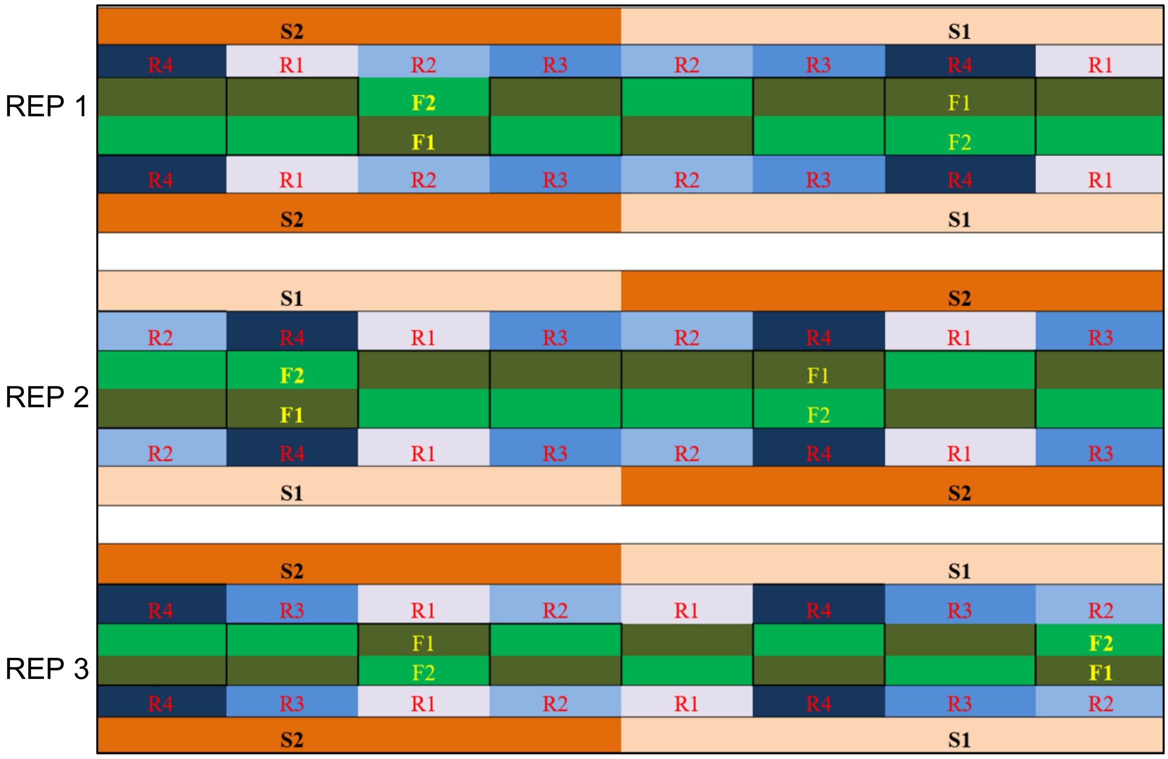

Figure 6.5: Field layout for the irrigation trial at ARC-VIMP. Investigation factors included tree spacing, soil water supply regimes and organic soil amendments.

6.2.1.3 Weather variability

Hourly and daily weather conditions during the experimental period were monitored through an automatic weather station (AWS) installed by the Agricultural Research Council – Institute of Soil, Climate and Water (ARC-ISCW) within the Roodeplaat area. The monitored parameters included maximum (Tx) and minimum (Tn) air temperatures, relative humidity (RHx, RHn), solar radiation (Rs), wind speed and rainfall. The reference evapotranspiration (ET_0) during the study period was computed using the Penman-Monteith equation (Allen *et al.*, 1998). Additional weather parameters (air temperature, relative humidity and solar radiation) were also monitored on-site using a Tinytag datalogger (Gemini Data Loggers, United Kingdom) and a net radiometer sensor (Campbell Scientific, USA) (Figure 6.6).

Figure 6.6: Tinytag datalogger used to measure air temperature and relative humidity (left) and net radiometer used to measure solar radiation (right), in the Moringa trials at ARC-VIMP.

6.2.1.4 Monitoring of changes in soil water content, determination of growth, physiological and yield parameters, as well as crop water use

Changes in soil water content were monitored daily on the upper and lower soil profile depths using 10-HS capacitative soil water content sensors installed at 30 and 60 cm within the crop root zone (Figure 48a). The data was automatically recorded using an EM50 datalogger (Campbell Scientific, USA) (Figure 48b). Tree growth, physiological and yield parameters were measured on-site, once at every harvesting throughout the entire growing season. A ceptometer (ACCUPAR LP-80, METER Group, USA) was used to measure leaf are index (LAI) and fractional interception of photosynthetically active radiation (FI_{PAR}), while a SPAD-502 meter (Spectrum Technologies, Plainfield, Illinois, USA) was used to measure leaf chlorophyll content (Figures 6.7).

Figure 6.7: A 10-HS capacitative soil water content sensor installed at 60 cm soil layer (a) and connected to an EM50 datalogger (b), measurements of canopy cover using a ceptometer (c), leaf chlorophyll content using a SPAD-502 meter (d) and rainfall using a manual rain gauge (e).

6.2.1.5 Crop water use determination

Moringa tree water use was determined using the soil water balance method, taking into account the following principles: (1) rain or irrigation reaching a unit area of soil surface could infiltrate into the soil, or leave the area as surface runoff; (2) the infiltrated water could evaporate directly from the soil surface or be taken up by the tree for productivity via transpiration; (3) drain downward beyond the root zone as deep percolation, or (4) accumulate within the root zone (Zeleke and Wade, 2012). The soil water balance calculations were based on the conservation of mass principle, which states that change in soil water content (ΔS) of a crop root zone is equal to the difference between the amount of water added to the root zone, Q_i, and the amount of water withdrawn from it, Q_o (Hillel, 1998) in a given time interval expressed as in Equation 19.

$$\Delta S = Q_i - Q_o \tag{6.1}$$

Then, ΔS was used to determine crop evapotranspiration (ET), as follows:

$$ET = P + I + U - R - D - \Delta S \tag{6.2}$$

where ΔS = change in root zone soil water content storage, measured automatically on a daily basis, using 10HS capacitative soil water content sensors; P = Precipitation measured by an automatic weather station and manual rain gauges installed on-site; I = Irrigation monitored using water meters installed on the main lines of each treatment; U = upward capillary rise into the root zone, R = runoff and D = deep percolation beyond the root zone were estimated using AquaCrop modelling version 4 (Raes et al., 2012). Groundwater table was assumed to be present at a constant depth of 2 m below soil surface, while values of R were estimated using the Curve Number method embedded in the AquaCrop modelling procedure. Soil physical characteristics (particle size distribution, bulk density, FC, PWP and typical hydraulic conductivity values for a loamy sand to sand clay "4-yr-old trees" and sandy clay loam "10-yr-old") were used for model parameterization, while model testing was conducted with the aid of actual soil water content measurements at different depths of the soil profile.

6.2.1.6 Statistical analysis of growth, physiological and yield parameters

Statistical analysis of variance (ANOVA) was performed on the observations of Moringa tree for the research treatments investigated, after testing the homogeneity of the experimental error variances using Bartlett's test. The residuals were examined for deviations from normality, and outliers causing skewness were removed. Fisher's least significant difference (LSD) was calculated at the 5% level to compare means for significant effects. Analysis was done using embedded Genstat for Windows 18th Edition (VSN International, 2015).

6.3. RESULTS AND DISCUSSION

6.3.1 Rain-fed trial

6.3.1.1 Weather variability during the crop growing period

During the experimental period (September 2021 to May 2022), minimum and maximum daily air temperatures fluctuated from 16.1-35.3°C and -0.6-18.9°C, respectively in 2021/22. Daily solar radiation reached a maximum of 30.5 MJ m^{-2} s^{-1} (Figure 6.8). The 2021/22 growing period had a total of 1166 mm of rainfall (with December as the wettest month with a total of 290 mm and May and the driest month with a total of 24 mm).

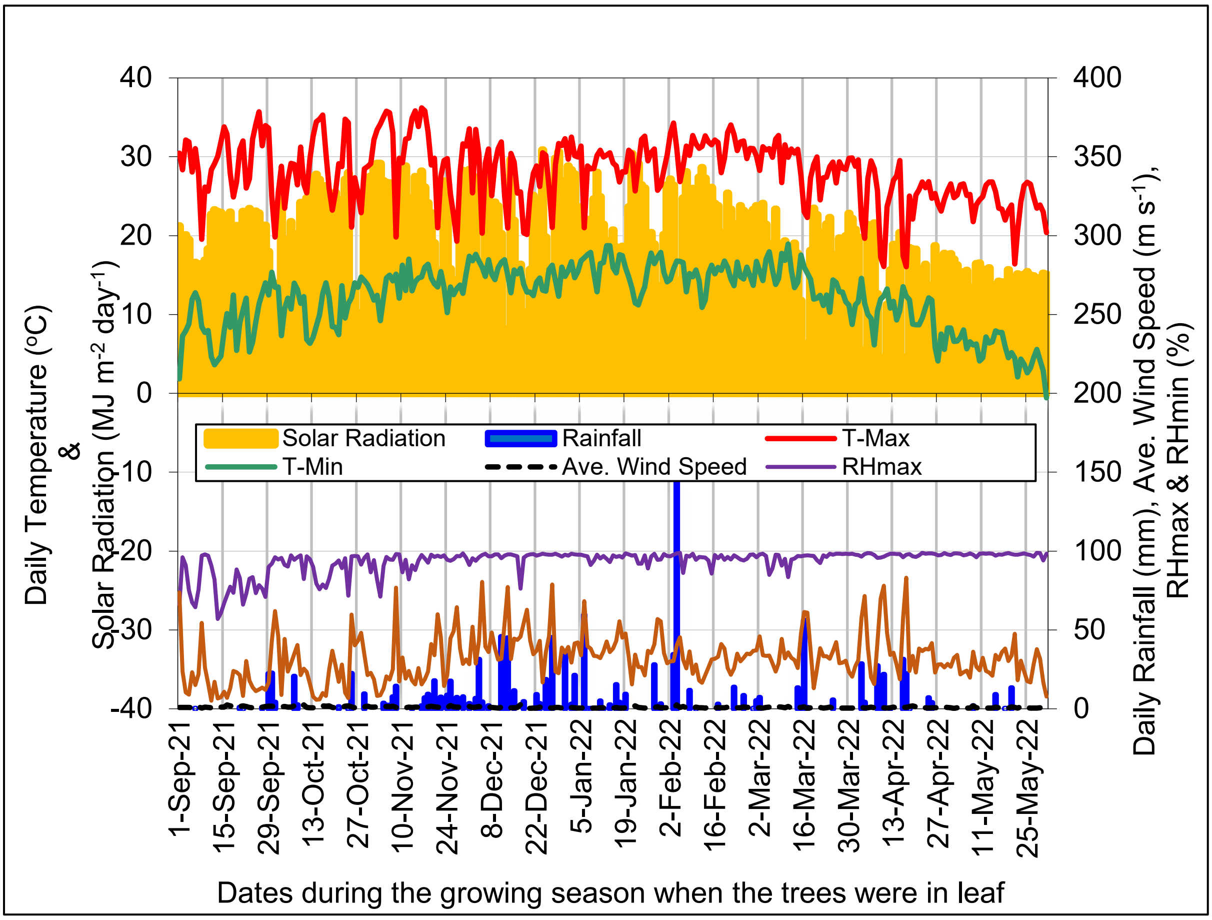

Figure 6.8: Daily weather variability (solar radiation, rainfall, maximum and minimum air temperature and relative humidity, as well as wind speed) during the 2021-2022 experimental period at Roodeplaat Experimental Farm of ARC-VIMP.

6.3.1.2 Changes in soil water content as influenced by harvesting strategy, rainfall and reference evapotranspiration

Soil water content was generally higher on the lower part of the soil profile (measured by the sensor installed at 60 cm below the soil surface) compared to the upper part of the soil profile (represented by the water sensor installed at 30 cm below the soil surface). Stripping method every 60 days (Figures 50d and 52d) conserved more soil water compared to the rest of the tested harvesting strategies. Stripping method every 60 days also had the lowest changes in soil water content throughout the growing season, which suggests minimal crop water use compared to other harvesting strategies. The highest profile soil water content was observed around December-January, period during which most of the rainfall occurred at the study site. There were unnoticeable effects of the changes in atmospheric evaporative demand (represented by ET_o), as the soil water content patterns remained fairly the same throughout the season, regardless of changes in ET_o (Figures 6.9 and 6.11), but mostly affected by rainfall. As the rainfall declined towards the end of the season (Figure 6.10), the soil water content levels also reduced. Changes in soil water content were more pronounced with the cut-back method every 30 days (Figures 6.10a and 6.12a), followed by the stripping method every 30 days (Figures 6.11c and 6.12c).

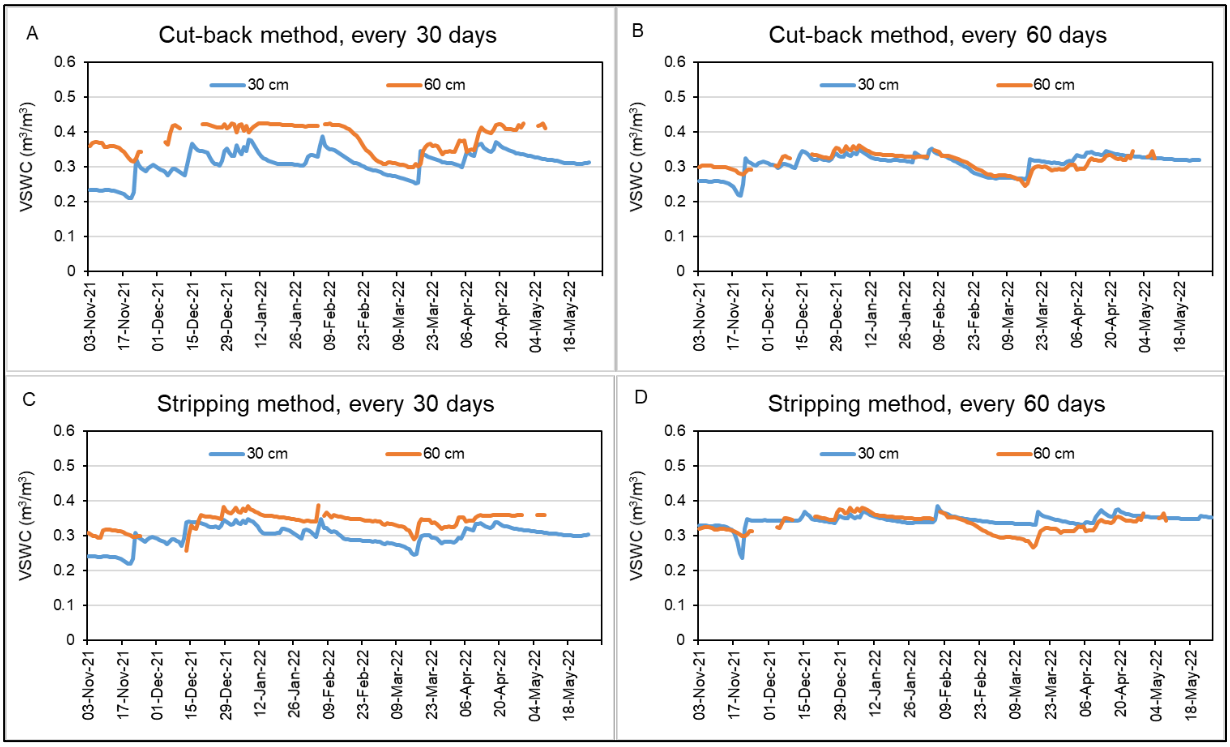

Figure 6.9: Changes in soil water content per soil layer on a 4-year-old Moringa plantation as affected by varying harvesting methods and frequencies (cut-back method every 30 days – a; cut-back method every 60 days – b; stripping methods every 30 days – c and stripping method every 60 days – d) at ARC-VIMP.

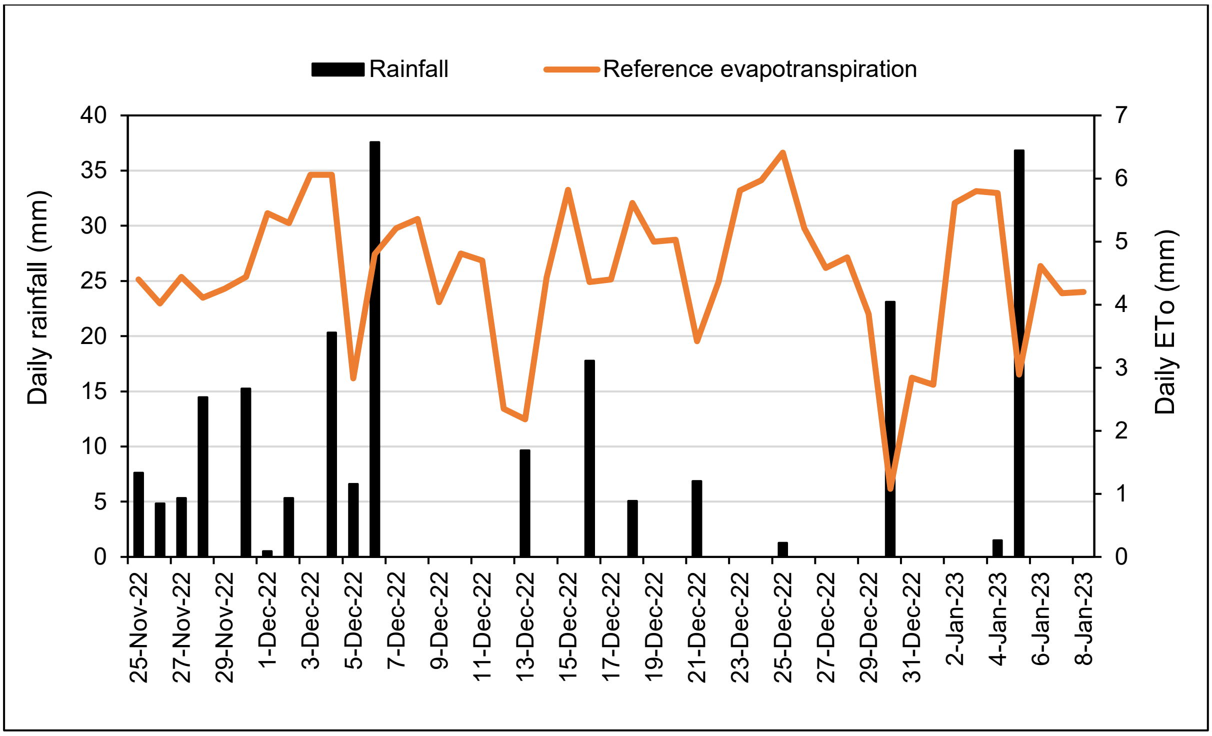

Figure 6.10: Daily rainfall and reference evapotranspiration during the experimental growing season 2021-2022 at ARC-VIMP.

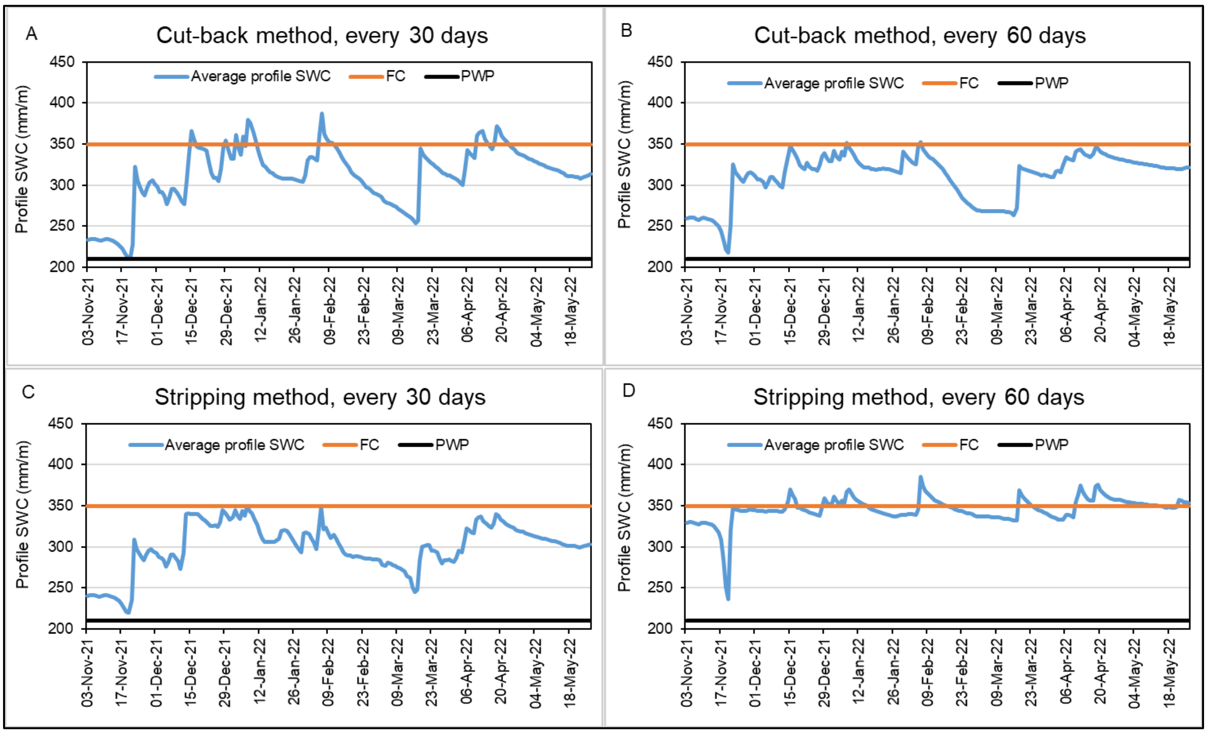

Figure 6.11: Average profile soil water content of 4-year-old Moringa trees as influenced by varying harvesting methods and frequencies under the in-situ rainwater harvesting system at ARC-VIMP

6.3.1.3 Moringa crop responses to different harvesting methods and frequencies under the in-situ rainwater harvesting and conservation method

The highest significantly different Moringa leaf productivity was obtained with the stripping method every 60 days (fresh mass = 11.3 ton/ha; FI_{PAR} = 58.4%; maximum tree height = 2.7 m and SPAD = 49.4), while the remaining three harvesting strategies performed the lowest (Table 6.3). Farmers typically harvesting Moringa using the cut-back method and have no information regarding optimum harvesting frequencies. Findings from this study revealed that cutting back Moringa trees affects the tree productivity negatively, irrespective of the harvesting frequency. This could be attributed to the tree need to invest in more energy to regrow new stems and twigs instead of leaves.

Table 6.3: Moringa crop responses to different harvesting methods and frequencies under the in-situ rainwater harvesting and conservation method.

Harvesting Method	Harvesting Frequency (days)							
	30	60	30	60	30	60	30	60
	Fresh mass (ton/ha)		FI_{PAR} (%)		Tree height (m)		SPAD	
Cut-back	5.2 b	4.4 b	56.8 a	64.5 a	1.4 c	1.7 bc	37.7 b	46.6 a
Stripping	4.5 b	11.3 a	18.7 b	58.4 a	1.9 b	2.7 a	38.3 b	49.4 a

3.1.4 Moringa crop water use as influenced by varying harvesting methods and frequencies under the in-situ rainwater harvesting and conservation system

The 4-year-old rain-fed grown Moringa trees were cultivated under non-limiting soil water supply conditions during the growing season 2021-2022. The cumulative amount of rainfall (1060 mm) was generally higher than the crop water use (224-380 mm) and reference evapotranspiration (790 mm). There were unnoticeable differences in crop water use between the harvesting strategies of cut-back and stripping every 30 days (Figure 6.13). Moringa trees cultivated under these two harvesting strategies consumed the highest amount of water, followed by the harvesting strategy cut-back every 60 days. Moringa trees consumed the lowest amount of water under the stripping method every 60 days. This could be attributed to exceptionally high canopy growth of Moringa trees, which contributed to shading of the ground surface, thus minimizing soil evaporation losses. In contrary, harvesting Moringa trees at a high frequency (every 30 days), particularly with the cut-back method, resulted in decreased canopy sizes which most likely increased soil evaporation losses.

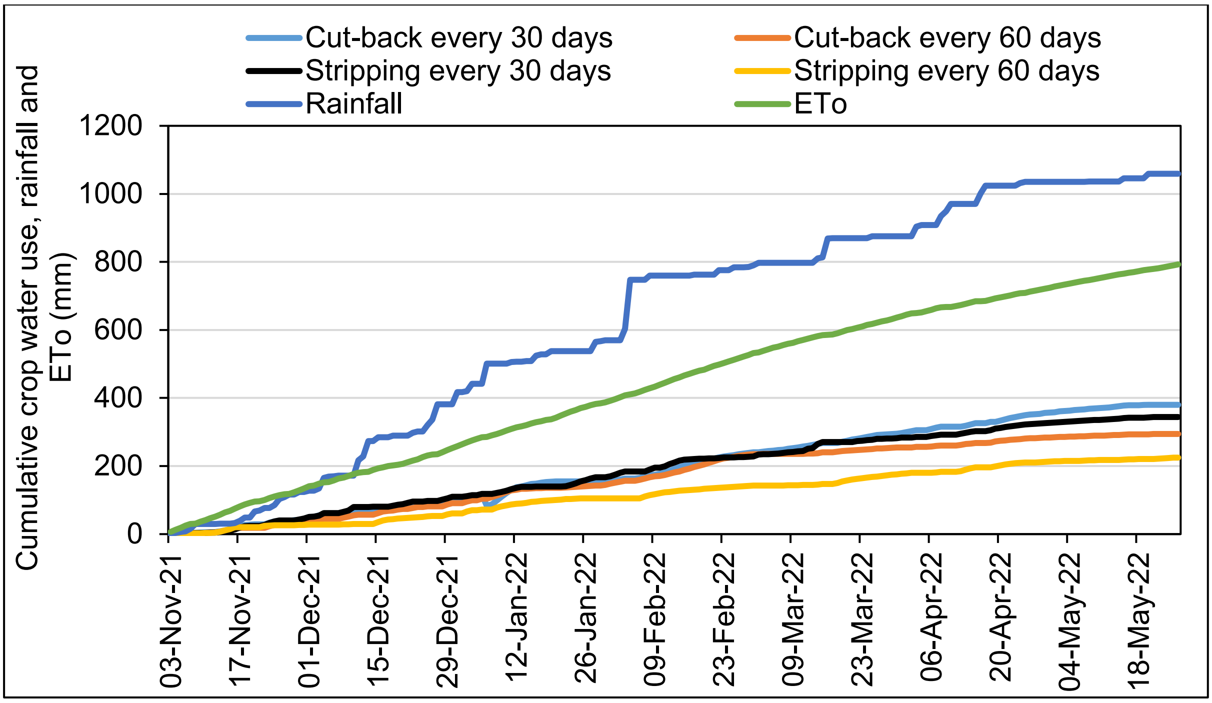

Figure 6.12: Cumulative rainfall, reference evapotranspiration and Moringa crop water use during the experimental growing season 2021-2022 under varying harvesting methods and frequencies within the in-situ rainwater harvesting and conservation system at ARC-VIMP.

6.3.2 Irrigation trial

6.3.2.1 Weather variability during the crop growing period

The weather conditions during 2022-2023 growing season, harvesting 1 period, were mostly comprised of clear sky days with daily solar radiation fluctuating between 20.6 and 31.1 MJ m^{-2} day^{-1}, accompanied by high air temperatures (reaching up to 33.7°C) and relative humidity (up to 98%) (Figure 6.14). There were a few overcast days (daily solar radiation varying between 4.4 and 11.1°C). These days registered relatively low air temperatures (24.4 to 25.9°C). Minimum air temperatures (describing mostly night-time periods) varied between 11.1 and 18.4°C). During the reported period (25 November 2022 to 08 January 2023), there was a total of 220 mm of rainfall and 204 mm of reference evapotranspiration. This shows that it was quite a wet period (cumulative water supply exceeded demand throughout the experimental period, Figure 6.15) and, as a result, irrigation was not administered.

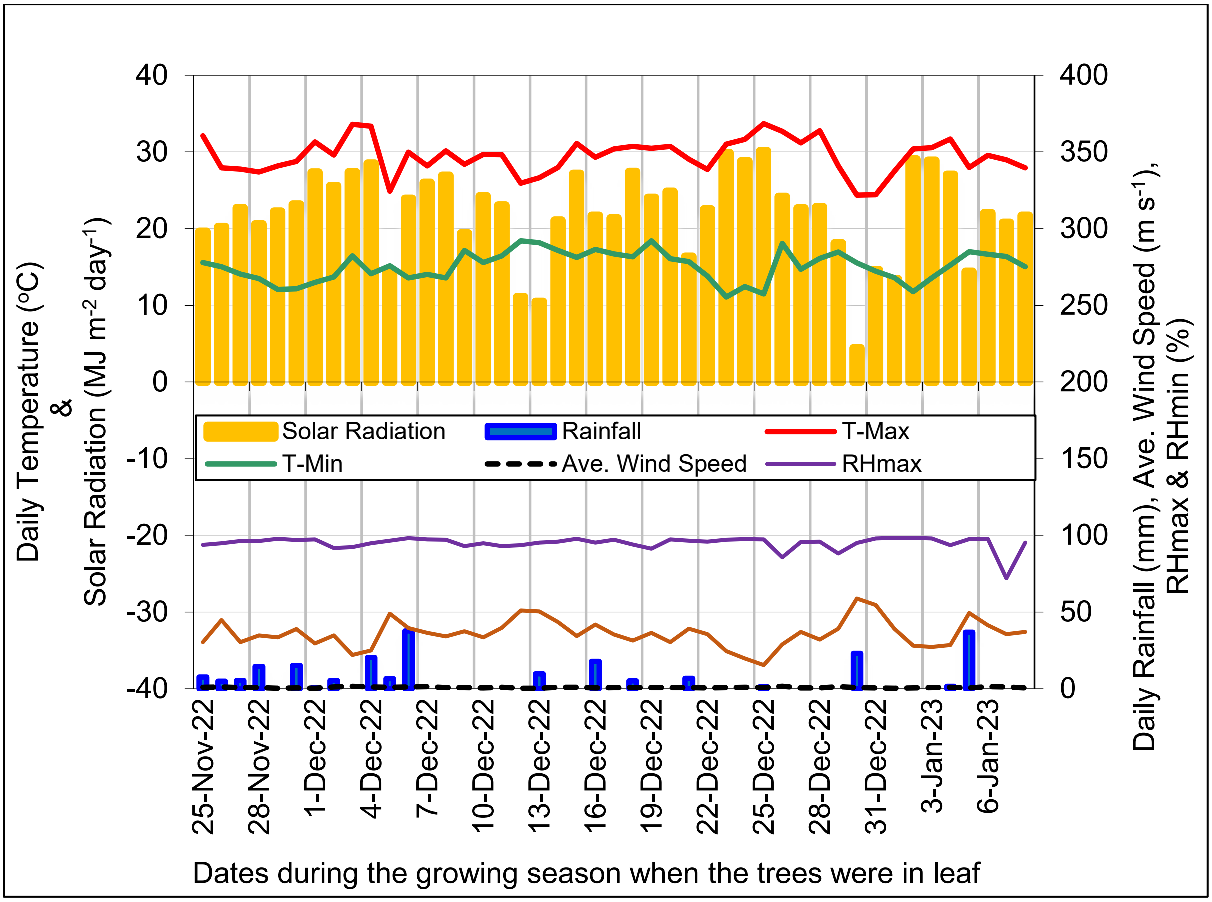

Figure 6.13: Daily weather variability (solar radiation, rainfall, maximum and minimum air temperature and relative humidity, as well as wind speed) during the 2022-2023 growing season, harvesting 1 period, at the 10-year-old Moringa plantation trial site located at Roodeplaat Experimental Farm of ARC-VIMP.

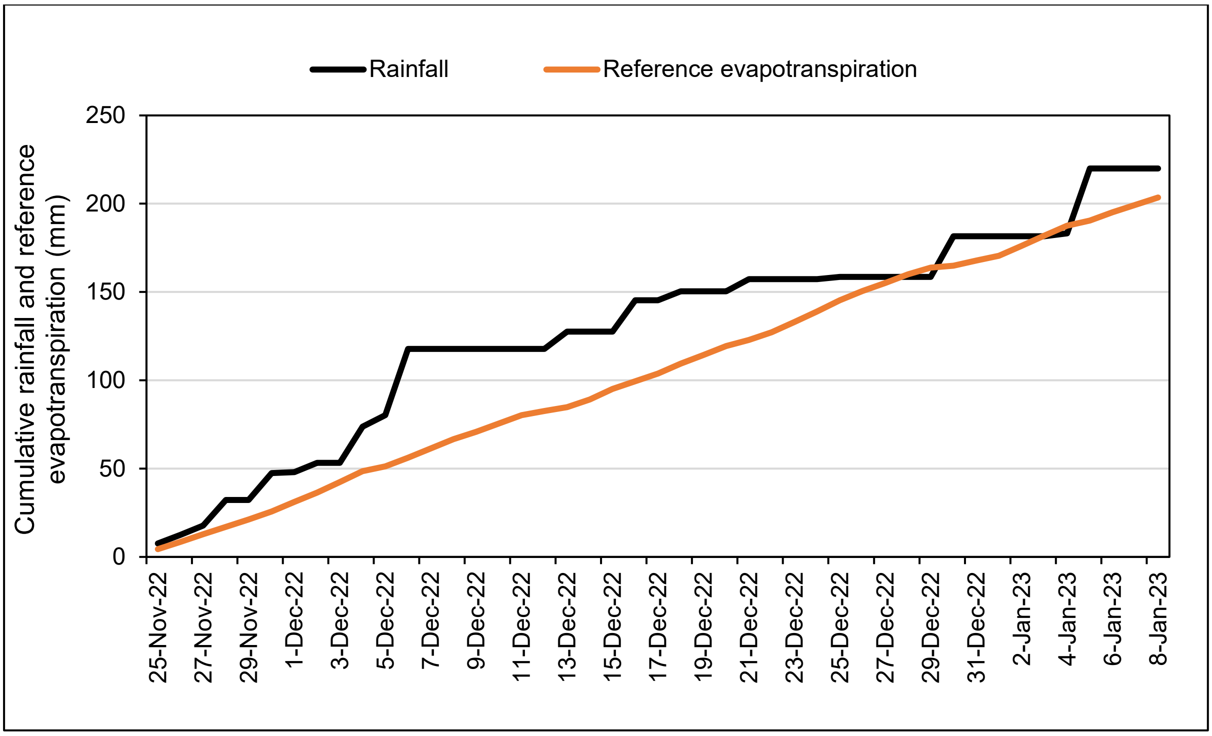

Figure 6.14: Daily rainfall and reference evapotranspiration during the experimental growing season 2022-2023, harvesting 1 period of the 10-year-old Moringa trial at ARC-VIMP.

6.3.2.2 Changes in soil water content as influenced by tree spacing, rainfall and reference evapotranspiration

The 1.0 x 1.0 m spacing conserved more soil water compared to the 1.0 x 1.5 m spacing (Figures 6.16 and 6.17). Narrower spacing improves radiation interception and radiation use efficiency compared to wider spacing which, in turn, contributes to lower soil evaporation losses and more improved soil water conservation. The lower soil layer (60 cm) registered lower soil water content levels compared to the upper layer (30 cm), particularly for the 1.0 x 1.0 m spacing (Figure 6.16a). An opposite pattern was observed for trees grown under the 1.0 x 1.5 m spacing, which may be explained by the differences in root volume along the soil profile (Figure 6.17b). Further analysis of root density across different tree spacing needs to be conducted.

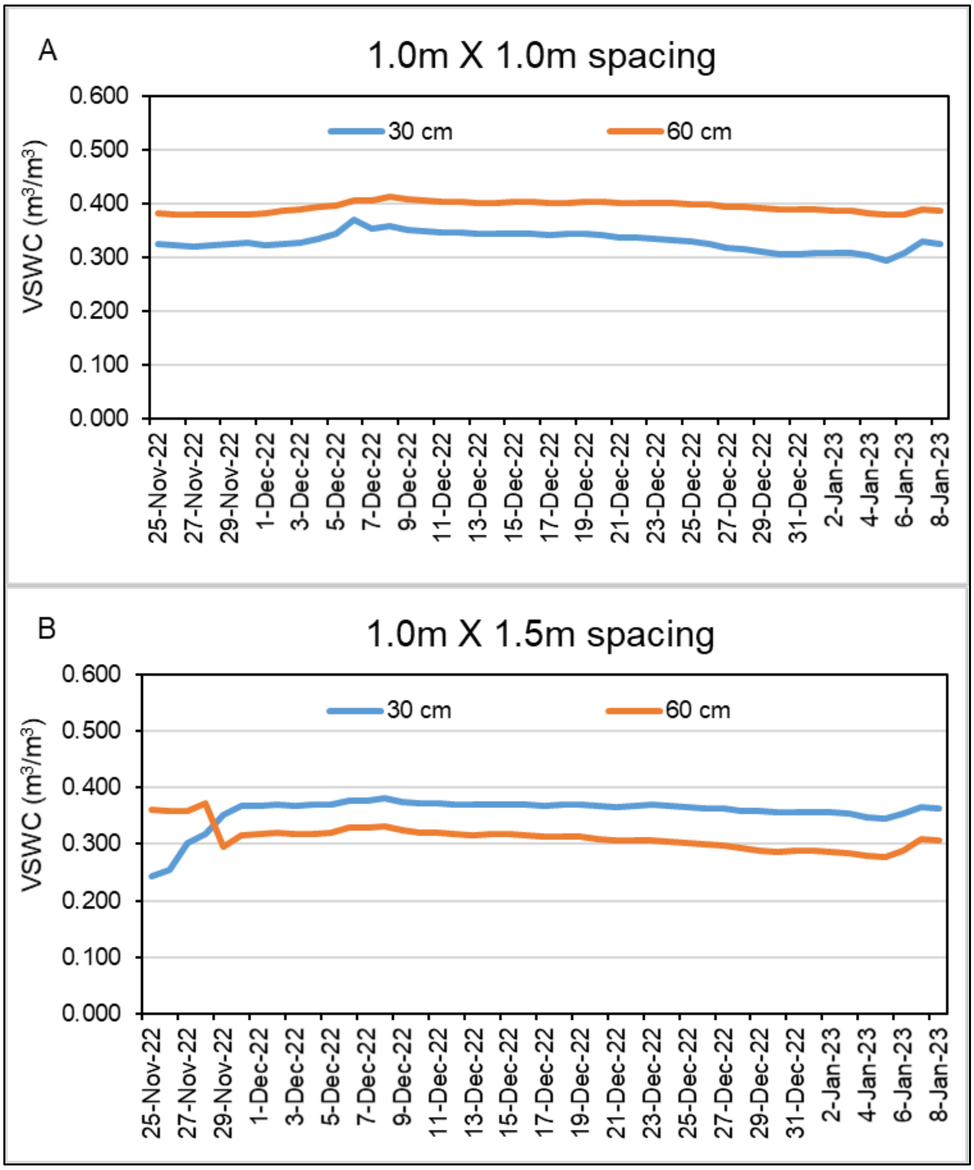

Figure 6.15: Changes in soil water content per soil layer on a 10-year-old Moringa plantation during harvesting 1 period of the 2022-2023 growing season, as affected by varying tree spacing (1.0 x 1.0 m – a; 1.0 x 1.5 m — b) at ARC-VIMP.

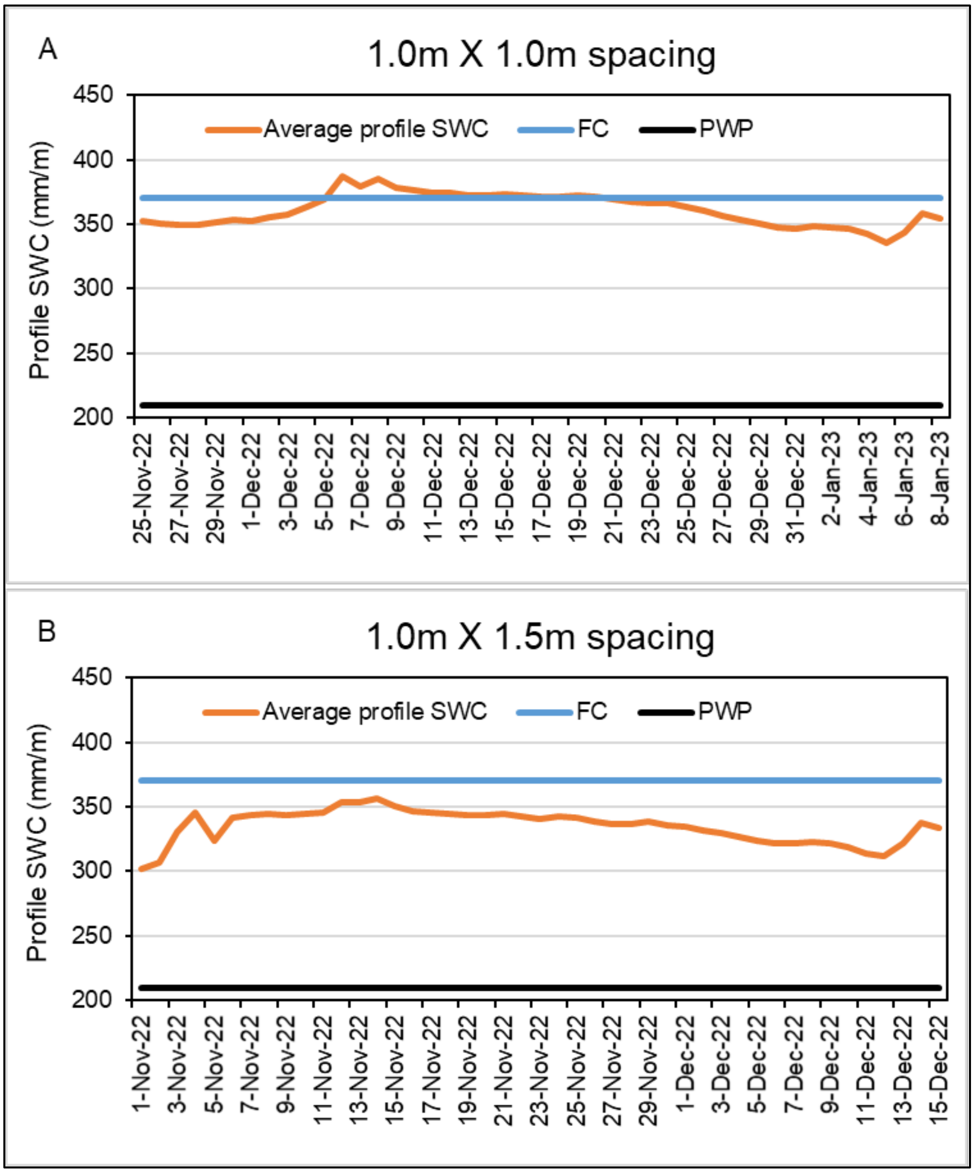

Figure 6.16: Average profile soil water content of 10-year-old Moringa trees as influenced by tree spacing 1.0 x 1.0 m (A) and 1.0 x 1.5 m (B) at ARC-VIMP.

6.3.2.3 Moringa crop responses to different tree spacing under irrigated conditions

Moringa crop response differences to the two-tree spacing investigated (1.0 x 1.0 m and 1.0 x 1.5 m) were insignificant (Table 6.4). The growth and yield of the crop was slightly higher under the wider compared to the narrower spacing, which suggests that the spacing of Moringa trees could be increased beyond 1.0 x 1.5 m, in other words, lower plant populations are encouraged for leaf production (lower than 6 666 trees per ha).

Table 6.4: Moringa crop responses to different harvesting methods and frequencies under the in-situ rainwater harvesting and conservation method.

	Growth, physiological and yield parameters				
Tree Spacing	Fresh mass (Ton/ha)	$FI_{PAR\ (\%)}$	LAI ($m^2\ m^{-2}$)	Tree height (m)	Leaf stomatal conductance (mmol $m^{-2}\ s^{-1}$)
1.0 x 1.0 m	1.8	77.0	4.2	101.1	783
1.0 x 1.5 m	2.1	84.0	4.4	107	700

6.3.2.4 Moringa crop water use as influenced by varying tree spacing, rainfall and reference evapotranspiration under irrigated conditions

Moringa tree water use remained fairly the same throughout the entire growing period, under the two tree spacing investigated. This could be attributed to the presence of sufficient water in the soil (the total amount of rainfall = 220 mm was higher than the total ET_o = 203 mm). Although the profile soil water content for the wider spacing trees was kept below field capacity, the trees were not affected by the imposed water deficit, demonstrating the tree tolerance to water stress (Figure 6.18).

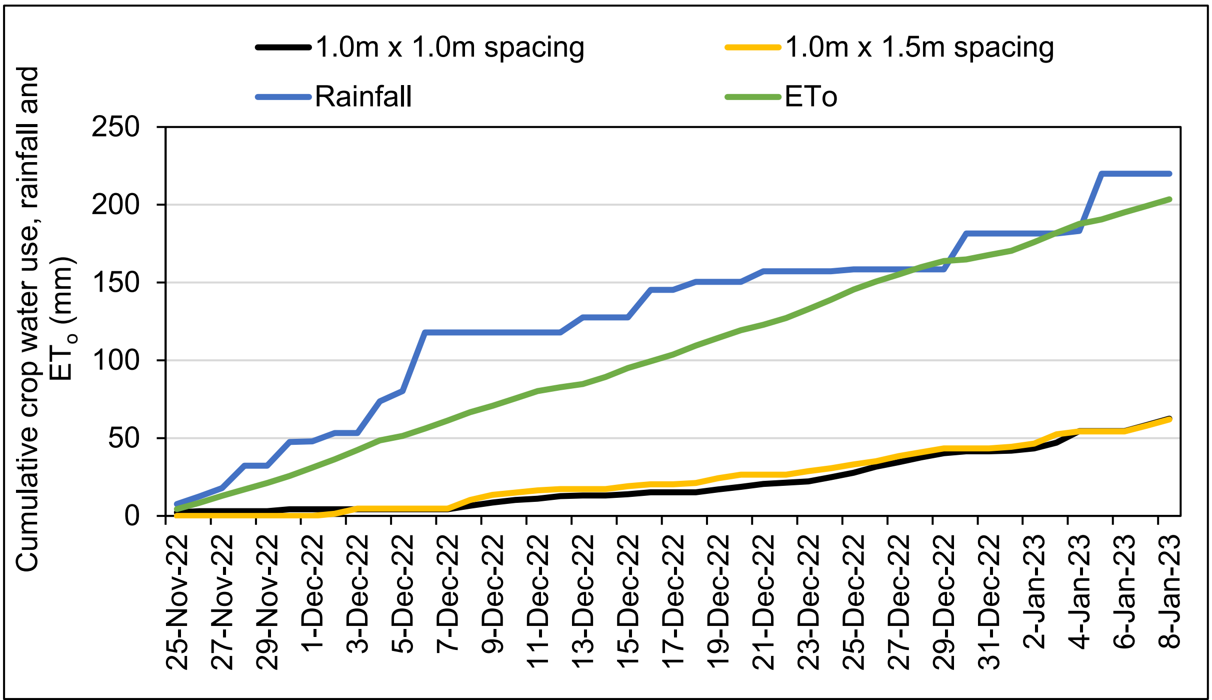

Figure 6.17: Cumulative crop water use, rainfall and reference evapotranspiration during the *experimental growing season 2022-2023, harvesting 1 period of the 10-year-old Moringa trial at ARC-VIMP.*

6.4 CONCLUSIONS AND RECOMMENDATIONS

The growth, physiology, yield and water use of four- and 10-year-old *Moringa oleifera* trees was investigated in response to varying crop management practices (tree spacing and harvesting strategy). The reported experimental period received sufficient rainfall for Moringa crop productivity and, as a result, irrigation was not applied. Harvesting Moringa leaves using the stripping method every 60 days resulted in the highest crop productivity (11.3 ton/ha) and lowest crop water consumption (225 mm) seasonally, when the trees were cultivated using the in-situ rainwater harvesting and conservation system. Cultivating Moringa trees using narrower (1.0 x 1.0 m) or wider (1.0 x 1.5 m) tree spacing did not have a significant influence on the crop productivity (1.8 to 2.1 ton/ha per harvesting). Similarly, the crop water use remained unnoticeably different between the two tree spacing investigated (62.01-62.51 mm per harvesting). Therefore, it is suggested that the Moringa tree be cultivated at wider spacing/lower plant population of less than 6 666 trees/ha. In areas receiving sufficient rainfall, the Moringa tree can be cultivated under rain-fed conditions, however, employing climate-smart production systems such as the in-situ rainwater harvesting and conservation has proven beneficial to the Moringa tree grown for leaf production.

ACKNOWLEDGEMENTS

This work was financially supported by the Water Research Commission of South Africa (WRC Project No. C2020/2021-00484). Technical support, data collection and processing by postgraduate students Mr Ambroise Ndayakunze and Mr Floyd Nwamba are highly appreciated. Ms Irene Nel (from ARC – Natural Resources and Engineering) is thanked for providing a complete set of weather data for the experimental site.

REFERENCES

Aditama, R.S., Sukria, H.A., Mutia, R., 2021. Evaluation of nutrient and antioxidant activity on steam blanching of *Moringa oleifera* leaves. E3S Web of Conferences. 306, 04016. https://doi.org/10.1051/e3sconf/202130604016

Adebayo, A.G., Akintoye, H.A., Shokalu, A.O., M.T. Olatunji, 2017. Soil chemical properties and growth response of *Moringa oleifera* to different sources and rates of organic and NPK fertilizers. Int J Recycl Org Waste Agricult. https://doi.org/10.1007/s40093-017-0175-5

Allen, R.G., Pereira, L.S., Raes, D., Smith, M., 1998. Crop evapotranspiration: Guidelines for computing crop water requirements. FAO Irrigation and Drainage Paper 56. FAO, Rome, Italy.

Bagula, E.M., Majaliwa, J.G.M., Basamba, T.A., Mondo, J.G.M., Vanlauwe, B., Gabiri, G., Tumuhairwe, J.-B., Mushagalusa, G.N., Musinguzi, P., Akello, S., et al., 2022. Water use efficiency of maize (*Zea mays* L.) crop under selected soil and water conservation practices along the slope gradient in Ruzizi Watershed, Eastern D.R. Congo. Land. 11, 1833. https://doi.org/ 10.3390/land11101833

Bufebo, B., Beyene, G., Addise, T., 2023. Analysis of selected soil properties in relation to soil and water conservation practices in Sibiya Arera, Soro District, South Central Ethiopia. Sci. World J. 1763367, 8. https://doi.org/10.1155/2023/1763367Diop,

Chirinda, N., Beniaich, A., El Gharous, M., El Mejahed, K., 2022. Soil and water conservation in Africa: state of play and potential role in tackling soil degradation and building soil health in agricultural lands. Sustainability. 14, 13425. https://doi.org/10.3390/su142013425

Du Toit, E.S., Sithole, J., Vorster, J., 2020. Pruning intensity influences growth, flower and fruit development of *Moringa oleifera* Lam. under sub-optimal growing conditions in Gauteng, South Africa. South African Journal of Botany. 129, 448-456.Hillel, D., 1997. Small scale irrigation for arid zones: Principles and options, Development monograph No. 2 , FAO, Rome.

Leone, A., Spada, A., Battezzati, A., Schiraldi, A., Aristil, J., Bertoli, S., 2015. Cultivation, genetic, ethnopharmacology, phytochemistry and pharmacology of *Moringa oleifera* leaves: an overview. Int. J. Mol. Sci.. 16, 12791-12835.

Mabapa, M.P., Ayisi, K.K., Mariga, I.K., Mohlabi, R.C., Chuene, R.S., 2017. Production and utilization of Moringa by farmers in the Limpopo Province, South Africa. Int. J. Agric. Res.. 12, 160-171.

Mabapa, M.P., 2019. Yield characteristics, carbon capture and chemical composition of *Moringa oleifera* under diverse planting population and agro-ecological conditions of Limpopo Province, PhD thesis, University of Limpopo. South Africa.

Mokgehle, S., Araya, N., Mofokeng, M., Makgato, M., Amoo, S., Maboka, K., du Plooy, C., Araya, H., 2022. Regrowth response and nutritional composition of *Moringa oleifera* to cutting back in three agro-ecological zones in South Africa. Hortic. 8, 963. https://doi.org/10.3390/horticulturae8100963.

Obala, D., Ng'ang'a, F. M., Kiruki, H., Mutiso, F., Ndung'u, C., 2022. Effects of *Negarim* Micro-catchment (MC) on growth and survival of two provenances of *Moringa oleifera* under different spacing in a semi-arid area of Kitui County, Kenya. EAJENR 5(2), 14-28. https://doi.org/10.37284/eajenr.5.2.927

Roose, E., 2015. *Restauration de la productivité des sols tropicaux et méditerranéens: contribution à l'agroécologie*. Institut de Recherche pour le Developpement (IRD): Montpellier, France.Vasconcelos, M.C., Costa, J.C., Sousa, J.P.S., Santana, F.V., Soares, T.F.S.N., de Oliveira Júnior, L.F.G., Silva-Mann, R., 2019. Biometric and Physiological Responses to Water Restriction in *Moringa oleifera* Seedlings. Floresta e Ambiente. 26(1), e20150165. https://doi.org/10.1590/2179-8087.016515

VSN International, 2015. Genstat for Windows 18th Edition. VSN International, Hemel Hempstead, UK. Web page: Genstat.co.uk.

CHAPTER 7

EVALUATION OF THE METRIC EEFLUX PLATFORM TO ESTIMATE WATER USE OF MORINGA

Knowledge Muchaonyerwa[1], Shaeden Gokool[1], Alistair Clulow[1,2] and Nadia Araya[3,4]

[1]*Centre for Water Resources Research, School of Agricultural, Earth and Environmental Sciences, University of KwaZulu-Natal, Pietermaritzburg, South Africa.*

[2]*Discipline of Agrometeorology, School of Agricultural, Earth and Environmental Sciences, University of KwaZulu-Natal, Pietermaritzburg 3209, South Africa*

[3]Agricultural Research Council – Vegetable, Industrial and Medicinal Plants, Pretoria, South Africa

[4]Agricultural Research Council – Natural Resources and Engineering, Pretoria, South Africa

7.1 INTRODUCTION

Over the years there has been a significant amount of quantitative research highlighting the benefits of using Moringa (Al-Alsmari et al., 2015, Tshabalala et al., 2021). There is enough evidence encouraging agricultural communities to consider commercializing this crop and create opportunities in the cosmetics and pharmaceutical industries with an increase in the scale of production (Al-Asmari et al., 2015; Tshabala et al., 2021). Results from validated research has shown that the plant can grow under relatively dry ecological zones (with a maximum of 400 mm of annual rainfall, Tshabala et al., 2021). However, there is limited information regarding optimal growing conditions of Moringa in South Africa (Bopape-Mabapa, 2019; Mashamaite et al., 2021, Akpor et al., 2022). For a successful implementation of large-scale commercial farming there is a need to develop a deeper understanding of the adaptability of *Moringa oleifera* to different climatic conditions, and its biomass production in relation to water availability (water use efficiency), especially under different water supply conditions and management approaches.

There are various ground-based approaches commonly used to measure crop water use; these include the soil water balance modelling, sap flow measurement and Eddy Covariance (EC) (Mashamaite et al., 2021). The EC system is currently the international standard in ground-based techniques for acquiring accurate predictions of crop evapotranspiration (ETc). Due to the high cost of equipment required to run the EC flux towers, there is a need to validate alternative methods such as Remote Sensing (RS), which has the potential of being more efficient (Anapalli et al., 2020). The RS technology is capable of capturing spatially explicit information of a heterogeneous environment in a way that saves time and resources (Nhamo et al., 2020, Brewer et al., 2022).

Remote sensing techniques integrated with cloud-based systems are effective in capturing real-time large data. The advantages of these new systems are: (i) efficiency in processing of data obtained by the sensors, using supercomputers that have larger processing power; (ii) low background knowledge requirement by the end-user due to minimized input data needed to utilize the platform (user friendly);(iii) Cloud-based tools create an opportunity for more complex studies to be conducted at lower costs over time, through compilation of results generated from similar studies in different parts of the world which enables developers to revise the models by identifying gaps in their conceptualization that could be causing inaccuracies. Technological advances in RS have resulted in the development of products that use the cloud-computing environment such as MOD16 (He et al., 2019), Mapping Evapotranspiration at High Resolution with Internal Calibration using the Earth Engine Flux (METRIC EEFlux)(Allen et al.,2015), and Surface Energy Balance for Land use Algorithm Improved Google Earth Engine (SEBALIGEE) (Laipelt et al., 2021). The function of a product utilizing the cloud-computing environment is to increase efficiency by reducing processing time for the end user (utilizing supercomputers and internet) and providing processed data in the form of imagery with minimal additional processing required to make informed decisions (Allen et al., 2015). The aim of this study was to validate the METRIC EEFlux application (which is a fully automated cloud-based RS system) by determining the water use of *Moringa oleifera* using in-situ EC measurements for ground reference data. The results from the study will aid in understanding the effectiveness in the METRIC EEFlux model conceptualization and quantify the uncertainty of the model outputs to establish whether it is an application that can be adopted for field-scale studies.

7.2 MATERIALS AND METHODS

7.2.1 Study site specifications

The study focused on obtaining actual ET measurements of a nine-year-old drip-irrigated Moringa plantation established on a commercial farm in Tooseng, Limpopo, South Africa (24˚26’59” S, 29˚32’58” E) (Figure 7.1). The planted field had an area of approximately 1 ha (100 m x 100 m), elevation of 822 m above sea level, and mean annual precipitation of 448 mm.

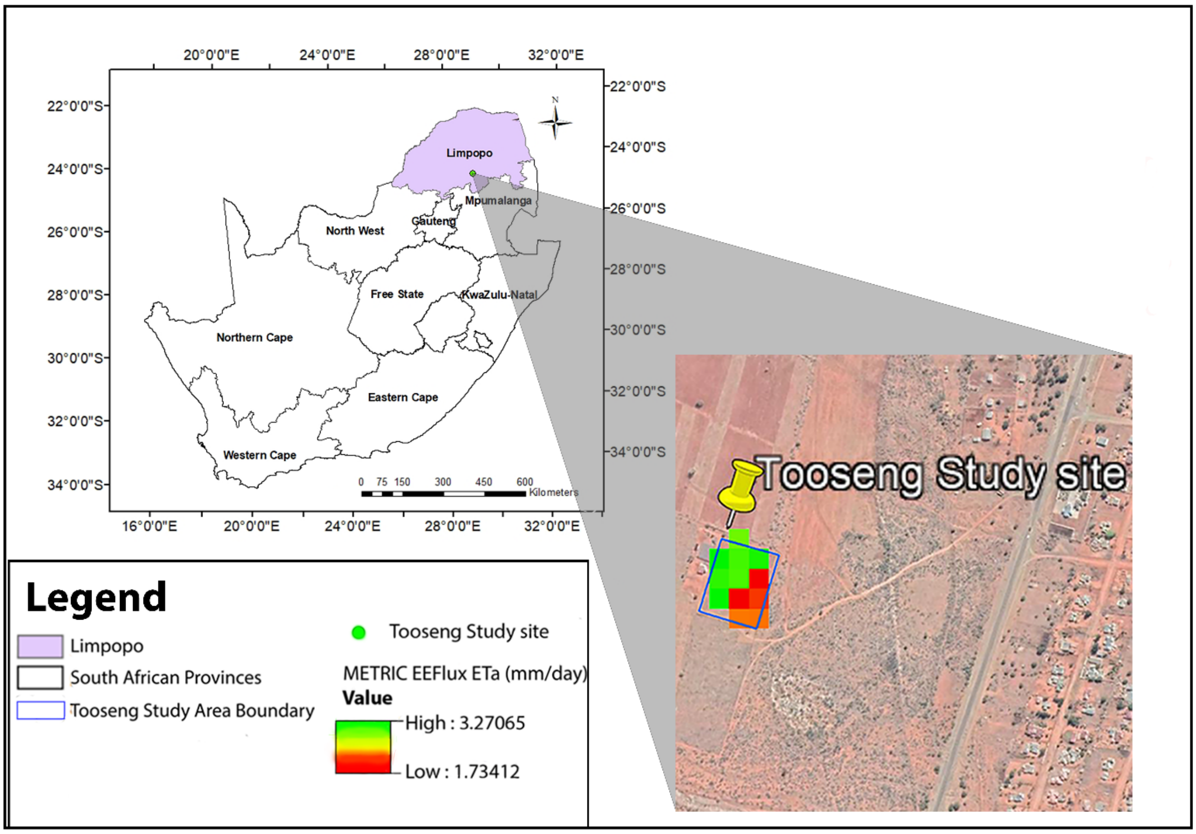

Figure 7.1: An overview of the location of the study site used for Remote Sensing predictions of Moringa water use.

The EC flux tower was selected as the appropriate ground-based ET measurement tool for obtaining actual Evapotranspiration (ETa) over the homogenous Moringa field, an output data was logged (CR5000, Campbell Scientific Inc., Logan, Utah, USA) at 30-minute intervals using a sampling rate of 10 Hz. The EC flux tower collected data from 17 December 2021 to 31 January 2022, when measurements ceased due to a field invasion by bush crickets. The three-dimensional wind velocity and variation in temperature (CSAT3, Campbell Scientific Inc.), the concentration of water vapor (EC 150 CO_2/H_2O open-path gas analyzer), net radiation (NR-Lite, Kipp and Zonen, delft, Netherlands), and soil heat flux (HFT-S, REBS, Washington, USA) were measured to determine ETa using the shortened energy balance method and to assess the closure error (19%, considered acceptable, Mashamaite et al., 2021) (Equation 21). Sensors installed on the mast were at least 0.5 m above the tallest part of the canopy. The shortened energy balance equation is expressed below.

$$Rn - LE - H - G = 0 \tag{7.1}$$

where:

LE is latent heat flux; Rn is net radiation, H is sensible heat flux and G is soil heat flux, all components expressed in W m^{-2}, where fluxes towards the surface are positive and away from the surface are negative.

7.2.2 Actual Evapotranspiration estimates using the METRIC EEFlux model

The METRIC EEFlux model estimates instantaneous LE (W m^{-2}) for every pixel in an image at the satellite overpass time for the region of interest (Equation 22):

$$LE_i = R_{ni} - H_i - G_i \tag{7.2}$$

where, the subscript "i" denotes measurements at the time of satellite overpass. Other components of the surface energy balance equation (Rn, H and G) are not provided directly as part of the products available in the METRIC EEFlux application s.

An instantaneous estimate of actual evapotranspiration (ETinst in mm hr^{-1}) is calculated for each pixel by converting LE in W m^{-2}, calculated as a residual from the surface energy balance (RSEB) equation, using constants of latent heat of vaporization "λ" (J/kg) and density of water "ρ_w" (kg m^{-3}), multiplied by 3600, a conversion factor to hours, expressed in Equation 23.

$$ETinst = \frac{LE}{\lambda \rho w} x3600 \tag{7.3}$$

ETrF is a fraction of reference evapotranspiration of alfalfa crop used as a vehicle for extrapolating ET from the overpass scene to the surrounding 24-hr period (Carrasco-Benavides et al., 2014). The METRIC EEFlux model provides an estimate of daily ETa through a multiplication of ETrF values for each individual pixel by the daily ETr computed from gridded weather data from Climate Forecast System Version 2 (CFSv2) for countries outside the contiguous United States (CONUS). Values of ETrF are derived following the equation below.

$$ETrf = \frac{ETinst}{ETr} \tag{7.4}$$

In this study, daily ETa values estimated by METRIC EEFlux using gridded weather data were compared to in-situ ETa data measured with the Eddy Covariance technique. As a way of assessing whether the METRIC EEFlux direct estimates of ETa could be improved, this study determined daily ETa by combining values of ETrF from the EEFlux application with in-situ ETr determined using meteorological weather data obtained from an automated weather station installed in close proximity to the experimental site. Consequently, daily ETa is obtained by the Landsat sensor which has a spatial resolution of 30 m using the equation below (Allen et al., 2013, Allen et al., 2015).

$$ETa = ETr \; x \; ETrf \tag{7.5}$$

Estimated daily ETa is the average computed from all the pixels within the area of interest (mm d^{-1}).

Figure 7.2 gives an overview of how ETa is obtained using an average value of all pixels within the boundaries of the experimental site. The same procedure was used to analyze other products provided by the METRIC EEFlux such as ETr and ETrF.

7.3 RESULTS AND DISCUSSION

7.3.1 Comparison between measured and estimated actual evapotranspiration using gridded weather data and ETrF provided by the METRIC EEFlux model

The METRIC EEFlux model generally overestimated crop ETa and ETrF values compared to the EC measurements (Figure 7.2). This is primarily attributed to an overestimation of ETr determined from gridded weather data (Figure 7.2). Kadam et al. (2021) also found an overestimation of ETa determined from the METRIC EEFlux model when compared to ETa measured using an EC system for grain crops grown under rainfed conditions in the USA. The overestimation was attributed to the choice of a relatively high cold pixel ETrF value of 1.05 in the METRIC EEFlux model. To address this limitation, these authors proposed a reduction of cold pixel ETrF, which is a parameter affected by sensor overpass time (from 1.05 to 0.85,), but emphasized that this adjustment could be variable depending on environmental conditions (Foolad et al., 2018). It is important to note that the trial took place over a short period during the rainy season (17 December 2021 to 31 January 2022), thus limiting the number of low cloud cover images that could be acquired for analysis.

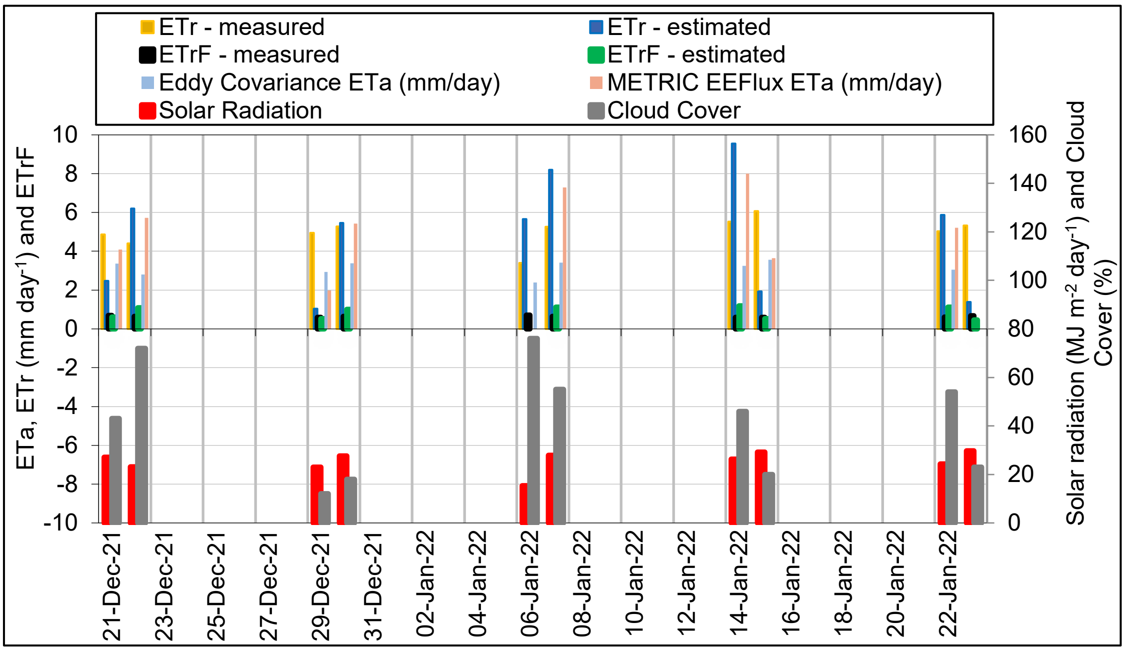

Figure 7.2: A comparison between measured and estimated actual evapotranspiration, reference evapotranspiration and fraction of reference evapotranspiration, under a range of cloud cover and solar radiation conditions at the study site.

The comparative statistics between the EC and METRIC EEFlux methods of crop ETa quantification (Table 7.1) were poor for the observed period when cloud cover ranged from 12 to 72%. It is important to note that cloud cover percentage for the satellite does not suggest that the area of interest will be affected, however a higher percentage does increase the probability of surface reflectance in the area of interest. The mean absolute percent error (MAPE) was on average 22%, which indicates that the model prediction accuracy was relatively low (Swanson, 2015; Hara et al., 2021). In addition, the coefficient of determination (R^2) and root mean square error (RMSE) results were poor (<0.5 and 0.67 mm/day, respectively), which demonstrated that the proportion of variation in the estimated ETa was poorly predicted by the METRIC EEFlux model.

Table 7.1: A statistical comparative performance between the Eddy Covariance and METRIC EEFlux crop ETa quantification approaches on Moringa.

Date	Eddy Covariance ET_a (mm/day)	METRIC EEFlux ET_a (mm/day)
21-Dec-21	3.36	4.09
29-Dec-21	2.93	1.97
15-Jan-22	3.56	3.64
23-Jan-22	3.62	3.01
MAPE (%)		22.23
RMSE (mm/day)		0.68
R^2		0.44

The relatively poor performance of the METRIC EEFlux model (Table 7.1), could be attributed to factors such as i) assuming ETrF to be constant throughout the day, ii) cloud contamination within the images, iii) sensor overpass time (in the acquisition of ETisnt), and iv) global gridded weather data (for estimating ETr). However, the impact of these factors can only truly be established following the completion of the trial. Despite these potential limitations, the METRIC EEFlux model incorporates an internal self-calibration procedure of sensible heat flux (H) for two extreme conditions (hot pixel and cold pixel), which reduces errors associated with spatial variability of crop ETa at a field-scale (Carrasco-Benavides et al., 2014). Hence, there is potential for the METRIC EEFlux modeling procedure to be improved to generate more accurate estimations of Moringa crop ETa. Findings obtained in this study also confirmed the importance of selecting satellite images with relatively low cloud cover with adequate incident solar radiation (at least 29 MJ m^{-2} day^{-1}) (Figure 7.3).

7.3.2 Assessment of the METRIC EEFlux products using local climate data for estimation of Moringa daily actual evapotranspiration

Results presented in Table 7.2 suggest a promising performance of the METRIC EEFlux model to predict Moringa crop ETa using estimated ETrF and ETr determined with in-situ measurements of weather variables, under optimum conditions of crop growth. The improved performance of the METRIC EEFlux model was assessed by comparing estimated values of ETa against measured values using the EC technique (Table 7.2). Values of MAPE and RMSE for the comparison between measured and estimated ETa reduced considerably from an average of 22% and 0.67 mm/day using ETa derived directly from METRIC EEFlux to 8% and 0.28 mm/day, respectively, with ETrF derived from METRIC EEFlux combined with in-situ meteorological data. Similarly, the R^2 value increased from 0.44 with the METRIC EEFlux direct procedure of estimating ETa to 0.91 using the alternative procedure.

Table 7.2: A statistical comparative performance between measured (with the Eddy Covariance) and estimated Moringa ET_a (using the local climate data as an alternative METRIC EEFlux modelling approach).

Date	Eddy Covariance ET_a (mm/day)	METRIC EEFlux ET_a (mm/day)
21-Dec-21	3.36	3.29
29-Dec-21	2.93	2.60
15-Jan-22	3.56	3.52
23-Jan-22	3.62	3.77
MAPE (%)		8.00
RMSE (mm/day)		0.28
R^2		0.98

7.4 CONCLUSIONS AND RECOMMENDATIONS

The evidence from this study has shown that local meteorological data could potentially be integrated with the output from the METRIC EEFlux model to provide fairly accurate Moringa ETa estimates. For a more in-depth evaluation of the METRIC EEFlux model performance, a longer period of in-situ measurements is needed to account for variations in canopy cover due to leaf senescence and harvesting periods. This will provide the opportunity to identify other possible gaps that could be affecting results produced by the platform, apart from cloud coverage and gridded weather data. It will also enable an evaluation of a range of scenarios to identify the most suitable conditions for improved estimates of crop water use. This study has contributed towards an understanding of the components within the METRIC EEFlux model algorithm, which could increase uncertainty of field scale ETa estimates. Some of the shortcomings of the METRIC EEFlux modelling approach can be counteracted by using semi-automated remote sensing tools such as the METRIC-GIS toolbox which utilises local meteorological data as modelling inputs.

ACKNOWLEDGEMENTS

The authors would like to acknowledge the Water Research Commission (WRC) for funding this research, which was conducted by the Agricultural Research Council (ARC) in collaboration with the University of KwaZulu-Natal (UKZN) under the Project No C2020/2021-00484, titled “Determining water use, water use efficiency and nutritional water productivity of Moringa under varying crop management practices”. We would also like to acknowledge the developers of the Google Earth Engine METRIC EEFlux application for providing further clarity on model operation technicalities.

REFERENCES

Al-Asmari, A. K., Albalawi, S. M., Athar, M. T., Khan, A. Q., Al-Shahrani, H. and Islam, M. (2015). Moringa oleifera as an anti-cancer agent against breast and colorectal cancer cell lines. PLoS One*,* 10**,** e0135814.

Allen, R. G., Morton, C., Kamble, B., Kilic, A., Huntington, J., Thau, D., Gorelick, N., Erickson, T., Moore, R. and Trezza, R. (2015). EEFlux: A Landsat-based evapotranspiration mapping tool on the Google Earth Engine. 2015 ASABE/IA Irrigation Symposium: Emerging Technologies for Sustainable Irrigation-A Tribute to the Career of Terry Howell, Sr. Conference Proceedings, 2015. ASABE, 1-11.

Anapalli, S. S., Fisher, D. K., Pinnamaneni, S. R. and Reddy, K. N. (2020). Quantifying evapotranspiration and crop coefficients for cotton (Gossypium hirsutum L.) using an eddy covariance approach. Agric. Water Manag., 233, 106091.

Bopape-Mabapa, M. P. (2019). Yield characteristics, carbon capture and chemical composition of *Moringa oleifera* under diverse planting population and agro-ecological conditions of the Limpopo Province. University of Limpopo.

Brewer, K., Clulow, A., Sibanda, M., Gokool, S., Naiken, V. and Mabhaudhi, T. (2022). Predicting the chlorophyll content of maize over phenotyping as a proxy for crop health in smallholder farming systems. Remote Sens. , 14, 518.

Foolad, F., Blankenau, P., Kilic, A., Allen, R. G., Huntington, J. L., Erickson, T. A., Ozturk, D., Morton, C. G., Ortega, S. and Ratcliffe, I. (2018). Comparison of the automatically calibrated Google Evapotranspiration Application—EEFlux and the manually calibrated METRIC application. doi: 10.20944/preprints201807.0040.v1

Hara, P., Piekutowska, M. and Niedbała, G. (2021). Selection of independent variables for crop yield prediction using artificial neural network models with Remote Sensing Data. Land, 10, 609. https://doi.org/10.3390/land10060609.

He, M., Kimball, J. S., Yi, Y., Running, S. W., Guan, K., Moreno, A., Wu, X. and Maneta, M. (2019). Satellite data-driven modeling of field scale evapotranspiration in croplands using the MOD16 algorithm framework. Remote Sens. Environ., 230, 111201.

Kadam, S. A., Stöckle, C. O., Liu, M., Gao, Z. and Russell, E. S. (2021). Suitability of Earth Engine Evaporation Flux (EEFlux) Estimation of Evapotranspiration in Rainfed Crops. Remote Sens., 13, 3884.

Mashamaite, C. V., Pieterse, P. J., Mothapo, P. N. and Phiri, E. E. (2021). Moringa oleifera in South Africa: A review on its production, growing conditions and consumption as a food source. S. Afr. J. Sci., 117, 1-7.

Nhamo, L., Magidi, J., Nyamugama, A., Clulow, A. D., Sibanda, M., Chimonyo, V. G. and Mabhaudhi, T. (2020). Prospects of improving agricultural and water productivity through unmanned aerial vehicles. Ag., 10, 256.

Swanson, D. A. (2015). On the relationship among values of the same summary measure of error when used across multiple characteristics at the same point in time: an examination of Malpe and Mape. IREF, 5.

Tshabalala, T., Abdel-Rahman, E. M., Ncube, B., Ndhlala, A. R. and Mutanga, O. (2021). Leveraging of hyperspectral remote sensing on estimating biomass yield of Moringa oleifera Lam. medicinal plant. S. Afr. J. Bot., 140, 37-49.

CHAPTER 8

PREDICTION OF MORINGA EVAPOTRANSPIRATION USING THE AQUACROP MODEL

Nadia Araya[1,3], Ntsieni Mulovhedzi[1,4], Stephen Amoo[1] and Zaid Belo[2]

[1]*Agricultural Research Council, Vegetable, Industrial and Medicinal Plants Private Bag X293, Pretoria, 0001, South Africa, Private Bag X293, Pretoria, 0001*

[2]*Agricultural Research Council, Grain Crops, Private Bag X1251, Potchefstroom, 2520, South Africa*

[3]*Agricultural Research Council[1]Natural Resources and Engineering, Private Bag X293, Pretoria, 0001, South Africa, Private Bag X293, Pretoria, 0001*

[4]*University of Mpumalanga, School of Agricultural Sciences, Private bag X11283, Mbombela, 1200, South Africa*

8.1 INTRODUCTION

Moringa (*Moringa oleifera* Lam.), also known as the miracle tree, horseradish tree or drumstick tree, is a relatively new promising crop because of its multipurpose uses, rich nutritional and phytochemical value, as well as drought tolerance (Daba, 2016; Devkota and Bhusal, 2020; Shyamli et al., 2021). All its parts (leaves, pods, flowers and seeds) are used for nutritional, medicinal and pharmacological purposes. The crop is highly nutritive in terms of its minerals, protein, and vitamins' contents; and medicinal due to its constituent phytochemicals including tannins, sterols, terpenoids, flavonoids, saponins, anthraquinones and alkaloids (Shyamli et al., 2021). It has been proven that the nutritional content of Moringa leaves is higher than that of the other parts of the tree (Gopalakrishnan et al., 2016). As a result, Moringa leaf is the most used part of the tree for agro-processing and product development. Other uses of this multifunction tree include water purification, biofuel production and conservation of soil and water natural resources (Shyamli et al., 2021).

Moringa is a slender, fast growing, deciduous perennial woody shrub or small tree reaching 9 to 15 m in height, with an umbrella shaped, open crown (El-Boraie et al., 2021). It is considered as drought tolerant plant that is easily adapted to various ecosystems (Shyamli et al., 2021). Its drought resistance characteristic is attributed to the tree's deciduous growth habit, displaying an acclimation mechanism in response to water stress by shedding its leaves, which consequently limits transpiration (Ezzine et al., 2023). Moreover, the tree has a tuberous root system with water and energy storage that allows the plant to grow new leaves when climatic conditions become favorable (Ezzine et al., 2023). Despite its genetic tolerance to sub-optimal growing conditions, it is reported that Moringa benefits from adequate water supply, particularly during critical growth stages such as seedling establishment and growth, as well as tree reproduction (Mulh et al., 2013). Moringa water requirements can be met through the development of appropriate irrigation scheduling strategies. This can be carried out through the use of a crop model. Crop models are one of the tools used to develop and test possible management strategies for optimal water productivity. Furthermore, crop models can assist as support tools for planning, decision making, yield predictions and evaluating the effects of climate change (Steduto et al., 2009a). As a result of all these advantages, crop models have been adopted as cost-effective and time-efficient tools to develop tailored crop water management strategies across a range of conditions. This, in turn, contributes to an optimization of the limited water resources, which is particularly important in semi-arid climates where the crop water demand often exceed its atmospheric supply (Kisekka et al., 2017).

Several crop modelling approaches have been reported to aid in irrigation water management of horticultural crops, including plant physiological and crop coefficient models (Ibraimo et al., 2016; Li et al., 2020; Jo and Shin, 2021). However, these modelling approaches are often suitable for scheduling irrigation under non-limiting water supply conditions, and do not provide direct feedback on how irrigation management decisions impact seasonal crop yields (Kisekka et al., 2017). In this paper, we present a performance evaluation of the AquaCrop soil water balance model, which unlike previous model examples, can be a useful tool for implementing tactical irrigation scheduling, while providing feedback on how irrigation scheduling decisions impact crop growth, yield and water productivity (FAO, 2023). The AquaCrop model generates these outputs by using a significantly lower number of parameters, while providing a better balance between simplicity, accuracy and robustness compared to other models (Steduto et al., 2014).

AquaCrop is a water-driven crop model that can be used for planning and decision making studies for a range of crops. The model has been successfully tested on several horticultural herbaceous crops, including leafy, root and tuberous vegetables (Bello and Walker, 2017; Nyathi et al., 2018; Wellens et al., 2022; Wang et al., 2023), grains (Bello and Walker, 2016; Jalil et al., 2020; Martínez-Romero et al., 2021; Feng et al., 2022; Zhang et al., 2022), grapevines (Er-Raki et al., 2021), and legumes (Nunes et al., 2021). Little to no information is available regarding the applicability of the AquaCrop model on woody crops, despite its conceptual framework allowing predictions for such crops (Poppe, 2016). This may be due to the carry-over effects from one year to another, the complexity of morpho-physiological processes and the more complicated evaporation and transpiration behavior of woody plant species. Thus, the aim of this study was to parameterize and validate the AquaCrop model for simulating Moringa growth, leaf yield and crop evapotranspiration under a semi-arid climatic condition. This serves as an opportunity to test the applicability of AquaCrop for woody crops and model serial harvesting of Moringa leaves, which have not been previously exploited.

8.2 MATERIALS AND METHODS

8.2.1 *Study area characterization and crop management*

Field measurements were conducted at the Roodeplaat Experimental Farm of the Agricultural Research Council – Vegetable, Industrial and Medicinal Plants (ARC-VIMP) (25°35'N, 28°21'E, 1164 m above sea level) in Gauteng Province, South Africa, on a 1- to 2-year-old, 500 m^2 Moringa stand, over two consecutive experimental seasons in 2018/2019 and 2019/2020 (Figure 8.1). The crop growing period, when research treatments began, was from 01 January to 07 June in 2018/2019 and from 17 December to 05 May in 2019/2020. However, the crop dormancy break is around October. After this period, the stand is left growing for about three months before it is leveled for uniformity of research treatment responses. The experimental region experiences summer rainfall, with an annual average of approximately 650 mm per annum (Nyathi et al., 2018). The climate is semi-arid, with average daily air temperature ranging from 8 to 34°C in summer and 4 to 23°C in winter (Mulovhedzi et al., 2020.

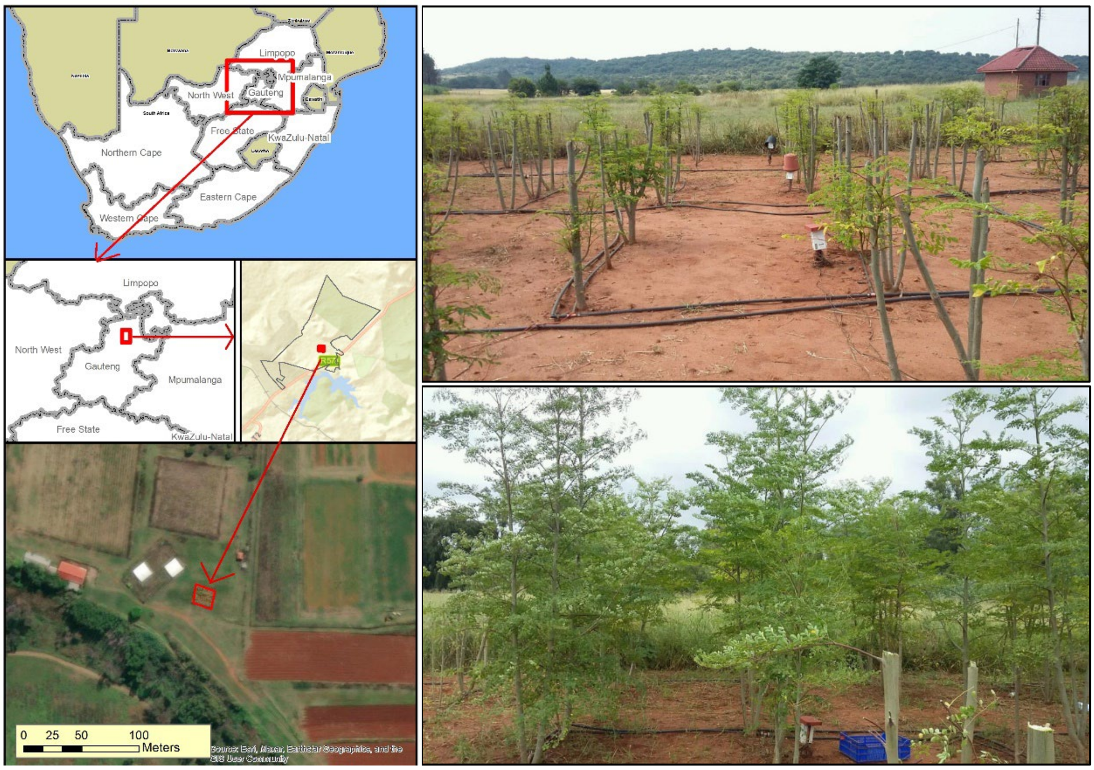

Figure 8.1: Geographic location of the study area, ARC-VIMP Experimental Farm, Roodeplaat, Pretoria.

Moringa seedlings were planted in rows that were 2 m apart with intra-row spacing of 1 m, maintaining a planting density of 5000 trees per hectare. Each plot was composed of four rows of 4 m long. Weeds were controlled manually and mechanically using brush cutters between rows. Based on the soil analysis test results and crop nutrient requirements, 150 kg ha^{-1} N [limestone ammonium nitrate (LAN) 28%] was applied at planting during 2018/19 season, phosphorus (P) and potassium (K) were sufficient, and a top dressing of 100 kg ha^{-1} N (LAN) was applied after each harvest. After planting, top dressing with the same fertilizer application rate was maintained during the 2019/20 season. In both seasons, fertilizer was applied around each plant and incorporated into the soil manually using hand hoes and rakes. From October to December each year, the crop was irrigated optimally to facilitate adequate growth before research treatments were introduced. During each growing season, the crop was harvested three times (keeping a 45-day harvest interval), by cutting all the biomass above a height of 0.50 and 0.9 m from the ground surface in 2018/2019 and 2019/2020 respectively.

8.2.2 Research treatments and statistical design

Four water supply regimes were tested, namely high [(20% management allowable depletion level (MADL)], medium (40% MADL) and low irrigation (60% MADL), as well as rainfed (without irrigation). The treatments were laid out in a randomized complete block design (RCBD), with three replications. The field was slightly sloped and, as a result, the statistical design was laid perpendicularly to the source of variation to account for the gradient effect.

8.2.3 Field data collection

8.2.3.1 Soil physical and chemical characteristics

Prior to the commencement of the trial in August 2018, a 1.5 m x 1.5 m x 1.5 m soil trench was dug for soil texture, volumetric soil water content (θ) at field capacity (FC), and permanent wilting point (PWP) determination. Soil samples were collected from 0-35 cm, 35-70 cm, and 70-100 cm depths for soil texture, while FC and PWP determination was done using standard laboratory procedures involving a hydrometer and pressure plate apparatus at the Natural Resources and Engineering Campus of the Agricultural Research Council in Pretoria. The extraction of soil samples was done using a manual soil auger. Thereafter, all soil samples were labeled and sent to the laboratory for determination of chemical and physical properties of the soil at the study site (Table 8.1). The soil at the site is classified as a Hutton soil form (Soil Classification Working Group, 1991) with a medium sandy clay texture and an average bulk density of 1.2 g cm^3.

Table 8.1: Soil chemical and physical characteristics across a one-meter deep soil profile at the study site prior to the commencement of the field trial in August 2018.

Soil characteristics	**Units**	**Soil layer**		
		0-35 cm	**35-70 cm**	**70-100 cm**
Chemical elements				
Phosphorous (P)-Bray 1	mg kg^{-1}	54.55	12.47	2.79
Potassium (K)	mg kg^{-1}	196	129	103
Calcium (Ca)	mg kg^{-1}	733	838	787
Magnesium (Mg)	mg kg^{-1}	204	278	268
Manganese (Mn)	mg kg^{-1}	26.9	17.4	15.4
Sodium (Na)	mg kg^{-1}	11.5	21.5	22.2
Iron (Fe)	mg kg^{-1}	10.8	8.06	7.68
Zinc (Zn)	mg kg^{-1}	6.88	1.09	0.97
Copper (Cu)	mg kg^{-1}	4.03	2.7	2.02
Ammonium-nitrogen (NO_4-N)	mg kg^{-1}	8.11	8.03	7.47
Nitrogen (N)	%	0.06	0.06	0.05
Nitrate-nitrogen (NO_3-N)	mg kg^{-1}	1.73	1.46	1.21
pH (H_2O)	–	7.16	7.21	7.15
Physical elements				
Sand	%	36.7	30.1	26.6
Silt	%	13.4	13.7	14.1
Clay	%	49.9	56.2	59.3
Field capacity	m^3 m^{-3}	0.337	0.351	0.358
Permanent wilting point	m^3 m^{-3}	0.21	0.21	0.21
Bulk density	kg m^{-3}	1241	1196	1113

8.2.3.2 Monitoring of irrigation of applications, changes in soil water content, determination of actual crop evapotranspiration and water productivity

Irrigation was applied using a high-density, pressure-compensated drip irrigation system. The system had a delivery rate of 2.5 ℓ hr^{-1}, at a pressure range of 100-150 kPa. The spacing between drippers was 1 m and one dripper line was installed per crop row, with one dripper per tree. Each irrigation treatment was equipped with a solenoid valve to control irrigation amount. Immediately after planting, the plots were irrigated optimally, in order to keep the soil profile at field capacity (FC) for 90 days until the plants were fully established.

Changes in soil water content were monitored daily, using 10-HS capacitative soil water content sensors connected to an EM-50 data logger (Decagon Devices, Campbell Scientific, USA) for automatic data logging. Sensors were installed at middle depths, between 0-35, 35-70 and 70-100 cm down the soil profile. Thus, one set of three sensors was installed in one of the representative trees per experimental plot. Soil water content, rainfall and irrigation application data was used to determine cumulative actual crop evapotranspiration per growing period, using the soil water balance method (Zeleke and Wade, 2012). Water productivity was determined as the ratio between leaf yield and cumulative actual crop evapotranspiration per growing period (Nyathi et al., 2019).

8.2.3.3 Measurements of tree yield, canopy growth and physiological attributes

Table 8.2 illustrates Moringa tree yield, canopy growth and physiological attributes measured during the experimental period.

Table 8.2: Moringa tree yield, canopy growth and physiological attributes measured during the experimental period.

Measurement type	Measurement frequency	Measurement device
Fractional interception of photosynthetically active radiation (FI_{PAR})	Once every week	Ceptometer (Decagon, Pullman, Washington, USA)
Leaf area index (LAI)	Once every week	Ceptometer (Decagon, Pullman, Washington, USA)
Leaf stomatal conductance	Once per harvest period	SC-1 Leaf porometer (METER Group, Inc. USA)
Tree fresh leaf yield	Once per harvest period	Weighing scale (Adam Equipment, UK)
Tree dry leaf yield	Once per harvest period	Oven and weighing scale (Adam Equipment, UK)

8.2.3.4 Weather variability monitoring

Daily reference evapotranspiration (ET_o) for the measurement period was calculated using the FAO-56 Penman-Monteith equation (Allen et al., 1998) from weather data obtained from an automatic weather station (AWS) installed within a 500 m radius from the experimental site. The AWS was installed and managed by the ARC – Natural Resources and Engineering. The weather parameters recorded were wind speed, solar radiation, temperature, relative humidity and rainfall. Quality assessment and quality control of the data was performed according to the procedures described by Allen (2008). Quality of the data was found to be good and no corrections were necessary.

8.2.4 AquaCrop model: Parameterization, calibration and validation

AquaCrop is a software system developed by the Land and Water Division of FAO in order to simulate the yield response to water by increasing water efficiency practices in agricultural production (Steduto et al., 2008; Araya et al., 2010). The AquaCrop model relates the soil-plant-atmosphere components through the water balance (Araya et al., 2010). The main input file for the simulation are: climate data (minimum and maximum air temperature, ET_o, rainfall and CO_2), crop data (time to emergence, maximum canopy cover, start of senescence, maturity), soil data (field capacity, permanent wilting points, saturated hydraulic conductivity), management data (irrigation, field management practices) and initial soil water conditions (Er-Raki et al., 2021).

This study used the latest version of AquaCrop model (version 7.1), which is suitable for crops with multiple harvests within a season. This is the case of Moringa cultivated for leaf production. This AquaCrop version does not cater for shrub crops that have hard woody stems and branches close to the ground. As a result, a perennial herbaceous forage crop with the C3 photosynthetic pathway was chosen as the study crop. Moringa's deciduous growth habit and leaf morphological characteristics as well as its photosynthetic pathway belong to those of C3 plants. The canopy cover after harvesting (CC_{ini}), and the generation or timing of the harvest events are specified in the field management file. By considering the CC_{ini} from the input in the field management file, the development of the canopy cover is simulated after each harvest. Soil water, soil fertility, soil salinity stress conditions during the experimental period are taken into account in the prediction of canopy development (Raes et al., 2023).

In semi-arid regions with relatively cool winter periods, the Moringa crop undergoes dormancy from June to August. AquaCrop gives an option for simulation of dormancy in perennial herbaceous crops, whereby early canopy senescence is triggered in the absence of rain and/or irrigation. To account for regrowth of the Moringa crop, in spring when environmental temperatures become warmer, the crop's dormant period is specified. During this period, it is assumed that the crop is not yet permanently wilted, and canopy cover (CC) remains above zero to allow the simulation of canopy expansion as soon as sufficient water becomes available for plant regrowth. Since the dormant period is expressed as a sum of daily ETo, its length (L dormant) is determined by the weather conditions. Hot dry weather shortens the dormant period, while cool weather lengthens the period (Raes et al., 2023). The dormancy and regrowth functions of the AquaCrop model have not been fully tested in this study. Here we present the ability of the model to conduct multiple harvests for perennial crops.

The AquaCrop model parameterization and calibration was based on the highest (20% MADL) water supply regime, using the available climatic data for the first season of experimental measurements (2018-2019). Model fitting and evaluation accuracy was assessed using several statistical parameters, as shown in Table 8.3. Fine-tuning of critical model parameters presented in Table 35 was done by fitting model predictions of canopy cover (CC), cumulative actual crop evapotranspiration (ET_a), seasonal fresh and dry leaf yield, as well as daily soil water content (SWC) to experimental data. Model performance was validated using an independent data set obtained for full irrigation during the 2019-2020 growing season.

Table 8.3: Statistical parameters used to assess the AquaCrop model fitting performance.

Statistical parameter	Symbol	Interpretation	Strength	Reference
Correlation coefficient (dimensionless)	r	Expresses a statistical measure of the strength of a linear relationship between two variables	>0.8	Nash and& Sutcliffe, 1970
Mean Absolute Percent Error (%)	MAPE	Indicates the percent of the average deviation of the simulated values from the measured ones	<25	Swanson, 2015
Root Mean Square Error	RMSE	Measures the discrepancy of simulated values around observed ones	Lower values are more acceptable	Singh et al., 2005
Normalized root mean square error (%)	CV(RMSE)	Calculated as the RMSE divided by the range of the observed values, expressed as a percentage	<25	Jadon et al., 2022
Willmott's index of agreement	d	A standardized measure of the degree of model simulation error which varies between 0 and 1	>0.8	Willmott and Matsuura, 2005

The main input parameters used for parameterization and calibration of the AquaCrop model are grouped into two classes: conservative and non-conservative (Table 8.4). The conservative parameters do not change with time, location, management or cultivar, while those that are non-conservative depend on environmental conditions and management practices (Er-Raki et al., 2021).

Table 8.4: Main input crop parameters used for the parameterization/ calibration of the AquaCrop model for Moringa during the 2018/2019 growing season, under the full irrigation treatment.

	Parameterization/ calibration stage 2018/2019	Validation stage 2019/2020	Method of determination
Conservative			
Base temperature (◦C)	6	6	L, O
Upper temperature (◦C)	40	40	L, O
Initial canopy cover, CC0 (%)	10	10	M
Canopy growth coefficient, CGC (%/GDD)	6.4	6.4	C
Canopy decline coefficient, CDC (%/GDD)	0.429	0.429	C
Maximum coefficient for transpiration, $KcTr_{,x}$	0.65	0.65	C
Maximum coefficient for soil evaporation, Kex	0.34	0.34	C
Upper threshold for canopy expansion, $Pexp_{,upper}$	0.2	0.2	C
Lower threshold for canopy expansion, $Pexp_{,lower}$	0.55	0.55	C
Leaf expansion stress coefficient curve shape factor	4.5	4.5	C
Upper threshold for stomatal closure, $Psto_{, upper}$	0.5	0.5	C
Stomata stress coefficient curve shape factor	3	3	C
Canopy senescence stress coefficient, $Psen_{, upper}$	0.85	0.85	C
Senescence stress coefficient curve shape factor	3	3	C
Reference harvest index, HI0 (%)	9	9	C
Normalized crop Water productivity, WP* (g/m^2)	11	11	M
Non-conservative			
Time from budbreak to full CC, days (CGDD)	61 (835.81)	46 (731.69)	M
Time from budbreak to maximum CC, days (CGDD)	166 (2 696.69)	122 (2048.26)	M
Time from budbreak to start senescence, days (CGDD)	227 (3 522.94)	198 (3256.69)	M
Time from budbreak to end of season, days (CGDD)	243 (3 596.98)	218 (3494.99	M
Maximum canopy cover, CCx (%)	67	75	M
Maximum effective rooting depth, Zx (m)	1.0	1.0	M

Notes: C: calibration; O: observation; L: literature; M: measured

Soil samples taken at each layer, as well as soil water content measurements, were used to determine the different parameters needed for the soil file of the AquaCrop model (Table 8.5). Values of saturated hydraulic conductivity were determined through model parameterization and calibration using the first experimental season (2018-2019).

Table 8.5: Soil hydraulic properties at the experimental site.

Soil hydraulic properties	Soil depth (cm)		
	0-35	35-70	70-100
Field capacity FC (m^3/m^3)	0.340	0.360	0.365
Wilting point WP (m^3/m^3)	0.270	0.270	0.270
Saturation SAT (m^3/m^3)	0.37	0.379	0.383
Saturated hydraulic conductivity, Ksat (mm/day)	35.0	35.0	35.0

8.3 RESULTS AND DISCUSSION

8.3.1 Weather variability during the experimental period

The study was conducted during two consecutive experimental seasons (2018-2019 and 2019-2020). The total rainfall during growing season 1 (339 mm) was slightly lower compared to season 2 (353 mm). The study area did not receive rainfall during the cool months, from May to September. Rainfall distribution during the experimental period (January to May) was relatively similar across the two growing seasons (Figure 8.2). The study region experienced frost during the winter period, with daily minimum temperatures up to -2.1°C (Figure 8.3). Total reference evapotranspiration during the experimental period was 578 and 543 mm in 2018/2019 and 2019/2020, respectively (Figure 8.4).

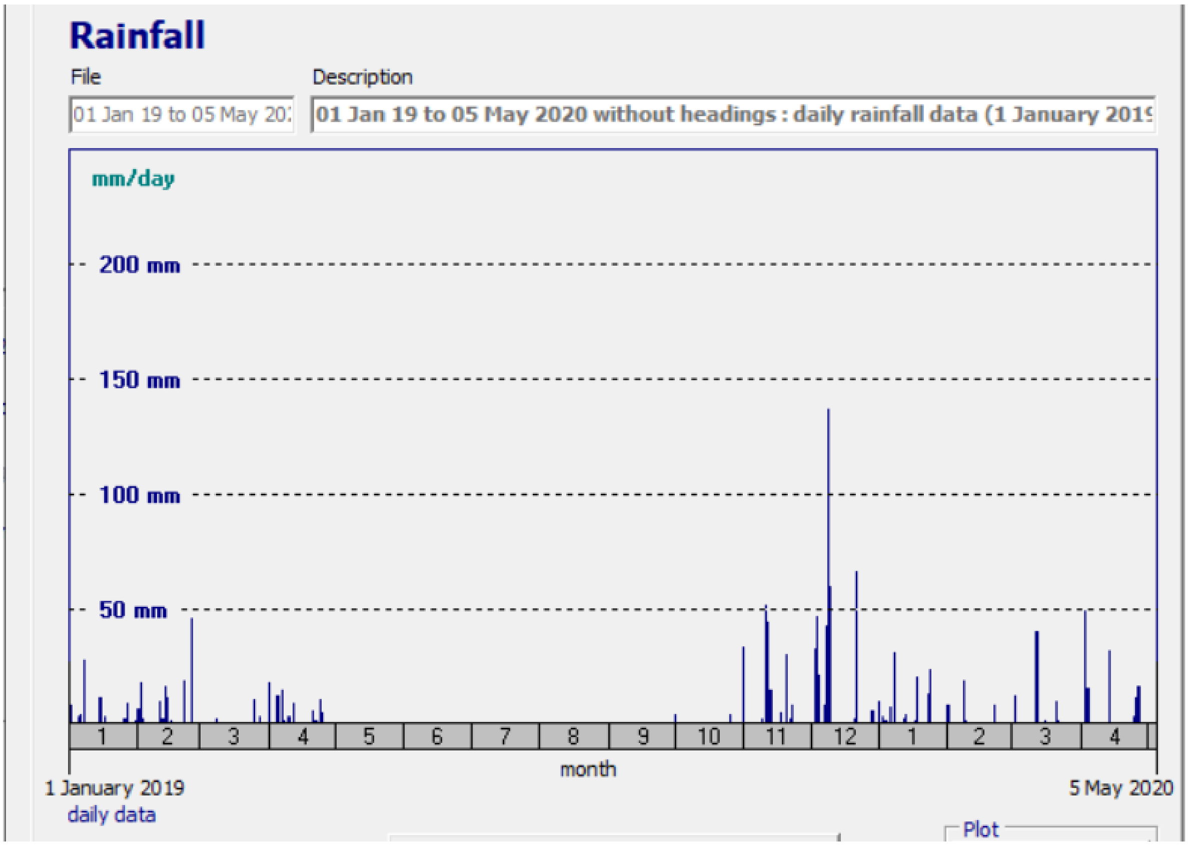

Figure 8.2: Daily rainfall variability during the experimental period at the study site.

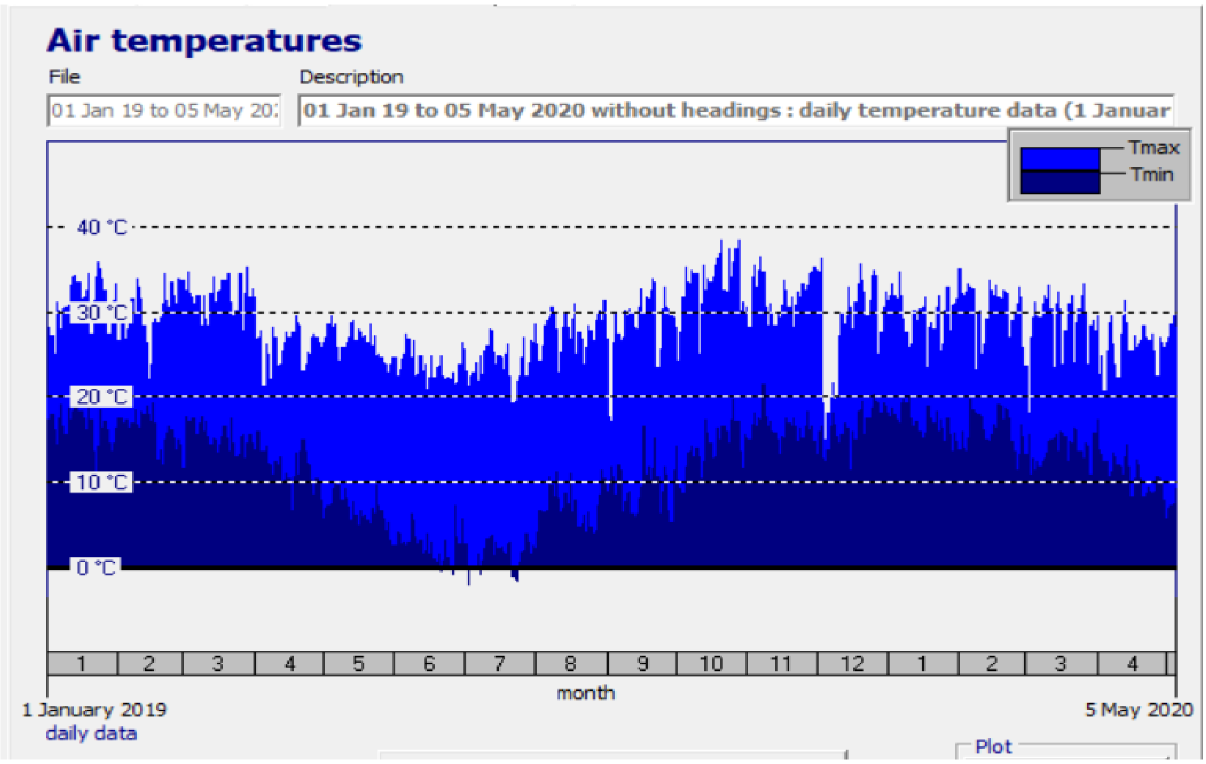

Figure 8.3: Daily variability of maximum and minimum air temperatures during the experimental period at the study site.

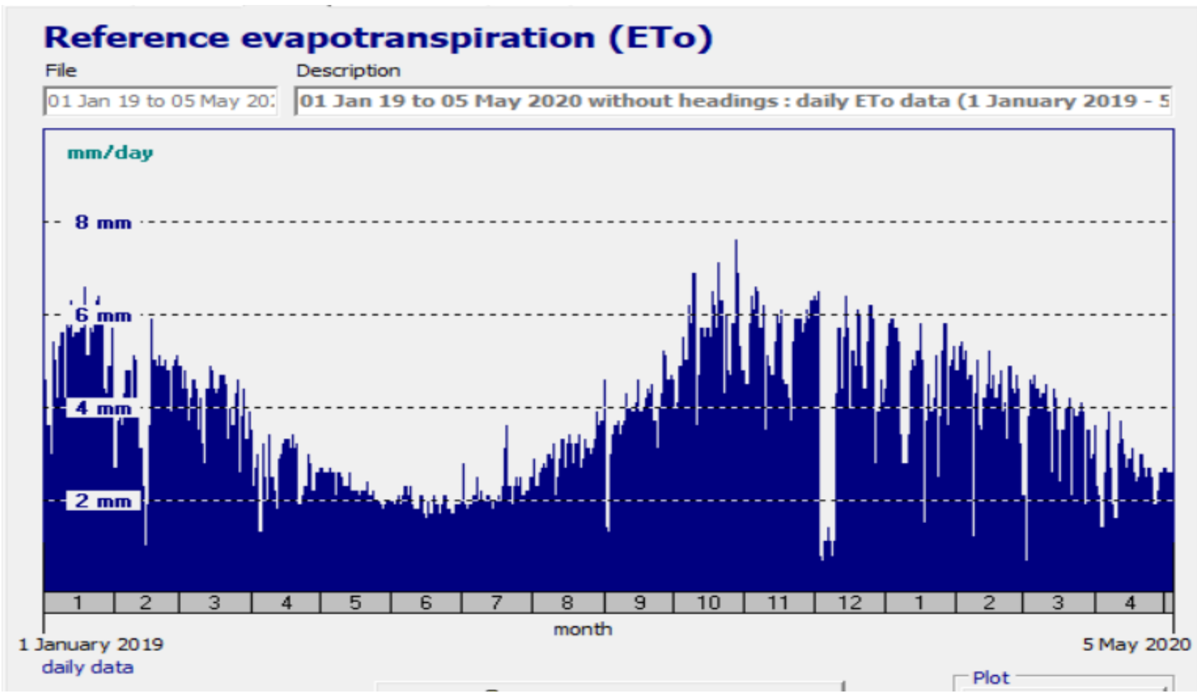

Figure 8.4: Daily variability of reference evapotranspiration during the experimental period at the study site.

8.3.2 Prediction of multiple harvests of Moringa leaves

The AquaCrop model was able to predict multiple harvests of Moringa leaf (Figure 8.4). Towards the end of the growing season (around May), when there was no rainfall or irrigation, the model predicted minimum canopy cover (CC=10%) throughout the entire dormancy period (June to August). The model assumes that, during the dormancy period, canopy cover should be kept at a minimum enough for the crop to be able to regrow once the environmental conditions become favorable after the winter period. The beginning of the regrowth period (in spring, around September), is generated by a temperature criterion, taking into account the base temperature (6°C) for the crop.

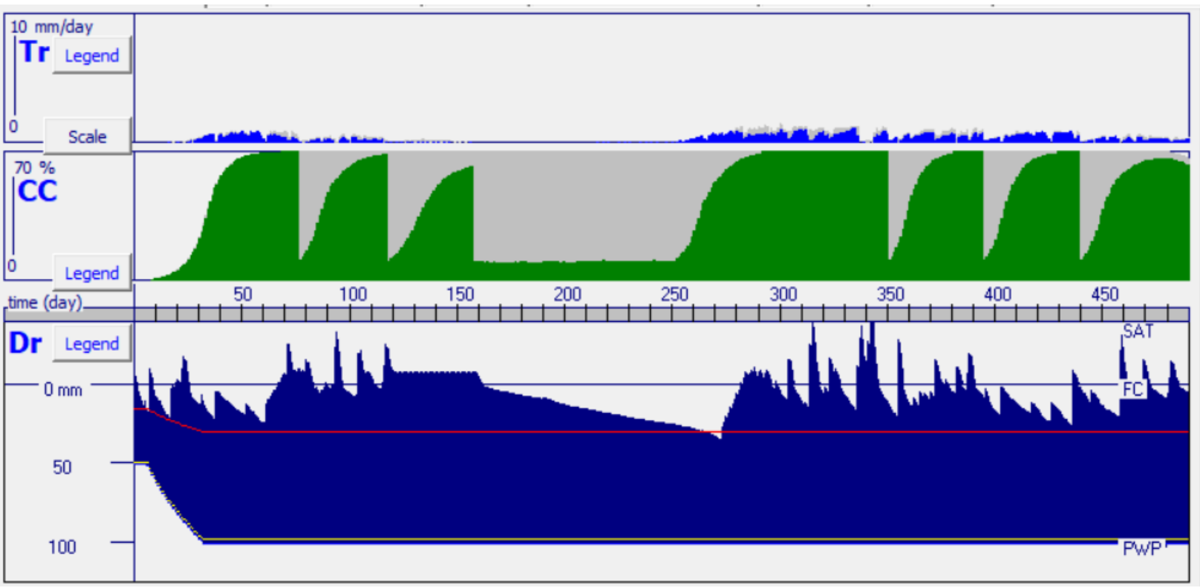

Figure 8.5: Daily actual transpiration fluctuations in relation to changes in actual canopy cover and root zone water depletion during the experimental period on a 1- to 2-year-old Moringa plantation established at ARC-VIMP, Roodeplaat, Pretoria.

8.3.3 AquaCrop model calibration assessment for prediction of green canopy cover, profile soil water content, Moringa fresh and dry leaf yield, as well as crop evapotranspiration

In the calibration phase, the parameter values adopted for the canopy cover (CC) simulation (Figure 8.5a) presented a good goodness-of-fit (r = 0.93, RMSE = 7.9%, CV (RMSE) = 20.2%, EF = 0.78 and d = 0.95). The simulation of CC throughout crop growth and development shows a slight tendency of overestimation in harvest 1. This is primarily attributed to the length of the growing period 1 (76 days, from 01 of January to 18 March 2019), which was longer than that in growing periods 2 (40 days, from 19 March to 28 April 2019) and 3 (40 days, 29 April to 07 June 2019). In addition, the AquaCrop model predicts a constant maximum canopy cover value (67% in this particular growing season – value assigned by the user), which does not reflect the true morphological characteristic of the crop.

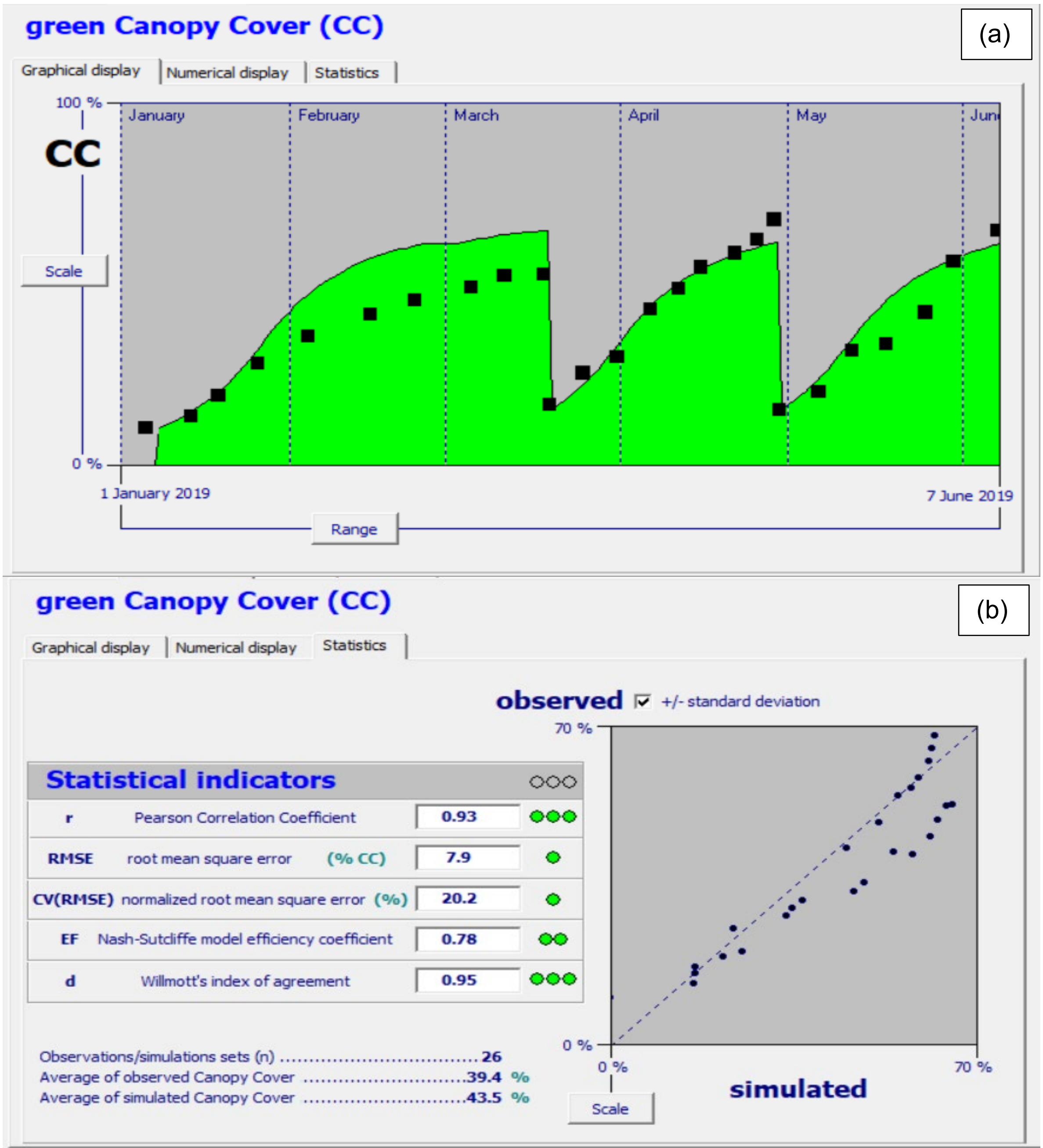

Figure 8.6: Comparison between observed (black squares) and simulated values (solid line) of green canopy cover for *Moringa oleifera* during model calibration under the full irrigation treatment (20% maximum allowable depletion level) in the first experimental season (a). Several statistical parameters have been considered for model performance assessment (b).

The irrigation simulation model performance can be evaluated through the dynamics of soil water content, which are based on field observations using capacitative automated soil water content sensors installed along a 1.0 m soil profile in each soil water supply regime tested. The model simulated changes in soil water content reasonably well along the period of experimental measurements (Figure 8.6).

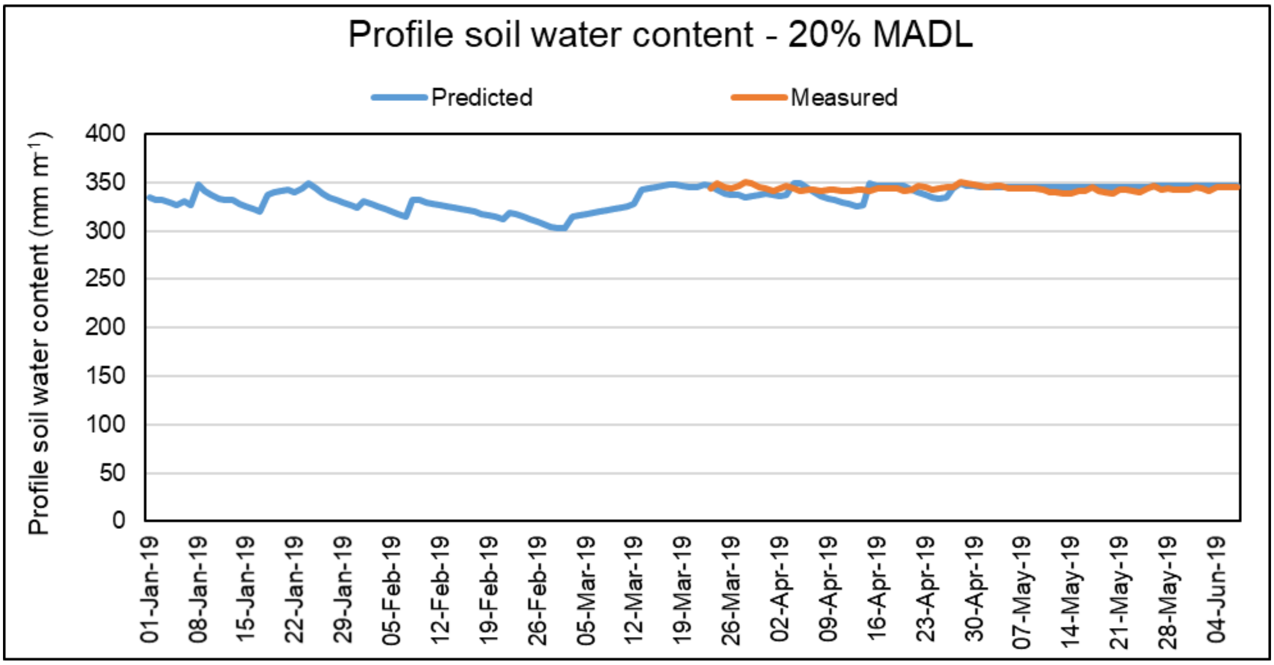

Figure 8.7: AquaCrop model calibration performance: comparison between observed (solid orange line) and simulated values (solid blue line) of soil water content along a 1.0 m profile planted with *Moringa oleifera* under the full irrigation treatment (20% maximum allowable depletion level) in the first experimental season.

Seasonal fresh and dry Moringa leaf yield was simulated quite well using the AquaCrop model. Mean absolute percent error (MAPE) between simulated and observed were 9.9 and 2.4% for fresh and dry yield components, respectively (Figure 8.7). However, model yield prediction per growing period were quite poor, which can be attributed to effects of growing period length and constant maximum canopy cover that are taken into account by the model when predicting crop yield.

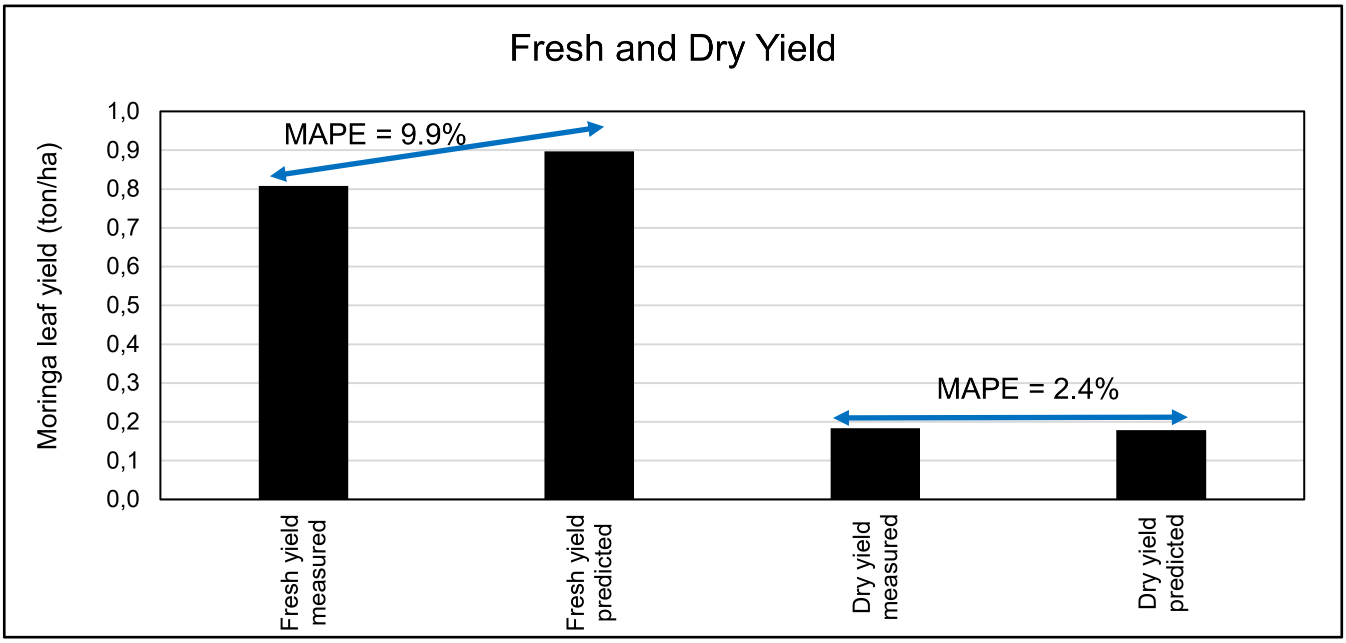

Figure 8.8: AquaCrop model calibration performance: comparison between measured and predicted values of *Moringa oleifera* crop yield grown under the full irrigation treatment (20% maximum allowable depletion level) in the first experimental season.

The AquaCrop model overestimated daily crop evapotranspiration, particularly during the beginning of the growing season. This is attributed to an overestimation of canopy cover and yield, leading to an increase in the transpiration component during that particular period. The discrepancy between predicted and measured cumulative crop evapotranspiration was a maximum of 33.3% (Figure 8.8).

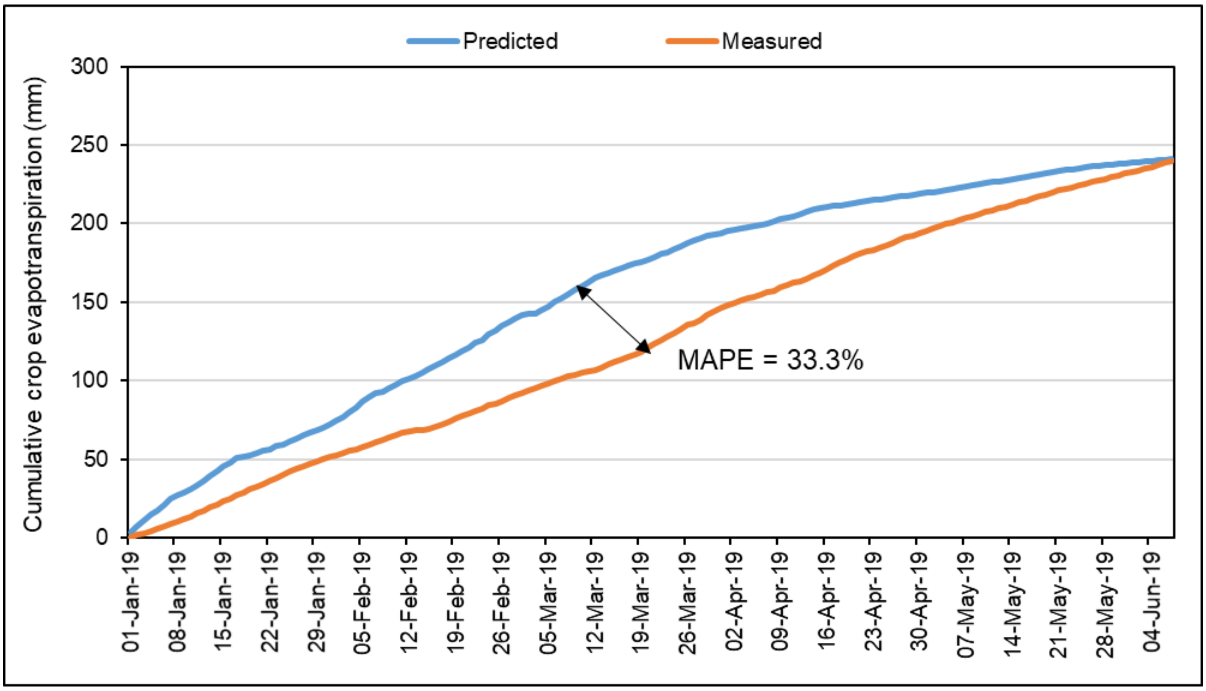

Figure 8.9: AquaCrop model calibration performance: comparison between measured and predicted cumulative crop evapotranspiration of *Moringa oleifera* grown under the full irrigation treatment (20% maximum allowable depletion level) in the first experimental season.

8.3.4 AquaCrop model validation for Moringa crop

Model validation was conducted using calibrated crop parameters obtained with a data set generated under the full irrigation treatment during the 2019-2020 experimental season. As shown in Figure 8.9, green canopy cover predictions compared quite well to measured values (r = 0.97, RMSE = 5.4%, CV (RMSE) = 12.0%, EF = 0.93 and d = 0.98). Model predictions during the second experimental season were better than the first season due to more uniform length of the various growth periods (44, 44 and 49 days for growing periods 1, 2 and 3, respectively).

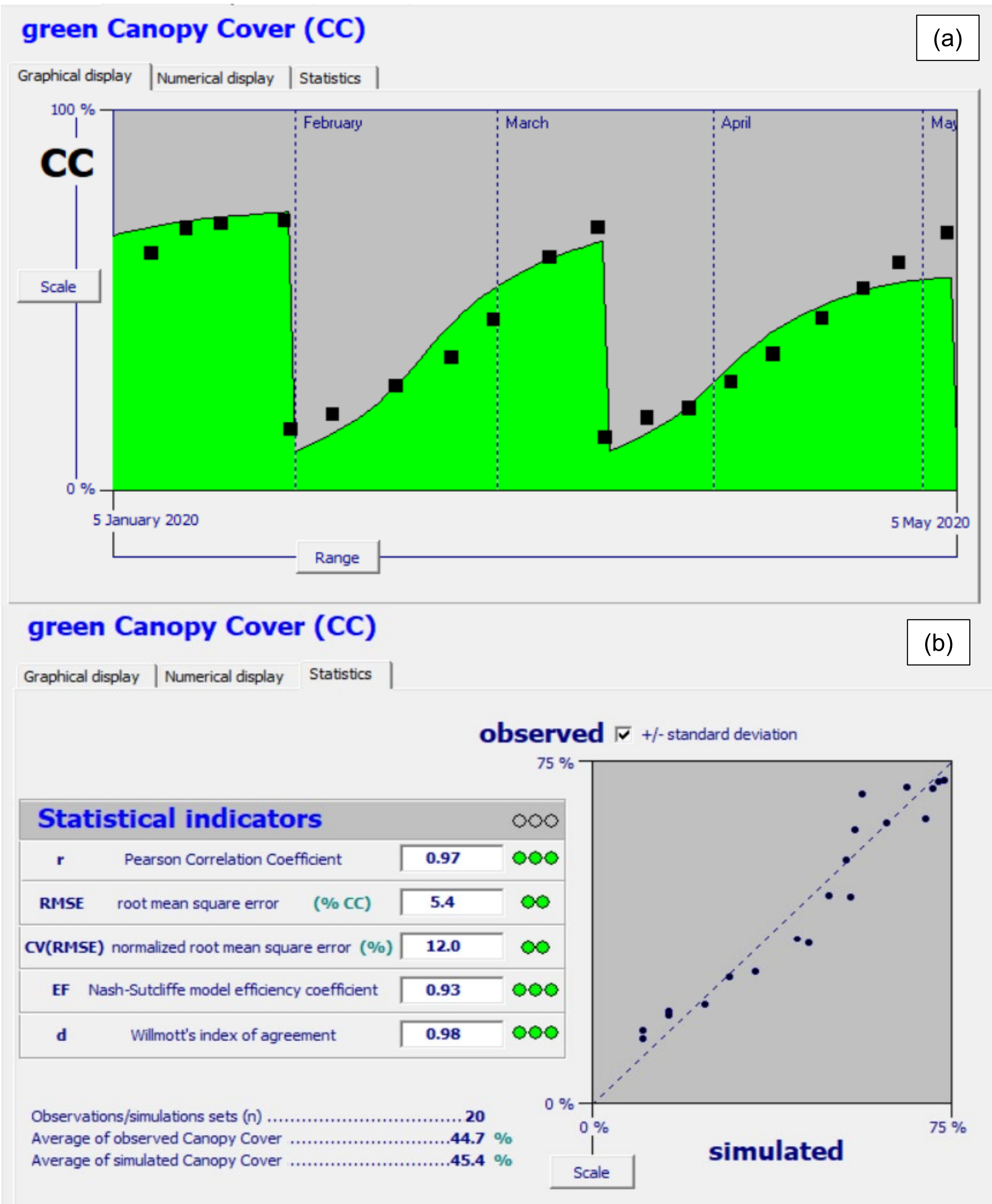

Figure 8.10: Comparison between observed (black squares) and simulated values (solid line) of green canopy cover for *Moringa oleifera* during model validation under the full irrigation treatment (20% maximum allowable depletion level) in the second experimental season (a). Several statistical parameters have been considered for model performance assessment (b).

The predicted profile soil water content was at the level of measured values (Figure 8.10). However, there were more pronounced fluctuations of soil water content compared to the trend of measured values. This aspect needs to be investigated further, to understand what factors contribute to such modelling response.

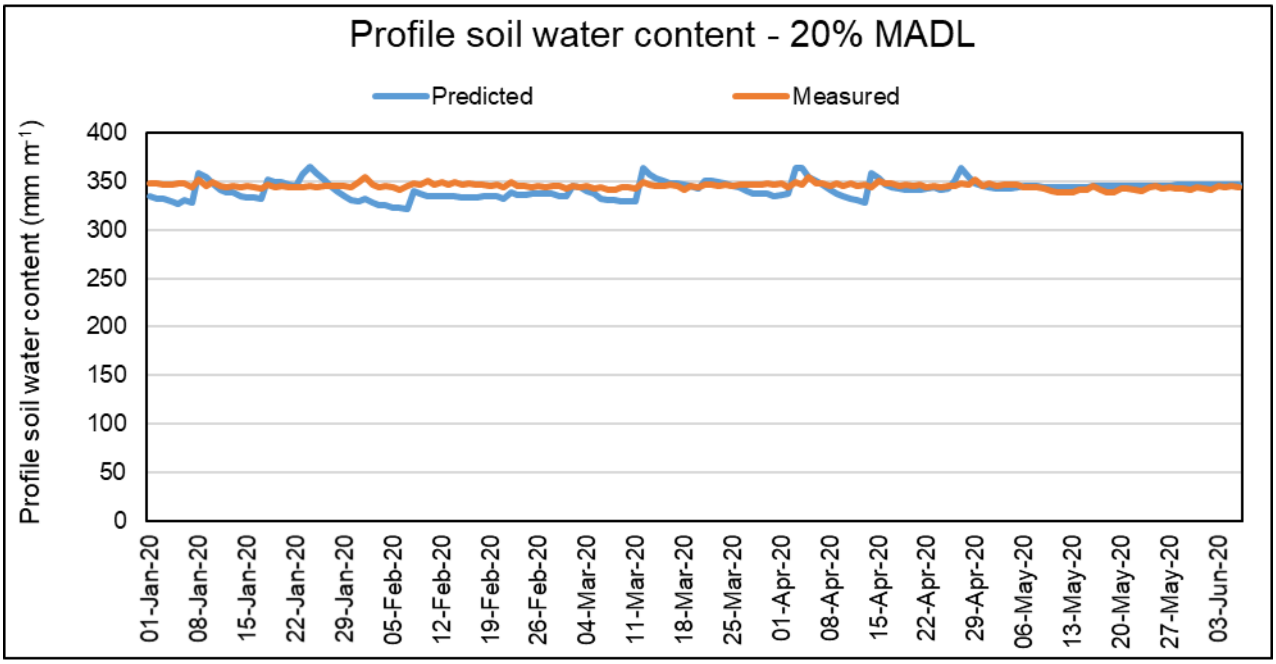

Figure 8.11: AquaCrop model validation performance: comparison between observed (solid orange line) and simulated values (solid blue line) of soil water content along a 1.0 m profile planted with *Moringa oleifera* under the full irrigation treatment (20% maximum allowable depletion level), in the second experimental season.

Model predictions of crop evapotranspiration were found acceptable, with maximum MAPE = 11.7. Similarly, predictions of fresh and dry leaf yield were acceptable, with MAPE varying between 21.5 and 24.1%. The model took into account the transfer of assimilates function embedded in the perennial herbaceous forage crops module, which assumes that, at the start of the next season, a fraction of the stored assimilates are mobilized by transferring them from the root system to the above-ground parts of the crop. Therefore, a portion of assimilates produced in season one were stored during the dormant period of the crops and made available in season 2 through movement (transfer) from the root system to the above ground parts of the crop (FAO, 2023).

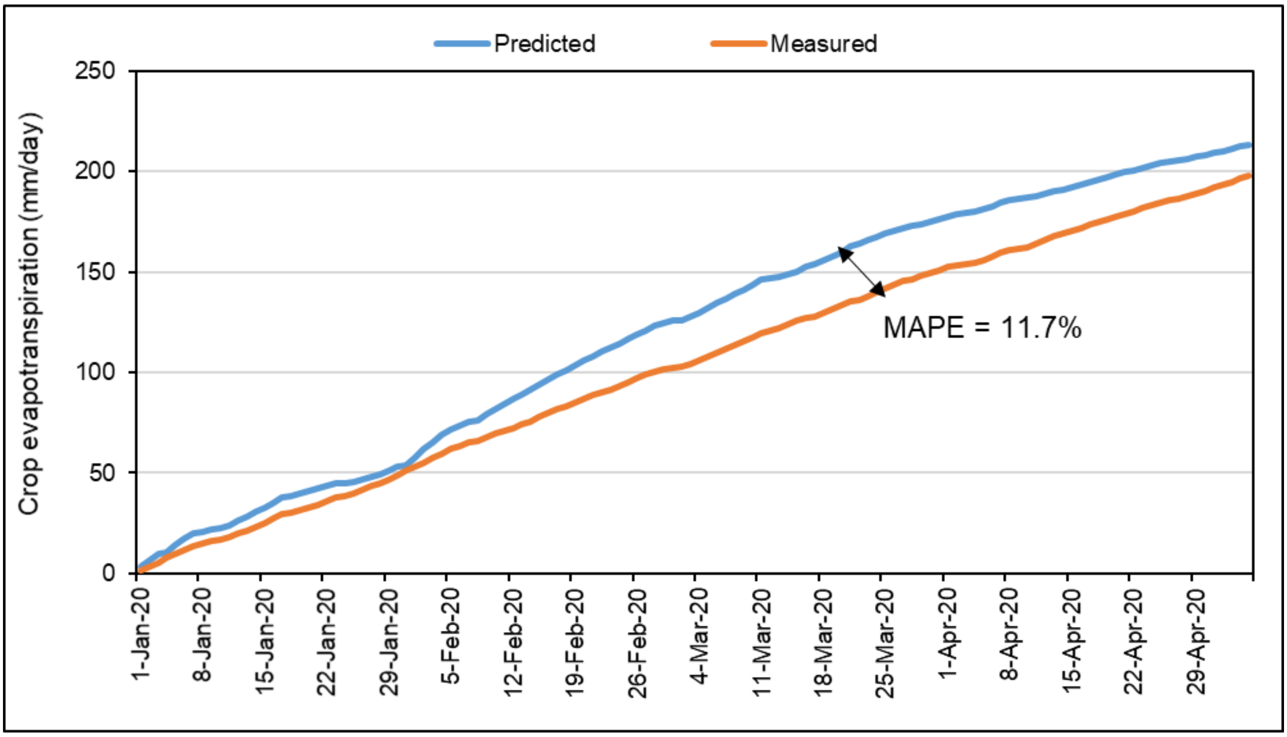

Figure 8.12: AquaCrop model validation performance: comparison between measured and predicted cumulative crop evapotranspiration of *Moringa oleifera* grown under the full irrigation treatment (20% maximum allowable depletion level) in the second experimental season.

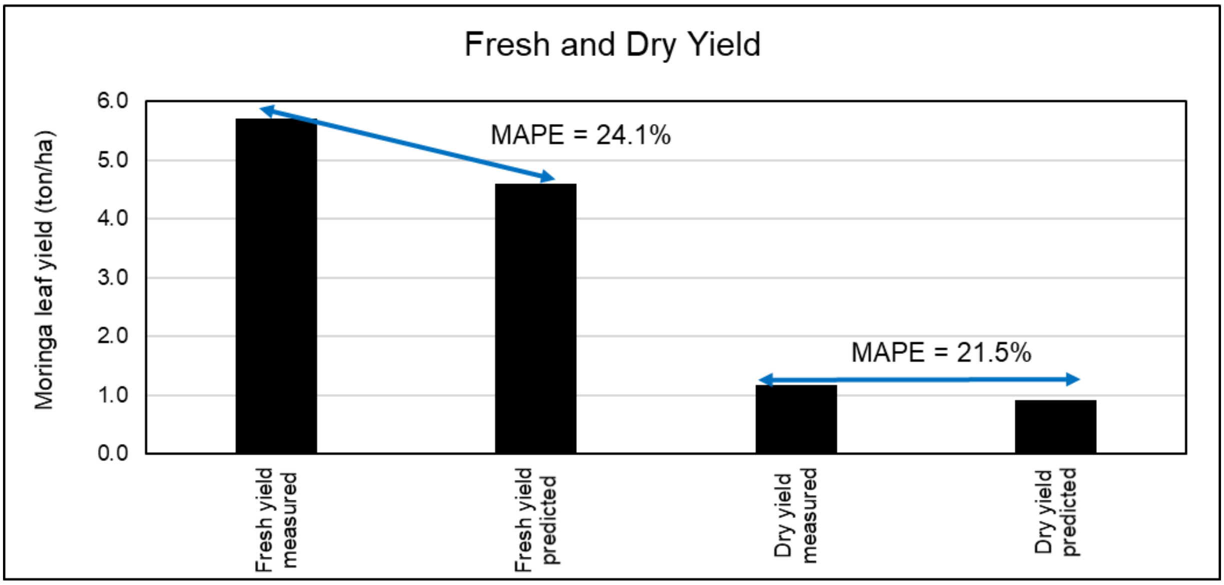

Figure 8.13: AquaCrop model validation performance: comparison between measured and predicted values of *Moringa oleifera* crop yield grown under the full irrigation treatment (20% maximum allowable depletion level) in the second experimental season.

8.4 CONCLUSIONS AND RECOMMENDATIONS

This study tested for the first time, the ability of the AquaCrop model to simulate green canopy cover, actual crop evapotranspiration, soil profile soil water content, and fresh and dry leaf yields of Moringa grown in a semi-arid region of South Africa. Simulations were conducted using the perennial herbaceous forage crops module embedded in AquaCrop model. The performance of the model simulations was assessed based on field data collected during two consecutive growing seasons, each comprising three growing periods. The first experimental season (2018-2019) was used for model calibration, while the second season (2019-2020) was for model validation. The ability of the model to simulate crop performance under varying water supply regimes was also assessed through evaluations of changes in soil water content and crop evapotranspiration. Simulation results showed that the model adequately simulated canopy cover, actual crop evapotranspiration, total soil profile water content, and fresh and dry leaf yields of Moringa. Nonetheless, further calibration and validation of the AquaCrop model for Moringa in other climatic conditions, geographic regions and water supply regimes are needed to improve the parameterization of the AquaCrop model for this crop. The results reported in this study provide an initial foundation for further research aimed at adapting the model for Moringa, which will broaden the model database. The following functions of the AquaCrop model need to be adjusted for more accurate predictions of Moringa crop performance:

- Canopy cover and yield reduction with age of the crop. Moringa biomass production rather increases with tree age, at least for the first 10 to 15 years;
- The perennial herbaceous crops module allows a minimum planting density of 10 000 plants per hectare for C3 species and 6 667 plants per hectare for C4 species. Tree crops like Moringa cultivated for leaf production can be planted at 5 000 plants per hectare or even at lower densities. The value entered for planting density has a direct influence on the initial canopy cover of the simulated crop;
- Canopy cover, biomass and yield within a growing period are strongly dependent on its length. In addition, the model assumes a constant maximum and minimum canopy cover throughout the entire growing season. While minimum canopy cover values can be met through crop management, maximum values are dependent on several factors, including prevailing weather, soil water conditions, plant nutrition, etc. These model limitations contribute to poor estimations of canopy cover and yield per growing period;
- AquaCrop models crop growth and development following published FAO-56 crop growth stages. For perennial herbaceous crops, these growth stages are from transplant to (1) recovery transplant; (2) maximum canopy cover; (3) maximum rooting depth; (4) start of canopy senescence and (5) end of season. There is a need to adjust these growing periods for Moringa crop growth and development stages, as follows: from bud break to (1) fully established canopy cover (2) maximum canopy cover (3) start of canopy senescence and (4) end of season;
- For perennial crops, the regrowth mode considers maximum canopy cover from the previous growing season as the initial canopy cover during the regrowth phase. This contributes to an overestimation of canopy cover in the beginning of the growing season.

ACKNOWLEDGEMENTS

This work was financially supported by the Water Research Commission of South Africa (WRC Project No. C2020/2021-00484). Technical support, data collection and processing by the postgraduate student Mr Ntsieni Mulovhedzi and staff from the Hydroponics Section of ARC-VIMP are highly appreciated.

REFERENCES

Abdelaty, H.S., Hosny, A.M., Abdelhamid, A.N., Abdalla, A.M., 2022. Effect of irrigation water quantity and salinity level on growth and internal chemical contents of Moringa plants. Egypt. J. Chem., 65(12), 79-85.

Araya, A., Habtu, S., Hadgu, K.M., Kebede, A., Dejene, T., 2010. Test of AquaCrop model in simulating biomass and yield of water deficient and irrigated barley (*Hordeum vulgare*). Agric. Water Manag., 97, 1838-1846.

Bello, Z.A., Walker, S., 2016. Calibration and validation of AquaCrop for pearl millet (*Pennisetum glaucum*). Agric. Crop Pasture Sci, A-M,http://dx.doi.org/10.1071/CP15226

Bello, Z.A., Walker, S., 2017. Evaluating AquaCrop model for simulating production of amaranthus (*Amaranthus cruentus*) a leafy vegetable, under irrigation and rainfed conditions. Agric. For. Meteorol., 247, 300-310.

Daba, M., 2016. Miracle tree: a review on multi-purposes of *Moringa oleifera* and its implication for climate change mitigation. J. Earth Sci. Clim. Change, 7(8), 1-5.

Devkota, S., Bhusal, K.K., 2020. *Moringa oleifera*: A miracle multipurpose tree for agroforestry and climate change mitigation from the Himalayas – A review. Cogent food agric., 6(1), 1-8.

El-Boraie, F.M., El Shafay, R.M.M., Elhagarey, M.E., 2021. Morphological and chemical characterizes responses of *Moringa oleifera* yield to localized irrigation systems, water restriction and fertilizers. Int. j. adv. Res, 9(2), 509-523.

Er-Raki, S., Bouras, E., Rodriguez, J.C., Watts, C.J., Lizarraga-Celaya, C., Chehbouni, A., 2021. Parameterization of the AquaCrop model for simulating table grapes growth and water productivity in an arid region of Mexico. Agric. Water Manag., 245, 1-10.

Ezzine, H., Metougui, M.L., Boukcim, H., Abbas, Y., 2023. Physiological responses of three field-grown species (*Ceratonia siliqua, Eucalyptus camaldulensis*, and *Moringa oleifera*) to water deficits in a Mediterranean semi-arid climate. Sci. Rep., 13, 1-10.

FAO, 2023. Chapter 2. Users guide. AquaCrop Version 7.1. Reference manual. Food and Agriculture Organization (FAO) of the United Nations, 1-370.

Feng, D., Li, G., Wang, D., Wulazibieke, M., Cai, M., Kang, J., Yuan, Z., Xu, H., 2022. Evaluation of AquaCrop model performance under mulched drip irrigation for maize in Northeast China. Agric. Water Manag., 261, 1-10.

Gopalakrishnan, L., Doriya, K., Kumar, D.S., 2016. *Moringa oleifera*: A review on nutritive importance and its medicinal application. Food Sci. Hum. Wellness, 5, 49-56.

Grosshagauer, S., Pirkwieser, P., Kraemer, K., Somoza, V., 2021. The future of Moringa foods: a food chemistry perspective. FRONT NUTR, 8, 1-9.

Ibraimo, N.A., Taylor, N.J., Steyn, J.M., Gush, M.B., Annandale, J.G., 2016. Estimating water use of mature pecan orchards: A six stage crop growth curve approach. Agric. Water Manag., 177, 359-368.

Jadon, A., Patil, A., Jadon, S., 2022. A comprehensive survey of regression based loss

functions for time series forecasting. arXiv:2211.02989v1 [cs.LG], 1-13.

Jalil, A., Akhtar, F., Awan, U.K., 2020. Evaluation of the AquaCrop model for winter wheat under different irrigation optimization strategies at the downstream Kabul River Basin of Afghanistan. Agric. Water Manag., 240, 1-8.

Jo, W.J., Shin, J.H., 2021. Development of a transpiration model for precise tomato (*Solanum lycopersicum* L.) irrigation control under various environmental conditions in greenhouse. Plant Physiol. Biochem., 162, 388-394.

Kisekka, I., De Jonge, K.C., Ma, L., Paz, J., Douglas-Mankin, K., 2017. Crop modeling applications in agricultural water management. Transactions of the ASABE, 60(6), 1959-1964.

Li, L., Chen, S., Yang, C., Meng, F., Sigrimis, N., 2020. Prediction of plant transpiration from environmental parameters and relative leaf area index using the random forest regression algorithm. J. Clean. Prod., 261, 1-13.

Martínez-Romero, A., L'opez-Urrea, R., Montoya, F., Pardo, J.J., Domínguez, A., 2021. Optimization of irrigation scheduling for barley crop, combining AquaCrop and MOPECO models to simulate various water-deficit regimes. Agric. Water Manag., 258, 1-16.

Muhl, Q.E., Toit, E.S., Robbertse, P.J., 2011. *Moringa oleifera* (Horseradish tree) leaf adaptation to temperature regimes. Int J Agric Biol ., 13, 1021-1024.

Muhl, Q.E., du Toit, E.S., Steyn, J.M., Apostolides, Z., 2013. Bud development, flowering and fruit set of *Moringa oleifera* Lam. (Horseradish Tree) as affected by various irrigation levels. JARTS, 114(2), 79-87.

Nash, J. E., Sutcliffe, J. V., 1970. River flow forecasting through conceptual models part I — A discussion of principles. J. Hydrol. 10, 282-290.

Nyathi, M.K., van Halsema, G.E., Annandale, J.G., Struik, P.C., 2018. Calibration and validation of the AquaCrop model for repeatedly harvested leafy vegetables grown under different irrigation regimes. Agric. Water Manag., 208, 107-119.

Nyathi, M.K., Mabhaudhi, T., Van Halsema, G.E., Annandale, J.G., Struik, P.C., 2019. Benchmarking nutritional water productivity of twenty vegetables – A review. Agric. Water Manag., 221, 248-259.

Nunes, H.G.G.C., Farias, V.D.S., Sousa, D.P., Costa, D.L.P., Pinto, J.V.N., Moura, V.B., Teixeira, E.O., Lima, M.J.A., Ortega-Farias, S., Souza, P.J.O.P., 2021. Parameterization of the AquaCrop model for cowpea and assessing the impact of sowing dates normally used on yield. Agric. Water Manag., 252, 1-14.

Poppe, M., 2016. Simulating the water footprint of woodies in Aquacrop and Apex. Master Thesis, University of Twente, Water Engineering and Management, 1-102.

Raes, D., Steduto, P., Hsiao, T.C., Fereres, E., 2023. AquaCrop Version 7.1. Chapter 3 Calculation procedures. Reference manual. Food and Agriculture Organization (FAO) of the United Nations, 1-163.

Steduto, P., Raes, D., Hsiao, T.C., Fereres, E., Heng, L., Izzi, G., Hoogeveen, J., 2008. AquaCrop: a new model for crop prediction under water deficit conditions.

Shyamli, P.S., Pradhan, S., Panda, M., Parida, A., 2021. De novo whole-genome assembly of *Moringa oleifera* helps identify genes regulating drought stress tolerance. Front. Plant Sci., 12, 1-14.

Steduto, P., Raes, D., Hsiao, T.C., Fereres, E., Heng, L., Izzi, G., Hoogeveen, J., 2014. AquaCrop: a new model for crop prediction under water deficit conditions. Options Méditerranéennes, Series A (80), 285-292.

Singh, J., Knapp, H.V., Arnold, J.G., Demissie, M.. 2005. Hydrologic modeling of the Iroquois River watershed using HSPF and SWAT. J. American Water Resources Assoc. 41(2): 361-375.

Swanson, D.A., 2015. On the relationship among values of the same summary measure of error when it is used across multiple characteristics at the same point in time: An examination of MALPE and MAPE. Review of Economics & Finance. ID: 1923-7529-2015-03-01-14, 1-14.

Wang, H., Cheng, M., Liao, Z., Guo, J., Zhang, F., Fan, J., Feng, H., Yang, Q., Wu, L., Wang, X., 2023. Performance evaluation of AquaCrop and DSSAT-SUBSTOR-Potato models in simulating potato growth, yield and water productivity under various drip fertigation regimes. Water Manag., 276, 1-20.

Wellens, J., Raes, D., Fereres, E., Diels, J., Coppye, C., Adiele, J.G., Ezui, K.S.G., Becerra, L., Selvaraj, M.G., Dercon, G., Heng, L.K., 2022. Calibration and validation of the FAO AquaCrop water productivity model for cassava (*Manihot esculenta* Crantz). Agric. Water Manag., 263, 1-10.

Willmott, C.J., Matsuura, K., 2005. Advantages of the mean absolute error (MAE) over the root mean square error (RMSE) in assessing average model performance. Clim. Res. 30, 79-82.

Zhang, C., Xie, Z., Wang, Q., Tang, M., Feng, S., Cai, H., 2022. AquaCrop modeling to explore optimal irrigation of winter wheat for improving grain yield and water productivity. Agric. Water Manag., 263, 1-10.

Zeleke, K.T., Wade, L.J., 2012. Evapotranspiration estimation using soil water balance, weather and crop data. Evapotranspiration – Remote Sensing and Modeling, pg 41-58.

CHAPTER 9

Nadia Araya

Agricultural Research Council – Vegetable, Industrial and Medicinal Plants, Private bag X293, Pretoria, 0001, South Africa

Agricultural Research Council – Natural Resources and Engineering, Private bag X79, Pretoria, 0001, South Africa

GENERAL CONCLUSIONS AND RECOMMENDATIONS

The morphological characteristics of Moringa (tree height, trunk girth diameter), seed/pod and leaf yields are highly variable depending on crop management factors (time of leaf harvesting, harvesting frequency, planting density, tree spacing, and type of production system), genetics (cultivar) and environmental conditions (soil type and climate). Moringa crop productivity is also likely to be influenced by variations in crop physiological and anatomical characteristics. Very few studies have investigated the influence of crop management practices and changes in environmental conditions on crop productivity, water use efficiency and nutritional water productivity. The available literature suggests that Moringa grows well in tropical and sub-tropical semi-arid climates, with warm and humid environmental conditions and a range of rainfall amounts (200-3000 mm) and soil types. This indicates that Moringa is quite tolerant to both drought and waterlogging conditions. However, very few studies have looked at Moringa crop responses to varying water supply regimes and soil types, which could lead to an underestimation of the crop potential yields, especially in areas where the crop has not been studied. The limited research that is available on Moringa has mostly been generated from the Limpopo Province. Hence, there is a need to conduct further research in other Provinces with potential for cultivation of Moringa such as the Gauteng Province.

This study investigated the first application of an eddy covariance technique to determine Moringa crop water use in order to develop site-specific crop coefficients. Daily crop ET varied from 2.45 mm day^{-1} on a cloudy day to 4.28 mm day^{-1} on a hot sunny day. Daily crop coefficients (K_c) remained steadily constant throughout the experimental period at about 0.6, suggesting the presence of a drought adaptation mechanism in Moringa trees. The cumulative ET during the period when the crop was actively growing (17 December 2021 to 29 January 2022) was 136 mm, while the atmospheric evaporative demand (ET_o) was 216 mm, resulting in an average K_c value of 0.62. During this period, the crop canopy cover increased from 49 to 86%.

In irrigated mature Moringa trees, the total branch SF diverged from the respective main stem SF by 25%. Moringa tree T was highly influenced by tree size (determined by the number of stems per tree and stem area, as well as by the changes in g_s). The major microclimatic influencing variables were ETo, followed by Ta_{max} and VPD. The growth, physiology, yield and water use of four- and 10-year-old *Moringa oleifera* trees was investigated in response to varying crop management practices (tree spacing and harvesting strategy). The reported experimental period received sufficient rainfall for Moringa crop productivity and, as a result, irrigation was not applied. Harvesting Moringa leaves using the stripping method every 60 days resulted in the highest crop productivity (11.3 ton/ha) and lowest crop water consumption (225 mm) seasonally, when the trees were cultivated using the in-situ rainwater harvesting and conservation system. Cultivating Moringa trees using narrower (1.0 x 1.0 m) or wider (1.0 x 1.5 m) tree spacing did not have a significant influence on the crop productivity (1.8 to 2.1 ton/ha per harvesting). Similarly, the crop water use remained unnoticeably different between the two tree spacing investigated (62.01-62.51 mm per harvesting). Therefore, it is suggested that the Moringa tree be cultivated at wider spacing/lower plant population of less than 6 666 trees/ha. In areas receiving sufficient rainfall, the Moringa tree can be cultivated under rain-fed conditions, however, employing climate-smart production systems such as the in-situ rainwater harvesting and conservation has proven beneficial to the Moringa tree grown for leaf production.

This study has contributed towards an understanding of the components within the METRIC EEFlux model algorithm, which could increase uncertainty of field scale ETa estimates. Some of the shortcomings of the METRIC EEFlux modelling approach can be counteracted by using semi-automated remote sensing tools such as the METRIC-GIS toolbox which utilises local meteorological data as modelling inputs. The evidence from this study has shown that local meteorological data could potentially be integrated with the output from the METRIC EEFlux model to provide fairly accurate Moringa ETa estimates. Furthermore, this study tested for the first time, the ability of the AquaCrop model to simulate green canopy cover, actual crop evapotranspiration, soil profile soil water content, and fresh and dry leaf yields of Moringa grown in a semi-arid region of South Africa. Simulation results showed that the model adequately simulated canopy cover, actual crop evapotranspiration, total soil profile water content, and fresh and dry leaf yields of Moringa. Nonetheless, further calibration and validation of the AquaCrop model for Moringa in other climatic conditions, geographic regions and water supply regimes are needed to improve the parameterization of the AquaCrop model for this crop.

APPENDIX A: KNOWLEDGE DISSEMINATION

Scientific publications

- Mokgehle S, Araya NA, Mofokeng M, Makgato M, Amoo S, Maboka K, du Plooy C and Araya H, 2022. Regrowth response and nutritional composition of *Moringa oleifera* to cutting back in three agro-ecological zones in South Africa. *Horticulturae*, 8, 963, 1-11.

- Ambroise N, JM Steyn, CP du Plooy and NA Araya, 2024. Measurement and modelling of Moringa transpiration for improved irrigation management. Accepted for publication in Agricultural Water Management.

- Muchaonyerwa K, Gokool S, Clulow A and Araya NA, 2023. Evaluation of the METRIC EEFlux platform to estimate water use of Moringa. Accepted for publication in Acta Horticulturae.

- Araya NA, Mulovhedzi N, Amoo SO, du Plooy CP, Gokool S and Clulow A, 2023. On-farm assessment of eddy covariance energy balance closure over a drip-irrigated Moringa plantation in a semi-arid region of South Africa. Accepted for publication in Acta Horticulturae.

- Mulovhedzi NE, Mokgehle SN, Seepe HA, Savage M, Amoo SO, and Araya NA, 2024. Nutritional water productivity of Moringa oleifera in response to varying water supply regimes under a semi-arid climate. Under review for submission to Scientia Horticulturae.

- Gokool S, Clulow A and Araya N, 2024. Cloud-based remote sensing for the water use estimation of Moringa Oleifera in South Africa. Under review for submission to Agricultural Water Management.

Scientific presentations

- Nwamba SF, Bello Z, Soundy P and Araya N. Simulating Moringa productivity under the in-situ rainwater harvesting system using AquaCrop modelling in a semi-arid area. Poster presentation at the Combine Congress 2023, Pretoria.

- Ndayakunze A, Araya NA, Truter M and Steyn JM, 2023. Can sustainable agronomic practices improve the edaphic and biotic dynamics of the Moringa rhizosphere? Oral presentation at the Combined Congress 2023, Pretoria.

- Sithole G and Araya NA, 2023. Investigating Moringa oleifera growth and yield under different organic soil amendment practices. Poster presentation – Awarded for best poster presentation at the Combined Congress 2023, Pretoria.

- Muchaonyerwa K, Gokool S, Clulow A, Araya NA, 2023. Evaluation of the METRIC EEFlux platform to estimate water use of Moringa. Poster presentation at the Xth International Symposium on Irrigation of Horticultural Crops, Cape Town.

- Araya NA, Mulovhedzi N, Amoo SO, du Plooy CP, Gokool S and Clulow A, 2023. On-farm assessment of eddy covariance energy balance closure over a drip-irrigated Moringa plantation in a semi-arid region of South Africa. Poster presentation at the Xth International Symposium on Irrigation of Horticultural Crops, Cape Town.

- Ndayakunze A, Araya NA, Araya HT, Amoo SO, du Plooy C.P. and Steyn JM, 2023. Measurement and modelling of Moringa transpiration using a canopy conductance approach. Oral presentation at the Xth International Symposium on Irrigation of Horticultural Crops, Cape Town.

Popular articles

- Mofokeng M, Mokgehle S, Araya N, Makhubele M, and Masondo N, 2022. Moringa value chain: seed and vegetative propagation. ARC-VIMP Newsletter No 13.

- Araya N, Mokgehle S, Mofokeng M, Makhubele M and Masondo N, 2022. Moringa value chain: cultivation strategies. ARC-VIMP Newsletter No 13.

- Masondo N, Mokgehle S, Mofokeng M, Makhubele M and Araya N, 2022. Moringa value chain: product development. ARC-VIMP Newsletter No 13.

- Mofokeng M, Mokgehle S, Araya H, Masondo N, Araya N, Amoo S and du Plooy I, 2022. *Moringa oleifera* – a nutritious naturalized tree adapted to South African conditions. AgriAbout No 109.

Farmers' days training events

- Ten emerging commercial farmers from the MOR-NUTRI Farm, Tooseng, Lebowakgomo, Limpopo Province. Optimum management practices for Moringa cultivation, from 2021 to 2023.

APPENDIX B: CAPACITY BUILDING

Post-graduate PhD students

Mr Ntsieni Mulovhedzi

Mr Ntsieni Mulovhedzi registered for a PhD degree in 2020, at the University of KwaZulu-Natal. His thesis is titled "Determining the yield, water use, water and nutritional water productivity of Moringa (*Moringa oleifera* Lam.) under varying water supply regimes". He conducted field experiments for two consecutive seasons on 2- to 3-year old Moringa trees in the semi-arid area of Roodeplaat, Pretoria. His thesis includes modelling the water use and productivity of Moringa using a soil water balance model. To date, he has compiled two manuscripts which are currently under review for submission to Scientia Horticulturae and Agricultural Water Management journals. His research work has been presented at several local scientific conferences. He is expected to complete his degree by December 2024.

Mr Ambroise Ndayakunze

Mr Ambroise Ndayakunze registered for a PhD degree in 2022, at the University of Pretoria. His thesis is titled "Sustainable agronomic practices for improved water use and nutritional water productivity of Moringa". He conducted field experiments for two consecutive seasons on 13-year old Moringa trees in the semi-arid area of Roodeplaat, Pretoria. His thesis includes modelling Moringa transpiration using a canopy conductance model. To date, he has compiled one manuscript which has been accepted for publication in Agricultural Water Management and attended and presented at several local and international scientific conferences. He is expected to complete his degree by December 2025.

Post-graduate MSc student

Mr Sihle Floyd N'Wamba

Mr Sihle Floyd N'Wamba registered for an MSc degree in 2022, at Tshwane University of Technology. His dissertation is titled "Investigating Moringa crop productivity in response to different leaf harvesting methods and frequencies under the in-situ rainwater harvesting and conservation production system". He conducted field experiments for two consecutive seasons on 3- to 4-year old Moringa trees in the semi-arid area of Roodeplaat, Pretoria. He presented his research findings at the Combined Congress 2023. He is expected to complete his degree by December 2024.

Advanced Diploma Intern

Mr Graig Sithole

Mr Graig Sithole completed his Diploma and Advanced Diploma degrees at Tshwane University of Technology, under the WRC-funded Moringa water use project C2020/2021-00484. He acquired extensive practical experience on Moringa cultivation through his involvement in a field experiment aiming to investigate the growth and yield of Moringa under different organic soil amendment practices. His research findings were presented at the Combined Congress 2023, where he received an award by the Southern African Society for Horticultural Sciences, for best poster presented at the Combined Congress 2023. He is currently looking to pursue his Honors degree on Moringa related research matters.

Agricultural Practitioner Research Assistant

Ms Tintswalo Mathonsi

Ms Tintswalo Mathonsi was affiliated to the Department of Agriculture, Land Reform and Rural Development when she joined the Agricultural Research Council – Vegetable, Industrial and Medicinal Plants as an Agricultural Practitioner. She acquired practical experience on Moringa cultivation for six months through her involvement in the Moringa research, under the WRC-funded project C2020/2021-00484.

Moringa Farmer

- Mr Mathabatha Thushego affiliated to MOR-NUTRI Moringa Farm.